

**Alkali-activated materials (AAMs) as Concrete Repair Materials**

**by**

**Eddy Mohd Fairuz Bin Mohd Yusslee**

**A thesis submitted in partial fulfilment of the requirements for the degree of Doctor of  
Philosophy**

**Supervised by**

**Associate Professor Dr. Sherif Beskhyroun**

**Department of Built Environment Engineering**

**School of Future Environments**

**Auckland University of Technology**

**New Zealand**

**August 2023**

## **Conference Presentations and Publications Arising from this Doctoral thesis**

1. The World Conference on Architecture and Civil Engineering, Berlin Germany  
11 – 13 March 2022  
Performance Evaluation of Hybrid One-Part Alkali Activated Mortar (Abstract) –  
Presenter
2. Global Meet on Civil, Structural and Environmental Engineering, Dubai UAE  
10 – 12 October 2022  
Performance Evaluation of One-Part Alkali Activated Mortar (Abstract) - Presenter
3. 4th International Conference on the Chemistry of Construction Materials, Karlsruhe  
Germany 26 – 28 September 2022  
Study on Alkali Activated Materials (AAMS) as Concrete Repair Mortar (Abstract)-  
Presenter
4. Performance Evaluation of Hybrid One- Part Alkali Activated materials (AAMs) for  
Concrete Structural Repair MDPI – Buildings (Publication) 18 September 2022  
[doi.org/10.3390/buildings12112025](https://doi.org/10.3390/buildings12112025)
5. The potential of one-part alkali-activated materials (AAMs) as a concrete patch mortar.  
Springer Nature - Scientific Reports (Publication) 23 September 2022  
[doi.org/10.1038/s41598-022-19830-0](https://doi.org/10.1038/s41598-022-19830-0)
6. The effect of water-to-binder ratio (W/B) on pore structure of one-part alkali activated  
mortar. Cell Press – Heliyon (Publication) 14 January 2023  
[doi.org/10.1016/j.heliyon.2023.e12983](https://doi.org/10.1016/j.heliyon.2023.e12983)

## **Acknowledgement**

First and foremost, all praise be to Allah, Most Gracious, Most Merciful!

I would like to thank my primary supervisor, Assoc. Prof Dr Sherif Beskhyroun for his ultimate support through my PhD study in AUT. Also, thank my co-supervisor Prof John Tookey for his undivided assistance. Thanks to the university for supporting me financially via scholarships.

Not to forget my family, parents, my wife, Huzaikha Awang and my son, Eddy Muhammad, for being with me together through thick and thin. To my wife, you helped make the impossible possible, and to my son, remember you got to beat me one day!

Finally, I am thankful to my sponsors and employer, who allow me to pursue study at this level.

Kia Ora! Thank you very much and terima kasih!

“Read! And your Lord (Allah) is the Most Generous,  
Who taught by the pen - Taught humanity what they knew not”

Quran: Al-‘Alaq 3 – 5.

## **Abstract**

Alkali Activated Materials (AAMs) is a new cement technology utilizing waste products to produce cementitious binders. The main precursors are activated with an alkali activator for the hardening process. The reaction between precursors and alkali activator will create hydrated gels of calcium aluminate silicate hydrates, C-A-S-H and/or sodium aluminate silicate hydrates, N-A-S-H for binding phases. FA and GGBFS contain a high amount of silica and alumina in their chemical components, thus making them suitable sources as aluminosilicate precursors for cement binders. AAMs are traditionally employed in the two-part system where the activator is liquid and activated dry precursor powder. However, it has handling problems due to corrosive activators that may affect worker safety, besides some performance issues such as rapid setting time and higher shrinkage issues that limit their application at real-site construction. Including ordinary Portland cement (OPC) mixed with aluminosilicate precursors, also known as hybrid, is an effort to modify the engineering properties of the dry mixture materials in one-part AAMs (dry activator system) in this study, diversifying its potential application.

One-part AAMs technology mainly focuses on concrete product purposes as an alternative to conventional OPC-based cementitious. A hybrid one-part AAMs mortar is being developed to reduce dependency on OPC in the form of mortar and cut the OPC volume as low as possible. Interestingly, the mechanical strength of the hybrid one-part AAMs mortar developed in this research is comparable to the OPC concrete, providing extra added value where no coarse aggregate is used, which the construction sector responsible for the waning of natural resources and environmental imbalances due to mining activities/rock excavations.

In this studies, all mortar samples were tested in the laboratory with controlled room temperature (18 – 22°C) and relative humidity, RH > 90%, to comply with EN1504–3:2005 standard, part 3: structural and non-structural concrete repair materials. The novel mix design formulation confirms it successfully replaces 30% of OPC volume with industrial by-product precursors as

the first step in diminishing reliance on the OPC and another effort to reduce clinker production, reuse waste products, and control CO<sub>2</sub> emissions. Nevertheless, using a less reactive alkaline activator with a low concentration level is beneficial for a cheaper cost, lower health risks and is not harmful to the environment. The hybrid one-part AAMs mortar in this study has mechanical strength that complies with European standards, EN-1504 specifications for Class R4 – Structural concrete repair materials. It has also had improved pore volume structures that reduce the porosity level – main drawbacks for one-part AAMs system while providing better engineering properties and durability for long-term applications.

One-part AAMs repair mortar as new innovative construction materials achieved another milestone as an effort to improve the construction sector towards the goal of sustainable construction to keep global warming increased to no more than 1.5 Celsius as called for in the Paris Agreement – emissions need to be reduced by 45% by 2030 and reach net zero by 2050 and also particularly for the zero carbon target in New Zealand - for domestic targets under the Climate Change Response Act (CCRA) Net zero emissions of all greenhouse gas (GHG) emissions other than biogenic methane by 2050.

## **Attestation of Authorship**

I hereby declare that this submission is my own work and that, to the best of my knowledge and belief, it contains no material previously published or written by another person (except where explicitly defined in the acknowledgements), nor material which to a substantial extent has been submitted for the award of any other degree or diploma of a university or other institution of higher learning.

Eddy Mohd Fairuz Binti Mohd Yusslee

25.8.2023

Signature:

## Co-authored Works

The contributions of the co-authors for the following chapters/papers are indicated below:

Manuscript 1: Eddy Yusslee, Sherif Beskhyroun (2022), **Performance Evaluation of Hybrid One-Part Alkali Activated Materials (AAMs) for Concrete Structural Repair**

published in the Buildings 2022, 12(11), 2025; <https://doi.org/10.3390/buildings12112025>

85%: Eddy Mohd Fairuz Bin Mohd Yusslee

15%: Associate Professor Sherif Beskhyroun

Manuscript 2: Eddy Yusslee, Sherif Beskhyroun (2022), **The potential of one-part alkali-activated materials (AAMs) as a concrete patch mortar**

published in the Scientific Reports|(2022)12:15902. <https://doi.org/10.1038/s41598-022-19830-0>

85%: Eddy Mohd Fairuz Bin Mohd Yusslee

15%: Associate Professor Sherif Beskhyroun

Manuscript 3: Eddy Yusslee, Sherif Beskhyroun (2023), **The effect of water-to-binder ratio (W/B) on pore structure of one-part alkali activated mortar**

published in the Heliyon 9 (2023) e12983 <https://doi.org/10.1016/j.heliyon.2023.e12983>

85%: Eddy Mohd Fairuz Bin Mohd Yusslee

15%: Associate Professor Dr. Sherif Beskhyroun

We, the undersigned, hereby agree to the percentage of participation in the chapters/papers identified above.

1- Eddy Mohd Fairuz Bin Mohd Yusslee

-----  
Date: 1 September 2023

2- Associate Professor Dr. Sherif Beskhyroun

-----  
Date: 4 September 2023

## Table of Contents

Conference Presentations and Publications Arising from this Doctoral thesis.....	i
Acknowledgement .....	ii
Abstract.....	1
Attestation of Authorship.....	3
Co-authored Works.....	4
Table of Contents.....	5
List of Figures.....	9
List of Tables .....	10
List of Equations.....	11
1 Introduction.....	12
1.1 Objectives of study .....	21
1.2 Aim of the study .....	23
1.3 Rationale and Significance of the Study.....	23
1.4 Scope and limitation of the study .....	23
1.5 Thesis Outline.....	26
2 Literature Review.....	29
2.1 Alkali activated Materials (AAMs) – One-part systems. ....	29
2.2 Aluminosilicate precursors .....	29
2.2.1 Fly Ash (FA).....	29
2.2.2 Ground Granulated Blast Furnace Slag (GGBFS).....	35
2.3 Ordinary Portland cement (OPC) .....	38
2.4 Alkali activators.....	41
2.4.1 Sodium silicate .....	43

2.4.2	Sodium hydroxide.....	45
2.4.3	Sodium carbonate .....	45
2.5	Mix design ratio and curing regimes. ....	46
2.6	Admixtures .....	54
2.7	Rheology of binder .....	57
2.7.1	Workability of one-part AAMs .....	57
2.7.2	Flowability.....	60
2.7.3	Setting Time .....	63
2.8	Mechanical properties of one-part AAMs. ....	68
2.8.1	Compressive Strength.....	71
2.8.2	Modulus of elasticity (MOE) and Poisson's Ratio.....	79
2.8.3	Bulk density.....	80
2.9	Flexural Strength .....	80
2.10	Tensile Strength.....	82
2.11	Shrinkage.....	83
2.12	Porosity.....	86
2.13	Microstructural Analysis .....	92
3	Introduction to Manuscript 1.....	98
4	Manuscript 1 .....	101
4.1	Introduction .....	101
4.2	Materials and Methods .....	106
4.3	Result and Discussion.....	110
4.3.1	Compressive strength .....	110
4.3.2	Flexural strength.....	117

4.3.3	Modulus of Elasticity.....	118
4.3.4	Tensile Strength.....	119
4.3.5	Drying shrinkage .....	120
4.4	Conclusions .....	121
5	Introduction to Manuscript 2.....	124
6	Manuscript 2 .....	126
6.1	Introduction .....	126
6.2	Materials and Methods .....	130
6.3	Result and discussion.....	133
6.3.1	Setting time of fresh mortar.....	133
6.3.2	Compressive strength .....	137
6.3.3	Pull-off bonding strength.....	140
6.4	Conclusions .....	141
7	Introduction to Manuscript 3.....	144
8	Manuscript 3 .....	147
8.1	Introduction .....	147
8.2	Materials and method .....	153
8.3	Result and discussion.....	157
8.3.1	Setting time and workability test .....	157
8.3.2	Compressive strength test.....	160
8.3.3	Pore structure analysis .....	162
8.3.4	Restrained drying shrinkage and expansion. ....	165
8.3.5	Scanning Electron Microscopy (SEM).....	168
8.3.6	Microstructural development.....	169

8.3.7	Characterization of reaction products using – SEM-EDX.....	172
8.4	Conclusion.....	174
9	Discussion.....	176
9.1	Discussion of Manuscript 1 .....	176
9.2	Discussion of Manuscript 2 .....	178
9.3	Discussion of Manuscript 3 .....	181
10	Conclusion.....	185
	References.....	189
	Glossary .....	203
	Appendices.....	208

## List of Figures

Figure 1: Schematic of AAMs Technology .....	101
Figure 2: Compressive strength at 7 days of curing age – Stage 1 .....	110
Figure 3: Compressive strength at 7 days of curing age – Stage 2 .....	110
Figure 4: Compressive strength at 7 days of curing age – Stage 3 .....	111
Figure 5: Compressive strength at 14 and 28 days of curing age .....	114
Figure 6: Compressive strength at 7, 14 and 28 days of curing age .....	115
Figure 7: (a) Cracked pattern failure for mortar sample mix 30 under compressive strength test; (b) Cracked pattern failure for mortar sample mix 26 under compressive strength test. ....	117
Figure 8: Flexural strength at 7, 14 and 28 days of curing age.....	117
Figure 9: Vicat penetration test for setting one-part alkali-activated repair mortar.....	133
Figure 10: Initial time for a one-part alkali-activated repair mortar (Setting Time Vs Water / Binder ratio).....	134
Figure 11: Initial setting time for a one-part alkali-activated repair mortar (Setting Time Vs Alkali activator). ....	135
Figure 12: Pull off mortar samples after 28 days of age (Mix 7).....	141
Figure 13: Setting time and workability test result of one-part AAMs mortar (paste samples). .....	157
Figure 14: Compressive strength result for mixed one-part AAMs repair mortar at 7, 28 and 56 days of curing age. ....	160
Figure 15: Pore structure distribution of hybrid one-part alkali-activated mortars.....	162
Figure 16: Restrained drying shrinkage behaviour (pull-off bond strength result).....	165
Figure 17: Porosity level vs compressive strength of one-part AAMs mortar.....	166
Figure 18: SEM Image of sample G2 (a) Overview and (b) Spherical structure.....	168
Figure 19: SEM Image of sample G3 (a) Overview and (b) Spherical structure.....	168
Figure 20: SEM-EDX of sample G2 (a) Image and (b) Weight (%) .....	172
Figure 21: SEM-EDX of sample G3 (a) Image and (b) Weight (%) .....	172

## List of Tables

Table 1: General Principles for Repair and Protection of Concrete Structures (European Standard 1504 – 9) .....	18
Table 2: Structural and non-structural repair of concrete structures (Table 3, European Standard 1504 – 3) .....	20
Table 3: Chemical compositions (%) and physical properties of Fly Ash (FA), Ground Granulated Blast Furnace Slag (GGBFS) and ordinary Portland cement (OPC) were obtained from the manufacturer. ....	108
Table 4: Mix composition and design of one-part Alkali Activated Materials (AAMs) .....	109
Table 5: Modulus of Elasticity (MOE) at 28-day of age .....	118
Table 6: Splitting tensile strength at 28 days of curing age .....	119
Table 7: Drying Shrinkage Measurement at 28 days of curing age .....	120
Table 8: Chemical compositions (%) of Ordinary Portland Cement (OPC) obtained from the cement manufacturer.....	132
Table 9: Mix design of one-part alkali-activated repair mortars.....	132
Table 10: Initial and final setting time of one-part alkali-activated repair fresh mortar .....	133
Table 11: Compressive strength at 7, 14 and 28 days of curing age.....	137
Table 12: Average pull-off bond strength results in protection and repair products of concrete structures at 28-days of curing age of one-part alkali-activated repair mortar. ....	140
Table 13: Chemical compositions (%) of Fly Ash obtained from XRF analysis.....	156
Table 14: Chemical compositions (%) of Ground Granulated Blast Furnace Slag (GGBFS) obtained from XRF analysis. ....	156
Table 15: Chemical composition (%) of Ordinary Portland Cement (OPC) .....	156
Table 16: Laser-diffraction Analysis (LDA) measured the particle size distribution.....	157
Table 17: Mix design ratio for one-part alkali-activated mortar.....	157

## List of Equations

Equation 1 .....	39
Equation 2 .....	41
Equation 3 .....	59
Equation 4 .....	79
Equation 5 .....	79
Equation 6 .....	81

# 1 Introduction

Alkali Activated Materials (AAMs) introduced in this study, also known as alkali-activated binders, are cementitious binders traditionally produced by a chemical reaction between aluminosilicate precursor and dry alkaline solutions, which are also known as two-part AAMs [1]. The AAMs have been getting popular and regarded as a green technology mainly composed of industrial waste materials and reduce carbon dioxide (CO<sub>2</sub>) emission in the atmosphere. It has 80% less CO<sub>2</sub> emission, low cost, better mechanical strength, and is a sustainable alternative to traditional Portland cement [2]. In comparison, limestone or calcium carbonate burned and decomposed into calcium oxide and released carbon dioxide to the atmosphere during cement production, which is reported to be responsible for 0.5 – 0.6 tonnes of CO<sub>2</sub> for every one tonne of Portland cement [3][4]. Aluminosilicate sources can be found in industrial by-products such as Fly Ash (FA), Ground Granulated Blast Furnace Slag (GGBFS) and Metakaolin (MK). Alkali activator sources consist of Sodium Hydroxide (NaOH) and Sodium Silicate (Na<sub>2</sub>SiO<sub>3</sub>), commonly used solely and/or combined as an alkali activator besides silica fume, which also employed as part of the alternative replacement for sodium silicate activator [5]. The conventional AAMs are prepared by two-part components, aluminosilicate precursor and alkali solution, for the hardening mechanism starts with the creation of cross-linked Si-O-Si, Al-O-Al and Si-O-Al bonds to the hydration gels product of calcium aluminium silicate hydrates, C-A-S-H and/or sodium aluminium silicate hydrates, N-A-S-H via the geopolymerization process [6]. Today, the development of AAMs products is in high demand in the form of concrete, thanks to its availability, low cost, and environmental friendliness behaviour. Many studies are showing that AAMs consists of anti-spalling properties, serve long service life performance and have excellent mechanical strength, which has made them suitable to be used in different forms of purposes such as paste for crack injection, mortar for section restoration and patch repair, therefore has potential to be used for concrete repair and become the new alternative to the existing commercial repair materials (RMs) in the market. On the contrary, few disparities related to AAMs' performance have been identified. Efflorescence and crack-shrinkage induced are the main drawbacks in two-

part AAMs owing to the problem with different pore structures in precursors, mainly due to high alkaline activator dosage.

Additionally, the two-part AAMs concept has setbacks in handling, mixing, and transportation issues besides extensive heat curing requirements to achieve required strength, making this product unsuitable for in situ construction. Researchers introduce the new method of one-part alkali-activated materials in the early 1900s as complementary to the conventional two-part concept. Aluminosilicate precursors are mixed with solid alkali activators to form a dry mixture, and water is added to initiate the geopolymerization process. The 'just add water' method has improved AAMs properties in terms of physical and mechanical properties, more extended durability, and fast application, making them easier to use. The experimental study in this report will be conducted in a laboratory, with controlled temperatures and relative humidity (RH) to stimulate the lab environment with the actual environment specified in the European testing Standard (EN). This study uses three primary aluminosilicate sources: FA, GGBFS and ordinary Portland cement (OPC). Modifying precursor mixtures with the combination of industrial recycled waste products with the OPC is commonly called 'hybrid' one-part AAMs. Including industrial waste materials will discourage dependency on the OPC, responsible for high CO<sub>2</sub> emissions and environmental pollution. On the other perspective, the engagement of OPC will indirectly compensate for the shortage of supply chain of raw materials of FA and GGBFS sources in the market of certain countries, vital to stabilize the market value for commercial materials (precursor) and avoid unnecessary monopoly and the speculated price at supply and demand stage. This research will focus on newly modified one-part AAMs (hybrid) characteristics, percentage relation in precursors mixture, alkaline activator ratio, additive proportions, design ratio, physical and mechanical properties, and durability under lab - controlled environments.

Moreover, their workability will determine the performance of the one-part AAMs in the fresh state, the mechanical strength in the hardened state and durability in the service state to comply with British and European Standard, BS EN 1504-3 for structural concrete repair materials - class R3 classification. Finally, these modified one-part AAMs technology or hybrid one-part AAMs,

will ensure the durable service life of concrete that will help to overcome the higher porosity and bonding shortcomings, promote low-cost repair material made from re-useable waste products, and finally, encourage the production of environmentally friendly materials in the construction sector. Reinforced concrete (RC) starts to deteriorate due to its ageing process. Apart from that, many reasons contribute to the deterioration of concrete structures. One of them is concrete spalling. Concrete spalling or delamination happens when areas of concrete cracked and are delaminated from the substrates. It can happen because of many factors, including freeze-thaw cycling, alkali-silica reaction, and fire heat, but the most common reason is the corrosion of embedded steel in concrete. Corrosion-induced deterioration affects RC structures' performance, serviceability, and safety when placed in higher CO<sub>2</sub> concentrations. Concrete deterioration often happens in ageing concrete structures. Many causes lead to deterioration in ageing concrete structures, but the most common factors are carbonation and chloride-induced reinforcement corrosion [7]. Carbonation is a process that initiates corrosion of embedded steel whereby the reinforcement rebar in concrete expands and creates an internal force on the surrounding concrete. Carbonation also occurred due to the chemical evolution of cementitious materials induced by the reactive diffusion of CO<sub>2</sub> in the porous media. Indeed, atmospheric CO<sub>2</sub> reacts with cement hydrates, dissolves portlandite and forms calcite. The main consequence of this chemical reaction is a significant decrease in pH in the porous solution that induces corrosion of the reinforcing steel. The kinetics of this degradation depends on temperature, atmospheric CO<sub>2</sub> pressure and relative humidity (RH), all parameters related to time and climate change [8].

Nevertheless, carbonation and chloride-induced corrosion penetrate cementitious materials via open pores propagated by cracks or from existing pore structures. Therefore, it is essential to control and improve the pore structures of hardened materials to prevent further intrusions that affect their structures and performances. The durability of the concrete patching repair is determined by its engineering properties, both physical and mechanical. Thus, choosing the suitable patch repair products available in the market is crucial. To evaluate the suitability of repair materials, it is essential to assess their overall properties, the interaction of these properties and their behaviour in actual service conditions before use. For instance, several techniques exist

to repair spalled concrete structures in buildings. Repairing spalled concrete using the patching repair method is quick and economical. Hand-applied patch mortar is the standard patching method if the spalled depth is between 25mm to 70mm and does not require replacing steel bars. The hand patching method can be applied for structural and non-structural concrete repair using cementitious products per EN 1504-3, European Standard for concrete repair materials.

Nonetheless, there are many concrete repair materials in the market. Each manufacturer claims their products comply with engineering standards and has proven their success with a list of past projects. The manufacturer might test and pass their products at specific quality control standards, but not all products are suitable for application under different service conditions. Tropical climate countries experience wet and dry seasons throughout the year. Tropical rainforest climate, a sub-type of tropical climate, has no dry seasons, and the seasonal rainfall is known to be heavy. Contrarily, temperate climates may record less rainfall but experience sudden temperature and seasonal change, prompting chemical attacks and freeze-thaw problems. The main difficulties are in selecting the correct physical and mechanical properties of concrete repair materials to be applied based on different climate environments. The pore system in hardened concrete, relative humidity level, hot temperature, and the rise of CO<sub>2</sub> in the atmosphere are the main factors affecting concrete carbonation that cause the concrete to spall. The impact of climate change today will further affect the long-term performance of the concrete rehabilitation process overall. The previous studies reported that one-part AAMs advantages include their ability to develop fast and good strength, higher resistance against severe climates, and outstanding concrete abrasion erosion resistance performance [9], which have made them suitable to be used in different forms such as paste for crack injection, mortar for section restoration and patch repair. However, further work is required to establish one-part AAMs as an innovative-ecological mortar mix for sustainable concrete repair materials to compete with existing RM in the market and explore its potential and strength in concrete technology for engineering purposes.

Numerous companies have played essential roles in producing concrete repair materials since the introduction of EN1504. Large engineering manufacturing firms such as Sika AG and BASF SE were among the pioneer conducting research and upgrading their products for quality

enhancement. They also encourage the production of environmentally friendly materials into the market as part of a carbon dioxide-controlled programme and energy reduction. Nevertheless, most of the concrete repair materials in the market are still dominated by Portland cement-based materials since they have been used for a long time and are already established in a worldwide market with massive supply-chain business operations. It is worth noting that every structure requires concrete, and every concrete is mainly composed of Portland cement. Even steel or timber structures are still required concrete for their foundation structures.

The clinker used to produce the Portland cement required excessive energy to burn, thus responsible for higher carbon dioxide released into the air and affecting the environment. Researchers started to study other alternative raw materials to replace Portland cement. They researched synthesizing plenty of waste products from industrial to agricultural waste materials to ensure this work reduces the tons of unused waste materials and can be reused and recycled, benefiting humans and saving the earth. However, issues with the shortage of waste products in certain countries make the supply cost higher. Also, some of the industrial product availability become lesser such as fly ash created from the ash of burning coal; some countries have stopped their coal production due to environmental impact, whereas other countries will follow whether to abolish it or scale down the coal burning activities permanently. Efforts have been made to diversify the source of raw materials, not only to depend on existing commercialized waste products but also to look for a new source and potential raw materials. Nevertheless, these measures have one aim in common; to reduce the dependency on Portland cement. Today, the usage of Portland cement is not only in the form of concrete but also widely used in another form of mortar and paste, whether for the construction of new structures or cementitious repair materials.

The European Standard EN 1504 for concrete products and systems took almost 15 years to design and bound by the experts in concrete repair technology since this topic was alarming over the past 40 – 50 years when the existing reinforced concrete structures, which were first built in the 1900s has achieved or exceeded their lifespan. Unlike modern buildings built with efficient protection

and durable materials that last longer with less maintenance, older buildings require extra repair and rehabilitation to safeguard their aesthetic features and historical background. The asset owner tends to keep the building functioning rather than demolish it for economic purposes besides avoiding complicated construction jobs, especially if new infrastructures surround the existing structures. Engineers, architects, and scientists began to examine concrete repair materials technology that can preserve concrete structures, maintaining their original shape and strengthening their load-bearing capacity. Today, most of these concrete structures have achieved their mid-life span and thus acquire attention. Still, due to limited options for concrete repair materials, some concrete structures experience severe levels of concrete deterioration because of chemical attacks that penetrate the concrete surfaces, corrode the embedded rebar, and are responsible for cracked and spalled concrete. In addition, an unsatisfactory understanding of the causes of concrete defect, subsequently leading to incorrect selection of repair materials, make the concrete problem worse, wasting time and effort for unnecessary repeated repair jobs besides incurring higher cost due to improper maintenance programme. Often complaints and unhappiness among concrete building owners and asset management operators on the performance of repair materials, especially for concrete surface patching repair applications, as early as within 1-2 years after the repair is completed [10].

Today, for newly constructed modern concrete structures like buildings - many types of concrete repair materials have been introduced in the market and give the professionals plenty of choices to have the best solutions from the engineering application point of view, low environmental impact and more economical. On the other hand, various options mean disadvantages too, where every manufacturer will claim their product is the best without addressing the importance of selecting the appropriate and relevant type of repair materials based on the intended applications, structural and non-structural, and surrounding environments in terms of chemical exposure, weather, moistures, and humidity. Not all types of concrete repair materials have the same quality. They may be differentiated externally, like branding, price, or type of applications, but their engineering performance might also differ. Therefore, an initiative has been taken to standardize the specifications for concrete repair materials where EN 1504 were introduced and came into

effect on 1st January 2009. This specification has emphasized the minimum performance requirements and standardized the testing method regarding apparatus, load, technique, duration, strength, and essential parameters, such as temperatures and humidity. EN 1504 has a group of 11 principles for consistent standards of practice. Also, it consists of 10 parts to provide key stages of assessment, identification and deciding the final approach of protecting, repairing and rehabilitating concrete [10].

EN 1504 Part 3 – *Structural and Non-Structural Repair of Concrete Structures* is one of 10 parts addressed in the EN 1504 document, which classifies four types of repair mortar classifications: R1 and R2 for non-structural repairs, R3 and R4 for structural repairs of concrete structures. Class R4 is the highest strength or high E-modulus mortar, while Class R1 is the lowest strength mortar. Nevertheless, all types of repair mortar comply with specific strength requirements and do not imply incompatibility or excellent performance. Still, it is rather than to indicate the most suitable repair mortar class to be employed according to the case-by-case situation and applications.

For instance, concrete used to transfer heavy loads must be repaired with high-strength products; in this case, it is a Class R4 mortar. This type of concrete is occasionally constructed as the main structural element, such as columns, beams, slabs, and footings for load-bearing structures like multi-storey buildings, bridges, etc. Lower concrete and transfer medium load strength should be repaired with the Class R3 mortar. For this purpose, the concrete still carries the load but with a lower capacity or less exposure to frequently applied loads such as walkaways, staircases, walls, or even for single-storey structures like ancillary buildings and storage units. Nonetheless, concrete that does not carry the load can be repaired with a higher strength of mortar Class R2 even though Class R1 can still be utilized. Generally, various types of mortar and concrete applications are covered under EN 1504, part 9, to restore and replace delaminated concrete surfaces. The field of applications is stated below:

Table 1: General Principles for Repair and Protection of Concrete Structures (European Standard 1504 – 9)

Principle no.	Principle Definition	Repair method	Reference method no.	Type of application
Principle 3	Restoring the original concrete of a structure element to the initially specified shape and function. Restoring the concrete structure by replacing part of it.	Concrete restoration	Method 3.1 Method 3.2 Method 3.3	Applying mortar by hand Recasting with concrete Spraying mortar or concrete
Principle 4	Increasing or restoring the structural load-bearing capacity of an element of the concrete structure	Structural strengthening	Method 4.4	Adding mortar or concrete
Principle 7	Creating chemical conditions in which the reinforcement's surface is maintained or returned to a passive condition.	Preserving or restoring passivity	Method 7.1 Method 7.2	Increasing cover to reinforcement passivity with mortar or concrete. Replacing contaminated concrete

EN 1504 specification (see Table 1) emphasizes the performance characteristic is defined with two engineering performance concepts *for all intended uses* and *certain intended uses*. This minimum technical performance parameter must be met for every application and specific intended uses for the repair system designed to resist harsh environments. Thus, this study aims to comply with **Method 3.1- applying mortar by hand – Class R3 for all intended uses** concept under concrete restoration type of repair - Principle 3. To elaborate further, there are five main performance characteristics for both structural and non – structural repair products (see Table 2) *for all intended uses*, classified as follows:

Table 2: Structural and non-structural repair of concrete structures (Table 3, European Standard 1504 – 3)

Performance Characteristic	Test Method	Minimum Requirement (Table 3 in EN 1504, Part 3)			
		Structural		Non-Structural	
		Class R4	Class R3	Class R2	Class R1
Compressive Strength	EN 12190	45 MPa	25 MPa	15 MPa	10 MPa
Chloride Ion Content	EN 1015-17	0.05%	-	0.05%	
Adhesive Bond	EN 1542	2 MPa	1.5 MPa	0.8 MPa	
Restrained Shrinkage	EN 12617-4	2 MPa	1.5 MPa	0.8 MPa	-
Durability Carbonation	EN 13295	dk > control concrete		No requirement	
Durability – thermal compatibility, freeze/thaw, thunder/shower, dry cycling Elastic Modulus Skid Resistance Coefficient of thermal expansions Capillary absorption (Water Permeability)		Only for specific intended uses.			

To develop one-part AAMs technology from a two-part system counterpart, the engineering parameter of the product will be changed significantly. Fresh properties, mechanical strength, and durability of one-part AAMs will be affected. In comparison, the two-part system has a quick setting time because the solution type of activator expedites the dissolution process of precursors particle for hydration products. A one-part system takes more time to set due to the more prolonged dissolution of the solid activator. The mechanical strength of the two-part system is also 30% higher than one-part due to the rapid dissolution of the fully dissolved activator, increasing the hydration rates for binding phases.

Furthermore, the one-part system recorded slow strength development between 7 – 90 days of age compared to the conventional two-part system. On the contrary, the two-part system has drawbacks in long-term performances where it has recorded higher porosity and water absorption level, and it possesses efflorescent problems besides visible autogenous and drying shrinkage [11]. Therefore, to introduce one-part AAMs as new concrete repair materials, attention must be given to compensate for all the shortages so that its engineering properties can be comparable to

or better than the two-part system. It is worth mentioning that the development of one-part AAMs has been carried out intensively but mainly limited to finding aluminosilicate precursors or still at the calcination and characterization stage. The use of one-part AAMs in the form of paste, mortar and concrete is still behind, and to the author's knowledge, one-part AAMs as concrete repair mortar has never been discussed. Therefore, this study is an initiative to introduce sustainable construction material into the market, diversify the application of AAMs technology in the field of one-part AAMs and, most significant effort to reduce air pollution due to high amounts of CO<sub>2</sub> released into the air from the production of OPC and control the environmental impact because of the increasing volume of unused industrial waste.

### **1.1 Objectives of study**

Few disparities have been identified related to the long-term performance of one-part AAMs. Higher porosity levels are the main drawbacks in one-part AAMs due to the problem with different pore structures in precursors, alkaline activator ratio and water content. As a result, the engineering application for one-part AAMs as concrete patching repair materials may not be efficient or become unpopular choices among industrial players, limiting this cement technology from broader adoption. Higher porosity levels will leave open pores to chloride or CO<sub>2</sub> intrusion, corroding the embedded rebar, affecting the cement-rebar bonding, and promoting crack and delamination. In other words, capillary stress has influenced water absorption in one-part AAMs, which subsequently affects the fluidity level of mortar at the fresh state, compressive and bonding strength at the hardened state, and shrinkage crack at the service state.

Nevertheless, mortar-based one-part AAMs potential has yet to discover compared to the concrete-based one-part AAMs applications and traditional two-part AAMs counterpart. Not all precursor materials can bond when applied vertically and horizontally; thus, selecting the main composition of precursor mixtures is crucial. The selection of the type of alkali activator and its concentration is essential in providing significant elasto-mechanical properties and durability performances of one-part AAMs where the higher the alkali content, the higher its mechanical strength and stronger physical structure are. An excessive alkali dosage, on the other way, will

harm the cementitious products due to many factors like loss of water, porosity, and shrinkage. A lower dosage of alkali activator can be employed to control the dissolution rates for the polymerization process and prevent early water loss at an early stage, control shrinkage crack, and reduce pore volume structures. As a result, a low alkaline environment will affect the strength development due to insufficient hydration gel products, thus disturbing the mortar's physical and mechanical properties. Though, including some chemicals could improve the performance of one-part AAMs mortar, reducing capillary tensile stress and water uptake, thus improving the microstructure by changing the pores structure of the repair material for better mechanical strength.

The conventional preparation of one-part AAMs will be modified by adding solid chemical additives based on the understanding that the expansion, reducer, and retarding behaviour of admixtures will complement the gap left in the current one-part AAMs technology, mainly for concrete repair application. Furthermore, including OPC as part of precursor sources will supply additional calcium to ensure the new creation of hydration gels of C-A-S-H, which is more stable than N-A-S-H gels under an alkaline environment[12]. In this study, one-part AAMs will be modified to provide practical application and improve the gap left by current research for its overall performance as concrete repair materials. A few possible admixtures will be added to the dry mix of solid aluminosilicate and alkaline sources. This research will focus on the characteristics of newly modified one-part AAMs (hybrid with OPC) by introducing a novel mix design formulation to determine the composition of aluminosilicate precursor and alkali activator, its additive proportions ratio, physical and mechanical properties, microstructure analysis and durability. Finally, the one-part AAMs, also known as hybrid one-part AAMs in this study, will ensure significant engineering properties of repair materials, improve the durability service life of concrete, offer low-cost raw materials, and provide efficient concrete maintenance programs. To summarize, three objectives have been identified to overcome the discrepancies above. The selection of objectives is carefully underline by applying (SMART) concept of setting the specific, measurable, achievable, relevant, and time-bound. The objectives are as follows:

- I. Establish a new mix design formulation for one-part AAMs repair mortar based on mechanical strength performance.
- II. To evaluate the mortar's compressive and pull-off bonding strength for concrete repair applications.
- III. To reduce the porosity level of one-part AAMs mortar used as structural concrete repair materials.

## **1.2 Aim of the study**

This research investigates the performance of one-part AAMs as an alternative concrete repair material to comply with European Standard, Class R3 – EN1504 specifications for structural concrete repair materials, so that the new cementitious product will meet international engineering standards and can be commercialized.

## **1.3 Rationale and Significance of the Study**

The significance of this research is included in the following:

1. Develop an innovative cementitious concrete repair material as an alternative to the existing OPC and RMs in the construction sector based on green technology.
2. Minimize environmental impact using eco-friendly waste materials, reducing clinker production for Portland cement application.
3. Enhance the service life of concrete structures by controlling the pore structure of the repair mortar to prevent early shrinkage cracking due to higher porosity levels.

## **1.4 Scope and limitation of the study**

A study on one-part AAMs as concrete repair materials is conducted based on lab experiments. Preparation of mortar samples will be carried out under controlled temperature and relative humidity as stated in EN-1504 specifications, while some experiments could involve a standard ambient curing method. The study was also limited to the form of hardened mortar samples by focusing on physical properties to understand their mechanical and pore structure behaviour. This

study will not investigate the raw materials characteristic at synthesis stages from a chemistry perspective but merely focus on its engineering application purposes that stimulate actual application at the site. Therefore, the experiment will not require a calcination process or excessive curing temperatures. Sources of supplies will utilize standard commercial materials available in the market rather than purely unprocessed raw materials or chemicals. Formulation from different percentages of precursor mixtures and different levels of alkali activator ratio will be tested with the inclusion of selected powdered chemical admixtures.

The one-part Alkali Activated Materials (AAMs) in this study will consist of three solid aluminosilicate precursors; Class F – Fly Ash (FA), Ground Granulated Blast Furnace Slag (GGBFS) and Ordinary Portland Cement (OPC). A low corrosive of Potassium Carbonate is used as an alkali activator to activate the precursors. The one-part AAMs mortar samples will be further analysed by adding expansion agents of powder Calcium Oxide - quicklime, CaO and powder Shrinkage-reducing Admixture (SRA) – reducer agent, based on the understanding that the additional expansions and reducer admixtures can control shrinkage level, where it will increase the volume of mortar during hydration instead of shrinking like typical cementitious materials. A fine natural aggregate used as part of mortar compositions and Sodium Lignosulfonate based superplasticizer (SP) as a retarder agent to control mortar from loss of water at an early stage in addition to low water content ratio used from standard tap water sources.

The proposed materials to be used in this experiment are listed below:

A) Materials

Aluminosilicate Precursor:

- I. Class – F Fly Ash (FA)
- II. Ground Granulated Blast Furnace Slag (GGBFS)
- III. Ordinary Portland Cement (OPC)

Alkali activator:

- I. Potassium Carbonate ( $K_2CO_3$ )

Expansion agent:

- I. Quicklime, CaO

Chemical admixture:

- I. Shrinkage-reducing admixture (SRA) - 90% Magnesium Oxide
- II. Sodium Lignosulfonate (LS) based - Superplasticizer (SP)

Aggregates:

- I. Fine natural aggregate from river  
(15% 1.18mm, 45% 600 microns, 25% 300 microns, 15% 250/150 micron)

Water:

- I. Fresh tap water

## B) Type of experiment

All mortar samples will be tested in the laboratory with controlled room temperature (18 – 22°C) and relative humidity, RH 90%, to comply with controlled temperature per EN1504–3:2005 standard, part 3: structural and non-structural concrete repair materials. Samples will be dismantled from the mould after 24 hours and cured under room temperature for 7 (early stage) and 28 days of age (later stage). All tests will be according to the American Standard Testing Method (ASTM), European Standards (EN) and British Standards (BS), respectively. However, a testing method might be adopted from previous researchers; some might not be listed in other established standards. In general, lab experiments for this study are based on the physical structure examination of hardened mortar and its microstructure analysis.

Lab Experiment type 1 – Physical structures:

- I. Workability test at the fresh state of a sample
  - Flow test (BS EN 13395-1-2002)
  - Setting time: The initial and final setting (Vicat setting time – BS EN196-3:2016)
- II. Mechanical strength test at the hardened state of a sample
  - Compressive strength (EN12190)
  - Modulus of Elasticity (BS 1881)

- Flexural strength the three-point flexural strength (BS EN 13892-2:2002)
- Bonding strength by a pull-off test (BS EN 1542:1999)
- Restrained drying shrinkage and expansion (Pull-Off Bonding Strength EN 12617-4)
- Tensile strength by splitting tensile test (ASTM C496)

III. Durability at the service state.

- Drying shrinkage (BS 1920-8:2009)

Lab Experiment type 2 – Microstructure Analysis:

The microstructure analysis will be carried out to characterize the samples by analysing the Scanning Electron Microscopy (SEM) image incorporated with the Energy Dispersive X-ray spectrometer (EDS). SEM and EDS will analyse the mixes' micromorphological features and elemental compositions as hydrated particles. Besides that, Mercury Intrusion Porosimetry (MIP) test will determine the porosity level of mortar, including its pore structure properties. Microstructure analysis samples will be taken from crushed hardened mortar samples at 28 days of age.

- I. Scanning Electron Microscopy (SEM)
  - Scanned the fractured mortar surfaces at 28 days
- II. Energy Dispersive X-ray spectrometer (EDS)
  - Observed the elemental composition in the samples
- III. Mercury Intrusion Porosimetry (MIP)
  - Analysing pore structural characterization

## 1.5 Thesis Outline

1. Thesis Abstract: The summary of the thesis focuses on crucial points such as current issues and background of the study, problems, the objective for writing, methodology, results, and implications of the research in AAMs technology – a one-part system for structural concrete repair applications.

2. Introduction: The background study of the research started with the introduction of current technology, trend, and shortage issues. Thus, the overall proposals of the study are presented comprised of the study's objective, aim, significance, and limitation and how the thesis is formatted and presented in the report. This section highlights three significant issues: the environmental issues associated with a negative impact on Portland cement production, issues on concrete repair works and the application of industrial by-products as concrete repair materials using AAMs technology.
3. Literature Review: Detailed engineering properties of raw materials and performance of one-part AAMs based on previously published works that include scholarly articles, books, reports, websites etc. The description of four main elements in AAMs are presented in this section; 1- Mix compositions: aluminosilicate precursors, alkali activators, admixtures, and design mix ratio; 2- Fresh and hardened state performances: curing conditions, rheology, and mechanical strength 3- Durability: shrinkage and porosity and 4- Microstructural study.
4. Summary of Manuscript 1: The short brief on research work for Manuscript 1. It summarizes the study's objective, the framework for selection criteria of raw materials and the stage of experimental study, a discussion of the result and recommendations for the subsequent study.
5. Manuscript 1: A detailed research report published, reformatted, and presented in the thesis report. The study aims to find the optimum composition of raw materials based on compressive strength results and study the reaction between precursors-activator-admixtures-aggregate/water content. Other mechanical performances were then evaluated for concrete structural repair application as per Class R3 – EN1504-3 specifications.
6. Summary of Manuscript 2: The short brief on research work for Manuscript 2. It summarizes the study's objective, further study on the mix design composition and suggestions for the next step in formulating the mix design composition, one part of AAMs mortar based on the experimental outcome.

7. Manuscript 2: A detailed research report published, reformatted, and presented in the thesis report. The composition of alkali activator, admixtures and water content are modified to understand the rheology behaviour of the mortar at fresh state, compressive strength, and pull-off bond strength at hardened state purposely for patch mortar application as per Class R3 – EN1504-3 specifications. The temperature and relative humidity (RH) also changed to evaluate the durability of the repair mortar under different exposed environments.
8. Summary of Manuscript 3: The short brief on research work for Manuscript 3. It summarizes the study's objective, limitations and shortage found in previous manuscripts and gives an overview of durability performance and microstructural study.
9. Manuscript 3: A detailed research report published, reformatted, and presented in the thesis report. The influence of water in activating dry cementitious binder is discussed from the perspective of rheology and mechanical performances, pore structure analysis and microstructural development. The formulation of repair mortar is finalized, and the class of repair materials specifications is concluded based on overall performance.
10. Discussion / Conclusion / Implication: The outcome summary from all manuscripts, research achievement and future recommendation works.

## **2 Literature Review**

### **2.1 Alkali activated Materials (AAMs) – One-part systems.**

Fly ash (FA), ground granulated blast furnace slag (GGBFS), and silica fume (SF) are the three main types of Supplementary Cementitious Materials (SCM), which are currently developed to replace the usage of ordinary Portland cement in the construction industry, therefore promoting environmentally products, improve cleaner production in terms of CO<sub>2</sub> emissions, air pollutants and solid wastes from mining and manufacturing of materials [13]. It was reported that approximately 4.2 billion tons of cement are produced annually, responsible for about 4 billion tons of CO<sub>2</sub> emission [14]. Nevertheless, the properties of AAMs are much influenced by the content and type of precursors and activators. According to Teo et al.[15], for precursors, the silicon dioxide/ Aluminium oxide (SiO<sub>2</sub>/Al<sub>2</sub>O<sub>3</sub>) molar ratio and calcium content of CaO play essential roles in determining the alkali activation process and hardened properties of AAMs. As for alkaline activators, the sodium oxide/silicon dioxide (Na<sub>2</sub>O/SiO<sub>2</sub>) ratio factor should be one of the criteria to establish the high performance of one-part AAMs applications. The reaction between aluminosilicate precursor with alkali activator will create a chemical bond environment of hydration products which, when water is added, will produce alkali aluminosilicate hydrates that act as a binder upon the hydration of the hydraulic types of cement as reported by Almalkawi et al.[16] on how the one-part AAMs cement functions. Researchers compared the influence of single and mixed precursors to improve the cementitious binder quality. In addition, a study combining aluminosilicate with OPC was also conducted since AAMs reported no stable geopolymer block or incomplete final products without a 3D geopolymer network. OPC has formed a crystalline phase of C-S-H that can strengthen the gel network of N-A-S-H [17]. The usage of OPC was tested in the form of new OPC cement or the form of recycled OPC concrete.

### **2.2 Aluminosilicate precursors**

#### **2.2.1 Fly Ash (FA)**

Fly ash is a by-product of thermal power captured at the top of the boiler, and class-F fly ash is the most used pozzolan in concrete. FA is an amorphous alumina and/or silica-rich material

composed of microsphere particles, making them blend easier in the mixtures [18]. FA is an industrial by-product of coal used for electricity generation in coal power plants. The shape of FA particles is spherical, contains up to 90% amorphous (remaining crystalline phases), and has a mineral composition of mullite, magnetite, quartz, hematite, and unburned carbon. The fineness of FA depends on coal burning conditions' temperature between 800 °C – 1600 °C. Typically, coal combustion at 1500 °C will produce the most suitable FA characteristic for the geopolymerization process; hollow particles, amorphous in nature and spherical shape, whose particle size is typically between 5 µm to 300 µm, help to increase the reactivity. There are two types of FA based on CaO content according to ASTM C618 standard. Class F-FA is a preferred source of precursor due to high SiO<sub>2</sub> (> 50%) and Al<sub>2</sub>O<sub>3</sub> (>2 0%) content, lower CaO (< 10%) and stable materials. Calcium contributes to the disordered nature of glassy phases in FA and also helps to increase the reactivity of the materials [19]. Conversely, Class C-FA has lower aluminium content, higher CaO (>10%) and Magnesium oxide (MgO) levels. However, a mineral containing Magnesium (Mg) generally does not participate in the geopolymerization stage, while the excessive calcium level may change the microstructure properties, thus affecting polymerization. Slow setting time and low early compressive strength are two main drawbacks of FA due to the low capacity of calcium content [17].

Xu et al.[13] explained and summarized the creation of industrial waste of FA during and after combustion, where the unreacted mineral particles within the coal undergo the process of liquifying, vaporizing and then condensing. The spherical and amorphous FA particles are formed because of surface tension force during the rapid cooling process in the combustion zone. The morphology of FA is dependent on the residual composition. In addition to heating and cooling conditions, some residuals may become glassy particles or crystallized product structures. Nevertheless, at high temperatures, the trapped volatile matter will expand inside and form a hollow cenosphere. FA particles, however, are primarily spherical in both solid spheres and cenosphere. Still, some irregularly shaped minerals and unburned carbon also can be observed and detected due to their larger size in the particle size distributions (above 200 µm). This report also suggests that low calcium fly ash was widely used for the geopolymerization process and

demonstrated outstanding performance than high calcium counterparts due to delayed ettringite formation of high calcium ash content. Besides, the high content of free CaO caused cement instability. FA has been used as an aluminosilicate precursor in AAMs technology for two- and one-part systems. FA is an aluminosilicate precursor made from coal, consisting of aluminate, amorphous silicate, mullite, hematite, and quartz [20]. FA class-C and FA class-F are commonly used in alkali-activated cementitious materials, as mentioned in ASTM C618-12a (2012). Also, other reports suggest that FA class-F, which has pozzolanic properties, is consisted of 70% of a high content of silicon dioxide ( $\text{SiO}_2$ ) + Aluminium oxide ( $\text{Al}_2\text{O}_3$ ) + ferric oxide ( $\text{Fe}_2\text{O}_3$ ) but has a low content of CaO, while FA class-C has a lower range of  $\text{SiO}_2 + \text{Al}_2\text{O}_3 + \text{Fe}_2\text{O}_3$  but has more CaO content [21]. An experimental study on FA reaction with alkali sources showed that the interface zone between the repair and substrate was denser and more homogenous and possessed better bonding compared to conventional commercial mortar repairs [2][22]. The study was conducted in a two-part system where 10 M sodium hydroxide solution (NaOH) and silicate solution (NS) used as alkali activators with regular alkaline to binder ratio of 0.60 hydroxide/silicate solution (NaOH/NS) ratio of 2.0 and then was mixed with FA and Portland cement as calcium additives that consisted 60.96% of chemical compositions of  $\text{SiO}_2 + \text{Al}_2\text{O}_3 + \text{Fe}_2\text{O}_3$  and 25.79% of CaO, has gained 32 – 38 MPa for the 28-day compressive strength test. The 28-day compressive strength of FA plus calcium hydroxide (CH) as an additive is 34 – 39 MPa, and FA without additives has shown low reactivity and only managed 25 MPa of strength. The alkali-activated FA mortar took a longer setting time (without the presence of slag), slowing the chemical reaction in the mixture, which resulted in slow strength development. However, alkali-activated FA-only mortar has the highest compressive strength after 56 days of curing compared to Ground Granulated Blast Furnace Slag/ Metakaolin (GGBFS/MK) alkali-activated mortar. Another study of alkali activator Fly Ash/ Ground Granulated Blast Furnace Slag (FA/GGBFS) exhibited excellent mechanical properties both of compressive and flexural strengths measured at 28 days, proving that the inclusion of GGBFS composition could improve both mechanical strengths [2][23][24][25].

Different type of FA, however, will have their particle distribution and composition, respectively. Three types of FA under the F-class, according to ASTM C618, have been studied. FA classified under Class I and II according to GB 1596-2017 were used, and another sample was super-fine fly ash (SFA) presents significant differences in characteristics. To achieve the required workability, the fluidity of fresh mortar must be first determined. The primary flow value of alkali-activated FA fresh mortar depends much on the fineness of its particle, where past studies proved the particle size range between 3 – 40  $\mu\text{m}$  would result from high fluidity. However, the higher content of FA alone could reduce the workability of the mortar because of its highly porous structure, which demands a high amount of water adsorption. The FA mortar's shrinkage was much higher than alkali-activated GGBFS and MK-based mortar due to a high amount of water in the FA-only mixture. Lower workability will increase permeability due to high porosity in the microstructure, subsequently affecting AAMs' durability [23]. The mixed composition of FA with slag has changed the reaction rate and affected the mortar's flow rate if it reacts with a higher alkali activator modulus. In addition, the higher percentage of GGBFS to FA has decreased the porosity level of AAMs and created denser C-A-S-H gel for better strength development.

However, the higher specific surface area of FA does not necessarily improve the mechanical strength of the mortar. This study showed not only the effect of the fineness level of FA but also the content of amorphous in FA and the molar ratio of  $\text{Na}_2\text{O}/\text{SiO}_2$  alkali activator were among factors involved to achieve better mechanical strength, provided that the mortar has good workability in the beginning. Alkali-activated FA-class II/GGBFS mortars have better compressive, flexural and bonding strength than alkali-activated FA-Class I/GGBFS and SFA/GGBFS mortars due to the high content of amorphous phases [2][26]. The typical alkali activator molar ratio for FA class-F was reported in the range ratio of silicon/aluminium ( $\text{Si}/\text{Al}$ ) = 1.5, sodium/aluminium ( $\text{Na}/\text{Al}$ ) = 0.48,  $\text{Si}/\text{Al}$  = 2.8 for NaOH activator, and  $\text{Na}/\text{Al}$ =0.46 for NaOH/NS activator [21]. Both activators were in the liquid form for AAMs in two-part systems. Alkali-activated FA mortar gives lower strength due to its low calcium. FA mortar's low reactivity happened because FA dissolution in the mixture was not completed before it hardened [23].

An additional additive, such as CaO, will increase calcium content in alkali-activated FA binders and enhance their mechanical properties. Many additives have been tested in alkali-activated FA binders as sources of high calcium content. Calcium carbide residue (CCR) is calcium-rich waste material used as an additive composed of Calcium hydroxide ( $\text{Ca(OH)}_2$ ). It will react with  $\text{SiO}_2$  and  $\text{Al}_2\text{O}_3$  from FA, where a study reported that the CCR level controlled the setting time of mortar. The reaction between CaO in CCR with a mild alkali solution activator generates heat in the polymerization process, which shortens the setting time. Additional C-S-H and C-A-S-H at the interface surface obtained from the CCR could increase the compressive and bonding strength of the alkali-activated FA mortar [27]. The ratio of 80% FA & 20% CCR and NS/NaOH=2.0 was the optimum composition for maximum compressive strength in 28 days, whereby excessive lime would affect the gel binder structures. The formation of C-S-H and/or C-A-S-H gel together with the existing gel of N-A-S-H from FA mixed with about 20% of CCR contain, improved bonding strength at the concrete substrate, exhibited higher bond strength compared to commercial polymer modified repair mortar and complied with the minimum bonding strength requirement according to ASTM C881/C881M-14 [24][26].

Both compressive and flexural strengths of alkali-activated FA can be further improved with the inclusion of GGBFS, where a study showed that high composition of CaO in slag materials could generate a higher CaO to  $\text{SiO}_2$  ratio, with the replacement of FA with 30 – 70% of GGBFS amount. Alkali-activated FA/GGBFS pastes were also tested, and maximum strength was recorded when up to 70% of GGBFS content was used in the mixture [26]. Another study on AAMs as concrete repair material showed that when alkali-activated FA concrete placing on top of Portland ordinary concrete surface as a patching application, it enhanced the reaction between calcium from the  $\text{Ca(OH)}_2$  with Si and Al from FA, subsequently improved the bond strength between the repair materials and concrete substrate [27]. GGBFS has a higher level of calcium-rich aluminosilicates that react well with low calcium of class-F FA, enhancing the system's reactivity, increasing CaO content for better compressive strength and reducing the need for heat curing. The excessive CaO, however, caused rapid hardening to affect the applicability of this cementitious technology. GGBFS has replaced the amount of FA between 0%, 10%, 15% and

20% by total precursors weight in one-part AAMs tested by Oderji et al.[28] and found that higher slag content will improve compressive and flexural strength but decrease the workability in the fresh state. In that report, 15% replacement with GGBFS is the optimum volume for AAMs binder activated with sodium silicate anhydrous ( $\text{Na}_2\text{SiO}_3$ ) for adequate workability (24 cm flow diameter within 15 minutes) and mechanical strength (up to 30 MPa). The compressive strength of one-part AAMs paste composed with the combination of class-F FA (70%) and calcined commercial kaolin (30%) only recorded 12 MPa at 28 days of age compared to FA/calcined ceramic waste at the same proportion and age of samples which has recorded about 25 MPa. This result explained the natural behaviour of calcined clay likely to absorb more water molecules when water is added to activate the geopolymer process of the binder. More water is required to control the kaolin mixtures' workability, which affects the quantity of water left for the system to transport all dissolved particles produced in alkaline environments to form the N-A-S-H gels, the main reaction product for the mechanical strength of AAMs. Furthermore, insufficient water creates undissolved particles containing large amounts of Sodium oxide ( $\text{Na}_2\text{O}$ ) embedded in the formed N-A-S-H gels. Later, the reaction with the N-A-S-H chains subsequently created defective regions in the material and decreased the compressive strength over time under all curing regimes, as discussed by [29]. 100% FA paste recorded low compressive strength of 10 MPa at 28 days of age. Still, when the volume of FA was replaced with 50% GGBFS at a specific activator dosage, the compressive strength increased to 24 MPa, indicating a combination of two or more precursors could fill the gap on each chemical composition to provide a better reaction of C-A-S-H gels due to high calcium content of FA/slag. The Si and Al concentrations were reduced during the creation of C-A-S-H gels, and the leftover alkali cations were used for the geopolymerization process. Nevertheless, insufficient Si and Al remain to promote the formation of highly polymerized structures after the consumption of calcium [30]. Unlike class-F FA, 100% class-C FA (high calcium) failed to harden even though activated with a higher dosage of alkali activator (12%) to demonstrate high calcium of FA has low reactivity and was unable to leach the Ca to the matrix to form N-A-S-H, C-(N)-A-S-H and C-A-S-H gels for binding purposes. Nevertheless, the greater the percentage of GGBFS, the greater the compressive strength and the inclusion of GGBFS

between 10% to 90% in the mixtures improved the compressive strength up to 90 MPa at 28 days of age [15].

### **2.2.2 Ground Granulated Blast Furnace Slag (GGBFS)**

Ground granulated blast furnace slag (GGBFS) is an amorphous pozzolanic material, currently becoming one of the most popular cementitious components used to produce alkali-activated materials. Blast furnace slag (BFS) is extracted initially from the ore smelting process for steel production. The BFS then grounded to the fineness of cement, known as ground granulated BFS or GGBFS, one type of BFS and the most suitable material for geopolymer binder. The particle size of GGBFS is between 5 – 25  $\mu\text{m}$ , which is crucial in providing a larger specific surface area and increasing reactivity. It has angular and irregularly shaped, containing higher CaO content (> 30%). The melting and rapid cooling process will form the glassy phase of GGBFS. It contains minerals like gehlenite, melilite and merwinite. Higher GGBFS will increase the temperature and improve hydration rates for fast setting and early strength development. However, excessive GGBFS will affect workability and has an early shrinkage crack problem[17]. Alrefaei et al.[31] analysed X-Ray diffraction analysis (XRD) slag pattern suggests high amorphous content, thus making its reactivity highly useful for geopolymerization. Previous studies have been conducted to evaluate alkali-activated materials based on GGBFS products in paste, mortar, and concrete. This type of binder is an industrial waste product used to make iron and is in the form of fine particle-containing approximately 95% non-crystalline calcium-aluminosilicates. It was then dried in the ground and produced fine powder [21]. It has the composition of  $\text{SiO}_2$ ,  $\text{Al}_2\text{O}_3$ ,  $\text{MgO}$  and  $\text{CaO}$  to form hydrated calcium-silicate (C-S-H) gels as the main reaction product in alkali-activated binders. GGBFS forms hydration products generated in a blast furnace. The process started with destroying Si-O-Si, Al-O-Al and Al-O-Si slag bonds to form the Si-Al layer on the slag grain's surface [20]. The final setting time for alkali-activated GGBFS fresh mortar was reported to be the fastest compared to FA and MK mortar. However, too short setting times may not be practical for its application [23]. Saeid et al. [32] have reported that the inclusion Micro-Silica (MS), another type of pozzolanic material mixed with GGBFS, produced extra C-S-H gel by reacting with calcium hydroxide that increased the compressive strength of alkali-activated

GGBFS/MS paste in the study. The previous research also showed that alkali-activated GGBFS/FA mortar cured at ambient temperature would perform better. At the same time, the reaction between GGBFS and OPC has a significantly low expansion value. Another study also found that the composition of 25% FA & 75% GGBFS mortars activated with an alkali activator of 10 M NaOH molar concentration and ratio  $\text{Na}_2\text{O}/\text{SiO}_2 = 1.0$  have shown significant mechanical properties in two-part AAMs system [26][32]. Ghasan et al. [26] investigated alkali-activated mortar containing mixed-FA and GGBFS as the source of CaO, where the FA consisted of 5.2% Ca, 57.2% Si, and 28.8% Al content, and the GGBFS consisted of Ca (51.8%), Si (30.8%) and Al (10.9%). The GGBFS content used in the range of 30 to 70% as replacement of FA, while the molarity ratio of alkali activator NS: NaOH and modulus of alkaline solution used were standardized for all two-part AAMs mixes. The result from this experimental program has proved the previous studies about the workability of alkali-activated mortar, where higher slag content could improve the rate of setting time. Viscous properties of the binder matrix play an important role in determining the workability of AAMs [23]. Incorporating slag with FA could reduce the water absorption rate, thus increasing the mortar's plasticity by reducing the number of spherical particles of FA and angular particles of slag. However, a high slag content volume could reduce the mortar's plasticity, decrease flow percentage and produce low workability. Slag can accelerate the hydration process and enhance the hardened properties of the alkali-activated FA-GGBFS mortar, subsequently providing incredible strength for its compressive and flexural properties. In short, the Al ions from the C-A-S-H gel of slag boost the polymerization process of C-S-H and N-A-S-H gels and improve the microstructure of alkali-activated mortar for the development of mechanical strength [26].

The alkali-activated binder can also be obtained from an aluminosilicate source of slag and natural pozzolan (NP) activated by an alkali solution. The chemical reaction between this kind of artificial material and volcanic pozzolan may establish another C-S-H, C-A-S-H and N-A-S-H gels described in previous studies by Rafael et al. [1]. NP, a sustainable industry by-product, was selected due to its availability in the market. GBFS will activate  $\text{Ca}^{++}$  ions concentration and replace low  $\text{Na}^+$  ions concentration in the alkali-activated matrix [26]. This experimental study

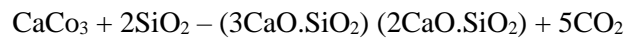
also showed that alkali-activated with a composition of 70% NP & 30% GGBFS and  $\text{Na}_2\text{O}/\text{SiO}_2 = 1.1$  ratios demonstrated higher compressive strength for 28 days of curing and complied with EN 1504-3 standard for 'structural repair mortar, class R3' type. Another parameter to satisfy this EN 1504-3 Class R3 type is that the tensile strength of repair material must be higher than the substrate's tensile strength in terms of its pull-of failure in the substrate's interfacial bonding zone (IBZ). The experiment conducted by Sabina et al. [23] showed that alkali-activated slag mortar layers delaminated on the vertical and horizontal surfaces of the concrete substrate during the curing period, which resulted in a low level of soluble silica, where previous studies confirmed adhesion bond depended on the high amount of Si and Na to increase the mortar bond strength. Yung et al. [20] studied that alkali activation of aluminosilicate waste material composed of 30% FA & 70% GGBFS used as bonding materials produced high-strength binder on concrete substrate. The adherence of the repair material to the substrate must be higher than 1.5 MPa for the Class R3 repair mortar. However, in this study, the tensile strength of the alkali-activated NP-GGBFS only satisfied Class R2 repair mortar for non-structural repair mortar due to factors like lower strength of the concrete substrate and content of alkali activator ratio.

Nonetheless, it may be improved with further study on chemical reaction formulation to achieve class R3 or R4 of structural repair mortar [1]. Vitor et al. [33] have experimented by testing 21 formulations of alkali-activated materials using MK and GGBFS as binders to determine compressive strength and modules of elasticity of repair mortar.  $\text{Na}_2\text{SiO}$  and NaOH solutions were used as alkali activators, while the molar ratio of  $\text{SiO}_2$  and  $\text{Al}_2\text{O}_3$  was set in the range of 2.0 to 4.6. The compatibility between repair materials and concrete substrate depends on mechanical strength and modulus of elasticity, where low modules elasticity prevents cracks in the concrete. Therefore, a highly alkaline environment with high percentages of slag could affect the formation of C-A-S-H gel. It also suggested that the formulation of 20% MK & 80% GGBFS with  $\text{SiO}_2 / \text{Al}_2\text{O}_3 = 4.2$  was the optimum formula to meet a similar modulus of elasticity of concrete substrate. In addition, at a low molar ratio of  $\text{SiO}_2/\text{Al}_2\text{O}_3$ , replacement MK with 20% GGBFS demonstrated good bonding strength at the interface zone of a concrete substrate due to higher silica modulus and lowered specific surface area slag.

In one-part AAMs, 90% GGBFS paste was mixed with 10% zinc fine tailings reported to have about 37 MPa compressive strength at 28 days of age. This mixture was activated with only 1.5% high silicate modulus water-glass powder, Na<sub>2</sub>O (by precursor weight), to control the fast setting of one-part AAMs slag. Adding 10% optimum zinc fine tailings assists the reaction process and strength development compared to solely slag content (31 MPa) when a lower dosage of the activator is used. Nevertheless, the compressive strength result did not comply with class R4, EN1504-3 for structural concrete repair materials ( $\geq 45$  MPa) at 28 days of age [34]. Other references on slag-based paste showed that 100 % GGBFS activated by solid sodium hydroxide and anhydrous sodium silicate powder only managed about 20 MPa compressive strength at 28 days of age, proving that excessive calcium in slag may cause higher drying shrinkage that affects the strength development [35]. On the other hand, 7% anhydrous sodium silicate was used to activate 100% GGBFS slag mortar and recorded about 60 MPa compressive strength at 28 days of age, 65 MPa (60 days), and 67 MPa (90 days). It is worth noting that early high strength is achieved at 28 days and keeps increasing. However, at 60 and 90 days of age, only about 10% of extra strength gained was recorded. To explain this trend, when water is added to the dry mixture, which is rich with calcium (slag), the temperature of the mixing water will increase due to the exothermic reaction, subsequently increasing the mixture's temperature in a fresh towards the hardened state. As a result, water will be lost quickly, and at the same time, the pH value rises when higher dosage of reactive alkali activator is dissolved in the water simultaneously. This phenomenon contributed to higher early strength for GGBFS-based mortar, as reported by [36].

### **2.3 Ordinary Portland cement (OPC)**

Portland cement, or in this study referred to as OPC has a rich amount of Ca. Alsubari et al.[37] highlighted that the chemical compositions of OPC typically has  $> 60\%$  CaO, AlO  $> 10\%$ , and Al<sub>2</sub>O<sub>3</sub> as a binder agent. Ralli et al.[17] explained that the production of OPC is from the calcination of limestone and silica aluminous materials to produce lime and also release CO<sub>2</sub> as per Equation 1 below:



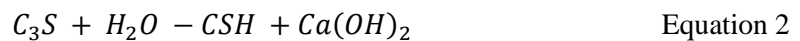
Equation 1

The hydration mechanism of OPC contributed to C-S-H gels, a stable gels chain because Ca is insoluble in water. Creating gels product of AAMs is similar to the OPC hydration system via total dissolution of precursors under an alkaline environment. It contributes to potassium or sodium aluminosilicate hydrate (K-A-S-H or N-A-S-H). However, the K or Na ions are chemically unstable compared to Ca; thus, incorporating OPC in the one-part AAMs system will create polymeric aluminosilicate chains of C-A-S-H and N/K-A-S-H, providing more stable hydrates. On the other hand, the inclusion of aluminosilicate precursor with OPC will compensate for the risk of having too much Ca in OPC that reduces sulphate resistance due to the formation of gypsum and ettringite caused over expansion and cracking, whereby for FA/GGBFS-based precursor, no gypsum and ettringite is formed [17].

One-part AAMs concrete composed of OPC has recorded a significantly high compressive strength value. Including 10% to 60% OPC in one-part AAMs showed the increment of the concrete's compressive strength from 33 MPa to 55 MPa at 28 days of age. The report explained by Askarian et al. [38] established how the concrete composed of 36% FA, 4% GGBFS and 60% OPC, also referred to as 'hybrid', recorded the highest compressive strength 27 MPa (1 day), 45 MPa (7 days) and 55 MPa (28 days) compared to the mixtures of FA, GGBFS without OPC, 0 MPa (1 day), 2 MPa (7 days) and 11 MPa (28 days). The microstructure of one-part AAMs concrete without OPC contains unreacted FA particles and a geopolymeric matrix, representing loose and amorphous structures. Higher OPC content will reduce its microstructure porosity due to amorphous Ca-Al-Si gels for strength development. In addition, hybrid one-part concrete without an alkali activator was recorded at 1 day of age (7 MPa), 7 days (28 MPa) and 28 days (44 MPa). Including OPC improves the early strength of AAMs concrete due to its rapid reaction behaviour and assisting geopolymeric acceleration when reacting with an alkali activator. Interestingly, the concrete mixtures without an activator could still achieve a significant compressive strength, proving the dominancy of 60% OPC in the mixtures to produce the cementitious binder and its potential to control alkali activator dosage for other applications such

as paste and mortar. Nevertheless, concrete samples in this experiment consisted of coarse aggregate as an added value to increase the compressive strength. Still, the study's lack of pore structures analysis may leave this concrete stability at stake. In the other report by Abdollahnejad et al.[12], one-part AAMs mortar composed of 26% OPC/58.3% FA and 8% slag of aluminate precursors can be effective as thermal insulation for floor heating systems and also has a promising cost efficiency. The compressive strength of the mortar, even though only achieved below 20 MPa at 28 days of age, with the addition of aluminium powder as a foaming agent, the mortar has a low thermal conductivity that complied with the Korean Industrial Standard code for foam concrete for floor heating systems. Coppola et al.[39] compared the compressive strength of mortar composed with Portland cement and slag-based one-part AAMs and recorded higher strength of about 47 MPa than slag mortar activated with GGBFS only ( 18 – 40 MPa). Nath et al.[40] used the OPC and reported that including OPC in Class-F FA has improved setting time and early strength properties in geopolymer concrete. A higher curing temperature is required for the geopolymerization process for setting time and strength development, but with the addition of OPC, the cementitious material can be cured at ambient temperature yet record comparable workability and mechanical strength. The microscopic images of OPC/FA also indicate an amorphous and calcium-rich hydration product where higher OPC content will increase the gel's compactness due to higher Si/Al essential for strength development. The greater amount of soluble silica could enhance the condensation process of dissolute precursors by increasing the reaction rates and crystallization productions. These findings support the past research by [41] on the influence of OPC (between 30 – 70% content) in geopolymer materials, suggesting that C-S-H formation from OPC has a more compact structure than N-A-S-H from FA, besides the C-S-H gels continue to form lower alkalinity in later stage ensure the strength keeps growing over the time. It is worth noting that calcium content could also be obtained from GGBFS, but OPC is already in the form of commercial cementitious binder products, which is more stable and does not require an activator for the hardening process, it will react immediately with water for a chemical reaction called hydration independently, on top of simultaneously supplying additional Si, Al, Ca and the covalent Si-OH-Al bond when dissolved with aluminosilicate precursors for geopolymerization process. On the other hand, GGBFS may also supply additional Si, Al, and Ca

but still need an alkali activator to activate the binder. As a result, the engineering properties of GGBFS-based materials still depend on factors such type and dosage of activator, curing temperatures and required additional additives to improve its physical and microstructural properties. Nonetheless, one-part AAMs cementitious materials composed with FA/GGBFS may achieve a satisfactory engineering performance without the OPC, but with hybrid technology – mixed with OPC, the engineering properties of AAMs is way much better, fast result and the most important is, more convincing products since the Portland cement has been well established and were used in the world market for many years. Moreover, the reaction between OPC and water will also produce calcium hydroxide,  $\text{Ca(OH)}_2$  which increase the pH level essential to speed up the dissolution process in the geopolymerization stage. The chemical reaction of OPC with water will releases  $\text{Ca}^{2+}$ ,  $\text{OH}^-$ , and a large amount of heat. The mixture reaches pH 11. Eventually, the system becomes saturated, and  $\text{Ca(OH)}_2$  crystallizes along with calcium silicate hydrate, CSH. It is described in the Equation 2 below:



#### 2.4 Alkali activators

Alkali dosage is one factor that determines the strength development in AAMs. Sodium silicate ( $\text{Na}_2\text{SiO}_3$ ), calcium hydroxide ( $\text{Ca(OH)}_2$ ), sodium hydroxide (NaOH) and sodium carbonate ( $\text{Na}_2\text{CO}_3$ ) are the most common activators to activate the one-part AAMs. However, sodium hydroxide (NaOH) has high hygroscopic properties and is often used in the solution. It is also known as NaOH micro-pearls or solid NH. As a result, potassium-based compounds replaced NaOH, especially potassium hydroxide (KOH) and potassium silicate ( $\text{K}_2\text{SiO}_3$ ). They were reported to have better alkalinity levels, as reported by Askarian et al.[30] who employed five different alkali activators to activate the FA/GGBFS to study the characterization of one-part AAMs. A high modulus ratio of sodium silicate ( $\text{Na}_2\text{O} = 27\%$ ,  $\text{SiO}_2 = 54\%$ , Ms ratio = 2.0) was used instead of a low modulus ratio sodium silicate - anhydrous (Ms = 0.9). In addition, industrial grade  $\text{Ca(OH)}_2$ , fine powder of potassium carbonate ( $\text{K}_2\text{CO}_3$ ) with 99.99% purity, Lithium hydroxide (LiOH) with 98% purity and sodium oxide ( $\text{Na}_2\text{O}$ ) were also tested. It was found that FA/GGBFS pastes activated with the combination of LiOH,  $\text{Ca(OH)}_2$ , and  $\text{Na}_2\text{SiO}_3$  activator has

recorded promising 38 MPa compressive strength at 28 days of age. A sole activator of sodium silicate produces weak and porous structures, while calcium hydroxide alone decreases the workability. Furthermore, it also mentioned in the report that slag activated with potassium carbonate reduces the workability of pastes samples, as recorded in the mini-slump test result. On the other hand, using sodium oxide has a setback on slow setting time. It is worth noting that the dosage of the activator used in the experimental study was between 4.5% to 12%, indicating that a low dosage of activator may not be sufficient to increase the pH level and create hydration gels in the polymerization process of one-part AAMs. Nevertheless, all types of solid activators in the study prove they can replace highly corrosive alkali solutions in conventional AAMs. The volume of the alkali activator is vital to ensure enough alkali environment for dissolving all particles. In contrast, excessive amounts of alkali activator may contain extra  $\text{Na}_2\text{O}$  (in addition to low water content causing undissolved particles) that remain embedded and will react with the formed N-A-S-H gels, affecting specific regions of materials and subsequently decrease the mechanical strength of AAMs [29]. Moreover, Askarian et al.[38] employed 7.5% potassium carbonate into one-part AAMs concrete containing 0 – 60% OPC replacing FA/GGBFS precursors' original content. The compressive strength increases from about 11 MPa (without OPC) up to approximately 55 MPa (60% OPC) at 28 days of age. When sodium silicate was added with potassium carbonate, not much difference was recorded for the compressive strength, unlike the additional 2.5%  $\text{Ca}(\text{OH})_2$ , which has recorded a more compressive strength level, resulting from increased pH solution, thus improving geopolymerization rates. AAMs concrete samples without OPC, activated with potassium carbonate and calcium hydroxide demonstrated approximate 37 MPa compressive strength at 28 days of age compared to hybrid 10% OPC concrete with a single potassium carbonate activator (33.4 MPa). The result of this report gives a valuable indication of the selection of an alkali activator and its mix design to activate a one-part AAMs system which is feasible and economical for site applications. Meanwhile, other factors may influence the mechanical strength outcomes such w/b ratio and added admixtures also play significant role on one-part AAMs properties.

### 2.4.1 Sodium silicate

Commercial sodium silicate powder was created by heating sodium carbonate and silicon dioxide to the temperature of 1200 °C. It still requires high energy for the degradation process, and from liquid to solid, sodium silicate manufacturing emits between 0.5 and 1.5 kg CO<sub>2</sub> equivalent per kg. A transportation charge may add to the overall cost of getting this product from countries with a scale of production like the United States of America, the United Kingdom, Australia, China, and India. In addition, exceptional care for handling makes it much more expensive. Three types of solid sodium silicate used depend on the amount of crystal water bound into the solid metasilicate phase of Na<sub>2</sub>SiO<sub>3</sub> anhydrous, solid sodium metasilicate pentahydrate, Na<sub>2</sub>SiO<sub>3.5</sub>H<sub>2</sub>O and Na<sub>2</sub>SiO<sub>3.9</sub>H<sub>2</sub>O. To summarize, sodium silicate activator has the disadvantage of cost, energy scale, handling, and safety issues. Still, researchers now focus on alternative silicate sources from common waste materials such as glass and rice husk ash [42].

Oderji et al.[28] used three types of solid alkali activators to study FA/GGBFS-based AAMs and described that the alkali dosage concentration influenced the mechanical strength of the pastes samples. An 8% anhydrous sodium metasilicate (Na<sub>2</sub>SiO<sub>3</sub>) was used to activate the precursors and recorded significantly high mechanical strength and excellent workability. However, when reduced below 8% dosage, the compressive strength dramatically dropped at 28 days of age. This phenomenon is attributed to the changes in Na<sub>2</sub>O content and the molar ratio, among the factors determining strength development in the alkali activation process. In this study, the Na<sub>2</sub>SiO<sub>3</sub> recorded the highest initial flow compared to NaOH and KOH. In contrast, NaOH had the lowest flow diameter due to higher heat released due to the exothermic reaction between the alkali activator and water. It subsequently lost its flowability within the first 4 minutes. Furthermore, microstructures analysis explained that more significant amounts of unreacted FA/GGBFS particles proved that dissolution of the precursor was not completed when less than 8% alkali activator dosage was used, as a sign of insufficient alkali activator content subsequently affects its mechanical strength.

A single activator of sodium silicate (12% of precursor weight) has been assessed to activate 100% FA paste, and it found that at 3 days of age, the sample did not set and only recorded about 10 MPa at 28 days under ambient curing. However, a combination of two or more activators increased the compressive strength at 28 days of age, where paste with  $\text{Na}_2\text{SO}_3/\text{Ca}(\text{OH})_2$  activator recorded 27 MPa, and 38 MPa with  $\text{Na}_2\text{SO}_3/\text{Ca}(\text{OH})_2/\text{LiOH}$  as reported by [30]. A higher dosage of alkali activator used in this study (12% and 21% weightage) accelerates the dissolution of aluminate and silicate ions from the FA. Therefore, it confirms the findings on the effect of higher alkali dosage towards the compressive strength as widely reported [34]. However, these mixes are uneconomic and have adverse environmental and safety effects besides exposure to the potential of efflorescent effect at a later stage. Samarakoon et al.[42] compared three types of alkali activators, namely dry activator (DA) consisting of water glass and solid sodium hydroxide, solid sodium metasilicate pentahydrate (NS) and sodium silicate/sodium hydroxide (NHNS) solution to activate 60% FA and 40% GGBFS paste. At 28 days of age, both DA and NS recorded about 30 MPa, while the NHNS activator contributed up to 48 MPa compressive strength. All samples showed an increment of strength from 7 to 56 days of age, whereas the NHNS solution in two-part AAMs showed the best mechanical strength performance. The result also confirms the rapid dissolution of solid precursors in liquid alkali activators compared to solid-type activators. Nevertheless, the early strength of one-part samples proved higher Na release from dissolution because of the kinetic reaction between FA and slag. Both DA and NS have comparable compressive strength results at all curing ages, related to the co-existence of sodium and calcium-based hydration products, indicating the potential of using other alkali activator products to replace uneconomic sodium silicate type. Alrefaei et al.[43] using 8% anhydrous sodium metasilicate to activate 50% FA and 50% GGBFS paste, achieving a significant 60 MPa compressive strength at 28 days. This result was similar to the findings reported by [15] using the same precursors and alkali activator (type and proportions) for paste samples, recorded compressive strength of about 60 MPa at 28 days of age. It is interesting to know that the higher the dosage of the activator, the higher the compressive strength. At 4% activator (by weight), the compressive strength recorded about 30 MPa, 10% activators about 70 MPa, and about 80 MPa using 14% activator explained the influence of alkali activator in determining mechanical strength

of AAMs. Azevedo et al.[29] used sodium hydroxide and sodium silicate to promote the formation of binders from the thermal treatment of precursors after adding water into dry mixtures. Increasing the alkali concentration of both activators can reduce unreacted FA particles and promote alkali carbonation reaction on the surface, mainly due to excessive  $\text{Na}_2\text{O}$  available in the system compared to  $\text{CaO}$ . A low alkali dosage of 1.5% water or alkali silicate glass with high silicate modulus,  $M_s = 2$ , activated slag-based pastes with 5 – 20% fine tailings. The low dosage of activator will slow down the dissolution rates of the binder with a long dormant period is well predicted, especially with low pH levels. Still, adding fine tailings compensates for the insufficient alkaline level and thus accelerates compressive strength development at the early curing stage.

#### **2.4.2 Sodium hydroxide**

One-part GGBFS (97%) mortar was activated with 3% commercial sodium hydroxide (SH) in the form of pellets has recorded about 25 MPa compressive strength at 28 days of age. However, this report by [44] compared the slag mortar composed of 77% slag, 15% desulphurization dust (DeS-dust) as an alkali activator and 8% micro silica (MS) as additional silica sources, has recorded 32.5 MPa compressive strength at same testing age. This situation is due to the higher Ca (Calcium) and Fe (Ferum) content in DeS-dust than in SH for better strength development over time. The additional MS, on the other hand, act as filler in the binder since MS has a lower dissolution rate, thus creating unreacted MS and filling the pores to provide a compacted and stable structure.

#### **2.4.3 Sodium carbonate**

Sodium carbonate ( $\text{Na}_2\text{CO}_3$ ) is an alkaline activator that can activate the precursors for binding purposes. However, using  $\text{Na}_2\text{CO}_3$  is not popular among researchers due to its low alkalinity. The functional group of carbonates ( $\text{CO}_{2/3}$ ) prevents the creation of hydrated products, thus limiting strength development. Lao et al.[45] reported that due to low pH values, combining  $\text{Na}_2\text{SiO}_3$  with other activators or additives effectively reduces setting time and improves the mechanical strength

of the geopolymer. It is worth noting that the production of  $\text{Na}_2\text{CO}_3$  has a lower environmental impact where the  $\text{CO}_2$  released in the air can be captured and reduced. In addition,  $\text{Ca}^{2+}$  from precursors will combine with  $\text{CO}_2$  to create  $\text{CaCO}_3$  or sodium-calcium carbonate phase as initial products from  $\text{Na}_2\text{CO}_3$  activation, subsequently acting as nucleation seeds to encourage the reaction and formation of hydrated products in AAMs technology. In contrast, sodium silicate ( $\text{Na}_2\text{SiO}_3$ ) and sodium hydroxide (SH) are the two most activator types used to activate the precursors because of their high alkalinity. However, the production of  $\text{Na}_2\text{SiO}_3$  required a higher temperature at  $1400\text{ }^\circ\text{C}$  to dissolve silica in molten sodium carbonate during the synthesis process, releasing more  $\text{CO}_2$  in the air. When the water-to-binder ratio decreases, the alkali activator dosage will be increased to expedite the dissolution process, increase the hydration rate, and contribute to a higher  $\text{SiO}_2/\text{Al}_2\text{O}_3$  ratio. The hybrid activator of  $\text{Na}_2\text{CO}_3$  and  $\text{Na}_2\text{SiO}_3$  recorded impressive compressive strength when tested for ultra-high performance geopolymer concrete (UHPC). On the other hand, sodium NaOH was reported to contain highly hygroscopic and corrosive when used at higher dosages, as published by [38]. In the report, the compressive strength of concrete hybrid OPC-AAMs was recorded up to 60MPa at 28 days of age when 12% of dry  $\text{Na}_2\text{CO}_3$  activator was used. The efflorescence potential also decreased because potassium has a stronger bond to the aluminosilicate gels, and its crystallinity is less visually apparent compared to  $\text{Na}_2\text{SiO}_3$  and NaOH. Xie et al.[46] suggest that sodium carbonate is the most cost-effective compared to sodium hydroxide and sodium silicate but has a much longer setting time. Lao et al.[45] analyzed the embodied carbon from alkali activator production of sodium carbonate and sodium silicate and found that sodium carbonate only released 0.110 metric tons of  $\text{CO}_2$  compared to sodium silicate, which has 10 times greater, approximately 1.860 of  $\text{CO}_2$  metric ton.

## **2.5 Mix design ratio and curing regimes.**

Many researchers used a series of water-to-binder (w/b) ratios to determine the compressive strength of one-part AAMs at a standard 28 days of curing age as the first reference to develop and improve the mechanical properties of cementitious materials for engineering applications. There are three types of cementitious materials samples commonly prepared in the form of concrete (with coarse aggregate), mortar (with fine aggregate) and paste (no aggregate). The

hydration and polymerization process of binders is vital to determine the density and durability of one-part AAMs product. Li et al.[47] reported that increasing the w/b ratio will change the rheology behaviour of one-part AAMs in the fresh state by decreasing yield stress and plastic viscosity. Gawwad et al.[48] explained that slag from GGBFS has lower hydration properties in the water. Still, if the precursors are thermally treated and curing time is extended for paste samples, the strength is continuously gained to increase the compressive strength. Excessive volume of water will promote evaporation and create more pores. Thus, gel products are required to fill these pores based on their chemical reactivity and available space for microstructural hydration, as reviewed by Nodehi et al. [49] on AAMs technology. Too compact a microstructure specimen can cause internal stress, leading to crack and strength loss when insufficient pore space is available in the new formation of hydration products. Also, a high temperature or longer curing process may cause more pores to appear due to high chemical reactivity, producing a higher C-A-S-H reaction that increases dissolution rates and shortens the setting time. The report also reviewed the effect of five main curing regimes, ambient, ovens and thermal, water immersion, wrapping/sealing, and microwave on AAMs. It can be concluded that ambient temperature between 20 – 30°C can cure the specimen under an alkaline environment of AAMs, induce densification of one-part AAMs samples, is cost-efficient, has less CO<sub>2</sub> and is most practical to be applied for construction. Curing at ambient room temperature enhances the refinement process of pore structure due to alkali activation with newly formed C/N-A-S-H gels, improved microstructure compactness and decreased microcracks. However, suppose a higher dosage alkaline activator is used; an exothermic reaction caused by higher temperature may reasons of water loss due to an increase in mixture temperatures, subsequently increasing the pH level since the concentration of alkali becomes higher, on top of the existing alkali activator powder that has already dissolved in the water, which finally upsurges the shrinkage and porosity level leading to cracks [36]. Zhang et al.[50] study the rheology of one-part slag pastes using a w/b ratio of 0.40, added 5 – 20% fine sand powder into the mixture, and record the highest compressive strength of 60 MPa at 5% fine powder added volume. A high dosage of solid water glass, 20% from precursor weight, was used to activate the one-part AAMs in the study to analyze its potential as semi-flexible pavement grouting materials. The findings also indicate that the mechanical strength of

pastes decreases with an increase of fine sand powder due to a decrease in gel content as in agreement with [51], suggested that for one-part AAMs in the form of FA-based concrete, compressive strength for samples cured under ambient and water are comparable to solar curing method regardless the binder-to-aggregate (b/a) ratios but in addition to that, by decreasing b/a ratio to 0.35 from 0.57 and 0.45, the mechanical strength of the concrete has increased. Higher aggregate content may cause the hydration product to be unable to wrap the surface of a fine powder, subsequently forming porous, brittle, and cracked physical structures of the one-part AAMs samples.

Luukkonen et al.[52] reviewed the suitable curing condition for one-part geopolymer products, preferably cured under saturated conditions such as 100% relative humidity to avoid water loss when heat is generated from the reaction between water with dry mixtures. Also, sealing the specimen can prevent dehydration, which is the main reason for efflorescent microcracks and finally affecting the compressive strength. By controlling water content via w/b ratios, for instance: a higher w/b ratio may help the formation of Al-rich, Si-rich gels for FA/sodium silicate samples. Still, a low w/b ratio on the other side leads to better compressive strength, as confirmed by Ye et al.[53], samples with a w/b ratio of 0.45 recorded about 32 MPa compressive strength compared to a w/b ratio of 0.50 (25 MPa) and a w/b ratio of 0.55 (20 MPa) for red-mud-based AAMs pastes. Almalkawi et al.[16] reported that AAMs cementitious binder has more significant shrinkage than OPC-based binder systems. Higher porosity levels and larger pore size of AAMs binder were observed in the report, and it found that excess water content from the water/binder ratio must be removed to produce a less porous polymeric microstructure. Elzeadani et al.[11] reviewed the water and aggregate ratio requirement for one-part AAMs technology and described the w/b ratio as the volume of water from the total volume of precursors and solid alkali activator or by total precursor volume only. Fresh water is the source of water used in preparing the cementitious material. Still, numerous studies have been introduced to employ sea water and reverse osmosis reject water (treated sea water) as an alternative to activate the AAMs mixtures. As a result, the mechanical properties are comparable and record fast settings with an accelerated hydration process. Conversely, its practicality in actual engineering practice and long-term effects

are still yet to be discovered, especially for large-scale production and engineering structural purposes. Silicious river sand has a  $\text{SiO}_2$  content of more than 95% for aggregate and becomes the primary source of fine natural aggregate for AAMs mortar. In contrast, a few types of aggregate were used for coarse aggregates, such as granite, basalt, limestone, dolomite, and clay granules, to prepare one-part AAMs concrete. In general, coarse is a granular material consisting of small rock fragments used as structural fill in concrete. Three main factors determining aggregate effects on hardened properties of AAMs are the irregular shape of the aggregate, its saturation level, and aggregate content used in the mixtures. Dry and unsaturated aggregates can absorb the free liquid solution, affecting the polymerization process and reducing strength. Pre-saturated porous aggregate will supply more water to the mixture during internal curing, increasing AAMs' setting time and workability. Still, excessive water significantly decreases the pH level and makes it susceptible to shrinkage problems [49]. Yet, recent studies suggest that alternative industrial waste products can replace the natural aggregate using crushed bricks, rubber, porcelain, and other ceramic products. This new type of synthetic aggregate can reduce  $\text{CO}_2$  emissions and does not harm the environment, especially from rock excavation and mining activities. Nevertheless, the availability of these raw materials may not sufficiently supply demand for construction use, and additional costs may incur to make this recyclable waste commercially ready in the market. Goncalves et al.[54] used waste sand from a biomass boiler as a replacement of fine natural aggregate for one-part AAMs mortar and found that a w/b ratio of 0.29 was not enough for geopolymerization reaction and only recorded about 40 MPa compressive strength compared with a w/b ratio of 0.33 and 0.35 with the increments of 55% and 70% compressive strength at 28 days of age, respectively. Higher water content is essential to dissolve smaller grain sizes of waste sand particles containing larger specific surface areas. A significant compressive strength recorded up to 70 MPa for the slag-based mortar activated with a 10% sodium metasilicate activator under ambient curing conditions, and further tests on other mechanical properties must be carried out to understand the performance of the mortar.

Azevado et al.[29] prepared one part AAMs paste composed with FA and calcined clay (commercial kaolin) and w/b of 0.90 and recorded about 12 MPa of compressive strength at 28

days of age. When commercial kaolin was replaced with calcined ceramic residue, the w/b was adjusted to 0.60 and recorded about 25 MPa of compressive strength at 28 days. Both compressive strengths, however, did not comply with the requirements for structural concrete repair materials as per EN 1504-3 standards. Askarian et al.[38] used a w/c ratio of 0.30 and b/a of 0.30 to activate one-part hybrid OPC-geopolymer concrete and achieved a higher compressive strength of about 55 MPa with 60% OPC, 52 MPa (40% OPC), 50 MPa (30% OPC) and about 40 MPa with 20% inclusion of OPC replacing the amount of FA and slag in the form of concrete. As a comparison, a paste sample containing FA and slag with a w/c ratio in the range between 0.20 – 0.45 under an ambient curing environment recorded a promising compressive strength of 38 MPa at 28 days of age for one-part AAMs paste composed with 50% FA and 50% slag respectively [30]. The performance of one-part AAMs slag paste with replacement between 0-20% fine tailings content was set to 0.45 and had about 37 MPa compressive strength maximum with 10% fine tailings replacement [34]. The FA/slag-based binder properties were tested by [6] using a w/b ratio of 0.50, where the paste samples were activated with two different alkali activators, solid sodium silicate and glass powder/micro-pearl (solid NH). The compressive strength results recorded that both paste-type samples achieved about 28 MPa – 32 MPa. Combination of slag and rice straw ash as precursors were tested by Yin et al.[35] in the form of paste using a w/b ratio of 0.41 but only recorded 18 MPa – 21 MPa compressive strength. Teo et al.[15] studied the influence of a w/b ratio between 0.40 and 0.55 on AAMs paste composed with high calcium fly ash (HCFA) and slag (GGBFS) and found that a higher w/b ratio will reduce the density of pastes sample subsequently decrease the compressive strength between 6 – 35% over 28 days of curing age. It is worth noting that the type of alkali activator used in this experimental investigation is sodium metasilicate anhydrous, which has higher corrosivity. Moreover, high-strength slag-based mortar blended with particle packing optimization has recorded 145 MPa compressive strength with a w/b ratio of 0.30, b/a ratio of 0.50 and concluded that an increase of w/b ratio from 0.25 to 0.30 will increase compressive strength. Still, the strength is reduced when the w/b ratio is 0.35. Optimum water content is required to dissolve solid sodium silicate and other Si/Al species in one-part AAMs, unlike a two-part system in which the alkali activator is already in the form of a solution to dissolve all the particles. The mortar samples in this study were carried out by Perumal

et al.[55] have both fine and coarse sand aggregate besides being activated with a 10 % volume of anhydrous sodium metasilicate to activate precursors' combination of slag, silica fume and phyllite dust. Haruna et al.[56] used a w/b ratio of constant 0.25 to analyze the long-term strength development of FA pastes and recorded between about 30 – 50 MPa compressive strength. An anhydrous sodium metasilicate activator was used between 8 – 16% of the volume as part of the total precursor volume, and the compressive strength kept increasing for up to 365 days. A higher dosage of an alkaline activator will increase the heat release rate, but a high exothermic reaction may harm the one-part AAMs due to efflorescence problems. The combination of slag with porcelain and raw ceramic as precursors for slag-based AAMs was tested by [57] under different curing methods to understand the microstructural and strength development of the mortar. The samples were composed with a w/b ratio of 0.35 and a b/a ratio of 0.50. Mortar samples with sealed curing conditions recorded the highest compressive strength, about 65 MPa, compared to samples cured with water and unsealed conditions. In this study, total porosity was increased with increased ceramic volume. Besides, high dissolution of rates of high calcium slag will make the mortar prone to cracking and strength loss, affecting the mortar's long-term durability, which was not covered in the study. Furthermore, a 10% sodium silicate was used to activate the slag mortar, and a higher dosage of an alkaline activator may also contribute to the higher compressive strength level at 28 days of age. Adesanya et al.[44] employed desulphurization dust, a waste material during the steel-making process, to replace commercial sodium hydroxide as an alkali activator with a constant w/b ratio of 0.45 and b/a ratio of 0.50 and a comparable compressive strength at 28 days of age. Adding micro silica into slag-based mortar improved the strength up to 33 MPa, still less than the compressive strength requirement for class R4, EN1-504-3. In addition, Samarakoon et al.[58] applied w/b ratio of 0.50 to study pastes sample composed with 60 % FA and 40% slag, activated with waste glass powder (blended with NaOH micro pearls to produce solid activator powder) has an average of 23 – 32 MPa compressive strength at 28 days of age. A 1% volume of high-strength fibre was added in 12 different mortar mix compositions with a constant w/b ratio of 0.30 and a b/a ratio of 0.60 to understand the mechanical properties of slag-based AAMs. The compressive strength showed it could achieve up to 50 MPa at 28 days of age by using steel fibre compared to other types of mineral fibre. Anhydrous sodium silicate used as

an alkali activator in this study may require extra caution when handling it, and higher costs may incur. It was also found that some fibres types were unstable in highly alkaline environments, affecting their strength and long-term durability, as reported by Shah et al.[59]. In this mortars samples composed of 80% FA / 20% slag, three types of fibres were added into the mixture, micro steel, basalt and polyvinyl alcohol fibre (PVA), to strengthen the mechanical strength with a w/b ratio of 0.30 and b/a ratio of 1. Approximately 45 MPa compressive strength was recorded with 2% additional PVA and 1% micro-steel fibre, while 42 MPa compressive strength for 2 % basalt. As a comparison. Luukkonen et al.[60] reported that slag mortar composed of 1% single fibre and activated with sodium metasilicate achieved a compressive strength of about 80 MPa with a w/b ratio of 0.45 and b/a ratio of 0.50. further study by Abdollahnejad et al.[61] on the effect of fibre-reinforced one-part slag/ceramic binders mortar recorded up to 70 MPa for 1%. Steel and PVA when cured in the water bath. In the report, the w/b ratio was constant at 0.35 with a b/a ratio of 0.50 and a high corrosive alkaline activator anhydrous sodium metasilicate was used to activate the precursors. Good adhesion of fibres in the matrix indicates that fibres could be undertaken as a bridge when the load is imposed, but tiny cracks also appear. As a result, water absorption increases with increased fibre volume in the mortar, which might affect its durability later. The w/b ratio of 0.35 and b/a ratio of 0.50 was used by Luukkonen et al.[62] to compare the alkali and silica sources in the slag-based mortar and record about 100 MPa compressive strength at 28 days of age when 10% sodium silicate is used, negatively affecting cost and has serious environmental impact.

Yang et al.[63] used the lowest w/b ratio of 0.10 to activate the slag pastes with additional 10% calcined dolomite and 10% solid sodium carbonate, recorded the highest compressive strength at about 40 MPa at 28 days of age and slightly increased to approximately 43 MPa at 60 days of curing age and cured at 20°C. The compressive strength has increased to 60 MPa when hydrothermal curing up to 50°C is applied, but such high temperatures require more energy besides not suitable for hand application at construction sites. The combination of slag pastes with 5% volume calcined oyster shell powder recorded 35 MPa compressive strength with a w/b ratio of 0.40 curing at a room-controlled temperature of 20°C. In addition, FA-based mortar containing

50% of FA and slag recorded up to 80 MPa compressive strength with a w/b ratio of 0.30 and b/a ratio of 1 but had a significantly high alkaline activator of 9% solid sodium silicate. The experimental study of this mortar was conducted under three different curing temperatures where for FA-based AAMs, it is easier to produce gel formation under ambient temperature. Hence curing at 30°C recorded better compressive strength at 28 days than at 20°C and 65°C. Also, higher early strength at 7 days of age was recorded with 30°C and 65°C curing temperatures in line with [64], on higher temperature released from high dosage of alkali activator and higher curing water temperature improved early strength development for slag pastes. This phenomenon is attributed to the high heat intensity that breaks the Si-O and Al-O bonds of SiO<sub>2</sub> and Al<sub>2</sub>O<sub>3</sub> to form new Si-O-Al products in the early hydration process. Adversely, shrinkage-induced cracking was observed with 50% slag content that might affect the mortar durability for long-term application [65]. Too rapid dissolution that accelerated hydration product formation, on the other way, will create more pores and less density as the reason for lower compressive strength. It is also worth mentioning that at 28 days of age, the compressive strength of the slag pastes recorded comparable strength regardless of the water temperatures used to cure the samples. Furthermore, one-part AAMs-based volcanic pumice has an average 22 MPa compressive strength when activated with a higher w/b ratio of 0.50 and b/a of 0.40 [16]. Coppola et al.[39] activate slag mortar samples with a w/b ratio of 0.55 and a b/a ratio of 0.33 recorded about 39 MPa compressive strength at 28 days of age lesser than OPC mortar compressive strength (48 MPa) with similar w/b and b/a ratios. Another study by Liu et al.[66] revealed that a w/b ratio of 0.45 was used to activate the slag pastes with a sodium silicate activator and honeycomb ceramic as an alkali activator. The compressive strength at 28 days of age was recorded at about 40 MPa and cured at 20°C. Nevertheless, a significant porosity level was detected by including the honeycomb ceramic in the paste samples. One-part AAMs slag concrete activates using a corrosive alkali activator type of sodium metasilicate pentahydrate with w/b ratio of 0.50 recorded compressive strength 65 MPa but has an issue with drying shrinkage due to high dosage of alkali activator and slag bases cementitious [67]. Gawwad et al.[68] employed w/b ratio of 0.25 to activate the slag paste composed of concrete waste successfully recorded about 28 MPa compressive strength. Moreover, Coppola et al.[69] used a w/b ratio of 0.50 to test slag-based mortar and has achieved

a compressive strength of 62 MPa without admixtures but experiencing loss of water and cracking in the plastic phase leading to shrinkage problems. A 50% FA/slag was activated with a w/b ratio of 0.42, and also use anhydrous sodium metasilicate was the source of an alkali activator that achieved up to 50 MPa compressive strength. One-part slag mortar activated with solid sodium metasilicate was cured at subzero temperature with a w/b ratio of 0.35, and b/a 0.50 can achieve up to 68 MPa at 56 days of age compared to OPC cement mortar only gained about 10 MPa. Nonetheless, lower curing temperature has caused the microstructure to become looser with limited gel content, which contributed to porosity problems in the long run [70].

## **2.6 Admixtures**

### **Superplasticizer (SP), Shrinkage Reducing Admixtures (SRA), Expansive agent (EA)**

One-part AAMs pastes are known for its set too quickly due to heat generated from the dissolution of solid alkali activator. Hence, a high range of water reducers or superplasticizers (SP) was used to improve the workability and rheology of samples and enhance the mechanical properties in concrete and mortar one-part-based AAMs. Many types of SP have been tested in past research, such as sodium lignosulfonate, modified polycarboxylate, naphthalene, and melamine-based compound. However, many SPs also work poorly in alkaline conditions; thus, the volume of SP must be examined to avoid degradation of the SP itself in the long run. Unlike two-part system counterparts, some SP types were not working efficiently with one-part AAMs [71]. Effects of water-reducing admixtures have been reported as beneficial to control the water level in AAMs mixtures. However, it also affects the mechanical strength of the hardened AAMs. Alrefaei et al.[43] added 0.5% to 3% polycarboxylate ether (PCEs) to the FA/GGBFS paste and found that its mechanical strength dropped compared to the control samples without added superplasticizer. The use of SP was also mentioned in a report by Askarian et al.[38] that may improve the workability level of hybrid OPC/AAMs concrete. The addition of citric acid - 1.5% volume of SP and 0.24% citric acid from total precursors weight were applied to all concrete samples that achieved a maximum compressive strength of about 55 MPa at 28 days of age for hybrid concrete composed with 60% OPC and 36% FA and 4% slag from GGBFS. In addition, 0.90% Polycarboxylate ether (PCEs-based superplasticizers) were used in AAMs paste composed with

50% FA / 50% GGBFS and achieved about 38 MPa compressive strength under an ambient cured environment as reported by [30]. A 5% borax – an admixture for water retarder was used by Shah et al.[59] to control the flowability and strength of one-part mortar composed with FA/GGBFS and compensate for the loss of workability and high water absorption from the added fibre. Abdollahnejad et al.[12] included 0.8% superplasticizer SIKA 3002 HE to maintain the workability of various AAMs mortar samples composed with OPC/FA/kaolin for floor heating system applications recorded up to 20 MPa compressive strength at 28 days of age. Moreover, further investigation by Abdollahnejad et al.[60] used 1.4% polycarboxylate-based SP to reduce the amount of water on AAMs FA/slag paste and concluded that adding SP would produce a high negative charge. Hence, particles will repel and deflocculates, releasing water from the mixtures, besides the electrostatic repulsions from the SP as a result of steric repulsion produced by the lateral ether chains on the molecule. To ensure a thixotropic consistency of FA/slag mortar, Coppola et al.[39] applied 0.5% SP based on Polycarboxylate ethers (PCE) to all mortar samples and recorded about 165 mm to 190 spread diameter superior to OPC mortar as a control sample (150mm spread diameter). Yet, the compressive strength of the one-part mortar only recorded 18 MPa at 28 days of age, even though it was using 8% of the alkali activator. Likewise, 0.35% Methylcellulose (MC) and 0.11% modified starch (MSt) were used as water retarders. At the same time, 1.5% ethylene glycol-based shrinkage-reducing admixtures (SRA) were added to control shrinkage problems with the addition of 3.5% CaO-based expansive agent to reduce shrinkage mortar at early stages as carried out by Coppola et al.[69]. These all types of admixtures (dosage used are based on total precursor) were combined and tested its function against shrinkage towards AAMs slag-based mortar and paste and found practical in reducing short- and long-term shrinkage, also preventing early cracking tendency in the plastic phase of one-part AAMs mixtures. All samples were composed of 100% slag and activated with three alkali activators: sodium metasilicate, potassium hydroxide and sodium carbonate. It can be found that the compressive strength of both pastes and mortar was reduced up to 20% with the inclusion of admixtures but still managed to achieve 50 – 61 MPa at 28 days of age for mortar and 78 – 97 MPa for pastes. The use of sole slag sources, however, may not be suitable for patching application as it is delaminated when applied; besides, the type of activators used in the study will

cost more. Another study on additional admixtures was explained by Zhang et al.[50] which used sodium carboxymethyl starch as a water retarder and latex powder as an anti-cracking mortar that improved the setting time of slag-based one-part AAMs mortar. Alrefaei et al.[43] incorporating 0.5% dosage (weight of precursor) of polycarboxylate ether (PCE) based superplasticizer on 50% FA/slag pastes to study the water retarder effects adsorption, reaction kinetics and rheology of one-part AAMs. The adsorption isotherms of PCE did not efficiently react (has no effect regardless of PCE dosage) with OPC systems prepared as control samples in the study, contradicting the AAMs system where the precipitation rate of PCE is lower (ineffective absorption) and well-integrated with the rheological behaviour of one-part AAMs. Furthermore, higher PCE content also reacts well with FA/slag mixtures. It has an effect on reaction kinetics where the heat released during the dissolution and polymerization process dropped with the addition of SP and but at the same time, prolonged the induction process. This phenomenon is well correlated with the reaction kinetics with added SP are related to the adsorption isotherms. Nevertheless, lower compressive strength at the early stage of curing recorded for the samples with 0.5% PCE, approximately 43 MPa, than control samples 48 MPa to support findings on the reaction kinetics and absorption result with SP addition in one-part AAMs could hinder the dissolution of precursors thus lower the compressive strength. Moreover, compressive strength at 28 days of age is also lower compared to control samples; hence it is agreed that adding admixtures will affect the mechanical strength of AAMs. An 8% anhydrous sodium metasilicate was used to activate the precursors with 0.39 of w/b ratio that can assist in reducing the yield stress and viscosity of fresh pastes, which contributed to better rheology behaviour of FA/slag pastes on top of superplasticizer effect as reported further in the study. Further investigations by Luukkonen et al.[72] on the suitability of commercial superplasticizer (SP) for one-part AAMs revealed that lignosulfonate (LS) based SP reacted efficiently with slag-based mortar and recorded better compressive strength at 28 days of age with about 40 MPa from 19 MPa (without SP). Adding LS into the mixtures will reduce yield stress and viscosity, which is beneficial to prolong the setting time of fresh AAMs mortars. Still, the yield stress development increases linearly over time without a drop, contrary to the two-part AAMs system. It also found that the maximum dosage of SP at 1.8% from precursor weight for practical workability. It's worth noting

that the  $\text{Ca}^{2+}$  chelation by LS improved the compressive strength, while the steric repulsion effect increased the workability as indicated by zeta potential measurements. However, the type and concentration of activator play significant roles in determining how the SP functions; therefore, the selection of SP and its dosage can only apply to specific one-part AAMs mix designs. In addition, three different types of superplasticizers were used (1% dosage) by Alrefaei et al.[31] to study its effectiveness in FA/slag pastes. Polycarboxylate (PCE) was the most effective SP compared to naphthalene and melamine SP. The PCE can be employed in a high w/b ratio above 0.36, while naphthalene performs better at a lower w/b ratio of 0.36 and below. However, the pastes are also activated with 12% anhydrous sodium metasilicate, where such a high concentration enhances the compressive strength of the pastes and may not require high water content due to increased alkalinity level for polymerization, but it can harm the stability of the admixture too as a setback. Coppola et al.[69] explained how ethylene glycol-based SRA and CaO-based expansive agents reduce the drying shrinkage of slag-based mortar. The combination of 1-2% SRA and 11% CaO modified the pore structure of the mortar, where the former was responsible for reducing the surface tension of pore water, thus decreasing internal stress during evaporation. In addition, the number of micropores in mortar samples also increased, which is beneficial for reducing capillary stress. For the latter, it has contributed to the delayed expansive of  $\text{Ca}(\text{OH})_2$  formation or, in other words, the transformation of calcium oxide to calcium hydroxide resulting in volume increment; hence, instead of shrinking due to loss of water, the samples will be expanding during an early stage of the hardening process. This phenomenon improved the drying shrinkage level of one-part AAMs. In addition, the  $\text{Ca}(\text{OH})_2$  from the reaction CaO with water will increase the alkaline environment for the geopolymerization process in one-part AAMs.

## **2.7 Rheology of binder**

### **2.7.1 Workability of one-part AAMs**

Many factors influenced the rheology behaviour of one-part AAMs. Apart from the effect on admixtures, w/b and aggregate-to-binder ratio (a/b) for rheology properties, the workability of

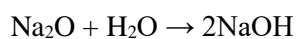
fresh mixes is also an essential element to understand. Low viscosity and high yield stress of one-part AAMs will ensure the compounds can flow efficiently and be stable for paste, mortar, or concrete applications. The workability of one-part AAMs can be measured by their flowability and setting time in the fresh state [47]. As reported in past studies, the workability of fresh one-part AAMs can be determined using a few methods. The slump test for new mortar can be performed according to EN 1015-3 specifications, while the setting time usually uses the Vicat needle method as per ASTM C191 guidelines [65]. Besides that, the flow table test, also known as the mini-slump test, is one of the methods used to determine the flowability of mixes over time following SFS-EN-12350-5 standard, EN 1015-3, ASTM C1437-15 [31][72], where the flow diameter of the compound will be observed until no further changes and the means of spread value will be obtained from flow table test. Haruna et al.[51] reported on the workability of one-part FA concrete activated with a 12% powdered sodium metasilicate activator which was measured using a standard slump cone test and recorded a very low slump value when a lower b/a ratio was applied. This trend was due to the mixture's low binder content, making it insufficient for aggregate to dissolve entirely and restricting its mobility. A slump value of 165mm recorded for a b/a ratio of 0.57 or about 60% total aggregate and 40% AAMs binder satisfied the typical slump value of between 165 mm to 220 mm for casting structural components. On the contrary, higher binder volume in b/a ratio may affect the concrete's compressive strength as enough aggregate is required to ensure a more stable structure, solid and better mechanical strength growth. In addition, it was reported that the dry mix of one-part AAMs has low workability compared to the two-part AAMs. Compared to the alkaline solution of sodium silicate and sodium hydroxide, the solid alkali activators composed of glass powder (GP) and NaOH has the lowest relative slump value in term of flowability but the longest setting time due to the inefficient dissolution process of Si ions from the glass powder in the water [42]. An experiment by Li et al.[73] on the rheology behaviour of one-part AAMs reported that with the amount of GP between 40% – 50% of one-part slag paste, w/b ratio between 0.325 – 0.35, and a/b ratio between 0.10 – 0.15 showed acceptable flowability and setting time, 100 mm – 190 mm of slump value and 60 mm – 90 mm of initial setting time. Many reports showed that the workability of fresh one-part AAMs would be reduced with the increasing amount of calcium-rich GGBFS. In addition, the additional

calcium from CaO content in the mixture could provide different nucleation sites for material to dissolve in the early stage due to the fast dissolution process resulting in quick hardening, shorten not only the overall setting time but also reducing the flow diameter of the one-part alkali-activated mixtures [65].

A highly alkaline environment significantly impacts the polymerisation process for the preparation of AAMs. With the increment of solid alkali activator dosage in the mixture, the flow diameter of one-part AAMs will also increase [64][65]. It was also reported by [39] that increasing alkali content activated by sodium silicate has a deflocculating and plasticising effect of increasing the workability of one-part AAMs. Meanwhile, Askarian et al. [30] reported that the type of solid activator had influenced the workability of one-part geopolymers, where sodium oxide was one of the most beneficial solid-powdered alkali activators able to increase the flowability of mixes. In contrast, blends activated by potassium carbonate have lower workability. The composition of 9% Na<sub>2</sub>O and 12% Na<sub>2</sub>SiO<sub>3</sub> were used to activate 100% Fly Ash. This research on the effect of one-part geopolymer started with different types of activators. The hydration process of solid Na<sub>2</sub>O is exothermic and more reactive than sodium hydroxide. Therefore, when it dissolved in the water, it will produce double reactivity of sodium hydroxide.

The reaction can be derived as

Equation 3 below:



Equation 3

Admixtures with retarding effect were reported to improve the workability of one-part AAMs mix significantly. Including a certain percentage of admixtures in the mixture, however, could lengthen and shorten the setting time and increase the flowability of the mix. Superplasticizer (SP), also known as water-reducing admixtures, is used to reduce the water content to enhance concrete's mechanical strength and durability. This type of admixture will plasticise and fluidise mixtures by electrostatic or steric repulsion mechanism and influence the flowability and setting time of one-part AAMs [31]. Superplasticiser-based admixtures can also adsorb particles and block the reactive sites, electrostatic and steric repulsion based on the superplasticiser type and cause the level of hydration and fluidity of one-part AAMs to be affected, as reported by

Luukkonen et al.[72]. Previous research also suggested that at 4% to 6% of Borax amount – another type of admixture added into the mixture has shown a consistent performance for its retarding function in one-part AAMs, both on flowability and setting time [74]. Coppola et al. [69] reported that including expansive-based admixtures reduced the workability in one-part AAMs mortar and pasted composed of high reactivity calcium-oxide by 20 – 30 min. In contrast, other shrinkage control-based admixtures such as methylcellulose (MC), modified starch (MSt), and ethylene-glycol-based shrinkage-reducing admixtures (SRA) did not affect the workability of the mixtures. Furthermore, the air-entraining admixture (AEA) is also recognised as one of the concrete admixtures used for freezing and thawing resistance. Therefore, it also plays an essential role in enhancing the workability of one-part AAMs reported by [39].

### **2.7.2 Flowability**

High water temperature used for mixing one-part AAMs mixtures will reduce the slump level and accelerate the slump loss rate. This phenomenon is because the heat released from the high temperature of the mixture increases the water evaporation level, resulting in more water loss. Alkali concentration will become dominant when water is reduced. The rise of pH could accelerate the formation of hydration products due to the formation of new physical and chemical bonds among products in the mixture. Besides that, higher alkali activator dosage also reduces the flowability level of one-part AAMs due to the flocculation of the suspended particles that appear in the mix [64]. Many researchers reported that including fibre in the one-part AAMs decreased the flowability performance of the paste in the mixture. When fibre is increased, the workability of the one-part AAMs will decrease where the micro-steel fibre was the lowest workability recorded, as reported by Shah et al.[59] previous research on the effect of fibre type and content in one-part AAMs mortar. The slump value between 165 mm to 220 mm with the standard compaction method was reported as acceptable workability for casting structural members of one-part alkali-activated concrete. The paste-to-aggregate ratio at 0.57 has recorded a 165 mm slump value, as Haruna et al.[51] conducted in the study on the effect of aggregate paste ratio for one-part alkali-activated concrete. The coarse aggregate's size varied from 20% of 20 mm, 20% of 14 mm, 30% of 10 mm and 30% of fine aggregate. A low volume of binder to

total aggregate could decrease the flowability of the mixture due to the aggregate's inability to move efficiently, associated with the size of the particles influencing the mixes' workability. This influence of the particle size on the flowability findings was supported by Chen et al. [34], where additional 20% fine tailings mixed with 80% GGBFS at constant water/binder ratio and alkali activator, the flowability level dropped to 170 mm compared to 190 mm of 100% GGBFS proved that the finer the zinc-mine tailings used, the lower its flowability was. Oderji et al. [28] suggested 15% GGBFS was the optimum amount to be mixed with Fly Ash to obtain adequate workability on geopolymer binder activated by an 8% dosage of  $\text{Na}_2\text{CO}_3$ . Adding 15% GGBFS, rich in CaO, could decrease the initial setting time to 40 min. Still, the flowability of the mixture was reduced when increasing the slag content up to 20% due to the increment of CaO. Another factor, such as the angular shape of the slag particles, could reduce the workability of the mix. Shah et al. [65] used 8%, 9% and 10% of  $\text{Na}_2\text{SO}_3$  to assess the early strength of one-part alkali-activated FA mortar where a mixture of 70% FA and 30% GGBFS activated by 10% of  $\text{Na}_2\text{SO}_3$  and 5% borax showed the highest flow diameter of 27 cm. When 8% of  $\text{Na}_2\text{SO}_3$  was used, the flow diameter was reduced to 17 cm within the range of acceptable slump value for concrete structure. Borax was also used as a retarder to prolong the hydration process in one-part AAMs. Borax forms a calcium–borax layer when dissolved in the water, reacting with  $\text{Ca}^{2+}$  ions. Due to this development, borax can retard the hydration process and prevent crystal disconnection of the cementitious structure [65][74]. Besides borax, it was reported that all superplasticiser-based admixtures increase the flowability-spread value up to 41% of one-part AAMs mortar composed of GGBFS and micro silica and activated by sodium hydroxide powder [72]. The flow diameter for the one-part FA/GGBFS binder activated by 8% of anhydrous sodium metasilicate ( $\text{Na}_2\text{SiO}_3$ ) has 28 cm and 15 min, w/b ratio of 0.32. In contrast, it has a 24 cm flow and 10 min duration for a w/b ratio of 0.28 which is not flowable. This finding was consistent with the report on the critical role of water content in FA-based mixtures for exothermic reactions, poly-condensation, and stabilising the geopolymerization process. With a retarder admixture of 4% borax, the flow diameter has increased by 33 cm and 40 min duration, while with 6% borax, it has a 34 cm flow diameter and 65 min duration [74].

The workability of AAMs mortar composed of GGBFS and shrinkage controller-based admixtures has recorded 140 – 160 mm, demonstrating the effect of admixtures can increase the flowability of the mixes as reported by [69] on the impact of shrinkage-reducing admixtures in one-part AAMs tested on mortar and paste samples. Adding air-entertaining admixtures (AEA) in one-part AAMs GGBFS mortar has 50% more workability than the mixes without AEA due to spherical air bubbles acting as a fine aggregate of meagre surface resistance. The mean value of flow tables for compounds with AEA was recorded between 185 – 220 min compared with compounds without AEA, which was between 160 – 190 min [39]. Furthermore, Teo et al.[15] using a high calcium Class, C-FA combined with GGBFS to produce one-part AAMs paste cured under ambient temperature, revealing its fresh paste properties on flowability. Replacement between 30 – 50% FA with GGBFS has improved the flow spread diameter from 196.5 cm to 214.75 mm, but when GGBFS exceed 50% volume, the fresh pastes become stiff and set quickly. The  $\text{Na}_2\text{O}$  ( $\text{Na}_2\text{O}/\text{SiO}_2$  ratio) concentration of precursor and solid activators determined the flow characteristic in terms of cohesivity and viscosity of AAMs. Via spread flow diameter test, the flowability of one-part AAMs correlated with the increase of  $\text{Na}_2\text{O}/\text{SiO}_2$  ratio and in this experiment, the ratio was between 0.118 to the optimum 0.167, with higher than this ratio may cause the flowability to decline. A higher alkali activator dosage of sodium metasilicate anhydrous between 4 – 8% was used to activate 50% FA/slag pastes to achieve desired  $\text{Na}_2\text{O}/\text{SiO}_2$  ratio on the other side, it is considered corrosive and may require extra precautions for handling at the site. The average diameter of spread flow was recorded as 238.0 mm for 0.118 ratios ( $\text{Na}_2\text{O}/\text{SiO}_2$ ) and 266.0 mm for 0.167 ratios ( $\text{Na}_2\text{O}/\text{SiO}_2$ ) and subsequently decreased to 249.75 mm, 214.75 mm, and 126.68 mm for  $\text{Na}_2\text{O}/\text{SiO}_2$  ratio of 0.19 (10% activator), 0.211 (12% activator), 0.232 (14% activator) to explained further on the  $\text{SiO}_2$  ( $\text{Na}_2\text{O}/\text{SiO}_2$  ratio) influenced from the amount of solid activator. Nonetheless, pastes with higher spread diameter in this report have lower compressive strength at 28 days of age compared to the paste's samples with lower spread diameter. Perumal et al.[75] reported that a higher (w/b) ratio from 0.25 to 0.35 will increase the percentage of spread value of one-part AAMs slag pastes. Excessive water content may lead to bleeding problems and not improve the spread diameter level. Moreover, the irregular shape of particles may require higher water demand to maintain the fluidity of the AAMs

mixtures, contradicting a larger type of particle size and lower surface area that is useful in reducing water demand. The report also mentioned including silica fume content in the slag-based paste will improve the cohesiveness of the cement paste compared to phyllite dust as a source of aggregates. Luukkonen et al.[71] conclude that one-part AAMs composed with FA/slag have thixotropic behaviour, which is useful for mixing and vibration to produce high workability. Still, its workability will be affected if a high amount of sodium silicate-alkali activator is employed. Moreover, as mentioned in the report, the workability level of one-part AAMs is about 35% lower than standard two-part AAMs. Zhang et al.[50] analyzed in detail the influence of fine sand powder–modified river sand as fine aggregate sources on the fluidity of AAMs slag mortar and explained that the more fine aggregate content, the larger fluidity of the slag mortar mixtures. Higher fluidity levels may cause bleeding and segregation as part of poor stability. On the other side, low fluidity will produce high viscosity of fresh mortar. It cannot depend on its gravity to spread over, limiting its application on grouting, injection or patching. To elaborate this phenomenon further, a larger specific surface area of fine aggregate than precursor required more water that produced thinner water film form by free water on the fine aggregate surface and undissolved precursor particles, increasing the frictional resistance between particles. After all, the shear stress of fresh mortar increases with fine aggregate increases. Furthermore, the gel proportion in fresh mortar reduced with the increment of fine aggregate volume in the mixtures and as a result, the lubricating layer formed by the hydration gel is unable to protect the surface of both precursor and fine aggregate that, leading to internal resistance, therefore, increase the yield stress of fresh AAMs mortar. Ren et al.[36] recorded that one-part slag pastes had a comparable spread flow diameter (239 mm) when comparing one-part AAMs slag mortar with conventional systems where the two-part system has recorded fluidity of 235 mm without sodium silicate dissolved in water, but when activating the dry mixtures of one-part AAMs, the mortar still demonstrated a homogenous fresh mixture, a firm with no bleeding and segregation.

### **2.7.3 Setting Time**

The initial setting time depends much on the water temperature and exothermic reaction when heat is produced from the dissolution of a solid activator such as alkali hydroxides in one-part

AAMs. These thermal factors, however, have influenced only the initial setting time, where the heat from the surrounding environment could affect the temperature of the mixtures at the final setting time [38][44][55][62][64]. In agreement with this literature, Yang et al. [63] used calcined dolomite (CD) to boost heat release from the polymerisation process of one-part AAMS activated by GGBFS and solid sodium carbonate. Adding CD has removed the carbon dioxide ions, expedited the reaction kinetics of  $\text{Na}_2\text{CO}_3$ , increased the cumulative heat release (J/g), and reduced the paste's setting time. A total of 10% of CD and 10% of  $\text{Na}_2\text{CO}_3$  from 100 grams of GGBFS were used in the experiment to study the effect of CD addition in one-part alkali-activated slag cement. Higher alkali dosage and lower activator modulus will accelerate the alkali activation process, thus decreasing the concrete's setting time. At 30 °C of water temperature and 8% of powder anhydrous sodium metasilicate activators, the setting time of one-part alkali-activated slag was recorded between 50 – 85 min as tested using a Vicat needle method as per ASTM C191-19 standard prepared by [64] in the previous report on the effect of mixing water temperature on one-part AAMs. One-part alkali-activated FA/GGBFS mortar activated with 8%  $\text{Na}_2\text{SO}_3$  and 5% Borax has recorded a setting time between 50 and 200 min [65]. Also, in the research conducted by Cun Liu et al. [66], a porous honeycomb ceramic (HCC) was used as the primary alkali activator mixed with solid sodium hydroxide to control the consistency of activator modulus has reduced the setting time of one-part alkali-activated slag paste. The initial setting time was decreased by 5 h and 10 h for 5% and 1% increments of HCC and NaOH content, respectively. The lowest setting time was recorded for the composition of 40% HCC and 6% NaOH from the total weight of GGBFS in the paste samples. Wei Lv et al. [76] replaced tap water with seawater to understand the performance of 80% GGBFS and 20% FA in one-part AAMs and found that the initial and final setting times were reduced and shorter than the ones mixed with tap water. This was because the formation of Calcium chloride ( $\text{CaCl}_2$ ) from seawater which released  $\text{Cl}^-$  ion and  $\text{Ca}^{2+}$  from the precursors, could accelerate the cement hydration of the mixes. The initial setting time for GGBFS mortar activated by micro silica (MS) and NaOH powder has the slowest setting time compared to the sodium silicate series. However, both sodium and silica alkali-activated sources had initial setting time recorded between 19 – 72 min and met with the required initial setting time for regular concrete within 45 – 75 min according to the EN 197-1:2000,

standard on the concrete strength class as reported in the previous research done by Luukkonen et al. [62]. This report also found that the MS and NaOH have the fastest final setting time at 135 min compared to the sodium silicate activator at 210 min where this finding satisfied the previously reported by other researchers on initial and final setting time for one-part AAMs between 23 – 150 min and 69 – 230 min. Too short of initial setting time, however, does not comply with ASTM C807 – 18 specifications for actual application, thus [60] replacing up to 80% of GGBFS with FA can extend the setting time of one-part alkali-activated mortar composed of GGBFS, FA and natural aggregates. Elijah et al.[44] have reported that the initial setting time for the mortar made from the composition of 85% GGBFS and 15% of desulphurisation dust (DeS-dust) has a shorter setting time at 60 minutes which was within the range of recommended initial setting time as per EN 197-1, 2011 specification - depending on the strength class. Des-dust was used to replace commercial sodium hydroxide as an activator for alkali activation in one-part AAMs mortar. Initial setting time was recorded longer with a high water-to-binder ratio, w/b, as reported by [74] in studying the influence of admixtures on the workability and strength of one-part FA/GGBFS binders. The initial setting time for the w/b ratio of 0.3 was about 35 minutes, and it was 60 minutes when the w/b ratio of 0.32 was applied.

However, when 8% Borax was added to the mixture, the longest initial setting time increased to 120 min. The slowest initial setting time with adding 2% borax was about 60 min compared to control mixtures without borax, which was about 40 min. However, lignosulfonate (LS) also has retarding effect on the setting time of one-part AAMs, as reported by Luukkonen et al. [72], where besides naphthalene, melamine and polycarboxylate-based superplasticiser [31] compared to another type of superplasticiser-based admixtures which has accelerated the initial and setting time of one-part AAMs mortar. The initial setting time was approximately 26 minutes compared to 13 minutes for the FA/slag pastes without SP. It has recorded about 48 minutes from 27 minutes (without SP) for the final setting time. These three superplasticizers work efficiently under high dosages of sodium metasilicate but have a comparable effect on the setting time because of the adsorption properties of superplasticizers on precursor material. L.Coppola et al. [69] reported the setting time for one-part AAMs to paste composed of GGBFS and shrinkage controller-based

admixtures mixed between methylcellulose, expansive agent and shrinkage reducing admixtures were recorded between 50 – 150 min of initial and final setting time, which beneficial for concrete patching repair application. Including methylcellulose, modified starch, and shrinkage-reducing admixture can lengthen the setting time of one-part AAMS. Still, in contrast, adding calcium oxide (CaO) based expansive agent admixtures could reduce workability and setting time. Askarian et al. [38] reported that the initial setting time was 60 min, and the final setting time was about 110 min for a one-part hybrid OPC geopolymer concrete. A total of 3% potassium carbonate was used as an alkali activator, and 20% of OPC, 8% GGBFS, and 72 % FA were the main aluminosilicate precursors composition used in the experiment. Besides that, one-part AAMs consisting of 40% OPC, 6% GGBFS and 54 % FA were tested and recorded for 40 min and 80 min for the initial and final setting times, respectively. Including OPC can accelerate the setting time, but the setting time will decrease if OPC is above 30%. However, the setting time of the mixes still can be controlled by using acid nitric, besides superplasticiser-based admixtures that functioned as accelerators and retarders. The more extended setting of concrete, however, will be caused low strength development, resulting in lower compressive strength in early curing age [66]. Yin et al.[35] replace 10% slag paste with rice straw ash (RSA) and found that the one-part AAMs paste has an initial setting time longer than sole slag content and shortens its final setting time. The RSA also contributed to higher yield stress in slag paste due to its porous nature, allowing for higher absorption capacity that can reduce the free water content of the paste samples for a better early compressive strength. In addition, weaker RSA reactivity, compared to slag, creates more unreacted RSA beneficial to increase consistency and control hydration rates at an early stage. The initial setting time for slag-based paste was 78 minutes but prolonged to 88 and 95 minutes with 5% and 10% RSA content, respectively. The final setting time decreased from 158 minutes to 145 and 120 minutes for each 100% slag paste, 5% and 10% RSA replacement. Nevertheless, including RSA also impacts higher pore volumes of the hardened paste samples besides creating larger gels and capillary pores diameters. In addition, higher lime kiln dust (LKD) content between 35 – 40% of precursor weight used as a solid activator has caused slow alkali activation in metakaolin-based pastes. LKD was added to supply extra  $\text{Ca}^{+2}$  alkaline cations to form extra  $\text{Ca}(\text{OH})_2$  beneficial for breaking and dissolving Si-Al chains, speeding up the alkali

activation reaction and enhancing the setting time. The more alkaline part becomes active, the longer setting time will be due to more dissolution product where the standard initial and final setting time for one-part AAMS was recorded between 23 – 150 minutes and 69 – 230 minutes, as reported by Kadhim et al.[77]. On the contrary, excessive unreacted activator sources and metakaolin may react with CO<sub>2</sub> in the air, forming efflorescent on the surface, affecting the strength of one-part AAMs. Abdollahnejad et al.[57] investigated the addition of ceramic waste as part of replacement in the slag-based paste and found that the setting time of the pastes was prolonged more than 30 minutes with 5 and 10% of ceramic volumes, regardless of its ceramic type, compared to 100% slag-based AAMs only recorded about 20 to 28 minutes of initial and final setting time, impractical for real applications. It is worth noting that mortar required a longer initial setting time due to aggregates and high water content; significantly finer particles that require more water to enhance the interaction with water and lengthen the setting time [54].

According to the standard EN 197-1, the initial setting time should be 45 to 75 minutes. Setting time can be increased if solid calcium carbonate decreased or sodium hydroxide were kept constant and when the amount of slag was added in the mixtures as elaborated by Luukkonen et al.[71]. It was reported that fine sand powder could lengthen the setting time of one-part slag used for semi-flexible pavement grouting materials, as described by Zhang et al.[50]. An addition of 5% fine sand powder recorded an initial and final setting time of 35 and 50 minutes, while a 20% addition recorded a longer setting time of 74 and 90 minutes, both initial and final setting times. This trend started when fine sand powder dispersed in the fresh mortar, with small particle sizes, helped to delay the reaction between silicon and aluminium ions for the hydration process. Also, adding this fine aggregate reduced the proportion of solid activator, thus weakening the dissolving and exothermic effect from the activator, subsequently delaying the endothermic reaction of calcium (Ca<sup>2+</sup>) produced from slag dissolution and silica gel polymerization. This overall phenomenon was explained by the report's increased initial and final setting time of one-part AAMs slag mortar activated with a higher dosage activator of solid water glass (20% sodium silicate). Alrefaei et al.[43] explained that two methods can be applied to add superplasticizer in one-part AAMs mixture; early addition and delay addition, where the latter has better influence

on rheology properties than the former. Delay addition of SP with mixing water can reduce the yield stress to compensate for the early loss of water for the dissolution process of FA/slag mixture at an early stage. Also, silicates species can be readily adsorbed in precursor without competition with SP for a smooth geopolymerization process and finally delay the overall setting time of the AAMs paste regardless of which addition method uses as the PCE-based SP delaying the hydration process by lowering the dissolution rates at an early stage of the hydration process. Ren et al.[36] reported that the one-part slag-based paste's initial and final setting time is higher than its conventional two-part system. The setting recorded between 123 – 310 minutes for a one-part system, much longer than the initial between 58 – 82 minutes for a two-part system. Nevertheless, in this study, a significantly high dosage of 7% anhydrous sodium metasilicate ( $\text{Na}_2\text{SiO}_3$ ) was used besides some evidence of crystals in microstructure analysis as an indication of efflorescence problem, which might affect the durability of this type of mortar. It is understood that dry slag and alkali activator mixtures were mixed first. This caused the gelation and condensation processing delay before water was added for the dissolving process, subsequently delaying the dissolution of silica and alumina species. A solid alkali activator was also mentioned as a reason for the slowing hydration rate compared to a liquid activator in a conventional AAMs system. Furthermore, the reaction between CaO, Si from the activator and Al from the slag when water is added could create a complex reaction shell surrounding slag particle surfaces that further hinder the hydration process of the fresh mortar.

## **2.8 Mechanical properties of one-part AAMs.**

The active dissolution of silica (Si) and aluminium (Al) in the polycondensation process enhances concrete strength development. It was reported that when Al content increased up to 1.5%, the compressive strength of one-part AAMs comprised 26% OPC, 58.3% FA and activated by 8% sodium hydroxide and 7.7% calcium hydroxide was increased [12]. Early strength development also depends on the concentration of activator dissolved in the mixes [18][66]. On the contrary, a decrease in concrete strength is known to be caused by microcracking [62]. Microcracking starts propagating as a natural process during the hydration process of cement mixes. This situation has been caused by other factors, such as compression load applied, environmental exposure or pre-

existing crack. Many factors could reduce the strength of concrete composed of one-part AAMs varying on its aluminosilicate part, solid activators, design mix, and admixtures' effect, besides curing regime factors, including temperature and relative humidity.

Water has played a significant role in the strength development of one-part AAMs. The former is vital for dissolution, polycondensation and the hardening stage of the geopolymerization process. Water exposure during the geopolymerization process is beneficial for rapid reaction in one-part AAMs due to the quick hardening process for higher and early mechanical strength development with calcium compounds and designated design mixes [38]. On the other hand, a high water-to-binder ratio could decrease the compressive strength of one-part AAMs, primarily samples composed of GGBFS [47][74]. Many reports that the amount of GGBFS was replaced by fly ash (FA) to control water proportion requirements [74]. This trend was further proved by Adriano et al. [29], which found that compressive strength value was higher for one-part AAMs composed of 30% ceramic waste, which required less water than conventional aluminosilicate precursors used to produce one-part AAMs. Askarian et al. [30] reported one part AAMs mortar sample with a w/b ratio of 0.35, which achieved 78 MPa compressive strength and 0.45 MPa for the paste sample.

There are three types of concrete curing: ambient curing, standard curing, solar curing, and water curing. Solar chamber and ambient curing are typically under laboratory temperatures between 23 – 25°C. Water curing usually submerges the samples at a temperature of 20°C, as recorded in a previous report by Sani et al. [51]. Relative humidity in the laboratory is usually below 50%. Curing in the air or sealed proved to have more effects on geopolymerization. The process could discharge the fraction of water molecules during reactions and require lesser water molecules than conventional Portland cement's hydration process [16].

Superplasticiser (SP) positively impacted the compressive strength of one-part AAMs. Higher superplasticiser dose and lower water contain amount could increase the 28-day compressive strength as recorded by Luukkonen et al. [72] though all types of SPs, when mixed with binder,

could affect the mechanical strength of AAMs due to the stability behaviour of admixtures in different alkali environment mainly on different type of alkali activator. While melamine and polycarboxylate admixtures may have a positive impact in one-part AAMs to develop early compressive strength at 1 – 7 days but for long-term strength development, i.e. 28-day, the experiment results have shown that the compressive strength decreased between 5 – 7% but still better than conventional two-part AAMs which recorded compressive strength dropped up to 43% [31]. It is also reported that 4% of retarder used in one-part FA / GGBFS mortar has significantly higher early-age compressive strength. On the other hand, using a 3% retarder could affect strength development at 28 days of age [65].

Sodium triphosphate (STP) and borax are suitable retarders to increase mechanical strength for one-part AAMs [74]. The use of silica fume (SF) as admixture could decrease the compressive strength, especially at an early age when its volume increased from 5% to 15% due to more silicon from SF countered with water creating more hydrogen gas that caused more pores found in one-part AAMs samples reported by Li et al. [47]. In contrast, L.Coppola et al. [69] said that the addition of admixtures, namely shrinkage reducing admixture (SRA), calcium oxide-based expansive agent (EA), methylcellulose (MC) and modified starch (MSt), could reduce compressive strength and modulus of elasticity of one-part AAMs even though these type admixtures may be beneficial to reduce shrinkage level of the AAMs mortar and paste and complied with standard strength requirement for concrete repair materials. For air-entraining admixture (AEA), however, enhance the freezing and thawing resistance of one-part AAMs mortar without affecting its compressive strength due to high pH level, which encourages the dissolution of silica and alumina of AAMs composed of GGBFS for the formation of denser microstructure subsequently produce higher compressive strength level [39].

The influence of alkali activators on the mechanical strength of AAMs was also discussed by Samarakoon et al. [42]. It was clearly understood that liquid alkali activators delivered a higher hydration reactions rate and offered more rapid dissolution on solid precursors than solid activators. However, due to factors such as worker handling problems, convenience, porosity and

cost, solid alkali activators were used to activate the AAMs, and the performance of the former was proved able to provide excellent and similar standard mechanical strength results as what liquid alkali activator has offered. Besides solid sodium hydroxide, NaOH and sodium silicate, Na<sub>2</sub>SiO<sub>3</sub>, the dry activator powder (DA) prepared by mixing glass powder and solid Na<sub>2</sub>SiO<sub>3</sub> were used as an alkali activator for one part FA/GGBFS AAMs showed compressive strength was about 30 MPa at 28 days of age which complied with mechanical strength requirement for concrete and the best choice for alternative alkali activator to develop since it was found cheaper and greener than commercial alkali silicates. Nevertheless, the retarded dissolution of solid activator (DA and Na<sub>2</sub>SiO<sub>3</sub> as a sole activator) has affected the strength development of one-part AAMs after 28 days of age compared to the two-part AAMs reported in this study.

It was reported that the yield stress of two-part alkali-activated pastes did not increase for up to 27 min of measurement. Some cases recorded increments for yield stress at first but gradually dropped due to the formation and destruction of the C-A-S-H gel. Several factors may enhance yield stress development, such as water content, type of aluminosilicate precursor and alkali activator, and the viscosity of the alkali activator. This report also confirmed that there was no drop in yield stress over time which is an advantage of one-part AAMs for their mechanical strength compared to their conventional AAMs counterpart, as explained by Luukkonen et al.[72].

### **2.8.1 Compressive Strength.**

H. Choo et al. [18] studied the compressive strength of one-part AAMs composed of fly ash (FA) activated by red mud and described that red mud as a solely NaOH supplier could increase the pH level of FA. It is known that the geopolymerization process was only efficient when the pH of the alkaline solution was more than 11. When the alkaline environment of the mixes increased, the dissolution of silica and aluminium from FA/red mud would promote the polycondensation process, subsequently increasing the unconfined compressive strength. To conclude this experiment, it was found that inorganic-FA activated by sodium silicate and sodium hydroxide can accelerate the polycondensation process more excellently than sodium hydroxide only and have better mechanical properties. The one-part FA triggered by red mud did not satisfy the

concrete strength requirement for structural use, but applying it to other construction materials with low strength requirements is helpful. Additional calcium hydroxide also contributes to the increased pH value to encourage the geopolymerization process. 60% of OPC volume was mixed with FA and GGBFS as the primary aluminosilicate precursor and has shown remarkably higher compressive strength than hybrid geopolymer samples without an activator. It was reported in past research that the inclusion of slag could increase 68 – 123% of one-part AAMs compressive strength at 28 days of age [30], while for this experiment, the compressive strength of geopolymer hybrid samples composed of OPC between 10% to 60% and activated by potassium carbonate recorded between 33 – 55 MPa at 28 days aged compared to the hybrid geopolymer control samples without activators which only managed to have between 18 – 40 MPa of compressive strength as reported by Mahya et al. [38] for the study on mechanical properties of OPC-geopolymer concrete subsequently explain the significant roles of alkali activator as well as the influenced of OPC, calcium-rich precursors in one-part geopolymer concrete.

A porous honeycomb ceramic (HCC) was mixed with sodium silicate solution used as a powder alkali activator with powdered sodium hydroxide for one-part AAMs activated GGBFS in research conducted by [66] to study the effect of HCC on the compressive strength of one-part AAMs. It was found that the compressive strength of the AAMs activated by 5 – 6% of NaOH and 40% HCC was 20 MPa and over 40 MPa tested at 3 and 28 days of curing age. HCC has about a 20% water absorption rate by mass, making it suitable as its porous carrier allows sodium silicate to be released slowly when it is in contact with water, subsequently extending the hardening process beneficial for controlling and supplying concrete to the site. Water curing and standard curing on one-part AAMs were reported to have a significant effect on the compressive strength of the mixes. A previous study found that the compressive strength of specimens stopped increasing and decreased after 7 days of using a water-curing system.

In contrast, the strength of specimens kept rising after 7 days when the standard curing system was applied. The strength of one-part AAMs relies on the geopolymerization process, the reaction degree, and the number of hydration products where these processes produce aluminosilicate gels

that can release water traps in the hardened mix [65]. Past research revealed that when a water curing system was used, the ions, mostly hydroxide ions, leached from the specimens to the water, decreasing the samples' pH value and reaction degree. Also, the reaction degree of water curing is influenced by undissolved activators. The compactness of the matrix and the addition of ultra-fine fly ash sinking beads (FASB) have improved the solidity matrix of one-part AAMs by reducing the leaching percentage of ions into the curing water. Besides, other factors that may disturb the strength development of one-part AAMs are the higher water-to-binder ratio, the more ions will be leaching out, and the amorphous level in aluminosilicate minerals also affects the chemical reaction in the geopolymerization process [78]. Apart from that, M. Almkhadmeh et al. [64] found that increasing up to 10% activator dosage resulted in higher early-age compressive strength at 1 day of age but had a minimal effect at 28 days. The former has indicated that increasing activator dosage will improve slag reactivity at 0 °C temperature of mixing water. The latter has proved a shorter orientation phase in the heat of the hydration process. In the early ages of the hardening process, one-part GGBFS / 10% anhydrous sodium metasilicate paste mixtures mixed with 0 °C water recorded higher compressive strength due to exothermic energy released from the activator hence increasing solubility and dissolution rate to boost the polymerisation process at early hardening ages.

In contrast, a higher temperature of mixed water, for instance, 30 °C, could accelerate product formation and create a higher porosity level, resulting in slow compressive strength development due to the low quality of hydration products besides other factors such as slow hydration process nature between slag and sodium silicate activator but higher later strength. Shah et al. [65] researched one-part FA / GGBFS AAMs mortar samples cured at 20 °C, 30 °C, and 65 °C room temperatures. They reported that the compressive strength increased at an early age test with increased curing temperatures (65 °C). This phenomenon was due to high rates of geopolymerization reaction, which is much required on heat intensity to boost the reaction and break the Si-O and Al-O bond from SiO<sub>2</sub> and Al<sub>2</sub>O<sub>3</sub> to produce new Si-O-Al products. The 30 °C cured samples have shown better compressive strength tested at 1, 7, and 28-day indicates that heat may help boost reaction at an early age but has no effect on the final products. However, a

higher temperature may draw a setback at 28 days of compressive strength due to extreme dissolution reaction intensity. This situation may cause the evaporation of excess water from the cavities, thus increasing porosity and subsequently affecting the strength development in the long term. The compressive strength of one-part AAMs activated by high-calcium class-C fly ash and granular sodium metasilicate activator tested with paste to aggregate ratio at 0.35 was recorded around 50 MPa for 3 days curing age, 70 MPa at 28 days and kept increasing up to 90 MPa at 90 days using solar cured regimes as reported by [51]. Crack propagation and pores volume of one-part AAMs is reported to be reduced at the early ages, where it was filled by the number of gels from the geopolymerization phase was the reason for the continuous development of compressive strength after 28 days, dissimilar with the one-part AAMs activated by GGBFS, which the strength reported decreased after 28 days of curing age. It is worth mentioning that in this experiment, for the paste-to-aggregate ratio, a higher volume of aggregate and a lower paste volume could increase the compressive strength of one-part AAMs due to the more stable structure offered by the aggregate, proving that the inclusion of aggregate has an accelerating role [30] besides no solid evidence for relating higher compressive strength value with the water curing system and standard curing. It was reported in past research that there was an alternative source to replace aggregate function in one-part AAMs.

Additionally, Z. Abdollahnejad et al. [79] researched the effect of ceramic waste used as aggregate in one-part AAMs activated by FA and GGBFS. The highest compressive strength is achieved when 10% slag is used to replace FA, but higher FA content will cause a lack of calcium to include in the mixture. Replacing natural aggregate with ceramic waste proved that it compensates for the strength loss. A result showed that at 28 days of age, 100 MPa was recorded for compressive strength while using 80% FA with a natural sand aggregate only achieved around 40 MPa at the same testing age. Ceramic aggregates are known to have a high aluminium and silica content. They can absorb a high amount of water in the mixture, subsequently increase the pH value, and lower the water/binder ratio, consequently improving the mechanical strength of AAMs composed of fly ash. Too low water/binder, however, could lead to surficial cracking. On the

contrary, the increasing water content will cause compressive strength to decline, as reported by Oderji et al. [74].

It was reported that higher alkali content would improve the one-part AAMs resistance against severe conditions [39]. The effect of alkali activator dosage in one-part AAMs was further investigated by Yang et al. [80], and found that 5% dosage (in terms of weight) of calcined oyster shell powder (COS) used as alkali activator for GGBFS paste has recorded higher compressive strength at 28 days testing compared to those paste activated by 10%, 15% and 20% demonstrated that strength development was also influenced by a dosage of activator at later ages while an excess of dosage harms strength development of one-part AAMs slag besides other issues such efflorescence [30]. Additional calcium sources significantly impact the geopolymerization process, where the former enables shortened setting time and improves the mechanical properties [38]. Therefore, higher alkali concentrations may increase geopolymerization rates. On the other hand, the excess amount of alkali used could decrease the compressive strength of AAMs due to the growth of calcium hydroxide, reducing the amount of existing calcium to form C-A-S-H gels [47]. However, due to the high amount of CaO in COS and the excessive intensity of hydroxide ions in gels precipitation, unused portlandite could publish early C-S-H formation and subsequently affect later-stage strength gain. The compressive strength of AAMs pastes activated by 5% COS in the report has recorded 13 MPa at 7 days and 35 MPa at 28 days curing ages. Askarian et al. [30] used 12% of binder weight for sodium silicate powder, 9% for calcium hydroxide powder and 6% lithium hydroxide to activate one-part AAMs paste composed of 50% FA and 50% GGBFS, and this specimen recorded 38 MPa of compressive strength tested at 28 days of age. Commercial solid water glass powder with an alkali dosage of 1.5 Na<sub>2</sub>O% activated one-part AAMs composed of GGBFS and fine lead-zinc mine tailings [34]. It was found that 10% was the optimum volume of fine tailings to enhance the development of compressive strength and achieved up to 30 MPa at 28 days which much linked to its influence on increasing pH value in pore solutions and sped up the reaction of binders at an early age (below 7 days of age) subsequently improved the compressive strength of one-part AAMs samples activated by low

alkali dosage of water glass which has lower Ca content that could decelerate geopolymerization process [47].

Peng et al. [81] reported that sodium silicate is more efficient for producing one-part geopolymers where the former has influenced the compressive strength and improves the water resistance compared to NaOH at the exact content of Na<sub>2</sub>O. This experiment also found that two-part geopolymers have more water resistance than the one-part due to faster completion of the hydration process, thus achieving the highest compressive strength within 3 days of curing. Still, the long-term compressive strength of one-part geopolymer increased after 3 days due to the continual hydration process. In other reports, a one-part geopolymer composed of 85% FA / 15% GGBFS and activated by 8% Na<sub>2</sub>SiO<sub>3</sub> only was the optimum composition by providing better compressive strength results tested at 28 days of age followed by a mixed Na<sub>2</sub>SiO<sub>3</sub> / NaOH activator, and the lowest was with KOH and NaOH only, and the activator mixed Na<sub>2</sub>CO<sub>3</sub> / NaOH. Lower strength development when reduced sodium silicate activator content is commonly noticeable and significantly caused by a change in molar ratios, especially the lower Na<sub>2</sub>O content. Na<sub>2</sub>O and SiO<sub>2</sub> will enhance reaction activities in one-part AAMs to create solid and stable structures after stiffening for better compressive strength development [29]. Besides the activator dosage factor, the type of alkali activator also plays an essential role in determining one-part AAMs' compressive strength. Adesanya et al. [44] reported that one-part GGBFS mortar activated by 15% DeS-dust has 32.5 MPa compressive strength level with the inclusion of 3% micro silica (MS) to increase the solvable silica content in the mixes at constant value 0.13 of Na<sub>2</sub>O. The Ca and Fe content in DeS-dust has contributed to the higher strength of one-part AAMs, where the dissolution of this additional element causing to hardened properties compared to the specimens activated by commercial NaOH following EN 196-1 of cement mortar specification method. The Na<sub>2</sub>SO<sub>3</sub> powder was used as the sole alkali activator to study the effectiveness of SP in one-part AAMs, where it found that polycarboxylate was the most effective admixture for higher w/b ratio (i.e., 0.4) and naphthalene performed better at lower w/b ratio (i.e., 0.36). The stability of admixtures depends much on the water where when the water is reduced, even has no significant

effect on the compressive strength, but the alkalinity level will increase and reduce the solubility process by solid activator and affect admixtures performance as reported by Alrefaei et al. [31].

The mechanical strength of one-part AAMs depends much on the pore structure and the capacity of the fibre itself to resist crack opening. One-part AAMs mortar reinforced with 1% volume of single steel type and PVA fibres have shown an increment in mechanical strength on 28-day of curing ages between 20 – 25% more (75 – 80 MPa) compared to a reference sample (60 MPa) which in the beginning activated by GGBFS and solid  $\text{Na}_2\text{SO}_3$  [60]. It also reported when the fibre is added to the one-part AAMs, the porosity will be increased due to air voids, but at the same time, the crack propagation will be reduced too. Previous research on the effect of fibre type and content on one-part FA/GGBFS mortar strength found that compressive strength of one-part AAMs reinforced with 1 – 2% fibre type consisting of micro-steel, PVA and basalt was increased at 7 and 28th day due to limitation of crack propagation in the specimen which also indicates that the induced porosity through fibre can be reduced too. Decreased porosity will increase the density and offer a better compressive strength level [12]. The highest compressive strength value recorded was 34 MPa and 45 MPa on the 7 and 28th day for one-part FA / GGBFS reinforced with 1% micro-steel [59]. These findings are similar to the result published by Z.Abdollahnejad et al. [61], where adding 1% PVA or 1% steel fibre reinforced in one-part AAMs recorded a higher increment of mechanical strength of mortar samples compared with using Polypropylene (PP) fibres reinforcement. It also found that the curing condition for one-part AAMs reinforced with fibres was more suitable by employing a water bath instead of sealing as it resulted from a higher rate of polymerisation to form more reaction products and reduce porosity. The compressive strength of one-part AAMs mortar composed of GGBFS / ceramic/sodium silicate and reinforced by 1% fibres achieved 60 MPa and above at 28 days of curing ages. The pore structure finesse also contributes to compressive strength gain in one-part AAMs, as Yang et al. [42] reported. GGBFS samples activated by 10%  $\text{Na}_2\text{CO}_3$  showed higher compressive strength than 10%  $\text{Na}_2\text{CO}_3$  activation. Adding calcined dolomite (CD) enhanced the alkali activation process initiated by  $\text{Na}_2\text{CO}_3$  produced gels that enabled to fill of the pore structure and decreased the pore diameter of the samples. Compacted pore structures of the one-part GGBFS paste sample

in this experiment have better compressive strength values up to 40 MPa after 28 days of curing at ambient temperature. Including carbonate reduces the release of Al and Si from fly ash but initiates the condensation of the species and polymerisation of the aluminosilicate gel. However, the reaction rate activated by alkaline carbonate could decrease due to factors such as low mechanical strength, porosity and pH system [30].

Luukkonen et al. [62] reported that one-part AAMs composed of GGBFS and activated by synthetic anhydrous sodium metasilicate showed the highest compressive strength compared to alkali activator of micro silica mixed sodium hydroxide and rice husk ash mixed sodium hydroxide. However, it was found that the compressive strength of the specimen activated by micro silica and sodium hydroxide has shown sufficient strength under ACI 318-11 (2011) standard for structural uses. The mortars activated by sodium silicate have faster-releasing silicate sources, which benefits early strength development and stability. However, mortars activated by slower-releasing silicate sources continued to increase strength over time because of the hydration process continuing. The compressive strength of mortar activated by sodium silicate achieved more than 100 MPa compared to about 32 MPa activated by micro silica mixed sodium hydroxide, tested at 28 days of curing age. Compared to FA-based, the compressive strength of one-part AAMs composed of GGBFS has developed better early. An increased slag amount in FA / GGBFS one-part AAMs mixture activated by 8% sodium silicate has produced higher strength due to a stable 3D network of silico-aluminates. High rates of C-A-S-H, C-S-H, and stability of microstructure were the reason for an early higher compressive strength gain for GGBFS - AAMs samples while at 28-day, the compressive strength increased with the increment of GGBFS content and activator dosage except for 10% Na<sub>2</sub>SiO<sub>3</sub>/ 50% GGBFS which showed declined in compressive strength due to crack formation caused by shrinkage and dry surface condition of AAMs under air curing regime. However, the result from this study showed that all design mixes for one-part FA/GGBFS mortars, activated by Na<sub>2</sub>SiO<sub>3</sub> at a constant water/binder ratio of 3 and temperature 30 °C has recorded about 60 MPa and above for 28-day curing ages and suitable for construction application [65].

### 2.8.2 Modulus of elasticity (MOE) and Poisson's Ratio

Haruna et al. [51] experimented to determine the modulus of elasticity and Poisson's ratio of one-part alkali-activated concrete with different paste-to-aggregate ratios and under different curing regimes. When applied to compressive load, Poisson's ratio determines the percentage of AAMs' lateral to longitudinal deformation. The values vary from 0.1 for high-strength concrete and 0.2 in contrast for weak mixtures. Concrete strength design is generally taken as 0.15 and 0.2 for serviceability criteria in compliance with The American Association of State Highway and Transportation Officials (AASHTO) guidelines and Euro code if the Poisson's ratio is not determined by any physical test [82]. The modulus of elasticity (MOE) is one of the crucial parameters for the structural design of concrete. It measures the resistance of concrete against elastic deformation when a force is applied. Cylinders of 150 mm diameter and 300 mm height were used and tested at 28 and 90 days of age to comply with ASTM C469 guidelines. Three samples were produced, and the mean value was recorded by using equations Equation 4 and Equation 5 as follows:

$$\text{Modulus of Elasticity, } E_c = \frac{D_1 - D_2}{E_2 - 0.00005} \quad \text{Equation 4}$$

$$\text{Poisson's Ratio, } u = \frac{EA_2 - EA_1}{E_2 - 0.00005} \quad \text{Equation 5}$$

Where  $D_1$  is the stress of longitudinal strain of 50  $\mu\text{m}$ ,  $D_2$  is compressive stress equivalent to 40% of the failure load,  $E_2$  is the longitudinal strain equal to  $D_2$ ,  $EA_2$  is the lateral strain at mid-height of the specimen similar to stress  $a_2$ , and the  $a_1$  is the lateral strain at the mid-height of the sample. The report concludes that the MOE of AAMs increased with a lower paste to the aggregate ratio of 0.35 and found that there is no significant difference impact when all the samples cured with three different curing regimes as strength also increased after 28 days showed the advantages of one-part AAMs compared to conventional two-part mixtures which required high temperature to gain the comparable mechanical strength. Poisson's ratio value lies between 0.15 to 0.17 at 28 days of age and 0.13 to 0.16 at 90 days of the curing period, equivalent to Poisson's ratio of OPC concrete, irrespective of curing requirements still influenced by the paste and aggregate content. On the other hand, the effect of admixtures on shrinkage reduction recorded up to 5% reduction

on the modulus of elasticity of AAMs paste samples corresponded to a 20% decrease in compressive strength as per the power-law model, which also applied to Portland cement-based – mortars and concretes [69]. In another report, the dynamic of modulus elasticity of one-part AAMs mortar was calculated using Ultrasonic Digital Indicator Tester at 28 days of age as per EN12504-4 standard found that flexural strength and elastic modulus of elasticity of Portland cement-based mixtures was better than one-part AAMs mortar due to crack propagation because of high shrinkage in alkali-activated material technology subsequently reflect the AAMs' elasto-mechanical properties. However, the higher the alkali content used, the higher the mechanical strength of one-part AAMs will be proved the importance of alkali content in the mixtures for long-term performance [39].

### **2.8.3 Bulk density**

Askarian et al. [30] weighed the 28-day AAMs samples to obtain their bulk density. They highlighted that type and combination of solid activators had influenced geopolymer density, although they found no correlation between the bulk density and the compressive strength of AAMs. The 50% Fly ash and 50% GGBFS activated by 12% and 9% weight from total mixtures weight has recorded 1680 kg/m<sup>3</sup> of density and 38 MPa at 28 days of curing age. Apart from that, the potential of one-part alkali-activated cement mixed with OPC to be used in thermal insulation applications was studied by Abdollahnejad et al. [12] only found that the aluminium powder mortar based - mixtures of 30% OPC / 58.3% FA / 4% CA and 7.7% CH were not a cost-effective although the used of aluminium powder is beneficial in obtaining foam materials with low thermal conductivity where a high content of aluminium powder in the mixture could increase the bulk density as a result of pore collapse in AAMs hybrid samples.

## **2.9 Flexural Strength**

The one-part AAMs were reported to have better deformation behaviour than the conventional two-part AAMs. The flexural strength test is vital for understanding the samples' deformation behaviour and determining the cracking level due to the load applied [51]. The test is generally

conducted using a three-point bending on prismatic beams size 40 mm x 40 mm x 160 mm as specified in ASTM C78 guidelines for the samples aged between 7, 14 and 28 days [60]. Shah et al. [59] reported two types of flexure behaviours of hardened concrete: deflection softening and deflection hardening. Modulus of rupture (MOR) in MPa for the former will consistently lower than the first peak load of the deflection curve, while for the latter, the MOR is more significantly lower than the first peak load of the deflection curve. The peak load is the first point on the load-deflection curve, with zero slopes. Still, when the point on the curve is unable to identify, the limit of proportionality (LOP) will be used in the case of stable deflection hardening behaviour as explained in ASTM standard C 1018-97. Adding any fibre and its higher content percentage in one part alkali-activated mortar increases the flexural strength at 7 and 28 days of age. At an optimum, 1.5% additional micro-steel fibres showed greater strength than PVA and basalt fibres. In comparison, 2% PVA has increased up to 16% more flexural strength and supported by the findings on hybrid fibres impact on flexural strength of one part alkali-activated slag mortars was more remarkable than its impact on compressive strength due to fibres bridging action thus introduced high ductility of material [60]. The increasing percentage of PVA and basalt fibres increased the peak flexural load of alkali-activated FA/GGBFS-based mortar. Both types of fibres were categorially under deflection hardening flexure behaviour wherefrom the flexure test result. It was noticed that the peak load was higher than the load at the first crack, and the deflection at the peak load was more extensive than the deflection at the initial cracked load, confirming the high ductileness of mixtures. The modulus of rapture was calculated using the formula given as Equation 6 follows:

$$MOR = \frac{PL}{bD^2} \quad \text{Equation 6}$$

where the P is a load at MOR in Newton (N), b is the breadth, d is depth, and L is the length of the beam in mm, respectively. It was reported that the flexural strength of one-part alkali-activated concrete is almost the same regardless of curing conditions. It is understood that OPC concrete strength keeps increasing over time due to its C-S-H development, and the one-part AAMs also have shown a similar trend, especially with the presence of high calcium content in fly ash class-

C activating the development of C-A-S-H gels in AAMs structures and increased high pozzolanic reaction at the later stage. The total aggregate content does not influence flexural strength; therefore, a lower paste/aggregate ratio could improve flexural strength. The paste/aggregate ratio was 0.35 used in the study by Haruna et al.[51] The highest flexural strength recorded at 90 days of age, ranging from 6.5 MPa to almost 9 MPa, was conducted under three different curing regime: water, air and solar curing conditions, respectively. A high temperature of the solar chamber is essential to increase the bond between paste and aggregate, enhance the geopolymerization reaction of the lower ratio of paste/aggregate and continue to develop after 28 days. However, heat will not influence the final product and is only beneficial to boost the reaction where the specimen cured at 30 °C showed better flexure strength than 20 °C and 65 °C, as reported by Shah et al.[65]. The acceleration effect of seawater for an early reaction also increased the flexure strength of one-part AAMs due to the extensive alkali activation process, where at 28 days of age, the flexure strength was 7.5 MPa satisfied the structure application purpose [76]. On the other hand, Oderji et al.[28] studied the effect of slag and alkali activators on one part AAMs and found that an additional 15% to 20% of GGBFS content could decrease flexural strength even though the compressive strength has much improved. The 15% GGBFS content replacement of fly ash was said to be the optimum percentage for one part alkali-activated composed of fly ash and GGBFS to meet the required mechanical strength where the excessive slag content not only reduces flexure strength but also could reduce the workability of the binders subsequently will be caused high potential of microcracks and autogenous shrinkage [28][65]. In comparison, 8% was the optimum dosage for the alkali activator of sodium silicate, which this combination has recorded 2.5 MPa of flexural strength at 28 days of age. The 4% of borax content was the optimum percentage to increase the flexural strength showing the influence of retarder content of one part AAMs for early strength development [65].

## **2.10 Tensile Strength**

It is essential to determine the load-carrying capacity of one-part AAMs. Splitting tensile stress is a method to understand the crack resistance at peak load and corresponding displacement. Brittle failure of the concrete matrix is the main factor in tensile strength drop. However, tensile

strength can be improved by the addition of fibres in fibres reinforced AAMs. For instance, the mixture between AAMs and micro-steel fibres will produce stable deflection hardening behaviour by reducing stress concentration at a crack point. This combination acts together to deform and resist the applied load.

Moreover, adding 2% PVA fibre replacement increased splitting tensile stress to 68%, followed by basalt fibres at 62% and basalt at 42%. It was noticed that poor bonding with hydrated mix was the primary factor basalt fibres recorded the lowest strength, as SEM images explained [59]. The low aggregate content of the binder was found to develop strength continuously after 28 days. The ratio paste/aggregate 0.35 and 0.45 relatively recorded high tensile strength due to a more robust interfacial transition zone (ITZ) between paste and paste aggregate. AAMs concrete cured under solar regimes has the highest splitting tensile strength up to 5 MPa due to a high degree of geopolymerization at an early stage of the hardening process followed by water cured and ambient cured at similar paste/aggregate (p/a) ratio of 0.35 and 0.45, respectively [51].

## **2.11 Shrinkage**

The microcracks development determines the durability of one-part AAMs due to autogenous and drying shrinkage. There are four types of shrinkage in AAMs which are: drying, autogenous (plastic), chemical (endogenous) and thermal (temperature). However, drying shrinkage is the most observed and tested based on its real engineering applications, besides the autogenous type of shrinkage. Shrinkage happens when negative pressures arise during alkalization, affecting the concrete capillary networks due to created contracting stress [49]. Elzeadani et al.[11] reviewed the shrinkage level of one-part AAMs and explained that autogenous shrinkage results from water demand during the hydration process where surface tension at capillary pores has caused length reduction in concrete. Drying shrinkage changes the concrete volume due to evaporation, as water is lost and released in unsaturated air when the concrete dries. As a result, capillary pores will experience hydrostatic tension that leads to microcracks. Shrinkage in one-part AAMs depends on five primary factors: 1) precursors, 2) activators, 3) water content, 4) aggregates and 5) curing conditions. Finer pores of slag, compared to FA, increase capillary stress and has a higher chance

of drying shrinkage. Higher alkalinity of sodium silicate followed by sodium hydroxide increase shrinkage level compared to carbonate and sulphate-based activator.

Similarly, high amounts of water contribute to higher shrinkage levels. The ability of natural sand to fill the gap between cement particles will reduce the pores, creating a more compact structure to resist hydrostatic tension, whereas the inclusion of waste glass (WG) and coal waste (CW) as alternatives to natural aggregate forming hydration products at the surface of aggregates for a more substantial interfacial transition zone (ITZ) subsequently restrained drying shrinkage. Among all curing methods, one-part AAMs samples cured at higher temperature has more excellent shrinkage resistance due to the high stiffness of the concrete matrix besides rapid mechanical strength development. FA/slag-based AAMs can be cured up to 1200 °C compared to OPC paste which loses its integration at 600 °C. On the contrary, mixing one-part AAMs paste with cold water has less drying shrinkage than dry mixtures mixed with warm water. Cold water is crucial to controlling the effect of early thermal deformation by reducing the difference between fresh samples' temperature and surrounding temperatures[64].

Carneiro et al.[83] studied on drying shrinkage behaviour of one-part AAMs found that the drying effect happened as early as at first four days after mixing due to the loss of water of free water during binding gel phases. As a result, the tension capillaries in micropores and nanopores increased. A higher dosage of activator and pore size distribution are causes of the drying shrinkage as the former increases the hydration rates and heat releases, thus reducing the amount of water in the mixes. On top of that, higher alkalinity levels will form structural binding of alkaline metal cations in the C-A-S-H gels that reduce the packing of the C-A-S-H layer, consequently causing the hydrated gels to be susceptible to collapse and redistributed after drying. For this reason, the sodium metasilicate activator recorded a higher drying shrinkage impact on AAMs based products. As for the latter, well distribution of capillary pores helps to release the water more accessible to the air via the evaporation process, thus experiencing less capillary stress that leads to drying shrinkage [66]. Nonetheless, water-to-binder ratio and shrinkage resistance admixtures can also control the drying shrinkage phenomenon in one-part AAMs. Coppola et

al.(combined) reported that a combination of shrinkage-reducing admixtures (SRA) and CaO-based expansive agents reduce shrinkage levels between 40 – 50%. Higher densification of microstructure in OPC paste, on the other hand, contributes to lower porosity level due to the formation of C-S-H and hydrotalcite, improving the microstructure and possessing higher stiffness resulting in lower drying shrinkage compared to the AAMs. Including OPC may compensate for the shortage of current one-part AAMs technology.

Further investigation by Yin et al.[35] on the effect of rice straw ash (RSA) in one-part AAMs slag, RSA contains lots of SiO<sub>2</sub> and Potassium oxide (K<sub>2</sub>O) where the reactive K and Si in RSA are involved in forming C-A-S-H. When activated with an alkali activator, RSA can assist in the hydrolysis of slag. Both drying and autogenous shrinkage of paste samples were evaluated in the report. It turned out that the replacement of slag with RSA between 5 – 10% reduced drying shrinkage of one-part AAMs up to 30% after 30 days. The drying shrinkage in the report recorded about 4900 µm/m at 30 days of curing age. The internal curing effect of RSA and the formation of crystals facilitate resistance against drying-induced shrinkage. Nevertheless, the coarser pore structure of RSA may expedite water evaporation from the matrix and prevent internal stress or smaller capillary pressure. As contrary, autogenous shrinkage for the paste sample was recorded higher than the OPC-based paste (control sample), but with the inclusion of RSA, autogenous shrinkage was reduced up to 42.6% and indicating the potential of RSA to be used as shrinkage-reducing admixtures for slag-based AAMs. Besides that, RSA also maintains the relative humidity, thus mitigating the self-desiccation of the AAMs paste. It is worth mentioning, based on this study, the physical structure of one-part AAMs is possibly be modified to control its shrinkage level based on the RSA reaction concept and give an early indication of the inclusion of OPC, which contains ettringite helps to expand the cement as part of precursors source may help to reduce autogenous shrinkage of one-part AAMs. Moreover, Sadeghian et al.[67] reported that silica fume (SF) as a co-binder source reduces the drying shrinkage of slag-based concrete up to 30% when SF content is used between 0 – 15%. The additional supply of Si, Al and N-A-S-H gels from SF compensates for the low Ca/Si ratio of C-A-S-H gels from the slag reaction, producing dense C-A-S-H gels with lower porosity. In addition, excessive amounts of water for

the chemical reaction in one-part AAMs lead to higher porous matrix (inconsistent pore distributions). Higher porosity then affects the mechanical strength and contributes to drying shrinkage problems when water in the samples evaporates and gets dried. Compressive strength for the slag-based concrete in the report recorded about 65 MPa at a w/b ratio of 0.50 but dropped to 60 MPa when the w/b ratio increased to 0.54 in water cured environment.

## **2.12 Porosity**

Porosity is a percentage of the volume of hardened material pores concerning the total volume of its overall structure. It can be air or water filled or somewhere in between penetrating the pores that affect the material's mechanical strength because pores cannot resist any load. The higher the porosity level, the lower the strength. Mercury Intrusion Porosimetry (MIP) is commonly used to measure the change in porosity of specimens subjected to various curing conditions. Typically, "porosimetry" refers to measuring a material's pore size, volume, distribution, density, and other porosity-related characteristics. Porosity is crucial to comprehending numerous materials' formation, structure, and potential applications. Porosity influences the physical and mechanical properties of a material.

The increase in porosity percentage in AAMs will cause a reduction in their mechanical strength. The cumulative pore volumes and pore size distributions can be obtained using Mercury Intrusion Porosimetry (MIP) test as carried out by [34]. AAMs composed of 30% calcined kaolin and 70% fly ash were recorded up to 40% porosity level after 28 days of curing age, much known due to the absorbent nature of kaolin. Wei et al.[78] explained the inclusion of fly ash and composite activators in one-part AAMs composed solely by GGBFS reduced the size of the harmful pores which any size greater than 50 nm [34][42] and contributed to the better pore size distribution of one-part AAMs products, therefore, improve its water resistance. However, the GGBFS-only samples have the lowest porosity percentage tested at one day of standard curing age compared to the AAMs mixture of 45% GGBFS and 45% ultra-fine fly ash sinking beads (FASB). Haruna et al.[51] explained that the smaller the pore volumes, the higher the strength of AAMs. This result is in line with the findings reported by Li et al.[47] on rheology behaviour of one part AAMs

with less than 10% silica fume (SF) content beneficial to increase the yield strength and decrease the plastic viscosity one part alkali-activated slag glass powder (AASG) for a better mechanical strength due to its fine size and spherical morphology. The sufficient aggregate content offers a stable structure and enhances strength development over time. Nevertheless, the lower paste/aggregate ratio is a result of less paste in concrete, where it risks some part of the mixing water being released via evaporation, and at a paste/aggregate ratio was 0.35, the AAMs mortar samples have recorded the highest percentage of porosity compared to 0.45 and 0.57 ratio where on the contrary, a higher porosity could decrease compressive strength due to more cracks appear [60]. Decrease in porosity is normally due to the improvement of pore structures which produce denser and compact structures. The addition of fine tailings was reported quicken the reaction of precursors by boosting pH development in pore solution that may help to reduce the quantity of harmful pores and help to optimize filling of solid granular particles [34]. The report also showed that less paste content in lower aggregate, p/a ratio reduced the pore volumes of AAMs, moreover it was noted that pores size that greater than 135 nm affected the strength and absorptivity of the hardened cement paste.

The pore's size can be defined as small gels pores for size less than 10 nm, size between 10 nm to 50 nm for large gels pores and considered voids if the size is more than 10  $\mu\text{m}$ . Moreover, the pore size is also referred to as three main groups: gel pores for size less than 10 nm, capillary pores for size between 10 to 5000 nm and macropores for any pore size greater than 5000 nm, as stated by [42]. However, the paste/aggregate ratio does not influence the pore volumes of AAMs due to the pore's structures controlled by the group of aluminosilicate gels through geopolymer matrix Si-O-Al network besides its hardened samples produced by a uniform alkali activator dosage, for instance, AAMs activated by 10 %  $\text{Na}_2\text{CO}_3$  activator will produce and C-A-S-H gel phase to fill the pore structures and reduce pore diameters as reported by Yang et al.[63] On the other hand, a lower paste/aggregate ratio will also reduce total water content, thus decreasing aggregate volume, whereby in the hardened concrete, the surface area for paste – aggregate interface transition zone (ITZ) could increase mainly for the mixtures with p/a ratio of 0.35.

How a substance can be used is determined by its adsorption, permeability, strength, and density, among other characteristics influenced by its porosity, as described by Abdollahnejad et al.[57]. Moreover, Bernal et al.[84] explained the pore structure of slag-based AAMs tends to be impenetrable or open, dependent on curing conditions, mix design and maturity. It was also controlled by the reaction mechanism where thermal curing is not necessarily effective in improving the reaction of AAMs slag binder, which differs from FA-based AAMs due to drying conditions. Nevertheless, a higher dose of alkali activator may be beneficial to refine the pore network. In addition, according to Elzeadani et al.[11], the porosity level of one-part AAMs depends much on its precursors, alkali activator and water content. AAMs activated with slag are much more compact pore structures than the sole precursor of FA. The combination of slag and FA will increase the overall pore volumes and improve the pore structures, not only responsible for reducing harmful pores at a range size of 20 to 200 nm but also replace the pore structures with a size range of less than 20 nm, known as harmless pore category. Larger pore sizes will allow high water absorption of AAMs. Higher water content in the pores is due to low pH levels and affects the dissolution rates of pore solution in the binder, subsequently creating coarser pores volume. Nevertheless, the decomposition of precursors in an alkaline environment is vital for polymerization and creating new gel products so that the pores' size, distribution, and homogeneity can be controlled and consistent, as reported by [49]. Additionally, sufficient water is beneficial for transporting dissolved particles under an alkaline environment and creating N-A-S-H gels, which are responsible for gaining mechanical strength. On the other hand, excessive water in the w/b ratio allows a higher permeability level that affects the durability of cementitious material. Nevertheless, water also can be found in wet aggregates. The optimum volume of the sand-to-binder ratio and its particle size is vital to prevent the gap formed by the aggregate. Still, porosity levels can be minimized but not entirely removed. By reducing the water content, cement granules can be brought close together, subsequently offering more space to the hydrated products due to less water leftover, more compact and reduced pores. On the other hand, too low of water content affect its self-desiccation process and cause pore drying because more water is required for local hydration reactions and leads to open porosity [75]. An excessive amount of aggregate in the sand-to-binder ratio will cause a reduction in gels proportion in one-part AAMs. As a result,

the insufficient gels to wrap the aggregate resulted in defects by generating pore structures and reducing the capacity of its mechanical strength due to the higher porosity level effect [85]. On the contrary, in the case of AAMs concrete, Haruna et al.[51] reported that lower binder content with an optimum sand-to-binder (s/b) ratio of 0.35 is beneficial to decrease the pore volume of concrete. Higher aggregate content will increase the surface area of the aggregate/paste ITZ because when the binder or paste is reduced, the release of mixing water on the aggregate through evaporation is resumed. The lower water content will decrease aggregate volume; therefore, the exterior surface area between aggregate and paste is increased, which subsequently segregates the water film's surface area from the fresh binder and increases the aggregate's adsorption level. Another way to control the porosity is by reducing the entrapped air pores in fresh cementitious materials to minimize the height drop or splashing for the fresh mortar to form and consolidate properly. Proper curing is required to make sure the hydration process works efficiently. Otherwise, the surplus or unreacted water can lead to the creation of pores. The mortar must be covered or sealed to maintain under the environment of higher temperature and humidity levels for ideal curing conditions. Alzaza et al.[70] examined the influence of curing temperature on the porosity level of one-part AAMs and found that the porosity level will be higher at lower and subzero curing temperatures. A study on slag mortar showed that although the total volume of gel pores ( $< 50$  nm) decreased, the macropores ( $> 50$  nm) increased with the decrease in curing temperature. This phenomenon is related to the low degree of alkali activation, thus producing less gel content. In contrast, curing process at room temperature encourage a continuous densification of slag mortar led to finer pore size distribution, reduce total pore volume, because of C/N-A-S-H gels form with high capability to filling the pores. A good selection of admixtures, such as water and shrinkage-reducing admixtures, could enhance the physical stability of mortar with optimum mix design proportions, reducing water demand and controlling excess water and porosity. Including Fly Ash and slag is also beneficial as the pozzolanic reaction helps to produce an excellent quality hydrated product [86].

Azevado et al.[29] analyzed the combination of FA and calcined kaolin showed a higher percentage of porosity between 35% (10% kaolin at 7 days of age) to 40% with 30% kaolin

content at 28 days. The absorbent nature of kaolin may contain more water responsible for large pores. There was little difference in porosity level when kaolin was replaced with 10% ceramic waste, slightly improving to  $32\% \pm 2\%$  at 28 days of age. This report gives essential information for using metakaolin-containing clay mineral products as main aluminosilicate precursors sources for AAMs, which possess high porosity levels that will affect their durability for long-term application. The selection of aluminosilicate precursors has influenced the geopolymerization development and its final geopolymer gels form. A 100% FA of one-part AAMs concrete was illustrated as having a porous structure containing higher particles of unreacted spherical structures of FA as a sign of an incomplete geopolymerization process. On the other hand, 50% slag was used to replace FA and recorded a very dense and compact matrix and developed higher early and final strength due to C-S-H gels formed in FA/slag reaction. This mixture has a higher Al level, and the calcium from slag can control the polymerization degree and help to avoid microcracks due to heat released from an intense reaction, essential for the pore size distribution and mechanical strength improvement. Nevertheless, the Ca/Si ratio of FA/slag mixtures is only about 0.6 may cause the products to face lower workability [30]. On the other hand, a higher calcium level of OPC may help to increase the Ca/Si level of one-part AAMs mixtures and can be a part of aluminosilicate sources. Further investigation revealed that forming amorphous Ca-Al-Si gels when OPC is added as part of precursor mixtures has reduced the porosity level, thus improving its mechanical strength, as Askarian et al.[38] reported. Less unreacted spherical fly ash structures are observed when 60% OPC is used, and the one-part AAMs concrete was also compact and less porous. In that report, this phenomenon can be explained by the coexistence between geopolymeric gels and C-S-H gels phases contributing to the hybrid products of calcium alumino-silicate hydrate (C-A-S-H) in the entire network. The mechanical strength of cementitious materials is much dependent on their porosity level. A higher porosity level presents a less dense microstructure that decreases compressive strength at a later stage [12]. Further investigation by Chen et al.[34] study on the use of zinc tailing waste as an accelerator in one-part AAMs paste containing GGBFS/zinc tailings and found that 10% fine tailings were the optimum volume that was useful to reduce porosity level down to 17% when low alkali activator dosage was used while accelerating the reaction of binders by improving the pH development in

pore solutions during the curing process. The compressive strength was recorded up to 28 MPa at 28 days of age. Nevertheless, all one-part AAMs slag/tailings samples possess microcracks, proving that slag-based AAMs tend to crack due to higher temperatures from the intensive polymerization reaction. Samarakoon et al.[42] carried out pore structure analysis on FA/slag AAMs paste with the ratio of 60:40 and activated with two types of alkali activator: dry activator (DA) and solid sodium silicate (NS). The porosity level for both samples was recorded at about 35% for the DA-based activator and 36% for NS. The FA/slag mixes were further activated with a liquid activator of sodium silicate/sodium hydroxide (NHNS), and the porosity level was about 36%. According to the MIP test result, 95% of pores are less than 5  $\mu\text{m}$  (5000 nm) for all samples categorized as capillary pores. Despite that, the sample with DA has recorded 39% of the pore fraction of the total porosity and 29% for NS, which is greater than 20 nm even though it is considered as less harmful pores. Coarser pore fraction ( $> 20$  nm) of one-part AAMs may affect their durability properties and be exposed to chemical attacks. On the contrary, two-part AAMs, which were activated with NHNS, only have 6% of  $> 20$  nm as the reason for the highest compressive strength (48 MPa) than DA ( $\sim 33$  MPa) and NS ( $\sim 29$  MPa) at 28 days of age. None of the paste samples satisfied Class R3 – EN 1504 requirement for structural concrete repair. An additional study by Shah et al.[59] The effect of fibre type and content on AAMs mortar described that the compressive strength could achieve up to 45 MPa at 28 days of age with an addition between 0.5 – 2.0% fibre volume showed that the creation of porosity through the fibre is lesser than its capacity to prevent cracks openings. Furthermore, if added more than the optimum value, tiny cracks will appear that cause a negative impact on the mechanical strength. Other issues observed in this study reveal the loss of workability and higher water absorption despite 5% of borax being used to improve its flowability. Consequently, they may affect its in-situ application, from mixing and transport to applying mortar on concrete surfaces. A study by [87] explained that one-part AAMs mortar with the addition of 1% single fibre could have a 13% up to 22% porosity level. Short-length steel type of fibre has recorded about 80 MPa compressive strength at 28 days of age and the lowest porosity level at 13 %. It is worth mentioning that the mix design for the samples mortar used comprising of 100% slag and activated with 11% solid anhydrous metasilicate of total precursors weight impacts corrosivity and safety issues. One-part AAMs slag

with 10% sodium carbonate activator and 10% calcined dolomite as an accelerator for the kinetic reaction of paste was tested on its pore structure and recorded about 21nm average pore size diameter or about 22 % of porosity level. The compressive strength at 28 days of age also recorded a significant 40MPa within the Class R3-EN1504 standard. Still, other mechanical properties must be carried out to make this cement fully comply with the concrete structural repair materials requirements. A higher dosage of alkali activator can lower the porosity level, denoted by lower shrinkage level, thus enhancing the mechanical strength [66][68], but it comes with higher cost and handling issues. Commercial alkali activators were replaced with natural waste activators as studied by [80] on one-part AAMs slag paste activated with 5% calcined oyster shell powder, which has a high contain calcium carbonate and recorded an average pore diameter of 14.1 nm and has 35 MPa of compressive strength at 28 days of age. Attention must be given to the calcination process for new raw materials since this step could easily require higher temperatures and greater amounts of energy that release a significant amount of CO<sub>2</sub> to the atmosphere, besides the cost of the cementitious materials need more binder volume for a paste application compared to the mortar or concrete counterpart.

### **2.13 Microstructural Analysis**

#### **Scanning Electron Microscopy (SEM) and Energy Dispersive X-ray Spectroscopy (EDS)**

In the one-part AAMs concept, the alkali activator is required for geopolymerization to form hydration products of gels that are beneficial for binding and mechanical strength purposes for cementitious material. Xun et al. [81] reported that the calcination process with alkali could break quartz's structure and subsequently increase the Si/Al ratio by capturing Si from the quartz. In contrast, quartz will not destroy bentonite without alkali, as tested in the report. Moreover, the SEM and EDS result confirm the alkali activator assists in destroying the minerals and also activate the geopolymerization. SEM micrographs are often used to observe and determine the microcracks, reacted/unreacted and hydration gels. Microcracks are attributed to the loss of water from the gels and the uneven shrinkage forces mentioned by Liu et al.[66] as a result of derivatized gels reacting with the particles during drying. Oderji et al.[28] used Scanning Electron Microscopy (SEM) to study the microstructure of the one-part AAMs consisting of FA and slag.

20% of slag samples showed the most homogenous microstructure. Lower  $\text{Na}_2\text{SiO}_3$  content has caused the low amount of geopolymerization products to show unreacted particles image of FA and slag. Moreover, even a 1% difference in alkali activator content could cause a higher loss of strength, indicating that the dissolution of precursors was not completed due to insufficient volume of alkali activator in one-part AAMs technology. In this report, Energy Dispersive X-ray Spectroscopy (EDS) was used to evaluate the morphology characteristic of the sample used for the SEM. It can be clearly shown that silicon, sodium, calcium, and aluminium were presented in the EDS images, confirming the co-existence of C-A-S-H and N-A-S-H gels. Also, FA particles can be observed via SEM in the form of spherical morphology even after contact with an alkali activator during the curing process as a result of the low reactivity of  $\text{Na}_2$  and  $\text{SiO}_2$  species available in calcined material (ceramic waste) as part of aluminosilicate sources as mentioned in the report by [29]. But when calcined material is added up to 30%, the spherical particles become lesser and embedded in the formed material, making it compact, thus improving the mechanical strength of the one-part AAMs. Askarian et al.[38] analyzed the microstructural images of crushed AAMs specimen using backscattered electrons at 28 days of age. The precursors contained OPC, FA and slag, and at a 60% OPC, compact and less porous structure images are well observed. A higher concentration of OPC will lower the porosity level and subsequently lead to the formation of amorphous Ca-Al-Si gels beneficial for gaining strength. Compared, one-part AAMs concrete without OPC microstructural images showed unreacted FA particles and geopolymeric matrix presenting loose and amorphous structures. Nevertheless, the SEM images proved the co-existence of the hybrid product of calcium alumina-silicate hydrate (C-A-S-H). Further analysis of the reaction of mixes using EDS for the OPC hybrid AAMs samples at 28 days of age explained that the CaO-to- $\text{SiO}_2$  ratio is influenced by OPC content. The oxide molar CaO-to- $\text{SiO}_2$  or Ca/Si ratio is one factor responsible for forming C-S-H gels. The Ca/Si ratio is decreased with low OPC content. At 60% OPC content in AAMs hybrid mixes, the Ca/Si ratio was 1.1, slightly lower than the Ca/Si ratio for the sole OPC based, which recorded between 1.2 to 2.3 but still comparable to the single OPC precursor that makes this hybrid mixes bring potential to be carried out for further study. A high Ca/Si ratio is required for forming C-S-H, vital for the early age of strength where hybrid AAMs may require it. The rich calcium content of OPC reacts with an activator to form a

semi-crystalline geopolymeric network and amorphous C-S-H, where the C-S-H keeps continuing to form due to decreasing alkalinity in the mixes. In addition, according to Kadhim et al.[88], low Ca/Si ratio in one-part AAMs indicates the increased reaction of both elements contributed to the formation of hydrate products of C-A-S-H. Further analysis by Askarian et al.[30] revealed that when FA was used as the sole precursor would have a high content of Si and Al, indicating unreacted FA particles within the binder even after 28 days of curing, with a lack of Ca. In SEM images, vast amounts of unreacted FA particles in the matrix indicate incomplete geopolymerization leading to low compressive strength. However, when 50% slag replaced FA, the micrograph showed significant Ca, as depicted in the EDS analysis. The morphology of these mixtures is also more compact and denser due to the contribution of Ca from slag-reduced polymerization degree for a better pore size distribution and early and ultimate strength development. However, higher slag content may cause excessive Ca, making one-part AAMs crack [34].

It is interesting to understand that not all microcracks appeared in SEM images due to the micro-pores or porous structures where water can escape during curing, as this occurrence can also be formed during the cutting, crushing or polishing of the specimen [44]. Almalkawi et al.[16] reported that some of the non-reactive phases, observed in SEM images, perhaps inherited from parents' material by the hydration products. Nevertheless, one-part AAMs paste composed of a 50:50 ratio of FA/slag has formed C-S-H gels, contained a higher amount of Al but still lacked Ca/Si ratio where the OPC has a potential source of Ca/Si to be included as part of aluminosilicate precursors. Furthermore, this report also confirms the formation of C-A-S-H gels and the co-existence of N-A-S-H / C-A-S-H gels after including calcium in FA-based precursors. Samarakoon et al.[42] described that to analyze the densification process of the binder with curing, the Backscattered scanning electron microscope (BSEM) images can be visualized as follow; brighter images if a more significant amount of calcium exists, especially for irregular-shaped slag particles, grey with spherical shape for FA particles, light grey or sometimes dark grey for hydration phase or reaction products (C-A-S-H gels) and pores are black. Additionally, smoother surfaces indicate the formation of hydration gels that fill micro-pores over curing time

[58]. The crystal shape on the surface commonly refers to the efflorescence that causes lower mechanical strength due to crystalline phase, defects and lesser C-A-S-H gels [36]. In the early stage of curing, the main hydration product is C-A-S-H gels showed the calcium-dominant reaction products from slag sources due to easier discharge of Ca ions than Si and Al ions. On the other hand, the inclusion of Al ions in the C-S-H products resulted in C-A-S-H gels in the early strength development of AAMs. It is worth noting that the combination of FA/slag in one-part AAMs confirmed the reduction of Ca content at a later stage, and in contrast, the amount of Si is increased in hydration products after 28 days of curing age. The report explains this phenomenon when the FA amount (60%) is more significant than slag (40%), and the incorporation of Na is favoured when the binder's composition has high Si content. Therefore, the N-A-S-H gels become dominant in a low calcium environment after 28 days of curing, but the co-existence of N-A-S-H / C-A-S-H is still possible. Moreover, the new formation of hydration products will become C-(N)-A-S-H, a more cross-linked structure for the FA/slag precursors. The C-(N)-A-S-H gels are more stable under chemical attack than C-A-S-H gels, especially in aggressive environments for most AAMs products. Ke et al.[89] reported that SEM images of red mud one-part AAMs have a low Si/Al ratio consistent with metakaolin-based AAMs with Si/Al ratios lower than 1.4, promoting highly porous microstructure and severe efflorescent problems. It was reported that significant elements of Ca, Si, O, Al, and Mg were found in the EDS result for forming hydration products of C-S-H gels in AAMs. Nevertheless, the ratio of Ca/Si in AAMs was lower than what OPC can offer. However, C-S-H gels with lower Ca/Si ratios also exhibited denser microstructures in slag paste. The Ca/Si ratio for the control sample containing the sole precursor of slag has recorded at about 1.38. Still, when the slag content was reduced between 5-10% with rice straw ash (RSA), the Ca/Si ratio dropped to 1.04 and 1.06, respectively, for a denser microstructure of slag-based AAMs. The Si/Al ratio also increased from 1.91 to 2.15 – 2.63, indicating the particles were not fully reacting at the early stage. Still, the total amount of hydration products is increasing because the geopolymerization process keeps continuing at a later stage for strength development. Three ratios of Ca/Na for control samples with the slag-only precursor, 95% slag and 90% slag indicate the difference in morphology and hydration products when RSA was included. Report by Luukkonen et al. [72] revealed that Ca/Si level increases as

LS included in AAMs mortar but in contrast, Na and Si decreases due to the dominant role of  $\text{Ca}^{2+}$  of lignosulfonate (LS) to facilitate the dissolution of slag based AAMs. With the inclusion of LS, the Na/Al ratio recorded as  $< 1$ .

Abdollahnejad et al.[57] carried out a study on the effect of using different types of curing regimes on one-part AAMs composed of slag and ceramic waste. Sealing the specimen showed that AAMs with ceramic waste have a very dense matrix resulting in higher compressive strength than other curing styles. Also, some cracks were detected when unsealed curing conditions were applied. Furthermore, EDX analysis measured the gel phase composition by the Al/Si and Ca/Si molar ratio. Different curing conditions affected the molar ratio for both element compositions. Curing with sealed in a plastic bag has recorded the maximum molar ratio, but subsequently, the ratio was reduced when applying unsealed and curing in the water. It is noteworthy that sealing affects the temperature requirement for chemical reactions; thus, only minimum reduction is detected for both Al/Si and Ca/Si ratio by sealing compared to another curing method. It is clear that the curing regime has influenced the dissolution rate of silicate and aluminate elements and affected the actual calcium content in the ion exchange process, as agreed with Luukkonen et al.[62] on longer curing with higher relative humidity could decrease the propagation of microcracks. As a result, it has also affected the molar ratio obtained from the EDX analysis. Additionally, unsealed curing conditions will decrease the curing temperature, leading to the presence of microcracks. When cracks happen, the ITZ could disrupt due to the ITZ region's pore size, as described by Alzaza et al.[70] on the effect of subzero temperature against one-part AAMs slag-based mortar. In addition, microstructure analysis on one-part AAMs curing with three different temperatures of 20 °C, 30 °C and 65 °C showed that incomplete geopolymerization process at lower curing temperatures and the reaction is accelerated to form denser microstructure towards higher temperature as a result of homogenous precipitation of geopolymer gels. In contrast, as Shah et al.[65] described, curing at elevated temperatures may encourage higher water evaporation levels and shrinkage that could create pores and microcracks. In the report, which also concludes that different curing temperatures and ages influenced the hardening mechanism and FA/slag-based mortar microstructure. Furthermore, the report explained that a lower temperature is insufficient

to cause dissolution, to assist calcium reacting with sodium silicate to form C-S-H, increasing the pH level that caused water content to be reduced. With higher alkalinity levels, the dissolution of existing aluminosilicate takes place for the hardening process and therefore, both of precipitated compound and formed geopolymeric gel of N-A-S-H and C-A-S-H contributed to the strength of AAMs mortar at a later stage with a curing temperature of 20 °C subsequently clarify on the slow geopolymerization process start as well as low early strength. On the other hand, the inclusion of fibre in one-part AAMs was observed by Abdollahnejad et al.[87] and found that steel and basalt fibres debonded from their surrounding matrix, but the PVA type of fibres was observed to be more dominant and form a rigid bond between fibre and matrix. However, in this study, including fibres also increased the total porosity of the samples mortar.

### **3 Introduction to Manuscript 1**

Alkali-activated materials (AAMs) in this manuscript 1 will be employed in a one-part system concept, which differs from the conventional two-part system. In the two-part AAMs concept, the alkali activator is used in the form of liquid or solutions, whereby for the one-part AAMs counterpart, only raw materials are in the form of solids before water is added to activate the dry cementitious mixtures. Demand for one-part AAMs material has been increasing lately due to its easy handling and durability. On top of that, awareness among industrial players in the construction sector on sustainability encourages more environmentally friendly products that reduce CO<sub>2</sub> emissions and recycle and reuse most industrial waste materials. As part of the construction community, this study was designed as part of an initiative to encourage green engineering materials to be introduced in the market not only to give more choices to the consumer but also first efforts to reduce clinker production, which is responsible for tons of CO<sub>2</sub> emitted to the atmosphere via Portland cement products. Thus, the one-part AAMs in this study were composed as part of Ordinary Portland cement (OPC) replacement, a 'hybrid' concept used as the cementitious binder in the form of mortar for structural concrete repair applications.

Four main elements must be formulated to compose a new mix design for one-part AAMs mortar. First, the type of aluminosilicate precursor must be determined. Fly Ash (FA), Ground Granulated Blast Furnace Slag (GGBFS) and Metakaolin (M) are rich in silica and alumina, commonly employed as aluminosilicate sources. Still, only two materials will be used in this study: Class-F FA, a low-calcium type selected with GGBFS, which possesses rich calcium, compensates for the former's shortage. Nevertheless, combining two different precursors was developed for a better mechanical performance than the sole aluminosilicate precursor source. Including OPC as part of the precursor will enhance the engineering properties of mortar as the former contributes calcium silicate hydrates, and C-S-H gels as the main product for binding purposes. The FA/GGBFS/OPC volume is subsequently adjusted to find the optimum ratio content so that they can react efficiently with the alkali activator for the geopolymerization process.

The second main element for AAMs technology is the alkali activator. Sodium hydroxide and sodium silicate are two primary dry alkali activators commonly used to activate the precursors due to their high alkalinity level compared to sulphate and carbonate activators with medium alkalinity levels. It is worth noting that higher alkalinity activators pose safety issues for the worker, are expensive and require higher energy levels to produce them. Hence in this study, a dry potassium carbonate activator will be utilized for all mortar samples to ensure low-risk application, cheaper and, most importantly, using environmentally friendly chemical products. As a benchmark, the alkali concentration (in weight) is initially set at 6% of the total precursor weight. It will be adjusted further to find the optimum dosage level based on its reaction with precursors. The third element includes solid admixtures in the dry mixtures as part of the additive to control and improve the mortar characteristic. Three types of powdered admixtures will be used sodium lignosulfonate (LS) as superplasticizer (SP), Shrinkage Reducing Admixtures (SRA) and calcium oxide (CaO). The use of SP ensures a higher workability level at the fresh state, while the combination of SRA and CaO is beneficial to control shrinkage levels at the hardened state. The volume of each admixture was also based on the total precursor weight.

The final element essential for formulation study is the ratio between aggregate and water to its binder. The volume of aggregate and water based on the total precursor must be determined. Mortar products only consist of fine aggregate or sand. The aggregate-to-binder, a/b, must be determined not only because the addition of sand can increase the mortar volume so that less cementitious binder can be used but it also contributes to resistance against early shrinkage cracking during the hardening process, thus will increase the density and workability for the mortar. Water is essential in activating the cementitious binder material to become the final product of mortar. The optimum water-to-binder w/b ratio will ensure overall engineering properties of mortar; workability level at fresh state, mechanical strength at hardened state and physical structures for durability purposes are at utmost performance. Finally, each of the elements will be chemically inter-connected with each other to produce hydration gels product N-A-S-H and C-A-S-H as a result of the geopolymerization process in AAMs technology that is

responsible for the strength development of the mortar over the time. The roles of each element are also discussed in detail in the manuscript.

There are 30 samples of mortar will be evaluated based on different design mix compositions in three stages of the experimental test. The compressive strength of all mortar samples will be determined to standardize the findings based on mechanical strength characteristics, beginning at 7 days of age, then up to 14 days of age, and finally at 28 days of age to achieve Class R3, EN01504-3, standard. The mortar samples will be prepared under controlled lab temperature to follow EN 12190 test method. The mortar samples with the best compressive strength result at stage 3 will be selected to further evaluate their other mechanical strength behaviour. Four more experimental tests will be involved in this study, where three of the tests; flexural strength test, modulus of elasticity (MOE) and splitting tensile test will be carried out to study its mechanical performance, while the last test will be done to understand the shrinkage level of the mortar for durability enhancement. All the mentioned tests, however, are not required under EN1504-3; thus, the temperature and relative humidity during preparation, curing and testing will be based on a lab ambient temperature of 29 °C and RH of 65%. Nevertheless, the testing method which will be applied to the mortar is still to follow European Standard (EN), British Standard (BS) and American Standard Test Method (ASTM). Overall, all the tests in this study will explore the performance of the one-part AAMs mortar used as concrete structural repair and determine its potential for other concrete applications.

## 4 Manuscript 1

### Performance Evaluation of Hybrid One-Part Alkali Activated Materials (AAMs) For Concrete Structural Repair

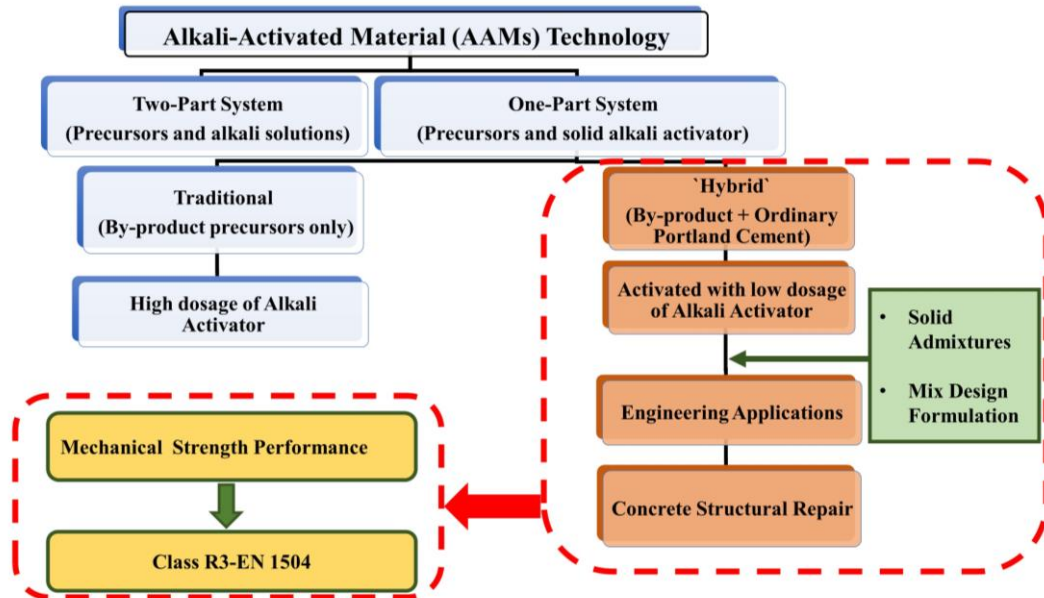


Figure 1: Schematic of AAMs Technology

#### 4.1 Introduction

Alkali-activated materials (AAMs) have been widely used and regarded as a green technology mainly composed of industrial waste materials and reduce Carbon Dioxide (CO<sub>2</sub>) emissions in the atmosphere (see Figure 1). This technology was brought to reduce construction dependency on ordinary Portland cement (OPC). The OPC contributes to CO<sub>2</sub> emissions due to higher energy consumption and heat from the calcination process [36]. In addition, many countries face deteriorated concrete structures as the building life span is approaching its limit. This situation contributes to the higher demand for cementitious material to construct the new building and repair and refurbish.

Furthermore, to keep the aesthetic value and heritage landmark for some buildings, many architects prefer those buildings to be refurbished to preserve them. As a result, sustainable building products are becoming popular among architects and engineers to ensure building

elements can resist the load and keep maintenance costs minimum. Thus, the AAMs have become a substitute for conventional Portland cement, which has higher mechanical strength and more extended durability [81]. The conventional AAMs are prepared by two-part components, aluminosilicate precursor and alkali solution, to create an amorphous three-dimensional structure via the geopolymerization process. Common aluminosilicate precursors used are alkaline by-products such as fly ash (FA), ground granulated blast furnace slag (GGBFS) and metakaolin (M) as alternative binders to replace OPC and produce a sustainable low-carbon cement material. Fly ash is an aluminosilicate product, mostly spherical particles but solid spheres and fines, which react with Calcium hydroxide ( $\text{Ca}(\text{OH})_2$ ) to form gel products [13]. GGBFS is obtained when the iron is manufactured. It is generated in the blast furnace and then slaked. Lower silica and  $\text{Na}_2\text{O}$  modulus in GGBFS benefit higher hydration products due to the heat released [20]. Both FA and GGBFS are presented in powder form and have fine particle sizes beneficial for mechanical strength development. AAMs composed of FA or metakaolin will produce sodium aluminosilicate hydrate or N-A-S-H gels as the main reaction product, while AAMs composed of slag create calcium aluminosilicate hydrate (C-A-S-H) gels, essential for cementitious binder materials [25]. In addition, FA and GGBFS have a higher content of amorphous phases that are favourable to accelerating the reaction scale for creating hardened products [2].

In addition, sodium hydroxide ( $\text{NaOH}$ ) and sodium silicate ( $\text{Na}_2\text{SiO}_3$ ) are alkaline solutions frequently used to activate the precursors and form a hardened matrix comparable to OPC in a two-part AAMs system [44]. On the contrary, the two-part AAMs concept has setbacks in handling, mixing, and transportation issues besides heat curing requirements to achieve the required strength, making this product unsuitable for in situ construction [59]. Researchers introduce the innovative method of one-part alkali-activated materials as complementary to the traditional two-part concept. Aluminosilicate precursors are mixed with solid alkali activators to form a dry mixture, and water is added to initiate the geopolymerization process [62]. This ‘just add water’ method has improved AAMs properties in terms of mechanical strength, porosity, durability, and fast application, which is easier to use. Kadhim et al.[88] explained the function of the alkali activator to provide an alkali medium and raise the pH for the reaction of mixtures

by assisting the dissolution process of aluminosilicate precursors in AAMs technology. Four main alkali groups are commonly used to generate the hardened binder of this solid precursor: alkali hydroxide, alkali silicates, alkali carbonates and alkali sulfates [47]. Anhydrous sodium metasilicate ( $\text{Na}_2\text{SiO}_3$ ) is reported as the most suitable activator for the geopolymerization process but possesses a higher  $\text{SiO}_2/\text{Na}_2\text{O}$  ratio that makes it challenging to handle as such a corrosive chemical. For that reason, the lower  $\text{SiO}_2/\text{Na}_2\text{O}$  ratio of solid sodium carbonate is being studied as an alkali activator due to its low alkalinity level to provide safe and easy activator handling, compared to the sodium silicate activator or alkali hydroxide, which costs more expensive and high  $\text{CO}_2$  emission. On the contrary, besides its corrosivity, the total cost of sodium hydroxide is almost 5-6 times higher than the calcium oxide type of alkali activator. Hence, it is crucial to minimize the usage of alkali activators in AAMs and make this technology safe, practical and cheap.

However, the investigation found that the one-part AAMs still have a low or inconsistent compressive strength, flexure strength and shrinkage cracking [59][60]. Numerous studies have been conducted to improve the compressive strength of one-part AAMs, but most studies are limited to only the synthesis and characterization stage. As a result, the application of one-part AAMs technology in the form of mortar for concrete structural repair has still lagged. The class F FA is a low reactive precursor that was combined with calcium-rich slag to expedite the system's reactivity, subsequently abolishing the heat curing prerequisite, but it causes rapid hardening, which is not applicable for actual site application. A 15% slag reported was the optimum dosage of one-part AAMs mixed with 85% FA that improved the mechanical strength of one-part AAMs. Unfortunately, it was also activated with an 8% activator dosage that is still considered corrosive and costly [28]. Another study on one-part alkali-activated mortar composed of 40% GGBFS / 60% FA and 10%  $\text{Na}_2\text{SiO}_3$  showed higher compressive strength up to 80 MPa but only managed recorded 7 MPa of flexural strength, less than 10% of its compressive strength [65] that affect its ability to resist bending for concrete repair application. The flexural strength ( $11 \text{ N/mm}^2$ ) and modulus of elasticity (27 GPa) for mortar composed of 100% GGBFS were the highest compared to a single precursor of FA and metakaolin. Nevertheless, slag mortar could not

bond vertically and horizontally, making it not applicable to concrete repair materials in the study conducted by [23]. The splitting tensile strength for one-part alkali-activated mortar with fibre can be achieved up to 3.5 – 11 MPa, yet a higher alkali-activated dosage of between 8 – 10% is required to achieve that standard strength [59][61].

Including the OPC in AAMs mixtures can improve and accelerate the reaction rate for strength development [90]. Moreover, this type of mixed or blended cement is cheap. OPC is a type of hydraulic cement composed of hydraulic calcium silicates. This cementitious material creates calcium silicate hydrate or C-S-H gels as the main hydration products used as binding agents responsible for the strength. The combination of by-product precursor with the OPC can be activated by non-hygroscopic alkali, which is beneficial in preventing the inclination for efflorescence, high permeability, and more severe water absorption problems. A 60% OPC added in one-part AAMs concrete recorded 55.0 N/mm<sup>2</sup> compressive strength at 28 days of age provides essential information in designing one-part AAMs in the form of mortar for patching concrete repair techniques. This concrete consists of coarse aggregate and has also been activated with a significantly higher 12% potassium carbonate (K<sub>2</sub>CO<sub>3</sub>) [38].

Furthermore, the inclusion of 15% waste concrete fines was reported to improve the mechanical strength of AAMs. Still, excessive waste construction (concrete) fines adversely impact the mechanical strength due to slow hydration degree and insufficient high calcium content, reducing C-A-S-H gels [91]. In addition, the recycled concrete powder also increases porosity in two-part AAMs due to low polymerization activity, creating a more porous microstructure [92].

AAMs' more significant shrinkage level was also the primary concern in both two-part and one-part systems. Hence, the presence of shrinkage-reducing admixtures (SRA) and calcium oxide (CaO) could control the expansion of hardened AAMs [69]. Moreover, combining SRA and CaO can stabilize the shrinkage effect [93]. A higher concentration of alkali activator may assist the degree of hydration, but higher heat release creates more expressive shrinkage after drying [83]. Adding CaO, which can provide extra alkalinity and calcium sources for forming C-S-H gels from

the cement binder, can reduce reliance on the alkali activator and increase the mechanical strength. This agrees that strength development is reduced when calcium content decreases [94]. Still, excessive content of both SRA and expansive additive of CaO may be causing other side effects such as fast setting and losses of water or moisture, thus ineffective in reducing drying shrinkage level [35]. To control the fast setting problems, a lignosulfonate-based superplasticizer (SP) was used to regulate the setting time of high calcium one-part AAMs and avoid setting too quickly, which is essential for transporting fresh materials from batching plant to the site [66]. The previous study on the potential admixtures for one-part alkali-activated materials (AAMs) also suggested that by adding SP to the mixtures, the water content can be optimized to improve the compressive strength of the mortar [72].

Therefore, this experiment aims to evaluate the mechanical strength performance of one-part alkali-activated mortar composed of different dosages of aluminosilicate precursors and activated with low dosages of solid alkali activators for concrete structural repair applications. The main precursor source used in this study was composed of the industrial by-product of FA and GGBFS combined with OPC, unlike typical one-part AAMs commonly composed of by-product powder only.  $K_2CO_3$  is a single solid alkali activator used to activate the precursors and as the source of alkali besides the existing sodium and potassium element ( $Na_2O$  and  $K_2O$ ) in the OPC. In addition, three powder admixtures were added and tested to stabilize the hardened material's physical properties. Furthermore, a test for drying shrinkage level for durability was also carried out. To the author's knowledge, no previous studies were conducted to evaluate the potential of one-part alkali-activated mortar composed of hybrid precursors and activated with a low alkaline solid alkali activator used for concrete structural repair application as an alternative to the conventional two-part AAMs system.

This study aims to comply with the compressive strength requirement with Class R3 – EN1504 standard for structural concrete repair materials. According to the EN1504 standard, for non-structural concrete repair materials Class R2, compressive strength must be above  $15 \text{ N/mm}^2$ . For structural concrete repair, Class R3  $\geq 25 \text{ N/mm}^2$  and  $\geq 45 \text{ N/mm}^2$  for Class R4 [5]. The novel

mix design formulation reported in this study is vital for the author's continued research on utilizing one-part AAMS technology for green and sustainable building products. The experiment was done in Kuala Lumpur, Malaysia – a country with a tropical climate, which is hot and humid throughout the year.

## **4.2 Materials and Methods**

Class f – Fly Ash (FA) and Ground Granulated Blast Furnace Slag (GGBFS) were used as precursors under ASTM C618 and ASTM C989, respectively. Ordinary Portland cement (OPC) was added as the primary binder source and activated with alkali-activated powder - potassium carbonate ( $K_2CO_3$  Purity  $\geq 90\%$ ). The chemical compositions and physical properties of all main precursors are shown in Table 3. Natural sand was used as fine aggregates with a specific gravity of 2.67 and an average particle size of 90.23  $\mu m$  (D50). In addition, a commercial ethylene glycol type of shrinkage-reducing admixture (SRA) and CaO were added as an admixture in the form of solid powder. At the same time, the sodium lignosulfonate powder-based SP was also used in the experiment as a retarder for the mortar samples.

### **Mix proportions**

The experimental study was conducted to understand the effect of aluminosilicate precursors with different volume ratios, with OPC as the main binder and activated with a low percentage of alkali-activated powder. Besides that, three powder-type admixtures were added to all mixtures to investigate the effect of these admixtures compared to the samples prepared without admixtures. There were three stages of the experiment. All the samples were marked as Mix 1 to Mix 30 and consisted of FA, GGBFS, and with/without OPC as main precursors with different volume percentages. Stage 1, Mix 1, was chosen as a control sample no.1, where the mixture contained only FA and GGBFS without OPC. For the second stage, Mix 10 was prepared as control sample no.2, which contained no admixtures. At the third stage, Mix 26 was chosen as control sample no.3 based on the findings on mechanical strength results for Mix 16 – 25 at 7 days of age (within the second stage experiment). The admixtures proportion for every sample was added into the mortar samples between 1.0 to 15.0 wt% of weight (based on total

aluminosilicate precursors weight). The water-to-binder ratio was set between 0.30 to 0.50, and the aggregate-to-binder ratio was between 1 – 3 to produce the mortar, tested in all 30 mortar mixture samples and cured under the lab ambient conditions. The mix design compositions of one-part alkali-activated mortars are further elucidated in

Table 4.

### **Sample preparations**

An electric mixer, EX-EM2000 EXTRAMAN 2000W, prepared all mixes. The FA, GGBFS, PCC,  $K_2CO_3$ , SRA, CaO, Sodium Lignosulfonate (SP) and fine aggregates were blended for 2 minutes according to their sample of mix compositions. After that, water was added slowly to the mixtures and continued blending for another 3 minutes to ensure the mortar paste was uniform. Then, all the fresh mortars were immediately cast into 50mm x 50mm x 50mm cubes for the compressive strength test, 40 mm x 40 mm x 160 mm for the flexural strength test, 150 mm x 300 mm diameter cylinder for tensile strength test and modulus of elasticity test and 75 mm x 75 mm x 280 mm for drying shrinkage measurement. All filled moulds were vibrated for 2 minutes using a shaking table. The mixtures were de-moulded after 24 hours before being cured in an ambient lab temperature of 29 °C, with Relative Humidity (RH) of 65 % until the testing day on 7, 14 and 28 days of curing age. For the compressive strength test, samples were collected for curing under standard laboratory climate (dry conditioning) for 7 days at  $21 \pm 2$  Celsius and  $60 \pm 10$  % RH.

### **Experimental procedures.**

To study mechanical strength, hardened mortar's compressive and flexure strength was evaluated at 7-day, 14-day, and 28-day curing age. Compression test machine AUTOMAX5 was used at a loading rate of 1000 N/s per the EN12190 test method and a three-point flexure test under a displacement-controlled condition where the load was applied at mid-span in compliance with BS EN 13892-2:2002. The mean value of three readings of each sample produced in triplicate for every test was recorded and taken as their final strength value. In addition, a test on the static modulus of elasticity mortars was conducted at 28-day of age with basic stress of  $0.5 \text{ N/mm}^2$ , and the stress increased at a constant rate within the range of  $0.6 \text{ N/mm}^2/\text{s}$  until the stress was equal

to one-third of the compressive strength of the concrete is reached in compliance with BS 1881. Three cylindrical specimens of 150 mm x 300 mm size for the selected mortar sample formula were prepared, and the average and standard deviation were calculated and reported. Indirect tensile strength was employed using a tensile splitting method on cylindrical mortars for the selected mortar sample and assessed at 28 days of age following ASTM C496 at a loading rate of 1 MPa/s. For drying shrinkage measurement, a test was done on the prism samples according to BS 1920-8:2009, tested at 28 days of curing age.

Table 3: Chemical compositions (%) and physical properties of Fly Ash (FA), Ground Granulated Blast Furnace Slag (GGBFS) and ordinary Portland cement (OPC) were obtained from the manufacturer.

<b>Chemical Compositions</b>	<b>FA (%)</b>	<b>GGBFS (%)</b>	<b>OPC (%)</b>
SiO <sub>2</sub>	55.94	35.91	23.97
Al <sub>2</sub> O <sub>3</sub>	22.60	16.56	5.27
Fe <sub>2</sub> O <sub>3</sub>	8.10	1.52	3.28
CaO	6.26	35.28	60.12
P <sub>2</sub> O <sub>5</sub>	0.36	0.36	-
MgO	1.21	6.01	1.36
K <sub>2</sub> O	1.66	-	0.51
TiO <sub>2</sub>	0.72	0.59	0.06
SO <sub>3</sub>	1.02	0.36	2.20
Na <sub>2</sub> O	0.62	1.76	0.23
Cl	0.03	-	-
LOI	1.48	-	2.00
<b>Physical Properties</b>			
Specific Gravity	2.20	2.90	3.15
Average Particle Size (D50)	14.08 μm	19.99 μm	16.32 μm

Table 4: Mix composition and design of one-part Alkali Activated Materials (AAMs)

Samples	Binder			Alkali activated	Admixtures			Design ratio	
	FA (%)	GGBFS (%)	OPC (%)	K <sub>2</sub> CO <sub>3</sub> (%)	SRA (%)	CaO (%)	SP (%)	a/b	w/b
*Mix 1	85	15	0	6	5	1	1	3	0.30
Mix 2	25.5	4.5	70	6	1	0.5	1.5	3	0.30
Mix 3	60	10	30	6	5	1	1	3	0.35
Mix 4	59.5	10.5	30	6	5	1	1	1.5	0.46
Mix 5	25	5	70	6	2	1	1	1	0.49
Mix 6	45	5	50	5	2	1	1	1.5	0.45
Mix 7	59.5	10.5	30	6	5	1	1	1	0.35
Mix 8	81	9	10	6	4	1	1	1	0.35
Mix 9	60	10	30	6	5	1	1	1	0.35
**Mix 10	60	10	30	6	-	-	-	1	0.35
Mix 11	60	10	30	6	4	1	1	1	0.35
Mix 12	60	10	30	8	4	10	1	1	0.35
Mix 13	60	10	30	10	5	15	1	1	0.40
Mix 14	45	5	50	8	4	10	1	1	0.35
Mix 15	45	5	50	10	5	15	1	1	0.40
Mix 16	30	-	70	8	4	10	1	1	0.35
Mix 17	30	-	70	10	4	15	1.5	1	0.40
Mix 18	30	-	70	8	4	10	1.5	-	0.45
Mix 19	30	-	70	10	4	10	1	1	0.45
Mix 20	30	-	70	8	4	10	1	1	0.45
Mix 21	30	-	70	8	4	10	1	1	0.50
Mix 22	40	-	60	8	4	-	1	1	0.45
Mix 23	30	-	70	8	4	-	1	1	0.45
Mix 24	20	10	70	8	4	-	1	1	0.45
Mix 25	25	5	70	8	4	-	1	2	0.45
***Mix 26	25	5	70	1.8	-	-	-	1	0.50
Mix 27	25	5	70	1.6	0.3	0.15	1	1	0.50
Mix 28	25	5	70	2	0.9	0.45	1	1	0.50
Mix 29	25	5	70	1.8	0.6	0.30	1	1	0.49
Mix 30	25	5	70	1.6	0.3	0.15	1	1	0.40

\*control sample no.1, \*\*control sample no.2, \*\*\*control sample no.3.

### 4.3 Result and Discussion

#### 4.3.1 Compressive strength

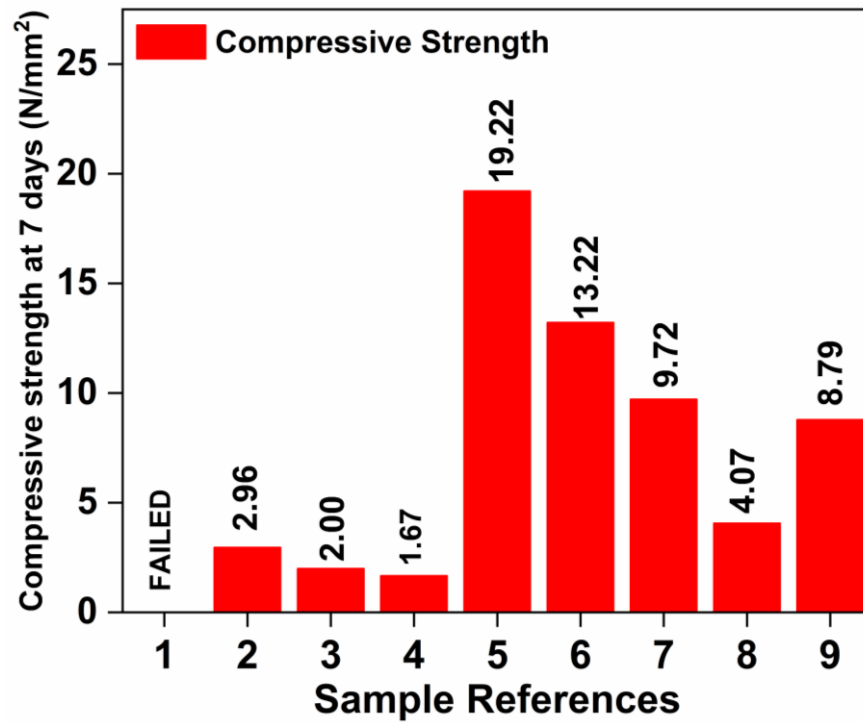


Figure 2: Compressive strength at 7 days of curing age – Stage 1

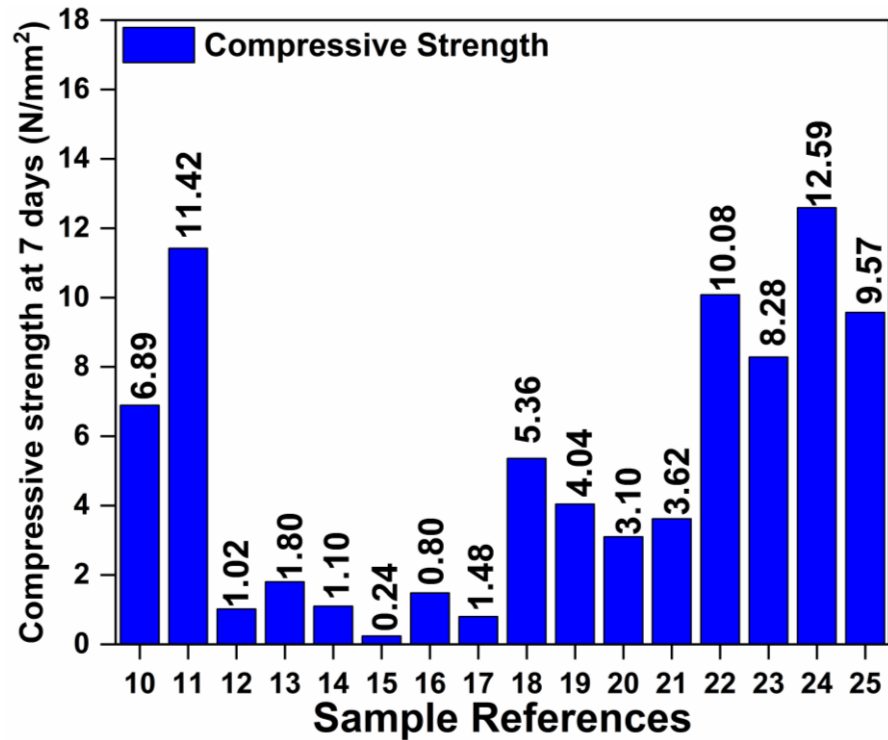


Figure 3: Compressive strength at 7 days of curing age – Stage 2

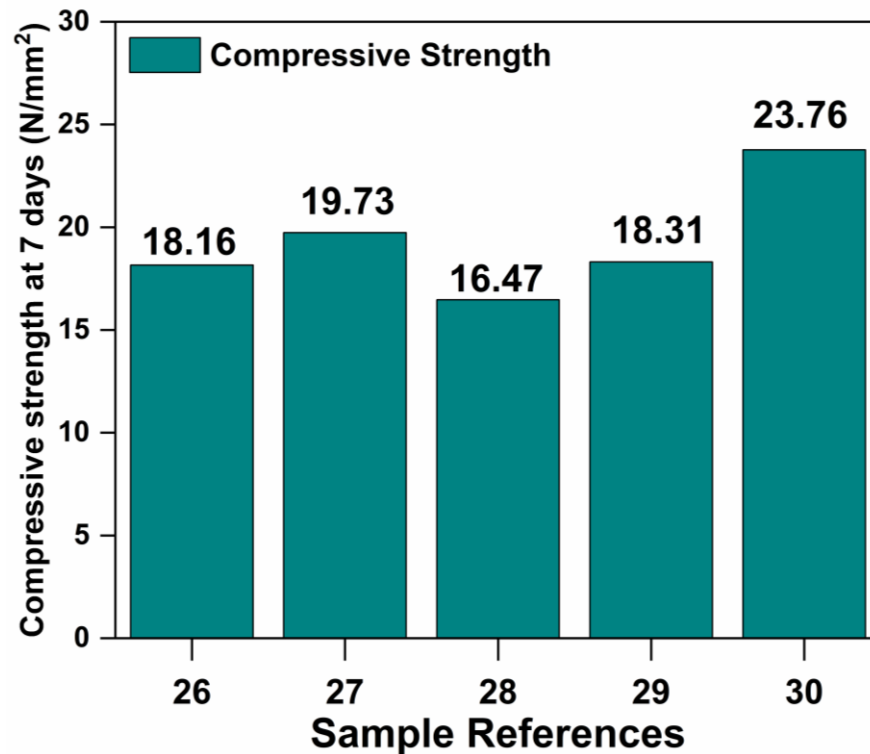


Figure 4: Compressive strength at 7 days of curing age – Stage 3

The 7-day compressive strength for 30 samples ranged from 2 N/mm<sup>2</sup> to 23 N/mm<sup>2</sup>, as shown in Figure 2 - Figure 4. Mix 30, composed of 25% FA, 5% GGBFS and 70% OPC, recorded the highest compressive strength with 23.76 N/mm<sup>2</sup>, nearing the minimum strength requirement at 28 days of curing age for structural repair products class R3 of EN1504-3 standard. For the mortar samples, Mix 5, 26, 27, 28, and 29 all recorded compressive strength above 15 N/mm<sup>2</sup> and had the potential to comply with the minimum strength requirement at 28 days of curing age for non-structural repair products class R2 of EN1504-3 standard.

Adding FA may slower the strength development of mortar at an early age and clarify the lowest compressive strength reported for samples. Mix 7 – 13 consisted of 60% - 80% FA. Without OPC, sample Mix 1 was prepared as a control sample consisting of 85% FA and 15% GGBFS and was activated by a 6% alkali activator, referred to as the first stage of this experiment for mortar samples 1 – 9 (see Figure 2). It was reported that the total aggregate content had not affected the flexural strength development of one-part AAMs [51]; thus, aggregate-to-binder ratios were set to 3 as a source of calcium and increased the mortar volume for the first three mortar samples,

Mix 1 – 3. However, these three samples were not hardened enough and immediately collapsed when the applied load was placed on the cube samples for testing.

Furthermore, these 3 samples were activated with a low water-to-binder (w/b) ratio of 0.3, contributing to lower compressive strength. As a result, the cube samples were brittle, sandy, cracked and failed due to insufficient water to initiate the geopolymeration process. The w/b ratio increased from 0.3 to 0.45 for Mix 3 - 9 and still only managed to get low compressive strength, except for Mix 5 (w/b ratio of 0.49), which was also designed with an aggregate-to-binder ratio of 1 and lower FA volume (than sample Mix 4) has recorded 13.22 N/mm<sup>2</sup> for 7 days of curing age offered important indication on the optimum design of aggregate-to-binder ratio. A higher a/b ratio between 1.5 to 3.0 in this study led to low compressive strength at 7 days of curing age due to the insufficient hydration of main gel products of C-S-H could not wholly wrap the surface of the fine aggregate, creating more porous structures that make it physically not solid [35].

Mix 10 was designed as a control sample no.2 without admixtures to evaluate the compressive strength trend for mortar samples. Mix 11 – 24 were prepared for the second stage (see Figure 3) in this compressive strength test experiment. The mortar samples Mix 10 has a 6% alkali activator and w/b ratio of 0.35 and recorded compressive strength of 6.89 N/mm<sup>2</sup>. In addition, a 1 – 10% CaO was added to the mortar because the CaO could supply additional calcium, increase the exothermic level for the hydration process, and react with silica and alumina from FA to produce additional C-S-H and C-A-S-H. Furthermore, the higher silica content in FA increased the dissolution and polymerization process. A higher Si/Al ratio in FA promotes low porosity microstructures, ensuring high sample compactness and enhancing compressive strength [95]. Excessive CaO, however, could lead to strength loss due to the fast chemical reaction of the matrix, subsequently generating unbalanced gel binder structures that affect strength development [24].

Further investigation found that a higher volume of CaO between 10 – 15% of mix composition was one factor in the poor compressive strength recorded for Mix 12 – 21. As a result, the volume of FA was reduced to 45% and 40% in Mix 14, 15 and 22 but still showed poor compressive strength. At the same time, samples with 30% FA without GGBFS continued a low compressive strength value trend below  $10\text{N/mm}^2$  as recorded for samples Mix 16 – 23, which gives a significant indication on the influence of GGBFS and its relation with FA to generate a stronger bond of prominent C-S-H gels.

A higher volume of GGBFS than FA in sample Mix 24 has shown slight improvement for 7-day compressive strength but is still within 50% of the targeted strength of class R3 standard. Nevertheless, it was reported that higher slag content is susceptible to autogenous shrinkage and cracking due to the rapid acceleration of the reactions [65]. Besides that, it was found that without CaO, the 4% SRA-only was inefficient in influencing the compressive strength performance of sample Mix 25. Therefore based on the compressive strength result at 7 days for Mix 10 - 15 (admixture effect) and Mix 16 - 25 (GGBFS effect), Mix 26 was designed as a control sample no.3 for the mix composition consisting of 25% FA and 5% GGBFS with the presence of 70% OPC and 1.8% alkali activator to produce the mortar, subsequently referred as the third stage of the experiment (see Figure 4). As a result, the compressive strength results for Mix 26 have an impressive early strength development up to  $18\text{N/mm}^2$  equivalent to 72% of the 28-day minimum compressive strength class R3 and successfully exceeded the 28-day minimum compressive strength for non-structural repair products class R2, both per EN1504-3 specification.

The concentration of alkali activators is crucial for early strength development [66]. A higher alkali activator dosage is required to complete the dissolution of raw materials. At lower alkali activator dosages, the dry mixtures were not fully reacted, causing the mortar to fail to harden at early curing ages. However, for this study, it was shown that a higher percentage had negatively affected its mechanical strength, as explained in samples Mix 1 – 25, which activated by 6 – 10% of alkali activators were unable to react well with precursors and an excessive amount of SRA (1 - 5%) and CaO (0.5 – 15%). Therefore, the alkali activator was set between 1.6 and 2.0% for this

third test stage. The SRA and CaO were adjusted to 0.3 – 0.9% of precursor volume for the SRA and 0.15 – 0.45% for CaO. The w/b ratio was maintained between 0.35 – 0.5. Also, a 1% superplasticizer (SP) and an aggregate-to-binder ratio of 1 were consistently applied to all samples. Therefore, the highest compressive strength value at 7-day of age was obtained from sample Mix 30 at an optimum w/b ratio of 0.4, where enough water supply was essential for the geopolymerization process at an early age essential for heat equilibrium, especially with the inclusion of 70% OPC and chemical admixtures (SP, SRA and CaO) that caused more heat released from the exothermic reaction.

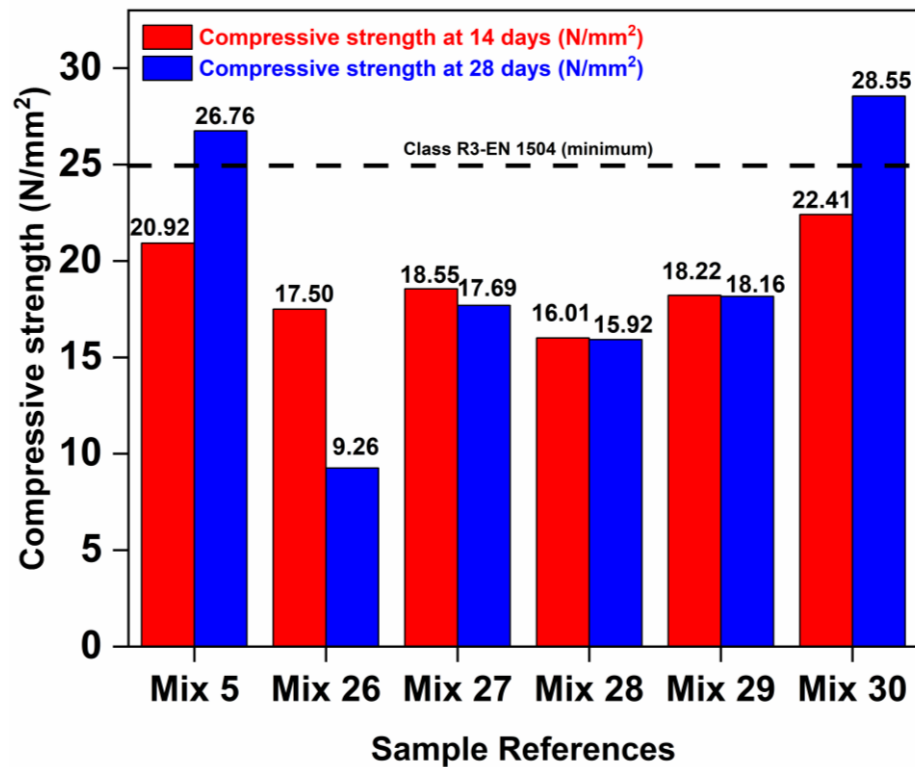


Figure 5: Compressive strength at 14 and 28 days of curing age

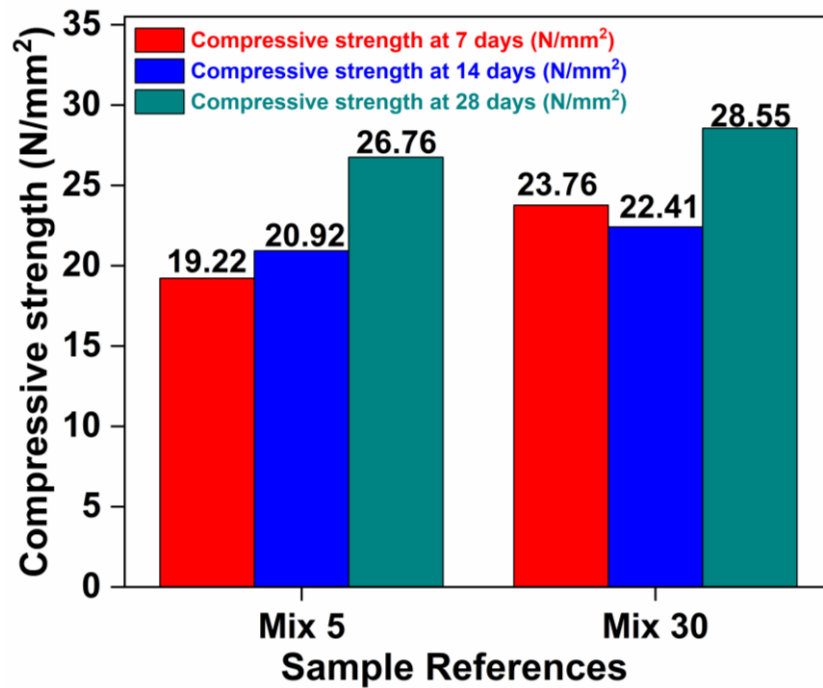


Figure 6: Compressive strength at 7, 14 and 28 days of curing age

Only 6 samples were selected out of 30 for compressive strength tests at 14 and 28 days of curing age, and the result is recorded in Figure 5. However, compressive strength for samples Mix 26, 27, 28, and 29 deteriorated on day 14 and dropped further toward day 28. It is worthing to understand that all mortar samples Mix 26, 27, 28 and 29 have higher water content with w/b ratios of 0.50 and 0.49 (Mix 29). These findings agreed with [5] on the effect of higher water content reducing the rheology of fresh mortar, subsequently affecting the mechanical strength at the hardened stage. Excessive water content may be caused extra gaps to occur between aggregates, creating voids filled by air when moisture vaporizes. The hardened materials then experience insufficient compaction and become less solid, which affects their strength [96]. Additionally, insufficient alkali cation ( $\text{Na}^+$ ,  $\text{K}^+$ ) to keep the pH raised for the reaction mixtures affects the dissolution process at 28 days of curing age.

Moreover, Mix 26 as a control sample was composed without admixtures, affecting the stability of the C-A-S-H gels chains and making them prone to chemical attacks. Crack formation due to shrinkage has also lowered the mechanical strength development. A combination of CaO and SRA was reported to control the shrinkage efficiently [69][93]. Still, too much CaO and SRA

content in Mix 28 and 29 did not react well with a low dosage of solid alkali activator and higher water content level factors in this report. The reaction rate between precursors and admixtures decreased in low alkali medium, causing low mechanical strength and porous structures [30]. This phenomenon is because low pH of carbonate delayed the initial reaction of one-part AAMs and might not be able to fully break down the Al-O and Si-O bonds of the aluminosilicate precursors with the presence of excessive admixtures content. The highest compressive strength recorded at 28 days was 28.55 N/mm<sup>2</sup> for sample Mix 30, followed by Mix 5, which recorded 26.75 N/mm<sup>2</sup>. These two samples have strength increases over time consistently from 7 days to 28 days of curing age, as shown in Figure 6 and exceed the minimum requirement for structural repair product Class R3 of EN1504-3 standard. The microparticle size of powder precursors FA, GGBFS and OPC in this study exhibit higher specific areas helpful in improving the reaction for better mechanical strength [2].

The cracked pattern of the cube samples for sample Mix 30 has little impact on faces in contact with the platens, cone and shear with fewer macrocracks, generally reflecting its rigidity supporting on higher compressive strength value as shown in Figure 7(a). In contrast, Mix 26 experienced an unsatisfactory type of cracked pattern failure, which indicates it's brittle and not solid, as illustrated in Figure 7(b). It was noted that a higher Si/Al ratio for 25% fly ash Class F used in this experiment is physically stable without significant structural disintegration, contributing to the excellent performance in compressive strength [97]. Si/Al ratio for FA was above 2 within the recommended ratio for higher compressive strength suggested by [95][98][99]. In addition, the main precursors are composed of rich calcium content supplied from GGBFS and OPC sources. Calcium is beneficial for creating C-S-H gels. The combination of FA/GGBFS expands the C-S-H gels chain by creating new C-(A)-S-H co-existed with N-A-S-H gels for excellent mechanical properties [25]. As a record, Coppola et al.[100] reported that a one-part alkali-activated mortar activated with a 4% alkali activator recorded compressive strength of 26.4 N/mm<sup>2</sup> at 28 days of curing age, lower than the findings in this study which activated with a minimal dosage of alkali activator.

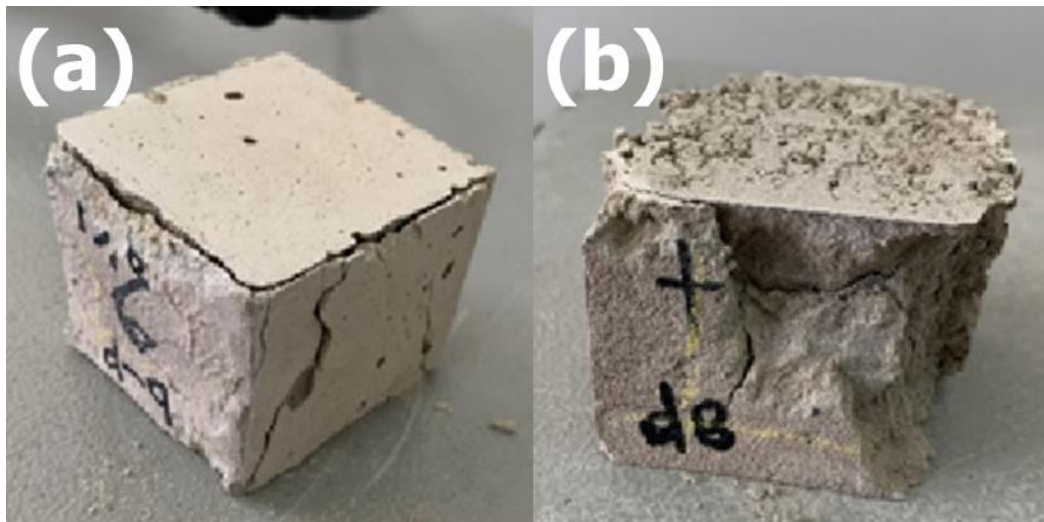


Figure 7: (a) Cracked pattern failure for mortar sample mix 30 under compressive strength test; (b) Cracked pattern failure for mortar sample mix 26 under compressive strength test.

#### 4.3.2 Flexural strength

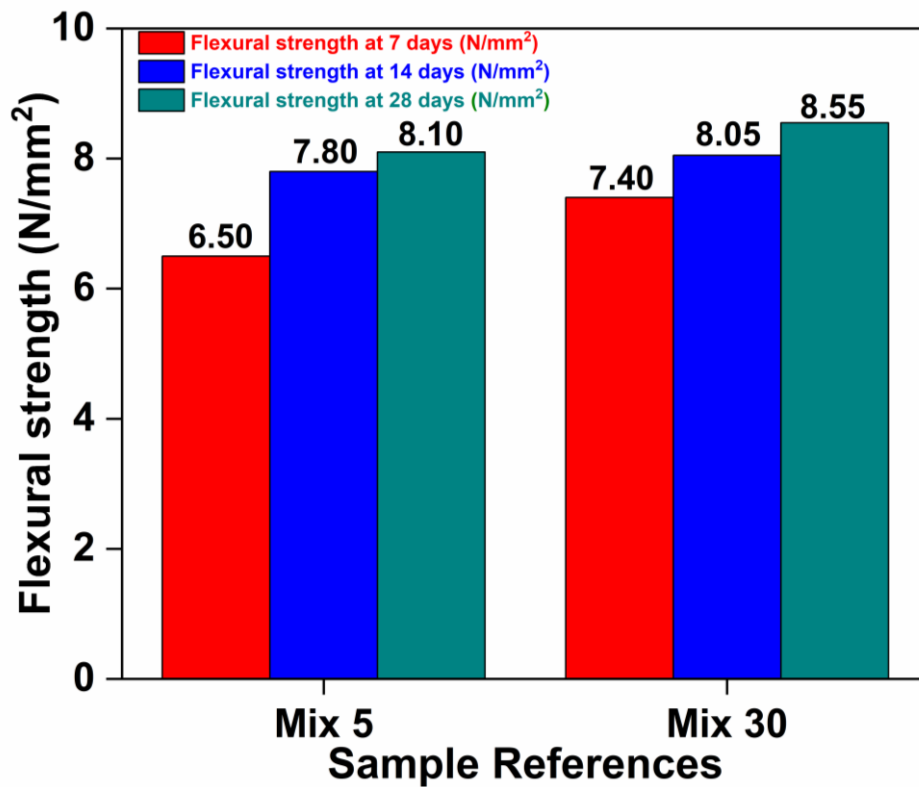


Figure 8: Flexural strength at 7, 14 and 28 days of curing age

The experiment in this report continues with the flexural test to determine the mechanical compatibility of the mortar and its bending resistance. The test will further explain its tensile strength ability indirectly. Sample Mix 5 and Mix 30 were selected to obtain their flexural strength

because their compressive strength at 28 days achieved the minimum requirement as per EN 1504-3 class R3 standard, subsequently referred to as control samples used for the rest of the experiment in this report. At 7, 14 and 28 days, the flexural strength for Mix 30 was 7.4 N/mm<sup>2</sup>, 8.05 N/mm<sup>2</sup> and 8.55 N/mm<sup>2</sup> and it was the highest flexural strength recorded between two control mortar samples, as shown in Figure 8, where the flexural strength development increased over time. Both mortar samples recorded above 8 N/mm<sup>2</sup>. The addition of 5% GGBFS improved the early mechanical strength of the mortar. At the same time, calcium from FA increased the pozzolanic reaction at the later stage. Besides, a more substantial bonding factor between the binder and the aggregate in the mortar is beneficial for bending resistance behaviour [51].

The flexural strength of Mix 30, however, was only around 30% of its compressive strength at 28 days of curing age. This result further explained that the unreinforced mortar cube samples used in this experiment are naturally brittle and very stiff. In addition, the growth of its mechanical strength over time dropped due to microcracks [33]. Nevertheless, the mortar used in the experiment was comparable to the conventional OPC concrete. The concrete standard's flexural strength or modulus of rupture is between 10 – 20% of its compressive strength, depending on the volume and size of the coarse aggregate used in the concrete. Also, the 8.55 N/mm<sup>2</sup> flexural strength of Mix 30 exhibited a higher strength value than other one-part alkali-activated materials, as published in past reports [65][69].

### 4.3.3 Modulus of Elasticity

Table 5: Modulus of Elasticity (MOE) at 28-day of age

Sample References	Modulus of Elasticity (GPa)
Mix 5	18.10
Mix 30	19.60

Besides the mechanical strength, alkali-activated mortar's higher modulus of elasticity is essential to offer durable repair materials by providing resistance against elastic deformation when force is applied. The lower aggregate-to-binder ratio reported increased the MOE of concrete activated

by one-part AAMs as written by [51]. The ratio of aggregate-to-binder in this experiment was 1, and the mortar samples for the MOE test were cured with water and ambient conditions.

As shown in Table 5 the modulus of elasticity of sample Mix 30 was recorded at 19.6 GPa, and Mix 5 has 18.10 GPa MOE, both complying with the minimum elastic modulus requirement for class R3-EN1504 standard, slightly higher than the modulus of elasticity for most of the two-part alkali-activated mortar, which has been recorded between 15 – 18 GPa [33][26]. Additionally, they did not require higher temperatures than the two-part AAMs [7]. However, similar to the flexural strength development, micro-cracks have affected the MOE of one part of alkali-activated mortar [39]. In addition, it is worth noting that repair materials and substrates may have different modulus of elasticity. For example, concrete substrates generally have an elastic modulus between 30 to 50 GPa. A lower modulus of elasticity of repair material than the substrates has more resilient elements that can take up more force and return to its initial structure [5], subsequently protecting mortar from cracking, thus providing better structural compatibility between the repair mortar and the existing concrete substrates [33].

#### 4.3.4 Tensile Strength

Table 6: Splitting tensile strength at 28 days of curing age

Sample References	Splitting Tensile Strength (MPa)
Mix 5	1.80
Mix 30	2.05

The higher aggregate content would increase the splitting tensile strength, and the strength developed over time follows a similar trend with compressive and flexural strength. However, the tensile strength after 28 days was lower than the mixtures with lower aggregate content reported by [51]. The highest splitting tensile strength between these two samples is Mix 30, which has recorded 2.05 MPa, equivalent to 10% of its compressive strength at 28 days of curing age, as shown in Table 6 and giving a good signal of its bond strength ability to achieve minimum adherence strength 2.0 MPa of class R4, EN1504-3 [1]. Nevertheless, Mix 30 with 2.05 MPa

tensile strength was within the range of tensile strength for typical plain cementitious mortar, as reported by [101]. It turns out that the incorporation of slag as a replacement for fly ash for mortar Mix 30 enhanced splitting tensile strength, as reported by [102]. It is worth noting that mortar is good in compression but weak in tension, like typical concrete. The interface Transition Zone (ITZ) is the weakest link in the hardened mortar, as observed from its microstructure. When a compressive load is applied, the ITZ bridges the load from one aggregate to another in the mortar. On the contrary, the outer surface of aggregates will break from each other when tensile stresses are applied to leave the ITZ to absorb all forces and cause failure.

#### 4.3.5 Drying shrinkage

Table 7: Drying Shrinkage Measurement at 28 days of curing age

<b>Sample References</b>	<b>Drying Shrinkage Measurement (microstrain)</b>
Mix 5	350
Mix 30	260

Shrinkage is one of the significant problems for alkali-activated materials, mainly caused by alkali activator involvement in accelerating the reaction. Jixiang et al.[2] reported that a higher sodium silicate and slag content dosage in alkali-activated materials increased shrinkage. In this report, a lower dosage of alkali activator and slag for the one-part mortar Mix 30 has a length change measured of 260 microstrains at 28 days, while for mortar sample Mix 5 has documented 350 microstrains, both recorded lower than 400 microstrains under ASTM C157 specification for drying shrinkage measurement as shown in Table 7, which is much better than the shrinkage level of the two-part alkali-activated materials counterpart. This result also agreed with [103] on the beneficial effect of the SRA in alkali-activated materials. The SRA admixture will limit the tensile stress stimulated by restrained shrinkage, thus avoiding the mortar from early cracks. Therefore, drying shrinkage measurement can indicate the mortar's ability to resist early crack formation and shrinkage-restraining stresses.

On the other hand, the low w/b ratio increased the mechanical strength of hardened mortar. Still, it could result in autogenous shrinkage and cracking, affecting the flexural strength over time. Sample Mix 30 mortar in this experiment has proved that even though it was composed of a lower water-to-binder ratio and a lower dosage of alkali activator yet recorded a lower level of drying shrinkage measurement within a maximum of 400 microstrains allowed. The result is also in agreement with [69][93], where the usage of shrinkage-reducing admixtures (SRA) and calcium oxide (CaO) as an expensive agent could reduce the shrinkage level of mortar. It is beneficial to determine CaO dosage in this experiment because the excessive level of calcium may precipitate as gypsum and expand, may damage the mortar's physical structures, but with an appropriate ratio, the gypsum may also block pores and minimize early corrosion attacks [104]. Furthermore, CaO is an expansive agent that induces a high exothermic reaction when it reacts with water to form a larger volume of hydrated lime particles, which helps the mortar to expand instead of shrinking and only stops expanding at the end of the curing process [93].

Other than that, the applied aggregate-to-binder of 1 for Mix 30 contributed to a better performance of tensile strength where it controlled the shrinkage level where the fine aggregate served as reinforcement to compact and stabilize the materials [1]. It is worthing to note that a higher percentage volume of all three admixtures created unbalanced gel structures and affected mechanical strength growth at the early and later stages of the hardening phase, as observed in all 30 mortar samples' compressive strength results in this study. Contrary to the conventional one-part alkali-activated mortar productions, the inclusion of admixtures and OPC reacted well with a low dosage of non-hygroscopic alkali activator, offering cheaper and safer construction products. This type of hybrid one-part AAMs has impressive mechanical strength and a low drying shrinkage level comparable to the conventional OPC mortar and the two-part AAMs mortar counterparts.

#### **4.4 Conclusions**

This study investigated the mechanical strength performance of one-part alkali-activated mortar for concrete structural repair application. The mortar was composed with different mixed design

compositions. As a result, mortar sample Mix 30 has the best mechanical strength performance out of 30 different mix design ratios, followed by mortar sample Mix 5. In Mix 30, the OPC binder content has been replaced with 30% by-product precursors consisting of 25% class-F fly ash and 5% slag from the GGBFS source. Interestingly, dry mixed precursors were activated with only 1.8% powdered alkaline activator of Potassium carbonate ( $K_2CO_3$ ). As a result, mortar samples Mix 30 has a water-to-binder ratio of 0.40 compared to Mix 5 activated with a w/b of 0.49. The mechanical strength results for mortar sample Mix 30 have complied with the minimum requirements for the compressive strength and modulus of elasticity (MOE) as per the Class R3-EN1504 standard for structural concrete repair materials and successfully achieved the aim of this study.

For one-part AAMs activated with low alkali activator dosage, a single aluminosilicate precursor will not be sufficient to produce the higher compressive strength of mortar. Combining two or three industrial by-product precursors with OPC demonstrates improved physical structures and mechanical strength. The combination of FA and GGBFS reacted well with the OPC under a low alkaline environment and exhibited acceptable mechanical strength performances. The flexural and splitting tensile strengths result for Mix 30 showed that the mortar has higher bending resistance and can resist the applied stress as a sign of solid bonding strength between mortar and concrete substrates, subsequently promoting its potential to be applied for concrete structural repair applications. Nevertheless, lower MOE of repair mortar than the concrete substrate is essential to ensure compatibility between two bonding materials to resist force while maintaining the bond at Interface Transition Zone (ITZ).

The combination of three powder admixtures enhances the mechanical properties of the mortar compared to samples without admixtures. Using SRA and CaO reduced the internal stress, controlled the expansion of the mortar and ensured reliable mechanical strength progress. Adding a superplasticizer (SP) lengthens the setting time and controls the hydration process rates.

Future studies will focus on the rheology behaviour of the fresh mortar using this new mix design formulation to ensure its consistency and flexibility when placed for the in-situ application. In addition, improved workability of mortar will offer better mechanical strength beneficial meant for the pull-off bond strength performance between the repair mortar and concrete substrate for concrete patching applications as part of concrete repair techniques.

## 5 Introduction to Manuscript 2

The mechanical performance of newly designed one-part AAMs mortar as concrete repair material was discussed in manuscript 1. A new formulation of the mix design composition of the mortar has been tested and can be improved to comply with another performance characteristic specified in Table 3, EN1504-3 standard. The highest compressive strength level in manuscript 1 recorded as 28 MPa exceeded the minimum requirement of Class R3, EN1504-3 standard ( $> 25$  MPa). Mortar samples have also recorded a splitting tensile strength of about 2 MPa, indicating its bond strength capability. In addition, the result from the drying shrinkage test gives a good impression of the mortar's ability to resist the expansion and contraction process during the early hardening process as a signal for an acceptable workability level at a fresh state and durable when exposed to environment. The outcome of these findings used as guideline to continue the second experimental study on improving the mix design composition with new formulation to ensure the final product of mortar is physically and chemically stable besides to explore another performance characteristic to satisfy Table 3, EN1504 requirement – adhesive bond using EN1542 test method: Pull off bond strength test.

The main composition of precursors was all fixed based on findings in Manuscript 1. However, alkali activator dosages were adjusted to achieve an optimum concentration level as minimum as it can be as a continued effort to develop innovative engineering materials. Since the geopolymerization of one-part AAMs mortar in this study is composed of a low alkaline activator, the admixtures will be modified to ensure they react well during hardening. Therefore, the combination of SRA and CaO was reformulated with a series of volume percentages while SP and a/b ratios were kept fixed based on previous findings. To understand the new performance of dry mix compositions, w/b ratios were adjusted accordingly. They were analyzed based on mortar workability at the fresh state and compressive and pull-off bond strength at the hardened state.

Ideally, the setting time for mortar should not be too fast or too long. Workers typically mix the cementitious binder in one volume for hand patching applications and start manually patching the mortar to the concrete. The patching process may require 1 – 2 hours based on volume, severity,

and location. Therefore, an initial setting time of about 120 – 150 minutes or within 2 hours is significant for actual site application – from start mixing to finish patching. In this study, an acceptable setting time level will be determined for the fresh mortar, which is essential as additional information to predict their mechanical strength performance at a later stage.

Furthermore, compressive strength tests in this study will be conducted with a higher lab temperature of 29 °C and low relative humidity of 65% to analyze the stability of the mortar when exposed to different environments. On the other hand, the consistency of mix design formulation can also be tested to determine whether the reaction among the materials composition is chemically efficient to produce solid engineering properties. Only mortar samples with the highest compressive strength will be picked up to evaluate their pull-off bonding strength and to make sure the repair mortar is not only practical and safe to use but also provide a good quality of bonding performance for patching mortar with hand application, under concrete restoration principal as per EN1504 guidelines.

For pull-off bonding strength, there are two main types of failure in determining the bond quality of the patch materials: interface failure or adhesion and substrate failure or cohesion. The best bonding performance is when the applied patch mortar has remained firm and only failed at the concrete substrate location. Both setting time and pull-off bonding strength will be done under controlled temperature as per EN-1542 and EN196-3 testing methods. All the tests in this manuscript 2 are designed to evaluate the behaviour of repair mortar as a patching mortar and aim to comply with Class R3, EN1504 for structural concrete repair materials. Furthermore, the findings in this manuscript will support and improve the mixed design composition formulated and discussed in Manuscript 1.

## **6 Manuscript 2**

### **The Potential of one-part Alkali-Activated Materials (AAMs) as a concrete patch mortar**

#### **6.1 Introduction**

Many concrete buildings are approaching or exceeding their designed service life and require substantial maintenance to ensure the structure can function to the end of its service life. Typically, concrete infrastructures are designed for 50 to 100 years or more. However, most concrete buildings were built in the past 50 years, when sustainable construction materials were not widely used and established. For economic reasons, building owners tend to repair and upgrade these ageing buildings rather than demolish them, and also from the ecstatic or historical point of view, which makes them want to keep the existing building [105].

Concrete degradation is most common due to corrosion, cracks, spalling, etc., and is repaired with different types of concrete repair techniques and strategies. Presently the maintenance program is focusing on developing eco-friendly materials such as geopolymer or other types of sustainable cement, which not only offers more environmentally friendly products but also improves its engineering properties like higher mechanical strength and better microstructure compared to the traditional ordinary Portland cement (OPC), which extensively used.

OPC has been used as a concrete binder due to its good mechanical properties and cheapness, making it a popular choice in construction [25]. However, many researchers have started looking for alternative binders to replace the OPC due to the environmental impact. Alkali-activated materials (AAMs) are a new binder introduced in the market. It is known for its recycle-friendly products by promoting and utilizing industrial waste as the primary aluminosilicate precursor source. Lately, the conventional two-part AAMs system has been deliberately replaced by one-part technology, also referred to as the 'just add water' concept, where the binder is composed of solid precursors, activated by a solid alkali activator before water is added to activate the mixture, unlike the two-part method that still required corrosive aqueous solutions of alkali activator, not convenient for handling purpose from mixing, transporting to the placing of the sticky concrete.

The one-part AAMs used as concrete proved similar and had better mechanical performance than the OPC.

On the contrary, AAMs applications as concrete repair materials are still not popular compared to commercial polymer-modified cement mortar and epoxy resin. Therefore, an effort has been made to ensure that mechanical strength compatibility will be better or comparable to conventional concrete repair materials. AAMs, as part of geopolymer cementitious technology, reported have better flexural bond strength than the OPC due to the creation of chemical bonds, especially C-S-H gels for interfacial bonding at the interfacial transition zone (ITZ)[25][106][107][2]. A study on the shear bond strength of two-part AAMs by [25] using a slant shear test suggested that the combination of fly ash and Portland cement improved the bonding strength of AAMs mortar and PCC substrates and recorded slightly above 25MPa, comparable to the bonding strength that applied with the commercial repair materials. The developed bond strength in the two-part AAMs mortar's trend is further supported by the findings from [2] on the combination of FA/GGBFS precursors exhibiting higher interfacial adhesion level as a result of conducting an interfacial flexural-tensile strength contributed to the better compressive strength of about 60MPa and flexural strength of about 6 MPa at 28 days of age.

However, for structural concrete repair materials Class R3 and Class R4, the pull-off bonding strength test method is required and must exceed 1.5 MPa for Class R3 and 2.0 MPa for Class R4 as per EN1504-3 Standard[23]. Salazar et al.[1] reported that the two-part AAMs mortar composed of 70% natural volcanic pozzolan and 30% ground granulated blast furnace slag (GGBFS), activated with sodium hydroxide (NaOH) and sodium silicate ( $\text{Na}_2\text{SiO}_3$ ), only recorded 1.24 MPa despite highest compressive strength at 28 days of age about 65MPa. Two-part alkali-activated mortar composed of a sole slag precursor collapsed when the patch was applied vertically and horizontally due to low pull-off bonding strength between repair materials and substrate. When the slag precursors were substituted and composed of Fly Ash (FA) only, the adhesion strength was 2.3 MPa at the vertical surface and 1.8 MPa horizontally. However, the two-part AAMs mortar activated by metakaolin-only recorded consistent pull-off bonding

strength reading at 2.0 MPa, both tested at vertical and horizontal surfaces. It is worth mentioning that the alkali activator reported in this experiment was between 8 – 14% weightage from the precursor's total weight and demonstrated the influence of the alkali activator where bonding strength will increase when the amount of Si and Na is boosted [23]. Too much alkali content, however, will cost more and affect the mechanical strength of efflorescent, especially metakaolin-based cementitious [81]. Nunes et al.[33] explained that the precursors composed with GGBFS/metakaolin under high alkalinity conditions tend to reduce adhesive strength due to the unreactive slag caused by high reactivity calcium precipitation that caused  $\text{Ca}(\text{OH})_2$  drops in the loss of C-S-H type of gels, risking the bond. The average pull-off bond strength recorded reported in this experiment showed that sole metakaolin precursor activated with a  $\text{SiO}_2/\text{Al}_2\text{O}_3$  molar ratio of 3.0 for alkali solution only achieved 1.78 MPa at 28 days of age and 1.74 MPa for precursors activated with 80% GGBFS & 20% metakaolin at a similar molar ratio of alkali solution. It is worth noting that both mortar samples recorded higher compressive strength of 50 MPa at 28 days of age.

In addition, the setting time of the one-part AAMs mortar is too fast if containing a higher percentage of OPC, as reported by [38], where one-part geopolymer paste recorded 22 minutes for an initial setting time even though it has remarkable concrete mechanical strength at 7 days of age at around 27 MPa with the inclusion of 60% of OPC, nevertheless, accelerate setting time does not favour the production and handling process at the construction site. Therefore, to overcome the shortcomings of these alternative concrete repair materials, attention should be given more to the mix composition of one-part alkali-activated mortar, particularly on the selection of raw materials as aluminosilicates precursors, type of solid alkali activator, admixtures and the ratio of water and aggregates in the mixtures.

As for the solid alkali activator, the sodium metasilicate series has recorded the shortest setting time for a one-part alkali activator mortar. Increasing the alkali activator amount has a linear growth in compressive strength, for which the flexural strength will follow the same trend. Regular concrete's required initial setting time is more than 45 – 75 min depending on the strength class [62]. Liu et al.[66] used honeycomb ceramic (HCC) as a carrier for the alkaline activator to

prolong the setting time of one-part alkali-activated slag paste to counter from short setting time of one-part AAMs. By taking into account the lowest dosage of alkali activator used for one-part alkali-activated slag mortar in the experiment by Almahadmeh et al.[64], colder mixing water temperature at 0 Celsius recorded a longer initial setting time, followed by 10 °C and 20 °C, whereby 30 °C of mixing water temperature shortened the initial setting time up to 30%, or the average of 50 – 60 minutes dropped for every 10 °C of mixing water temperature difference compared to mortar samples activated with 0 °C of water which explained the influence of mixing water temperature in controlling the initial setting time of fresh one-part AAMs.

Askarian et al.[38] reported that one-part alkali-activated paste composed of fly ash and slag only did not set within the first 24 hours. With the inclusion of ordinary Portland cement (OPC), fresh paste's initial and final setting time was significantly decreased. The superplasticizer (SP) effect on one-part alkali-activated slag mortar was studied by Luukkonen et al.[72] and found that the lignosulfonate-based superplasticizer was the most suitable retarder admixture to lengthen the setting time of the AAMs slag mortar by increasing the SP and water amount. The delay in setting time was due to adsorption activities by the SP towards binder particles under an alkaline environment [31]. Coppola et al. [69] reported the influence of admixtures in one-part alkali-activated slag where the calcium oxide, CaO used as an expansive agent for the paste samples reduced both initial and final setting time, and the combination of CaO and shrinkage-reducing admixture (SRA) effectively decreased shrinkage level of the mortar samples.

Wang et al.[2] reported that three systems were applicable for the compatibility between repair material and its substrate: mechanical interlocking, Van de Waals forces, and chemical bonds. Teixeira et al.[5] explained the requirement for repair mortars according to EN 1504 standard used in Europe and highlighted the importance of AAMs properties in fresh and hardened states for sustainable repair and reinforcement elements.

Study on one-part AAMs has been conducted extensively at the synthesis stage to determine the new by-products, chemical activators, and compositions. However, using one-part AAMs as

concrete repair materials has not been studied profoundly. Nevertheless, One-part AAMs can be used in concrete and are helpful as mortar. In this experiment, a one-part alkali-activated mortar was carried out to establish its potential as a concrete repair material in terms of compressive strength and also the mortar's bonding strength which was evaluated by pull-off bonding strength method against OPC substrate to satisfy class R3 and Class R4 – EN1504-3 specifications for structural concrete repair materials. In addition, the volume ratio for aluminosilicate precursors was kept constant (25% FA, 5% GGBFS and 70% OPC). The main objective of this paper is to determine the capability of the one-part alkali-activated mortar used as a patching mortar as an alternative concrete repair material product for structural repair purposes class R3 and R4 EN1504-3 specifications.

## **6.2 Materials and Methods**

Class f – Fly Ash (FA) and Ground Granulated Blast Furnace Slag (GGBFS) were used as precursors under ASTM C618 and ASTM C989, respectively. Table 8 shows the chemical composition of Ordinary Portland cement (OPC), which was added as the primary binder source and activated with alkali-activated powder - potassium carbonate ( $K_2CO_3$  Purity  $\geq 90\%$ ). Natural sand was used as fine aggregates with a specific gravity of 2.67 and an average particle size of  $90.23 \mu m$  (D50). In addition, a commercial ethylene glycol type of shrinkage-reducing admixture (SRA) and calcium oxide (CaO) was added as admixture and expansion agent in the form of solid powder. At the same time, the sodium lignosulfonate powder-based superplasticizer (SP) was also used as a water reducer in high-strength concrete.

### **a. Mix Proportions**

The experimental study was conducted to understand the effect of aluminosilicate precursor and OPC as the main binder, activated with a different low dosage of alkali activator powder. Adjusted water content to improve the mortar workability, compressive strength, and bonding strength for patch mortar application and meet the Class R3, EN-1504 standard for structural concrete repair material.

All the samples were marked as Mix 1 to Mix 7 and consisted of FA, GGBFS and OPC as main precursors with different volume percentages. The admixtures proportion for every sample was added into the mortar samples between 1.0 to 15.0 wt% of weight based on total aluminosilicate precursors (binder) weight. The water-to-binder ratio ranged from 0.30 to 0.50, and the binder-to-sand ratio was constant at 1 to 1 to produce the mortar applied to all mixtures. The compositions of one-part alkali-activated mortars are further elucidated in Table 9.

#### **b. Sample preparations**

An electric mixer, EX-EM2000 EXTRAMAN 2000W, prepared all mixes. The FA, GGBFS, PCC,  $K_2CO_3$ , SRA, CaO, Sodium Lignosulfonate (SP) and fine aggregates were blended for 2 minutes according to their sample of mix compositions. After that, water was added slowly to the mixtures and continued blending for another 3 minutes to ensure the mortar paste was uniform. Then, all the fresh mortars were immediately cast into a 50 mm x 50 mm x50 mm cube for the compression strength test. All filled moulds were vibrated for 2 minutes using a shaking table. The mixtures were demoulded after 24 hours before being cured at an ambient lab temperature of 29 °C, with RH of 65 % until the testing day on 7, 14 and 28 days of curing age.

For setting time test of fresh mortar, it follows the same procedure. Still, after 3 minutes of mixing with water, the samples are immediately cast into Vicat moulds (see Figure 9) before the penetrating process begins at a specific time interval. The preparation of fresh mortar for setting time and pull-off strength test was under a controlled temperature of 21 °C and RH > 90%. The age of the concrete substrate is 56 days, and the test specimen is 28 days after curing age.

#### **c. Experimental procedures.**

The one-part AAMs mortar was mixed following the dry mixing method in previous studies. The compressive strength of hardened mortar was evaluated at 7 days, 14 days, and 28 days of curing age to study mechanical strength and properties. The compression test machine AUTOMAX5 was used at a loading rate of 1000 N/s. The mean value of three readings of each sample produced in triplicate for every test was recorded and taken as their final strength value. Test on the setting

time of mortar was conducted by penetrating the fresh mortar in Vicat moulds, set with 120 minutes for its first interval. The height of the Vicat mould is  $40 \pm 0.2$  mm, and the initial setting time was recorded when the  $34 \pm 3$ mm was obtained, and the final setting time was recorded at 0.5mm penetration depth obtained as per MS EN 196-3: 2016 specification. A 50 mm dolly size was used for the pull-off strength test, and the core drill depth was 15 mm into the substrate material as per BS EN 1542:1999 requirement.

Table 8: Chemical compositions (%) of Ordinary Portland Cement (OPC) obtained from the cement manufacturer.

Chemical compositions (%) OPC	CaO	SiO <sub>2</sub>	Fe <sub>2</sub> O <sub>3</sub>	MgO
	60 – 65%	17 – 25%	0.5 – 6.0%	0.1 – 4.0%
	Al <sub>2</sub> O <sub>3</sub>	Na <sub>2</sub> O + K <sub>2</sub> O	SO <sub>3</sub>	
	3 – 8%	0.2 – 1.0%	1.0 – 2.75%	

Table 9: Mix design of one-part alkali-activated repair mortars

Samples	Binder			Alkali activated	Admixtures			Design ratio	
	FA (%)	GGBF S (%)	OPC (%)	K <sub>2</sub> CO <sub>3</sub> (%)	SRA (%)	CaO (%)	SP (%)	Binder to sand	Binder to water
Mix 1	25	5	70	6	2	1	1	1	0.49
Mix 2	25	5	70	1.8	-	-	-	1	0.50
Mix 3	25	5	70	1.6	0.3	0.15	1	1	0.40
Mix 4	25	5	70	2.0	0.9	0.45	1	1	0.40
Mix 5	25	5	70	1.8	0.6	0.30	1	1	0.40
Mix 6	25	5	70	1.6	0.3	0.15	1	1	0.35
Mix 7	25	5	70	1.6	0.3	0.15	1	1	0.30

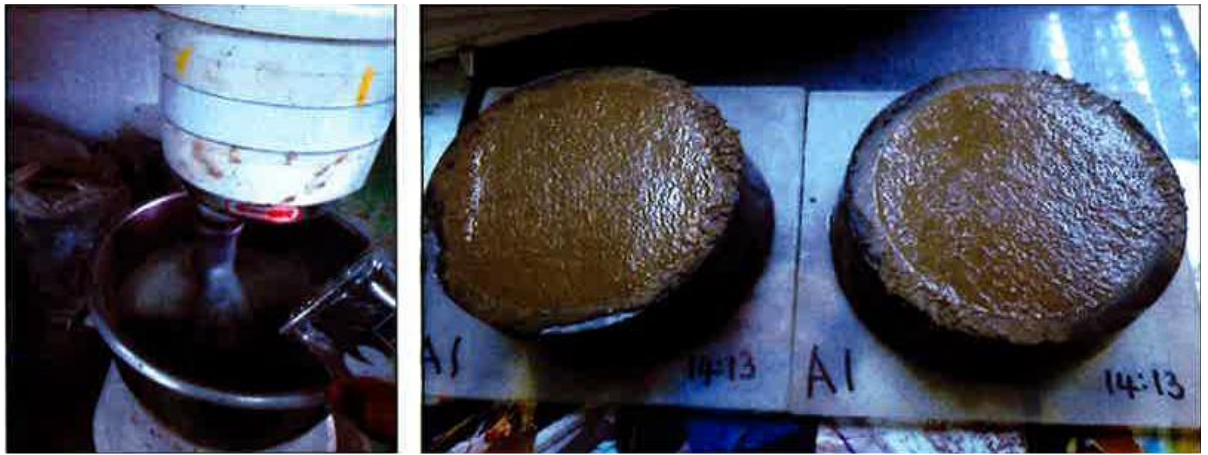


Figure 9: Vicat penetration test for setting one-part alkali-activated repair mortar

### 6.3 Result and discussion

#### 6.3.1 Setting time of fresh mortar

Table 10: Initial and final setting time of one-part alkali-activated repair fresh mortar

Mix Samples	Initial setting time (min)	Final setting time (min)
Mix 1	320	401
Mix 2 (control sample)	243	319
Mix 3	177	302
Mix 4	170	289
Mix 5	175	295
Mix 6	158	279
Mix 7	147	274

The initial setting time for the one-part alkali-activated mortar is essential for in situ application. The initial setting time is when fresh mortar starts losing its plasticity, and the final setting time is when the mortar completely loses its plasticity. Too long of an initial setting time will cause mortar or concrete to lose strength. This parameter will control the handling process from mixing to the casting stage. The initial setting time for Mix 2 (control sample) was 243 min or 4 hours compared with Mix 7, which recorded 147 min, a 39% reduction in initial setting time as shown in Table 10. The result also met the previous report's findings on the initial setting time range for one-part AAMs between 23 – 150 minutes [62]. Higher water-to-binder ratios for Mix 1 and Mix 2 affect the overall setting time of the fresh mortar, where the initial setting time was recorded at 320 minutes and 243 minutes, respectively. When the water content is reduced to a 0.40 water-binder ratio, both initial and final settings for Mix 3, Mix 4 and Mix 5 decrease in the range of

180 minutes to 175 minutes for the initial setting time and between 302 minutes to 295 minutes or about 5 hours for the final setting time. The fastest initial setting time was recorded for sample Mix 7 at 147 minutes, followed by sample Mix 6 at 158 minutes, where both samples contained low water-to-binder ratios of 0.30 and 0.35. As illustrated in Figure 10, the overall pattern of initial setting time decreased against lower water (w/b) content levels.

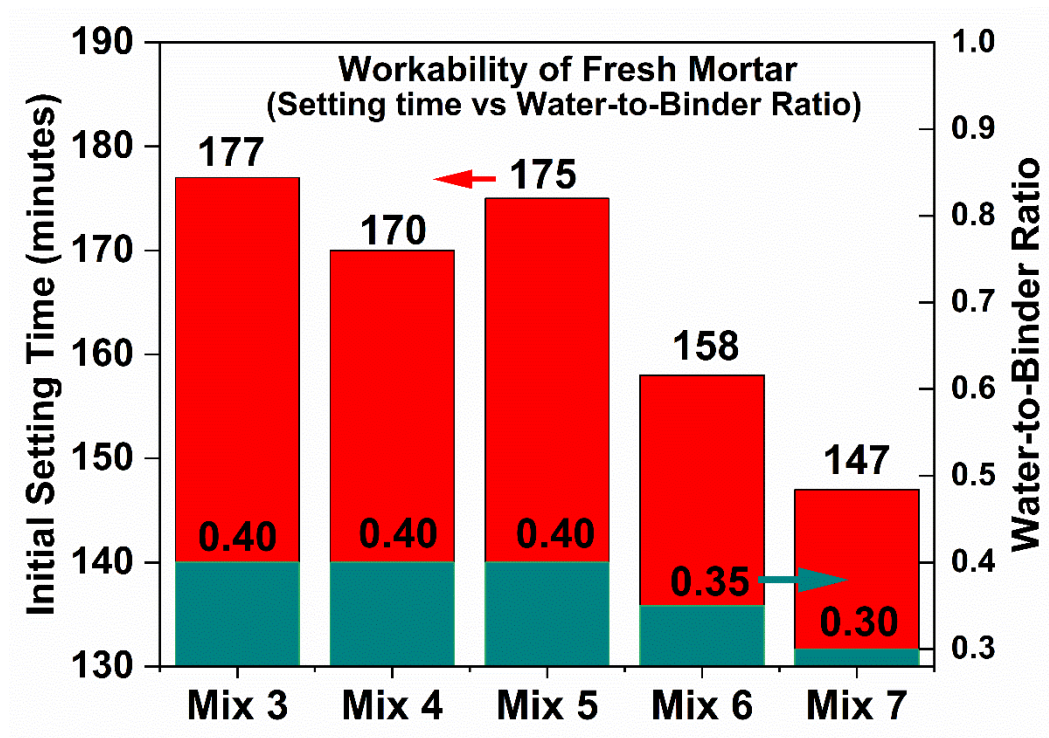


Figure 10: Initial time for a one-part alkali-activated repair mortar (Setting Time Vs Water / Binder ratio)

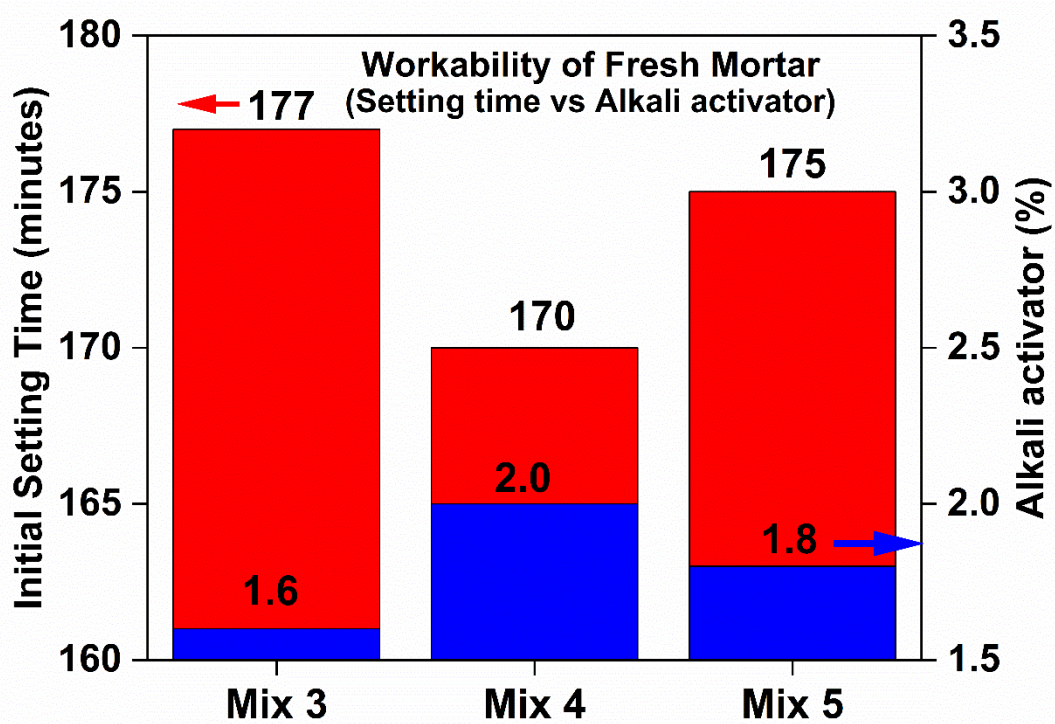


Figure 11: Initial setting time for a one-part alkali-activated repair mortar (Setting Time Vs Alkali activator).

It was reported that the common problem with one-part AAMs was they were set too fast and had a typical initial setting time in the range of 60 min, as reported by [44]. The longer setting time recorded in this experiment agrees with [12] that the presence of slag and solid potassium carbonate could reduce the workability of a one-part geopolymer. As shown in Figure 11, three mortar samples Mix 3, 4, and 5, have similar water-to-binder ratios of 0.40. Still, the longer initial setting time for Mix 3 was mainly contributed by the low alkali activator dosage of potassium carbonate, which only consists of 1.6% of total precursors weight because the higher the activator dosage, the shorter the setting time of one-part AAMs. Furthermore, all samples were prepared under a colder controlled temperature of 21 °C, which could be why the initial setting time was lengthened due to the thermal effect factor as agreed with [64]. Furthermore, 70% OPC content used as primary aluminosilicate sources for the binder was also the possible reason for a longer initial setting time due to a large group of cement particles occurring when the former reacts with water for the hardening process subsequently increased yield stress and plastic viscosity of the mortar for a longer setting time [47].

The potassium carbonate powder used in this experiment is a chemically non-hygroscopic alkaline. It has been reported to have a minimal impact than typical hygroscopic-based activators such as sodium hydroxide and sodium silicate that could harm the product in terms of efflorescence and water absorption level [38]. However, the slower dissolution of solid potassium carbonate activators, especially K ions in water, caused a slow hardening process at an early stage [42]. This experiment also confirmed the additional 1% (of binder weight) lignosulfonate-superplasticizer (SP) and higher water content could prolong the setting time of one-part alkali-activated mortar reported by [72]. Activated by a constant low dosage of alkali activator in resulting longer initial setting time of more than 100 minutes for both mortar samples respectively, the difference composition between the control samples Mix 2 and Mix 3 was that the addition of SRA and CaO provided more calcium to Mix 3 for a rapid reaction at an early stage on top of the existing 70% OPC for all mortar samples Mix 1 to Mix 7. Thus, SP was added to control the setting time of all samples with rich calcium examined in this experiment.

Comparing the initial setting time between Mix 2 (without admixtures) and Mix 1, 3 – 7, the strong influence of admixtures can shorten the setting time and improve the mechanical strength of one-part alkali-activated mortar. However, without admixtures, the control sample Mix 2 has recorded a longer initial setting time and low compressive strength at 28 days of curing age and does not comply with class R3 EN1504-3 standard.

It is worth noting that the non-hygroscopic alkaline with low alkali activator content of 1.6% was used in this experiment yet achieved not only mechanical strength comparable to the one-part AAMs activated by a conventional higher dosage of hygroscopic activator type but also a more extended initial setting for the mortar to become not too short or not too long and improved the setting time issues on one-part AAMs system.

### 6.3.2 Compressive strength

Table 11: Compressive strength at 7, 14 and 28 days of curing age.

Sample References	Compressive strength at 7 days (N/mm <sup>2</sup> )	Compressive strength at 14 days (N/mm <sup>2</sup> )	Compressive strength at 28 days (N/mm <sup>2</sup> )
Mix 1	19.22	20.92	26.35
Mix 2	18.16	17.50	9.26
Mix 3 (control sample)	23.76	22.41	26.75
Mix 4	19.16	19.03	14.41
Mix 5	18.0	18.83	13.88
Mix 6	21.90	29.24	36.27
Mix 7	21.45	31.14	36.80

Table 11 above shows the compressive strength of one-part alkali-activated mortar composed of mixed OPC, by-products of fly ash and GGBFS. All samples were activated by a low alkaline activator which is not corrosive, greener, yet cheaper. Mix 3 was referred to as a control sample based on the workability result activated by the lowest dosage of alkali activator at a w/b ratio of 0.40. At the same time, Mix 2 was composed without admixtures.

At the early stage, the highest compressive strength was recorded for Mix 3, with 23.76 N/mm<sup>2</sup>, followed by sample Mix 6 and sample Mix 7, with 21.90 N/mm<sup>2</sup> and 21.45 N/mm<sup>2</sup>, respectively. It is understood that one-part AAMs have a rapid reaction at an early stage due to the dissolution process of solid alkali activator with the presence of rich-calcium oxide content in precursors. The least amount of slag in this experiment, however, has been compensated by adding calcium oxide (CaO) powder as an expansive agent [69] together with the higher volume of calcium-rich OPC to provide more calcium, subsequently offering additional nucleation sites for dissolved materials under rapid dissolution process at an early stage, contributed to the fast hardening [38][65].

At 14 days of curing age, samples Mix 1, Mix 5, Mix 6, and Mix 7 recorded an increment in strength, contrary to samples Mix 2 (without admixtures), Mix 3 (control sample) and Mix 4,

which recorded slightly decreased strength over time. Mix 7 recorded the highest compressive strength with 31.14 N/mm<sup>2</sup>, followed by Mix 6 with 29.24 N/mm<sup>2</sup> and Mix 5 with 22.42 N/mm<sup>2</sup>. Further examination of the mortar's mechanical strength later confirmed the strong growth over samples Mix 1, Mix 3, Mix 6, and Mix 7. The highest compressive strength recorded was 36.80 N/mm<sup>2</sup> for Mix 7. The compressive strength slightly dropped for Mix 6 with 36.27 N/mm<sup>2</sup>, followed by Mix 3 and Mix 1, which recorded little difference in the strength, 26.75 N/mm<sup>2</sup> for the former and 26.35 N/mm<sup>2</sup> for the latter. The compressive strength at 28 days of curing age for all four repair mortar samples also complied with a minimum requirement for class R3, EN1504-3 specification for concrete structural repair materials. On the other hand, Mix 2, Mix 4, and Mix 5 continued suffered strength inclination between 30% – 50% over time.

The early mechanical strength of one-part AAMs contributes to the fast reaction due to the rapid dissolution of solid alkali activators in the binder to generate heat and make them lose their plasticity earlier than the two-part AAMs system. Consistent compressive strength levels in the range of 18 N/mm<sup>2</sup> to 21 N/mm<sup>2</sup> recorded at an early stage proved the rapid geopolymerization process begins immediately after water is added. Samples Mix 3, Mix 4, and Mix 5 were composed with a low alkaline activator (below 2.0% dosage). In contrast, sample Mix 2 activated without admixtures caused low compressive strength compared with the samples containing added admixtures. Samples Mix 4 and Mix 5 mortar have a double and triple volume of SRA and CaO compared to Mix 3 mortar, where SP dosage was kept constant at 1% for all samples. Samples Mix 1 – Mix 5 had compressive strength rise and dropped between -5% to +10% within 7 days to 14 days of age, in contrast with standard hardened mortar, which is usually springing up to its strength and achieve 90% compressive strength at 14 days of curing age.

The reduction in activator concentration would decrease the mechanical strength of hardened one-part AAMs [28]; thus, the dosage of alkali activator increased to 1.8% and 2.0% for samples Mix 4 and Mix 5, and additional Ca was obtained from SRA and CaO powder. However, the trend showed that the dissolution of an alkali activator for both samples Mix 4 and Mix 5 reached its peak at 7 days, whereby the lack of an alkali activator did not make sufficient to react with the

excessive amount of calcium resulting in incomplete reaction and inadequate binding between precursor and aggregate, creating more pores and crack propagation prevent the compressive strength growth at a later stage. Also, declined compressive strength over time was found in the fact that one-part AAMs were not water-resistant compared to the two-part AAMs system and subsequently encountered a slow hydration rate [81], associated with a higher water/binder ratio of 0.4 to 0.5, in addition to the low dosage of alkali activator used to compose these mortar samples.

Moreover, samples Mix 6 and Mix 7 recorded the highest compressive strength, about 36 N/mm<sup>2</sup> higher than the 25 N/mm<sup>2</sup> set as minimum compressive strength at 28 days of age for class R3-EN1504-3 specifications. Both mortar samples have similar mix compositions except for the water/binder ratio, 0.3 for Mix 7 and 0.35 for Mix 6.

Likewise, it is interesting to know that the low dosage of alkali activator has activated both mortar samples with 1.6% only than sample Mix 1 mortar activated by 6% yet achieved consistent and higher compressive strength. Insufficient Si and Al ions would dissolve due to a low alkalinity environment, and the resulting reduction in aluminosilicate precursors subsequently affects the rates of geopolymeric reaction [20]. On the other hand, Coppola et al.[100] reported that a higher dosage of alkali activator is required to lower the water demand. The lower alkaline activator incorporated with a lower w/b ratio contributed to the higher compressive strength. Li et al.[47] however, explaining the effect of the water-to-binder ratio plays a vital role in determining the rheological parameters of a one-part AAMs system. A lower w/b ratio will significantly increase yield stress and plastic viscosity for one-part AAMs and ordinary Portland cement (OPC). Luukkonen et al.[71] claimed that less water will increase the compressive strength of one-part AAMs, and adding a superplasticizer can further reduce and control the water. This experiment also confirmed that the presence of CaO and SRA restricted the growth of mechanical strength of one-part alkali-activated repair mortar as in the agreement with Coppola et al.[69]

### 6.3.3 Pull-off bonding strength.

Table 12: Average pull-off bond strength results in protection and repair products of concrete structures at 28-days of curing age of one-part alkali-activated repair mortar.

<b>Samples references</b>	<b>Tensile bond strength (MPa)</b>	<b>Mode of failure</b>
Mix 3 (control samples)	1.885	A and B interface / Adhesion
Mix 6	1.757	A and B interface / Adhesion
Mix 7	2.565	A – substrate / Cohesion

Based on the compressive strength result shown in Table 11, which was recorded above 25 MPa, only 3 samples were selected for compression testing. Pull-off bond strength for all samples complied with the required strength requirement Class R3 – EN1504-3 standard for structural concrete repair materials. The highest pull-off bond strength was recorded for sample Mix 7 mortar with 2.565 MPa (Class R4 – EN504-3 standard), Mix 3 with 1.885 MPa and Mix 6 with 1.757 MPa, as shown in Table 12 above. This experiment's pull-off test also confirmed the adhesion mode of failure at the interface between mortar and concrete substrate for Mix 3 and Mix 6, a cohesion mode of failure for Mix 7 (see Table 12). Both types of failure are considered ideal types of failure classification for the pull-off test as per EN1542 standard, indicating the one-part AAMs repair mortar as a good bonding material. In addition, the higher pull-off bond strength recorded indicates that this type of mortar can provide higher adhesive force [20]. The variety of material compositions sought for mortar mix design in this experiment influences the bond strength of the one-part AAMs system [94].

The reaction between alumina and silica from FA and calcium ions from ordinary Portland cement (OPC) could form C-(A)-S-H gel co-existed with N-A-S-H, enhancing the alkali-activated materials (AAMs) properties as reported by Phoo-ngernkham et al.[25]. The surface of OPC substrates is rich with calcium hydroxide ( $\text{Ca}(\text{OH})_2$ ) will bond chemically by reacting with the alkaline one-part alkali-activated repair mortar for positive ions such as  $\text{Ca}^{++}$  to balance the negative charge of the  $\text{Al}^{3+}$  and  $\text{Si}^{4+}$  from FA and GGBFS for geopolymeric reaction, in addition of the formation of calcium carbonate hydrate from the reaction between potassium carbonate

powder and calcium hydroxide of OPC later improved the adherence between repair mortar and substrates [1][108]. Additional C-S-H and/or C-A-S-H gel was established with N-A-S-H gel enhancing the bonding concentration at the contact area [24].

This experiment proved that one-part alkali-activated repair mortar, known as the third mortar category, can be used for concrete structural repair to replace conventional organic and inorganic binders in the construction sector [109]. Once again, the low dosage of alkaline activator used in this experiment successfully activated the one-part AAMs system and performed better than the two-part AAMs system counterpart.

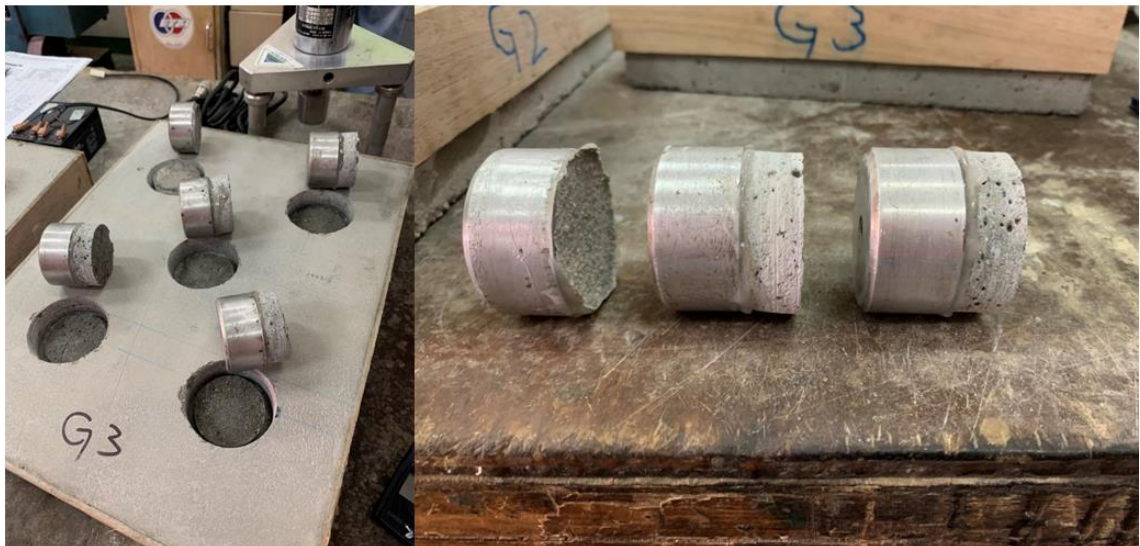


Figure 12: Pull off mortar samples after 28 days of age (Mix 7)

#### 6.4 Conclusions

The experiments in this report were conducted to investigate the mechanical properties of compressive and the pull-off bonding strength of one-part alkali-activated mortar against OPC substrate used as concrete patching materials as stated in EN1504-3 guideline for structural concrete repair material specifications. Hybrid precursors of fly ash, ground granulated blast furnace slag and OPC were used as the source of aluminosilicate binder. A low alkali activator of potassium carbonate in powder form was used to initiate the geopolymerization process and further adjusted with some admixtures, water, and aggregates for optimum mortar mix design. A

longer setting time is essential for transporting a large quantity of mortar to the construction site to maintain workability. The initial setting time for the mortar sample in this experiment achieved 147 minutes, in line with previous reports on the setting time of one-part AAMs. In addition, the highest compressive strength and bonding strength at 28 days of age were recorded for Mix 7 with  $36.8 \text{ N/mm}^2$  and  $2.565 \text{ MPa}$ , respectively. Therefore, they complied with Class R4 – EN1504 for structural concrete repair materials.

Another conclusion that can be highlighted in this paper is as follow:

1. Two-part AAMs composed of a single precursor such as fly ash, slag or metakaolin only have higher early compressive strength and better mechanical properties. Still, they are not suitable for concrete repair material due to lower pull-off bonding strength. In addition, two-part AAMs mortar activating with sole precursors also does not comply with mechanical requirements for repair materials (pull-off strength class R3 and R4, EN1504 standard) and is often delaminated. However, all these industrial wastes can be utilized by incorporating Portland cement in one-part AAMs technology to promote better chemical bonding between repair mortar and concrete substrates at the interface zone regarding pull-off bonding strength.
2. A short initial setting time for AAMs mortar is the main problem for supplying process at the construction site. Therefore, a longer initial setting time for the one-part alkali-activated repair mortar recorded in this experiment benefits the in-situ application. The main aluminosilicate mortar sample Mix 7 precursors were 25% FA, 5% GGBFS and 70% OPC. They exhibited 147 minutes for the initial setting time within the range of 23 – 150 minutes as reported for the initial setting time of one-part AAMs. Furthermore, it is worth noting that countries with hot and dry climates possess a higher rate of hydration. This result enlightened the sustainability of this type of repair mortar which has a flexible range of initial to final setting time when exposed to the higher surrounding temperature that may shorten the setting time of the fresh mortar up to a 30% reduction. Therefore, it is applicable to be applied in hot climate countries.

3. A lower dosage of solid admixtures is used to enhance the fresh and mechanical properties of one-part alkali-activated mortar that meet the requirement for class R3 and class R4, EN1504-3 specifications for structural concrete repair materials together with the optimum admixture dosage of 0.3% for SRA, 0.15% for CaO and 1% of SP from the total weight of precursors. In addition, a lower water-to-binder ratio at 0.30 has increased the repair mortar's pull-off bonding strength following higher compressive strength recorded at 28 days of curing age.
4. The repair mortar assessed in this experiment is composed of fly ash and slag as part of the mix composition, whereby this type of by-product can be developed further to enhance its potential and exploited as cement binder used as concrete patching materials, subsequently overcoming the limitations on the pull-off bonding strength properties as the weakest part of the system as reported. Therefore, future studies should focus on the microstructure analysis of the one-part AAMs mortar to enhance its potential to be used as a concrete repair material.

## **7 Introduction to Manuscript 3**

In manuscript 2, it was found that when water content reduced to a w/b ratio of 0.35 and 0.30, the compressive strength of one-part AAMs mortar has a comparable 36 MPa at 28 days of age. The result has far exceeded the minimum requirement of Class R3, EN1504-3 strength, but it is still behind the minimum compressive strength level of the Class R4 counterpart. Nevertheless, at a lower w/b ratio of 0.30, the mortar samples have recorded better pull-off bonding strength up to 2.5 MPa and subsequently comply with Class R4, EN1504-3 standard compared to the when w/b ratio of 0.35 used (1.7 MPa). Mortar samples with lower w/b ratios also recorded acceptable initial and final setting times of about two hours, making it practical to apply for concrete repair application. It is worth noting that mortar samples for the compressive strength test were prepared at slightly higher temperature levels with lower relative humidity, which may affect the consistency of the mortar due to the loss of water. All these findings further signal the influence of water in determining the complete engineering performance of the one-part AAMs mortar for the overall study. Thus, in this manuscript 3, the effect of the w/b ratio was evaluated not only to complete the formulation of a novel mix design for repair mortar but also to study the effect of water on the pore structure of one-part AAMs mortar and subsequently to improve its durability by controlling porosity and shrinkage level.

Three w/b ratios, 0.40, 0.35 and 0.30, were applied to activate the dry cementitious binder based on one-part AAMs technology. Firstly, the fresh mortar's workability in paste was analyzed to understand its rheology behaviour. Higher workability will ensure practical engineering application and safeguard mechanical strength development. Two tests will be carried out in this regard, setting time and spread mortar test. Next, compressive strength will be done based on 7, 28 and 56 days of age. It is essential to understand how the water assists in the strength development of hardened mortar over time under geopolymerization reaction composed with a low dosage of alkali activator and different microstructure properties of FA, GGBFS and OPC as precursors. In addition, unlike conventional OPC mortar, AAMs have a continuous strength gain

beyond 28 days of age due to the ongoing geopolymerization process. This phenomenon will further enhance the materials' durability for a longer lifespan.

As part of the durability measurement, the porosity level of the hardened mortar will be investigated using Mercury Intrusion Porosimetry (MIP). The pore structure analysis of the mortar can be verified based on different water content levels to explain further the capability of less reactive and low dosage types of alkali activators to refine the pore size of the mortar, which contains different types of raw materials and size distribution. A lower porosity level will justify higher compressive strength, while a higher porosity level is responsible for the shrinkage problem. In manuscript 1, the drying shrinkage result for the mortar was within allowable measurement, thus giving indication efficiency of mix design formulation for repair mortar to resist the expansion and contraction phenomena not only in the fresh state – during the early hardening process but also at hardened state when the mortar exposed to the environment. In this study, the measurement of restrained drying shrinkage and expansion will be done using pull-off bond strength as per the EN12617-4 test method. The mortar samples' bond strength will be compared in three different environments: curing in water for 28 days, under control lab temperature for 56 days, and in wet conditions for 56 days of age. From the pull-off bond strength test result, the stability of hardened mortar will be determined based on their strength changed trend. On top of that, the findings on the compressive strength test, pull-off bond strength and restrained shrinkage/pull-off bond strength in this manuscript 3 can finalize the classification of class repair materials whether it belongs to Class R3 or R4, EN1504-3 for structural concrete repair materials.

To evaluate further how the formulation of mix design works, the microstructural study will be done by studying the Scanning Electron Microscopy (SEM) images for micromorphological features and Energy Dispersive X-Ray analysis (EDX) to study the elemental composition of the hardened mortar. It is crucial to understand how the geopolymerization process contributes to the hydration gels product of N-A-S-H and C-A-S-H for one-part AAMs mortar in this study. Thus, the chemical reaction between precursors and alkali, admixtures, and aggregate at different levels

of w/b ratios will be discussed in detail based on the findings in SEM and EDX. Overall engineering properties performance stated in this manuscript 3 will conclude the novel mix design formulation investigation in manuscript 1 and manuscript 2 and classify the type of repair material class as per EN1504-3.

## **8 Manuscript 3**

### **The Effect of Water-To-Binder Ratio (w/b) on Pore Structure of One-Part Alkali Activated Mortar**

#### **8.1 Introduction**

Alkali-activated materials (AAMs) are synthesized from solid aluminosilicate precursors and alkali activator reactions. They become greener alternative cementitious materials to the traditional ordinary Portland cement (OPC) [66]. The AAMs technology does not require clinker for cement hydration products. In contrast, the excessive energy consumption required for clinker up to 5 GJ per ton is needed to burn limestone and silicious materials to manufacture clinker [110]. OPC emits tons of CO<sub>2</sub> that contributes up to 7% of greenhouse gas emissions resulting in global warming and climate crisis [111]. Therefore, industrial by-products in AAMs were introduced as a partial substitute for OPC cement for construction purposes. Conventional AAMs are produced with two products: solid aluminosilicate precursors and the aqueous solution of alkali activators. A higher alkalinity level is required to ensure the best performance of the cementitious products, although it means costly, besides highly corrosive chemicals that might risk the health and safety of the worker. Nevertheless, using a viscous aqueous activator makes it sticky and prevents it from an extensive in-situ application on the construction site. Therefore, the alkaline solution is replaced with a dry alkali activator in one-part AAMs technology for more practical applications.

However, without relevant formula, the one-part AAMs have some significant drawbacks on their long-term durability from the perspective of microstructural and nanostructural levels, which further affect the mechanical strength and durability, causing this type of geopolymer binder is still not famous for a commercial adaption at present [84]. Many reports have been established on the development of one-part AAMs. Fly ash consists of high silica content beneficial to improve the reaction rates in the geopolymerization process. However, its low calcium prevents it from strengthening the C-S-H gels for binding products. Adding calcium-rich slag filled the shortage by supplying additional calcium. Combining these two precursors creates an additional

3D network of N-A-S-H gels that co-exist with C-A-S-H gels from the primary parent product of C-S-H [25][75]. The FA/GGBFS precursors exhibited higher mechanical strength in one-part AAMs in concrete. However, too high GGBFS content will cause rapid hardening, water loss and higher shrinkage. Thus, OPC, which has a significant amount of calcium, was added in one-part AAMs as part of the precursors. OPC has been widely used as concrete and cementitious mortar. Still, with the presence of by-product precursors, the dependency on the OPC can be reduced, indirectly cutting down its volume. Askarian et al.[38] explained on one-part AAMs activated with the combination of by-product precursors and OPC in concrete can achieve up to 55.0 MPa with 60 % of OPC content at 28 days of curing age. However, its mechanical strength in the form of repair mortar is still not yet established. Luukkonen et al.[52] reviewed past studies on hybrid one-part AAMs performance and found that it has higher mechanical strength subject to a different percentage of OPC inclusion. The report comprises a few studies, including a 60% OPC mixed with 40% fly/bottom ash, which has recorded 32 MPa compressive strength at 28 days of curing age but has a higher w/b ratio of 0.5 and a tendency towards shrinkage. In addition, 20% OPC / 40% GGBFS and 40% kaolin/bentonite mixtures recorded compressive strength with promising 32 MPa at 28 days of age but had inconsistent w/b ratio of 0.3/0.5 besides being triggered with slightly higher alkali activator (5% solid sodium carbonate). Solid sodium hydroxide was used to activate the mixed precursor composed of OPC / FA/ kaolin has an efflorescence effect due to the lower reactivity that causes some sodium to be replaced by calcium. Nevertheless, this hybrid AAMs has recorded sufficient 27 MPa compressive strength (at 28 days). Moreover, in this review report, a patented geopolymetric cement containing 3-30% OPC has been tested at 28 days of age and recorded 35 MPa (30% OPC) of compressive strength. However, the pore structure of the hardened cement for all 43 patented dry mix cement compositions samples was not reported, making its durability uncertain.

In addition, minimal study on the effect of low alkaline activators is used to activate the one-part AAMs cementitious materials because higher alkalinity is more significant to complete the geopolymerization process to produce standard quality cement binder. Excessive alkalinity, on the other hand, causes significant drawbacks to the pore structures of the hardened products and

is prone to chemical attacks in a harsh environment. Yang et al.[63] mentioned that the slag paste was activated with a 15% sodium carbonate alkali activator, which has demonstrated a bigger pore diameter and pore volume than a 10% sodium carbonate, suggesting an excessive alkali activator could be coarse in the pore structures. Another study reported by Azevedo et al.[29] proved that with a higher dosage of alkali activator, the average pore diameter decreased from 24.29 nm to 21.48 nm and documented higher compressive strength up to 41 MPa at 28 days, subsequently supporting the fact that the elevated concentration of alkali activator encourages the hardened product to be more dense and solid without decreasing any unreacted particles.

Still, it has also affected the porosity between 30 – 40% for one-part AAMs composed of calcined commercial kaolin and ceramic waste. Gel pores and capillary pores are two significant matters in the strength of cementitious products where gel pores are unlikely to affect much strength properties but are reported to be influential on creep and shrinkage [42]. However, not all finer pores are harmful. There are four ranges of pore sizes that influence the compressive strength of hardened AAMs, which are classified as harmless pores for sizes below 20 nm, less harmful pores for 20 – 50 nm, harmful pores if 50 – 200 nm and more harmful pores if exceed 200 nm [34]. It was reported that two-part AAMs composed with a single metakaolin precursor used as concrete repair materials recorded 2.0 MPa maximum bond strength, but 20% replacement with slag showed an increment in pull-off bonding strength as an indication of mixed aluminosilicate precursors exhibit greater strength than a single type of binder precursor source. Both compositions have documented about 14% porosity level [33].

A fully reacted microstructure pattern on the surface could be formed by increasing the alkali activator in a dry mixture, as reported by [29]. Yet, excessive alkali content in the mixture can migrate to the surface and react with CO<sub>2</sub> in the atmosphere, consequently causing carbonation. The use of hybrid one-part AAMs concrete studied by [38] explained that the inclusion of 30% OPC in the mixes has more compact microstructures and less unreacted fly ash particles compared to 0 – 20% of OPC content but has a more porous structure than 40% and 60% of OPC content. In that report, the compressive strength for one-part AAMs concrete with 60% OPC was about

55.0 MPa. In comparison, adding 40% OPC and 30% OPC in one-part AAMs concrete composed with a single precursor of metakaolin recorded compressive strength of about 52.0 MPa and 50.0 MPa at 28 days of age, which was activated by 3 to 5% of alkali activator. It is worth mentioning that one-part AAMs composed of single precursors of metakaolin promote a highly porous structure, heterogeneous with unreacted particles that affect its mechanical strength and durability as illustrated in SEM images [89]. In contrast, one-part AAMs composed of two aluminosilicate precursors of fly ash and slag have denser microstructure than fly ash only mixes to confirm that combination of aluminosilicate precursors contributes better mechanical strength, rich in Al but has a substantial low Ca/Si ratio which the hydrated OPC has the advantage to offer a higher Ca/Si ratio and compensate this shortage [30].

At the current stage, one-part AAMs technology mainly focuses on concrete product purposes as an alternative option to the conventional OPC based cementitious. One-part AAMs mortar is to be developed to reduce dependency on OPC mortar and be comparable to other mortar repair materials in the market. Combining more than one precursor was designed to be mixed with the OPC as an initial approach towards promoting green and sustainable construction materials by utilizing industrial by-products as the primary aluminosilicate precursors source and cutting down the OPC volume as low as possible. Furthermore, a lower dosage of the solid alkaline activator is beneficial for a cheaper cost, lower health risks and is not harmful to the environment. First, the effect of a low alkaline activator used in one-part AAMs must be observed on its reaction with main precursors. For this reason, the w/b effect will support the geopolymerization process before conducting a microstructural study to deliver more understanding of the mechanism of its physical property's behaviour. Yusslee et al.[112] reported that the one-part AAMs' mechanical strength has compressive strength and pull-of bond strength level that complied with Class R4-EN1504-3 standard, indicating the potential of this type of geopolymer binder to be used as concrete patch repair mortar. However, the constancy of pore structures of the hardened mortar has yet to be proved; thus, its durability stays doubtful.

It is crucial to understand how pores start created during the hardening process as the water content difference affected the hydration products and strength development. Many researchers activate dry mixtures for one-part AAMs application with different w/b of ratios [29][30][38]. Luukkonen et al.[52] reported that in one-part AAMs, four steps occur after water is added to cementitious materials, beginning with ion exchange, hydrolysis, network breakdown and release of Si and Al, which differentiate the one-part technology from the conventional two-part AAMs. It is worth mentioning that as the geopolymerization cycle continues, the cracks and pores formed at the early stage were filled with an increasing amount of gels and justify compressive strength development over time as the result of a reduction in the accumulated volume of the pores, mainly from C-A-S-H gels phase fill the pore structure to reduce the pore diameter [51][63]. The compressive strength of one-part AAMs containing fly ash, OPC and slag as the main component reacted with an alkali activator to produce gel formation of sodium aluminosilicate hydrate (N-A-S-H), calcium aluminosilicate hydrate (C-A-S-H) and stable 3D network of silico-aluminate structures that enhance polycondensation process that contributes to the higher compressive strength [65].

The addition of commercial solid additives will be added and formulated in the one-part AAMs dry mixtures to control and stabilize the hardened products of mortar. The inclusion of lignosulfonate (LS) type superplasticizer (SP) as high range water reducing admixtures improved the dissolution of slag and reduced water content for better mechanical properties [31][71]. At the same time, the addition of OPC and CaO powder provided more calcium. As a result, it increased the compressive strength on the effect of water content for high compressive strength of AAMs cementitious products[71]. Differences in SP effect on one-part AAMs depend much on the stability behaviour of admixtures in a different type of solid activator. Quicklime-type of Calcium Oxide (CaO) was used as an expansive agent in mortar. Adding the CaO with Shrinkage Reducing Admixture (SRA) has increased the mortar volume instead of shrinking it like conventional cementations materials. Hence, the initial impression on the selection and composition of solid admixtures for the mix design of this study was based on the above findings and the previous study by [112].

Undeniable, the one-part AAMs have become a popular option in the form of concrete. Current studies largely focus on the synthesis and characterization to determine the new type of precursor-green products. Researchers utilize various types of waste products from agriculture and construction on top of traditional industrial by-products, fly ash, slag and metakaolin [91][92][113][114]. However, the engineering application for the one-part AAMs in other cementitious-based materials has still lagged. On the contrary, mortar composed of two-part AAMs systems has been tested as concrete repair products and reported to have great potential to be commercial in the construction industry [5][22]. The one-part AAMs must be developed not only to focus on their compressive strength but must have robust physical structures, higher consistency and be chemically stable.

The motivation to carry out this study is to analyze further the fact that the higher water content could decrease the yield stress and plastic viscosity of fresh cementitious materials and affect their rheology behaviour and performance at the hardened stage [47]. Nevertheless, the water content in the w/b ratio can be adjusted to change yield stress and plastic viscosity. Still, in actual construction, the w/b are conventionally controlled to ensure homogeneity of the mortar or concrete, besides operated practical handling from mixing and transporting to pouring time. Moreover, unlike the conventional one-part AAMs, which traditionally utilize industrial waste or/with natural pozzolanic materials as main aluminosilicate precursors [115], hybrid one-part AAMs, on the other hand, combine the industrial by-products with the OPC used as the main source of the cementitious binder in this study [38][52].

Therefore, the objective of this study is to examine the effect of w/b content on the pore structures of fly ash/slag precursors mixed with the OPC for repair mortar application. This study aims to reduce the porosity level of one-part AAMs by controlling the pore structure size of the hardened mortar with appropriate water content and safeguarding its mechanical strength against shrinkage effect after 28 days of curing age for concrete patching mortar application. Consequently, the hybrid one-part alkali-activated mortar in this study was activated by different w/b ratios of 0.40, 0.35 and 0.30 to encounter previous findings, which stated that alkali-activated materials exhibit

higher porosity levels and larger pore size than those reported in ordinary Portland cement (OPC), hence by controlling w/b ratio, it could produce less porous polymeric microstructure [16]. Thus, the optimum w/b ratio will complete the novel contribution of a new mix design formulation for Class R4 - EN1504-3 standard for structural concrete repair mortar application previously developed by the author [116]. Furthermore, the hybrid one-part alkali-activated in this study was activated with low alkalinity of solid alkali activator as part of the research in developing sustainable cementitious product technology by the author for engineering application.

This new type of repair mortar could efficaciously reduce clinker cement production and mitigate the carbon footprint linked to the construction industry. Furthermore, the reported result from this study will stipulate the prerequisite of understanding the interrelationship between compositions of solid materials ingredients with their physical properties when water reacts with a dry mixture of precursors, activators, aggregates, and admixtures (dissolution process of solid particles).

## **8.2 Materials and method**

The experiment conducted in this report used three main aluminosilicate precursors: Fly Ash Class-F as per ASTM C618, Ground Granulated Blast Furnace Slag as per ASTM C989 and ordinary Portland cement (OPC). A powdered Potassium Carbonate ( $K_2CO_3$ , purity  $\geq 90\%$ ) was used as the sole alkali activator. First, three solid admixtures were added to the mix design formulation: sodium lignosulfonate as a superplasticizer additive (SP), shrinkage-reducing admixture (SRA) – commercial ethylene glycol type, and calcium oxide powder (CaO). Both SRA and CaO control the effect of drying shrinkage of the mortar. Next, natural sands were added to increase the mortar volume and source of additional calcium with a specific gravity of 2.67 and an average particle size (D50) of 90.23  $\mu m$ . Finally, water is added to activate the mortar mix for testing in a fresh and hardened state. The chemical compositions of FA, slag and ordinary Portland cement are shown in Table 13, Table 14 and

Table 15, respectively. In addition, the particle size for each material is measured with the Laser Diffraction Analysis (LDA) and elaborated in Table 16. This report's materials and mix design formulation were according to the author's previous study in developing novel mix design

formulation for one-part alkali-activated mortar used as structural concrete repair materials [112][116].

#### **a. Mix proportions**

This study aims to reduce the porosity level of the one-part AAMs mortar by analyzing the pore structures of the structural repair mortar activated with one-part AAMs technology at three different water content levels of 0.40, 0.35 and 0.30 w/b ratio. Samples were marked with G1 composed with the highest w/b ratio of 0.40 (high water content), G2 has a w/b ratio of 0.35 (medium water content), and G3 has the lowest w/b ratio of 0.30 (low water content). Sample G1 was selected as the control sample in order to compare the pore structure behaviour if the w/b is decreased and its influence on determining the workability in the fresh state, mechanical strength and durability in the hardened state. Three admixtures were added in the mix design with a constant proportion of 0.30% of SRA, CaO (0.15%) and 1% SP from total aluminosilicate precursors weight. The sand content was fixed at 1 (b/a ratio) for all samples. The mix design formulation of the mortar is shown in

Table 17. All samples were cured under controlled temperature per EN1504-3:2005 standard, part 3: structural and non-structural concrete repair materials.

#### **b. Sample Preparation**

Dry mixtures of FA, GGBFS, OPC, SP, SRA, CaO and fine aggregates were blended for two minutes using an electric mixer (EX-EM2000 EXTRAMAN, 2000W). Next, water was added to the mixtures and blended for three minutes until the mortar paste was uniform. Finally, the fresh mortar was filled into the 40mm x40mm x160mm steel moulds for the compression strength test and vibrated for two minutes and dismantled form moulds after 24 hours. All samples were cured under the lab-controlled temperature of  $\pm 20$  °C and relative humidity of RH > 90% before being tested at the 7th, 28th and 56th days of age. The experiment on the cementitious paste was done without aggregates using Vicat moulds for the penetration process to check its consistency. The setting time measurement and pull-off bonding strength test also used similar temperatures and RH. The flow table test was also carried out under lab temperature of 29 °C – 30°C and RH

between 55 – 60%. For this test, the fresh mortar was filled and compacted into truncated conical moulds at the flow table platen before jolting the samples.

### **c. Experimental and procedures**

A compression strength test machine, AUTOMAX5, was used to determine the compressive strength of hardened mortar at the 7<sup>th</sup>, 28<sup>th</sup> and 56<sup>th</sup> days of age with an applied loading rate of  $2.4 \pm 0.2$  kN/s. Samples were produced in triplicate for each test, and the mean value of three readings was taken as the final strength value. Setting time cement paste was set for 120 minutes as the first interval time. The Vicat moulds used are  $40 \pm 0.2$  mm in height, and the first setting time is recorded when the penetration depth of  $34 \pm 3$  mm is obtained, while for final setting time, it is recorded when 0.5 mm penetration depth is achieved to comply with EN 196-3: 2016 standard. For the flow table test, after the truncated conical moulds are removed, the flow table is jolted 15 times and measured using a calibrated calliper. The average of two spread dimensions was recorded to get the flow value according to BS EN 13395-1-2002 standard. To examine the shear strength and tensile strength level, the pull-off test is carried out by means of determining restrained drying shrinkage or expansion impact after the hardening process stops at 28 and 56 days of curing age under three different curing conditions as per EN 12617-4 test method as part of the durability checking in EN1504-3 guidelines. Analyzing pore structural characterization, crushed samples from mechanical strength tests were used and measured with Mercury Intrusion Porosimetry (MIP) using a MicroActive Autopore V9600 machine. Scanning Electron Microscopy (SEM) and Energy Dispersive X-Ray analysis (EDX) were employed to analyze the mixes' micromorphological features and elemental compositions in the form of hydrated particles. The SEM scanned the fractured mortar surfaces at 28 days of age while the EDX (BSE/20KV) observed the elemental composition in the samples.

Table 13: Chemical compositions (%) of Fly Ash obtained from XRF analysis

<b>Chemical Composition</b>	<b>Percentage (wt %)</b>	<b>Chemical Composition</b>	<b>Percentage (wt %)</b>
SiO <sub>2</sub>	55.94	TiO <sub>2</sub>	0.72
Al <sub>2</sub> O <sub>3</sub>	22.60	Cr <sub>2</sub> O <sub>3</sub>	-
Fe <sub>2</sub> O <sub>3</sub>	8.10	MnO	-
CaO	6.26	SO <sub>3</sub>	1.02
P <sub>2</sub> O <sub>5</sub>	0.36	LOI	1.48
MgO	1.21	Cl	0.03
K <sub>2</sub> O	1.66	Na <sub>2</sub> O	0.62

Table 14: Chemical compositions (%) of Ground Granulated Blast Furnace Slag (GGBFS) obtained from XRF analysis.

<b>Chemical Composition</b>	<b>Percentage (wt %)</b>	<b>Chemical Composition</b>	<b>Percentage (wt %)</b>
SiO <sub>2</sub>	35.91	TiO <sub>2</sub>	0.59
Al <sub>2</sub> O <sub>3</sub>	16.56	Cr <sub>2</sub> O <sub>3</sub>	-
Fe <sub>2</sub> O <sub>3</sub>	1.52	MnO	-
CaO	35.28	SO <sub>3</sub>	0.36
P <sub>2</sub> O <sub>5</sub>	0.36	LOI	-
MgO	6.01	Cl	-
K <sub>2</sub> O	-	Na <sub>2</sub> O	1.76

Table 15: Chemical composition (%) of Ordinary Portland Cement (OPC)

<b>Chemical Composition</b>	<b>Percentage (wt %)</b>	<b>Chemical Composition</b>	<b>Percentage (wt %)</b>
SiO <sub>2</sub>	23.97	MgO	1.36
Al <sub>2</sub> O <sub>3</sub>	5.27	K <sub>2</sub> O	0.51
Fe <sub>2</sub> O <sub>3</sub>	3.28	TiO <sub>2</sub>	0.06
CaO	60.12	SO <sub>3</sub>	2.20
Na <sub>2</sub> O	0.23	LOI	2.00

Table 16: Laser-diffraction Analysis (LDA) measured the particle size distribution

Samples	D10 ( $\mu\text{m}$ )	D50 ( $\mu\text{m}$ )	D90 ( $\mu\text{m}$ )
FA	2.682	14.08	54.92
GGBFS	2.819	19.99	57.25
OPC	2.690	16.32	47.96
K <sub>2</sub> CO <sub>3</sub>	299.1	448.4	645.6
SRA	2.334	12.81	35.20
CaO	1.728	4.949	20.61
SP	16.12	35.88	56.86
Sand	11.16	92.95	220.8

Table 17: Mix design ratio for one-part alkali-activated mortar

Samples	Binder		Alkali activator		Solid admixtures			Design ratio	
	FA (%)	GGBF S (%)	OPC (%)	K <sub>2</sub> CO <sub>3</sub> (%)	SRA (%)	CaO (%)	SP (%)	Binder/Sand	Binder/Water
Mix G1	25	5	70	1.60	0.30	0.15	1	1	0.40
Mix G2	25	5	70	1.60	0.30	0.15	1	1	0.35
Mix G3	25	5	70	1.60	0.30	0.15	1	1	0.30

### 8.3 Result and discussion

#### 8.3.1 Setting time and workability test

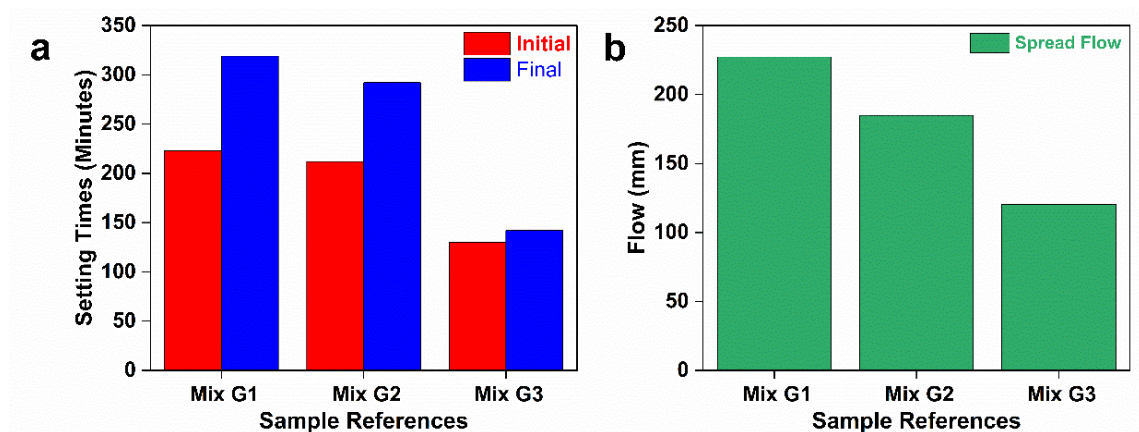


Figure 13: Setting time and workability test result of one-part AAMs mortar (paste samples).

The workability of the one-part AAMs mortar determines by observing how easily the fresh mortar deforms when stress is applied. Figure 13a above shows that sample Mix G3, activated by the water-to-binder (w/b) ratio of 0.30, has the shortest initial and final setting time, followed by sample Mix G2 and control samples Mix G1. All cement paste samples recorded more than two hours (> 120 minutes) of initial setting time, but what makes them different is low water content effectively expedited the final setting time to 142 minutes for cement paste sample G3 compared to mortar samples G1 and G2, which have recorded much longer time above 290 minutes (> 4 hours). An extended initial setting time in this result due to a low alkaline medium delayed the chemical reaction and geopolymerization process, contrary to the higher activator content, which has a more rapid reaction for a faster setting time. Furthermore, the inclusion of superplasticizer (SP) also has a retarder effect on the development of hardened mortar attributed to the adsorption properties of SP on the precursors material particles of FA, slag and OPC, as documented by [31].

Nevertheless, water content was the main factor differentiating between all paste samples in this study. The lower w/b ratio can shorten the setting time due to heat generation from solid activators when reacted with water. Askarian et al.[38] found that the paste only contained FA and GGBFS and failed to harden in 24 hours but recorded the shortest setting time by incorporating 60% OPC in the mixes. However, a short setting time could prevent proper casting at the construction site besides transporting issues from the batching plant. As for the flow table test, the higher water content in sample Mix G1 spread up to 227.24 mm makes it less viscous because of excess water compared to the samples with lesser water content, Mix G2 (184.95 mm) and G3 (120.40 mm) as shown in Figure 13b. These findings represented a 47% reduction in mortar spreading capacity when the w/b ratio of 0.40 was reduced to 0.30. It is worth noting that the finer the particles are, the lower the spreading flow is [34]. Though all mortar samples were spread firmly, no segregation was found on the flow table. This trend also confirmed the roles of CaO as one of the admixtures used in mix design, favouring the formation of homogeneous materials, low viscosity and reduced segregation of fresh materials [115]. The workability of the mortar is beneficial when applied as a repair patching material to ensure the patched mortar remains firm, set, and bonded well on a substrate. Nevertheless, the w/b ratio has influenced cementitious mortar's yield stress

and plastic viscosity. When cement particles come into contact with water, it begins to dissolve and are hydrated. Positive and negative charges will occur because of this reaction, encouraging electrostatic activities among cement particles and leading to the flocculation of the particles. Finally, cement particles absorb the amount of water, and as a sequence, the free amount of water will be diminished, leading to a higher content of solid volume fraction. As a result, yield stress and plastic viscosity level will subsequently rise, which improves the workability of the fresh one-part AAMs mortar [47]. In this study, the lower water content of the w/b ratio 0.30 delayed the hardening process (low plastic viscosity) but was shorter than the w/b ratio of 0.35 and 0.40. Higher yield stress and lower plastic viscosity ensure the fresh mortar is more stable and flows consistently, but too viscous could be a disadvantage if applied as sprayable mortar as it is not easy to be pumped out from the pipe. On the contrary, lower w/b with higher slag content also reported a setback in autogenous shrinkage and cracking [65] due to its porosity and pore size reported larger than the OPC [16], which is further discussed in the later section in this report.

It can also be concluded that with the optimum w/b ratio of 0.30, the reaction between precursors (composed with only 70% OPC content) with low alkaline activators as main synthesized products can lengthen the one-part AAMs setting time within an acceptable allowable range that beneficial for mixing, transporting, and pouring operation at the site.

### 8.3.2 Compressive strength test

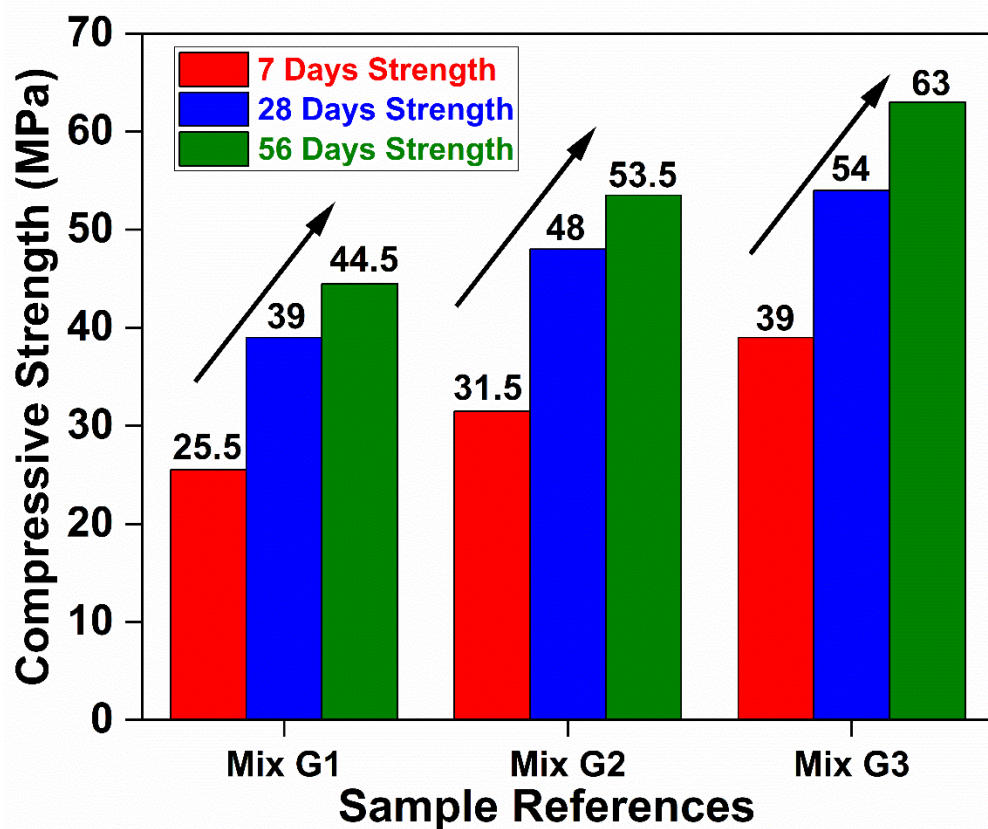


Figure 14: Compressive strength result for mixed one-part AAMs repair mortar at 7, 28 and 56 days of curing age.

Compressive strength development for all mortars increases with time regardless of the w/b ratio, illustrated in Figure 14. Mortar sample Mix G3 has recorded higher compressive strength for all curing periods beginning at 7 days of curing age and continues to develop later. Mortar sample Mix G3 has recorded the highest strength at 54.0 MPa, followed by mortar sample Mix G2 with 48.0 MPa and sample Mix G1 with 39.0 MPa at 28 days of age. Both mortar samples, Mix G2 and Mix G3, recorded above the minimum requirement for class R3 and subsequently met the class R4 - compressive strength standard as per EN1504-3 specification. At lower alkaline medium, mortar sample G3 managed to record the highest compressive strength at 63.0 MPa, followed by samples G2 and G1 at 53.5 MPa and 44.5 MPa, respectively, at 56 days of curing age.

The w/b ratio significantly influences cementitious materials for proper workability and strength. This result confirmed that the lower the w/b ratio, the higher the hardened mortar's compressive strength. Moreover, the lower binder-to-aggregate ratio used in this study was set to 1, beneficial to acting as reinforcement in the matrix and providing high dimensional stability to the mortar, improving mechanical performance and adherence level [1]. Apart from that, the compressive strength of one-part alkali AAMs product in this experiment keeps increasing after 28 days of age and confirms the geopolymerization process remains in force.

The use of a low w/b ratio of 0.30 successfully reduces the water content and has improved the compressive strength in line with the findings on the compressive strength development is correlated with the fine and large pore's diameter [31]. To understand it better, this report's latter part investigates the compressive strength result from the pore structure perspective. The inclusion of a combination shrinkage-reducing admixture (SRA) and CaO – expansive agent contributed to the higher compressive strength for mitigating shrinkage by reducing the surface tension of pore water and micropores. When water is added, the SRA helps decrease internal stress during evaporation, while CaO counteracts the shrinkage's effect by reducing the capillary stress. The porosity level, however, can be controlled by diminishing the capillary stress of the water generated by SRA during the mortar mixing process, although the usage of ethylene-glycol-based admixture reported has a setback in affecting the elasto-mechanical properties [69]. The expansion of mortar is extended with the addition of CaO during the hydration process and only starts to shrink when the wet curing is stopped. The combination of CaO and SRA reported gave a better performance concerning the cracking resistance of the mortar due to the shrinkage effect, which is valuable for better mechanical properties of hybrid one-part AAMs [93].

### 8.3.3 Pore structure analysis

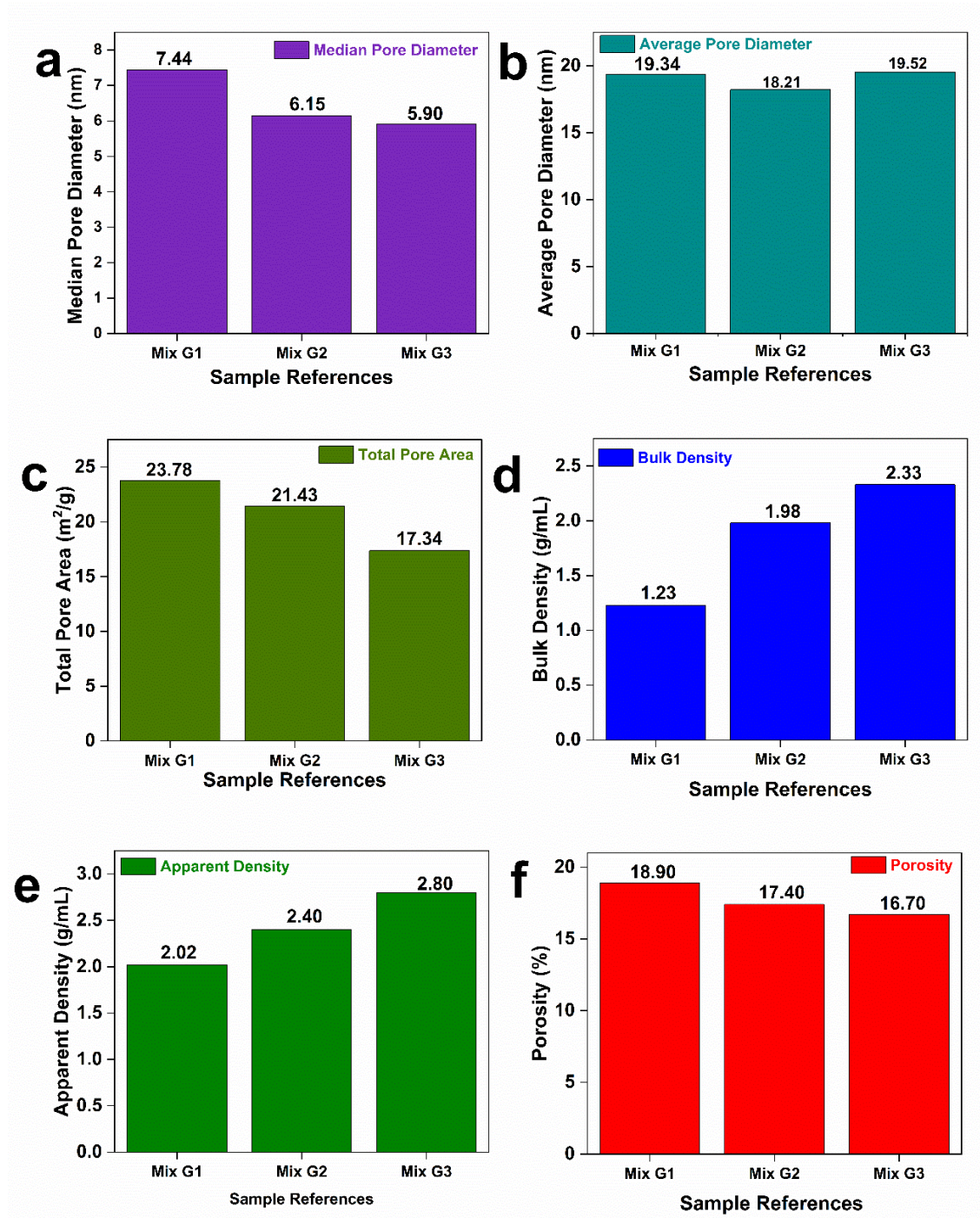


Figure 15: Pore structure distribution of hybrid one-part alkali-activated mortars.

Pore structure distribution of mortar samples Mix G1, G2 and G3 were analyzed with Mercury Intrusion Porosimetry (MIP). The results are shown in Figure 15 a - f. The mortar specimens were collected from the crushed cube samples from the 28-days compressive strength test. The median pore diameter is mainly distributed between the range of 5.90 nm to 7.44 nm (Figure 15a). The

average pore diameter for all mortar samples has no significant difference and is measured at 19.34 nm, 18.21 nm, and 19.52 nm for mortar samples G1 (w/b of 0.40), G2 (w/b of 0.35) and G3 (w/b of 0.30), respectively (Figure 15b). It is worth noting that pores sizes in the range of 3.5 – 10nm are commonly described as small gel pores type, while 10 – 100 nm are better known as large gel pores [66], 50 nm – 10 µm as capillary pores that cause detrimental to the strength of hardened samples and voids if the pore size is more than 10 µm [51]. However, voids or air bubbles have less impact on the strength during the sample preparation process triggered by vibration or mould defects [80]. Gel pores size found in this experiment as a sign of the complete reaction process of the products that can fill capillary pores with the addition of slag may decrease polymerization degree and improve pore size distribution of the mixes and strength development as reported by [30].

Increasing the porosity percentage will also reduce mechanical strength performance on the one-part AAMs [29]. The sample Mix G3 has an overall better pore structure distribution in terms of a low total pore area of 17.374 m<sup>2</sup>/g (Figure 15c), higher density of 2.33 g/mL (Figure 15d), smaller median pore diameter (Figure 15e) and as a result, Mortar G3 has a low percentage of porosity of 16.655% (Figure 15f), compared to mortar sample Mix G2 and G1.

This contributed to the inclusion of the OPC able to decrease microstructure porosity with the formation of amorphous Ca-Al-Si gels [38] and was discussed further in this report's SEM images analysis section. In comparison to other one-part AAMs, Samarakoon et al. [42] reported that the porosity level for one-part FA/slag-based materials was 35.96% (activated by sodium silicate/sodium hydroxide solution), 39% porosity (activated by soda lime glass powder/ sodium hydroxide) and 29% porosity activated by solid sodium silicate. On the other hand, for two-part AAMs, Kramar et al. [23] stated that a higher porosity level was recorded for metakaolin-based mortar (16.5%) followed by FA mortar (13.2%) and slag mortar (11.1%). As published in the report, it is interesting to note that only metakaolin-based mortar has complied with the class R4 standard and class R3 standard for FA-based AAMs, as per EN1504-3 specifications. However, a more extensive range of average pore diameter between 20 – 140 nm detected in two-part AAMs

mortar samples in that report compared to the mortar samples in this study showed that the introduced hybrid one-part AAMs has not only improved the existing one-part AAMs performance but also comparable to the two-part AAMs system for concrete repair application. Furthermore, the total pore area occupied under controlled lab temperature curing mortar at a w/b ratio of 0.35 is 23.778 m<sup>2</sup>/g but significantly reduced to 17.374 m<sup>2</sup>/g for mortar samples with a w/b ratio of 0.30. A 26% decrease in porosity is contributed to the enrichment of pore structures as an effect of the dense and compact hybrid one-part alkali-activated mortar where the group of aluminosilicate C-A-S-H gels characterized the geopolymer matrix Si-O-Al network that reflects porous fundamental structure in geopolymerization process to refined the pores [51]. The ongoing alkali activation at a later stage encourages more pore structure refinements, contributing to the better compressive strength performance for samples Mix G2 and Mix G3 at 28 days in this report. On the other hand, one-part AAMs activated by the dry activator of NaOH micro-pearls powder have a coarser pore fraction of more than 20 nm at a w/b ratio of 0.1 and subsequently prone to chemical attacks and potentially lower resistance against severe curing conditions than two-part AAMs counterparts [42]. Contrary, findings from this report indicate that a lower dosage of potassium carbonate reacts well with the optimum w/b ratio of 3.0 in the geopolymerization process, capable of refining the pore size of the mortar by filling the capillary pores, subsequently increasing the degree of microstructure densification and justified the higher compressive strength results in this report.

### 8.3.4 Restrained drying shrinkage and expansion.

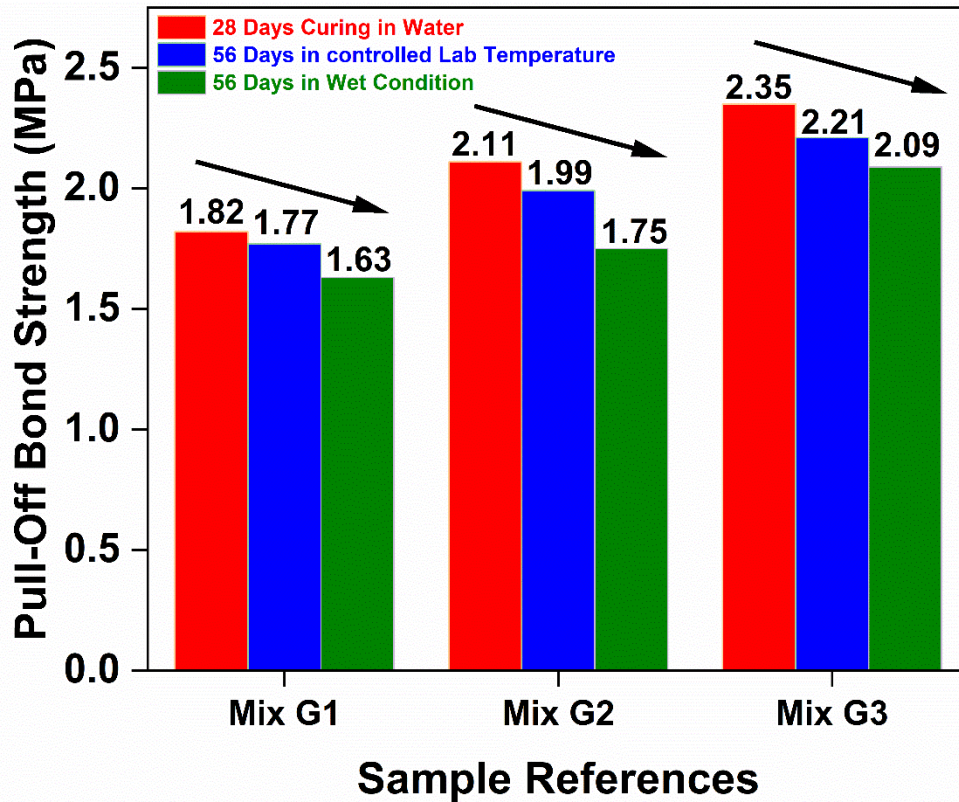


Figure 16: Restrained drying shrinkage behaviour (pull-off bond strength result).

The hybrid one-part alkali-activated mortars continue to be tested to determine their shrinkage impact by conducting a pull-off bond strength test under three different curing conditions between 28 days to 56 days of age as per EN 12617-4 test method. The pull-off bond strength trend for all mortars declines over time for all mortar samples, as shown in Figure 16 and confirms that each mortar sample was shrinking after the hydration process was completed or drying (loss) of capillary water/moisture for curing. When hardened mortar shrinks, tensile stress increases, leading to cracking and other internal deforming, thus affecting its homogeneity and compactness. Consequently, the hardened mortars' shear and tensile bond strength at repair and the concrete substrate surface will be weakened and influence the adhesion interface. Mortar samples cured for 28 days were soaked in the water as control values showed the highest pull-off bonding strength for each mixed sample, followed by 56 days curing under lab temperature, and 56-day wet curing condition (wrapped with water bath) was the lowest pull-off bonding strength amongst all. It is interesting to understand that pull-off bond strength for mortar sample G3 activated with

a w/b ratio of 0.30 has recorded above 2.0 MPa for all curing conditions and thus complied with the Class R4 ( $\geq 2.0$  MPa) while both mortar samples G1 and G2 even though recorded pull-off bond strength  $> 1.5$  MPa, they were only satisfied the Class R3 standard. It is vital to note that the pull-off bond strength of control values for mortar samples G3 only dropped slightly to its lowest recorded strength (-2.55%) compared to its counterpart, G1 (-10.44%) and G2 (-17.06%) and explain on the little effect of internal stress because of low shrinkage level. It does not affect the shear and tensile strength of the hardened mortars, indicating higher adhesive force [112]. The result of this experiment was in good agreement with the fact that the lower alkali activator dosage will have lower shrinkage and thermal effects on the hardened samples [64]. It also confirmed water content's vital role in controlling porosity levels in limiting drying shrinkage in alkali-activated materials systems.

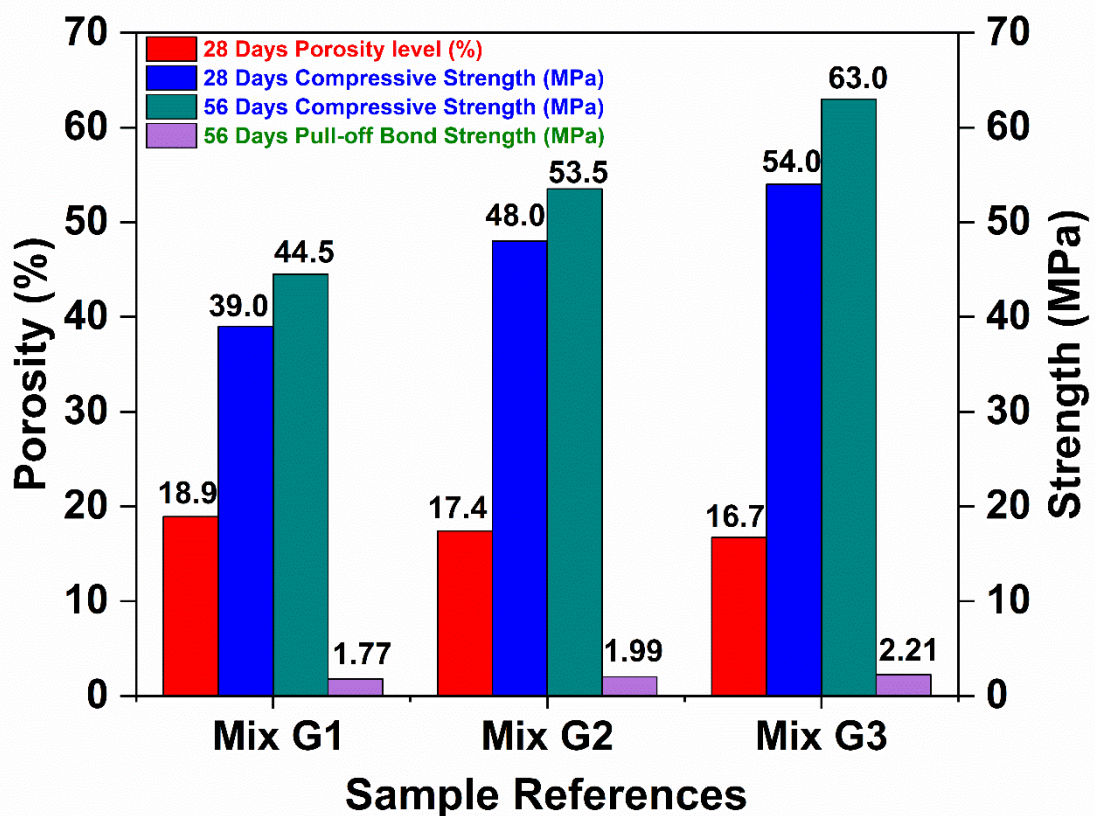


Figure 17: Porosity level vs compressive strength of one-part AAMs mortar.

The correlation between the porosity level of one-part AAMs mortar and mechanical strength before and after hardened mortar shrink at 56 days of curing are shown in Figure 17 above. At the constant mix design ratio for the mortar mixture, the influence of the w/b ratio is essential to

activate the geopolymerization and control the microstructural properties of the mortar. Reduction in porosity and drying shrinkage depends on excessive hydration product content in alkali-activated binder technology. When the water is added, the chemical reaction known as hydration is initiated and produces the final hardened material products by forming the calcium silicate hydrate (C-S-H) gels to fill the open pores to form a solid microstructure. A lower w/b ratio ensures a low porosity level of mortar sample G3 (w/b of 0.30), with 16.7%, followed by mortar sample G2, with 17.4%, and mortar sample G1 recorded the highest porosity level at 18.9%. At a lower porosity level, Mix G3 recorded 54 MPa, the utmost recorded strength for 28-days age. Furthermore, at 56 days, the compressive strength continued to develop up to 63 MPa and recorded the highest pull-off bonding strength of 2.21 MPa. This understanding explained the intercorrelation between porosity level and mechanical strength to control the shrinkage level of the mortar.

A lower porosity level ensures that the hardened mortar has a compact microstructure and fewer pores to avoid intrusion of water, gas, or other potential chemical attacks helps to increase the mechanical strength on both compressive strength's development at 28 days of curing age uninterruptedly to a last 56 days of age as reported in this study. In addition, FA consists of rich silica content that improves the process of dissolution and polymerization, contributing to low porosity microstructures [95]. Moreover, the input of Si is more efficient with low water content [117]. As a result, the pull-off bond strength remains consistent above 2.0 MPa for of mortar sample with the lowest w/b ratio (mortar sample G3) encountering the shrink-hardened mortar at 56 days of age and shows the water content effect on monitoring drying shrinkage and expansion behaviour (by means of pull-off bond strength result) subsequently complies with structural repair products of class R4 – EN1504-3 standard. These findings also confirmed that hardened mortar with a low porosity level corresponds to the lowest drying shrinkage and better mechanical strength [68].

### 8.3.5 Scanning Electron Microscopy (SEM)

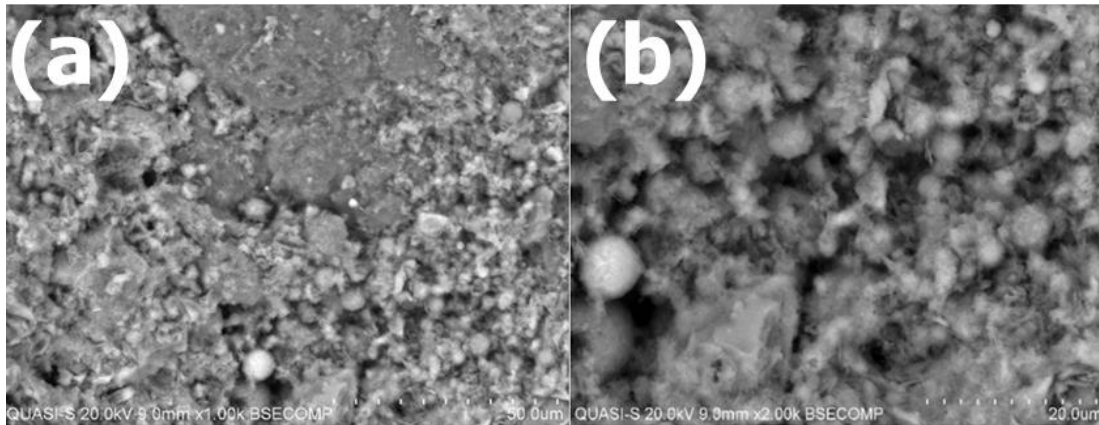


Figure 18: SEM Image of sample G2 (a) Overview and (b) Spherical structure

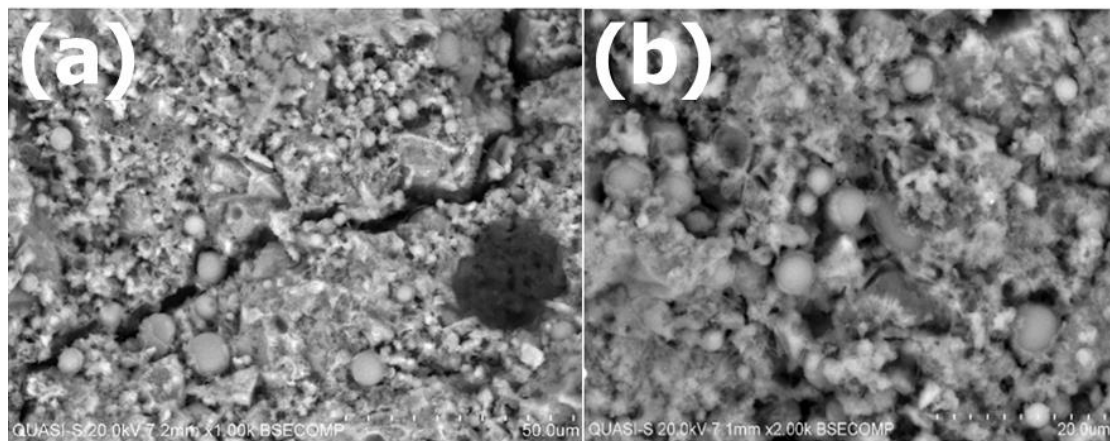


Figure 19: SEM Image of sample G3 (a) Overview and (b) Spherical structure

The microstructure of one-part alkali-activated materials was studied using Scanning Electron Micrograph (SEM). The hardened mortar was produced with different percentages of mix composition consisting of fly ash which contains 25% of total precursors weight, 5% slag and 70% ordinary Portland cement as main aluminosilicate precursors, which is donated to the densified microstructure of the mortar. Few spots were captured for the SEM images of mortar samples G2 and G3, and only images with overall textures, i.e., pores, cracks, and compacted surfaces, are shown in this report to understand the microstructures of the hydrated particles. Figure 18 and Figure 19 showed that both SEM images for samples G2 (Figure 18a) and G3 (Figure 19a) are well hydrated in general, compact and homogenous with new calcium sodium aluminosilicate hydrated gels on their surfaces. Interestingly, using a 1.8% dry activator type of

potassium carbonate still contributes to lesser unreacted calcium as a sign of effective chemical reaction between precursors, admixtures, and low alkali activators with appropriate water content. Nevertheless, the morphology of the two mortar samples is similar from the perspective of porosity and aggregate-mortar interface, including some unreacted particles pattern. Both images also depict the micropores and microcracks marks but exhibit a glass-like surface representing the geopolymeric gel. The microcracks frequently occur due to irregular shrinkage forces among gels and particles throughout the drying process, besides the loss of water in gels [66]. SEM images zoomed in to 20 $\mu$ m, focusing on spherically shaped areas, revealed that sample G2 has a less spherical structure than sample G3, which consists of more spherical spots, as shown in Figure 18b and Figure 19b. However, it can also observe in this image that the pores of sample G3 are more prominent, which supports the pore structure distribution result for the mortar sample with a low water content of w/b ratio of 0.30, has higher average pore diameters than the mortar sample G2.

### **8.3.6 Microstructural development**

All raw materials used in this study, from aluminosilicate precursors, alkali activators and solid admixtures, have good reactivity, are chemically stable in reaction and are well dissolved when in contact with water. Optimum w/b content ensures the hydrolysis of all these solid activators takes part to facilitate the network breakdown of solid precursors. Dissolved ions would undergo gelation and condensation, as reported by Lv et al. [76]. A higher Si/Al ratio obtained from fly ash is beneficial to encourage low porosity microstructure, improving sample compactness for better mechanical strength [95][97][99]. Adding GGBFS/OPC further supplies calcium and balances the short supply in FA, assisting in stronger chemical bonds for hydration products.

A higher volume of OPC is beneficial to wrap the water in the cement particles and reduce the amount of free water in the fresh mortar mixes, subsequently increasing adequate solid volume friction for better compactness and leading to higher mechanical strength [47]. Three exothermic reactions after the addition of water in one-part AAMs are the dissolution of raw materials (NaOH and hydration of CaO), bond breaking (attack of OH<sup>-</sup> on Si-O and Al-O bonds) and release of Ca, Si and Al and formation of gels via polymerization as reported by [52]. Unreacted particles

decrease in quantity with a longer curing time and a higher dosage of alkali activator in the system. However, lower alkali activator dosages were used in this experiment. Only 70% of OPC content was used in the mix, yet it contributed to a more compact and less porous structure and less unreacted fly ash particles, as agreed by [38]. FA particles composed of microspheres, amorphous alumina and/or silica-rich materials can be dissolved in alkalinity [18]. The spherical particles will be embedded in the form of material and contribute to better mechanical strength over time. Spherical structures are spotted in this study's SEM image, commonly known as the unreacted fly ash component, in agreement with Azevedo et al.[29] on the fact that fly ash particles remain even after contact with alkaline materials in all curing periods, probably caused by low alkaline reactivity. In this report, mortar sample G3, which has more spherical shape particles, recorded growth compressive strength from 7 days (39.0 MPa) to 28 (54.0 MPa) and 56 days (63.0 MPa) of curing age and retained its pull-off bond strength at an average of above 2.0 MPa at 56 days of age. It proves that the spherical/unreacted FA particles were still experiencing geopolymerization after 28 days of age. It was also helpful to understand that some unreacted particles are inherited from the parent material of hydration products, as suggested by [16].

A compact structure shows good adhesion and explains the increase in mechanical strength of the mortar. The compaction of microstructures improved with a more extended curing period, confirming the increment of strength over time for both mortars [68] samples as recorded in the compressive strength test at 7, 28 and 56 days of curing age in this report. Therefore, the unreacted particles in the SEM images may act as micro fillers in the mixes and improve their compactness. Both images have shown microcracks spots. Although a line of microcracks is more visible in the mortar sample, the G3 image may indicate the loss of water [62] or temperature cracks due to the heat generated from the reaction between the sodium oxide of the alkali activator and water [30] and uneven shrinkage forces between derivatized gel and the particles. All take place during the curing period [66]. The cracks' formation could degrade the mechanical performance of the mortar over time. Though, Almalkawi et al.[16] reported other factors on why microcracks could appear or get visible areas due to the drying process of the specimen for SEM. The clear microcracks image proves that the mortar sample G3 (19.52 nm) has a higher average pore diameter than G2

(18.21 nm), in line with the MIP test result for pore structure distribution. It was reported that an 8% solid activator (by weight %) used to activate FA/GGBFS one-part AAMs only achieved about 30 MPa at 28 days of curing age, where more unreacted particles were observed in SEM image [28]. In contrast, as the low alkaline level of the alkali activator (1.6%  $K_2CO_3$  by weight) used in this study observed, fewer unreacted particles were found on both SEM images for samples G2 and G3. Yet, they achieved significant compressive strength value, proving that this type of mortar samples initiated with a low amount of alkali activator have substantial potential to improve the current technology of one-part AAMs.

Alkali activated materials concept is much contributed by the dissolution of aluminosilicate precursors with the formation of geopolymeric gels of low atomic order favourable for hardened materials cementing properties [29]. The preparation of samples in this study was conducted under controlled temperatures and not exposed to high temperatures that could trigger dissolution. On the other hand, the geopolymerization begins with the calcium reacting with potassium carbonate to create C-S-H gels, consequently elevating the pH of the alkaline mix and reducing water content. Under an alkaline environment, the dissolution of aluminosilicate precursors was initiated, subsequently ameliorating polycondensation and polymerization reactions for the hardening process. The precipitated compounds and geopolymeric gels of N-A-S-H and C-A-S-H contributed strength and remained to develop higher over time as the geopolymerization continued.

On the contrary, at a higher temperature level of 65 °C, the dissolution of aluminosilicate precursors quickens to form geopolymeric compounds at an early age for higher early strength [65]. Still, it may also cause incomplete dissolution of aluminosilicate compounds given that geopolymeric slurries could cover the undissolved precursor, limiting further dissolution besides water evaporation and excessive shrinkage problem creating more cracks and pores and finally decreasing the strength of the mortar. Samarakoon et al.[42] reported that at the early age of curing, the hydration product for one-part AAMs mainly comprises C-A-S-H type gels. However, the reaction products are C-S-H dominant due to higher reactivity, and easier discharge of calcium

ions can be found as early as 1 day of curing age. At the same time, the other portion of silicon and aluminium remains unreacted on the surface of the reacted phase. After 28 days, calcium content will be reduced. Still, silicon involvement in hydration products is increased because higher portions of fly ash could promote zeolite formation at the later curing stage when the composition of the binder is SiO<sub>2</sub>-rich; the incorporation of Na is also favoured, later confirming the co-existence between C-A-S-H and N-A-S-H with a potential cross-linked structure of C-(N)-A-S-H type gels at subsequent curing. In this report an optimum w/b of 0.30 effectively initiate the chemical reaction and created C-(N)-A-S-H type gels which assist the hardened mortar with low porosity level not only able to resist leaching through its open pores but also offer more stable geopolymeric link gels against chemical attacks and maintaining its mechanical strength, beneficial for one-part AAMs long-term effectiveness.

### 8.3.7 Characterization of reaction products using – SEM-EDX

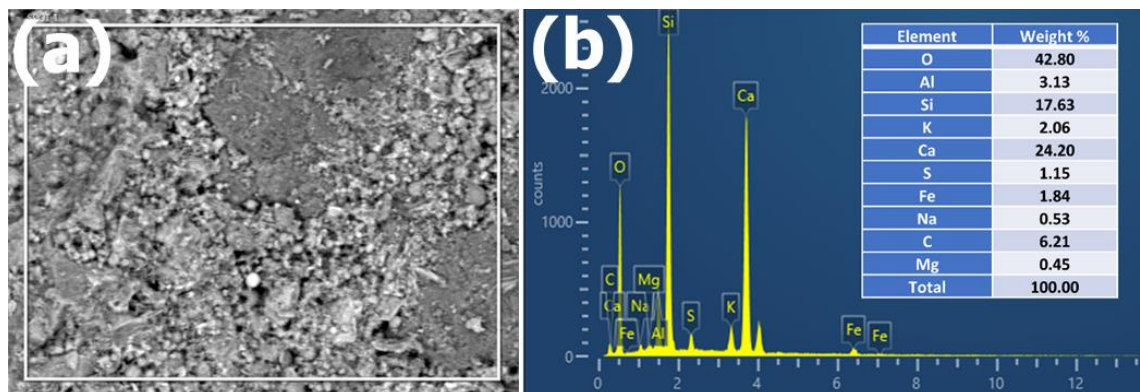


Figure 20: SEM-EDX of sample G2 (a) Image and (b) Weight (%)

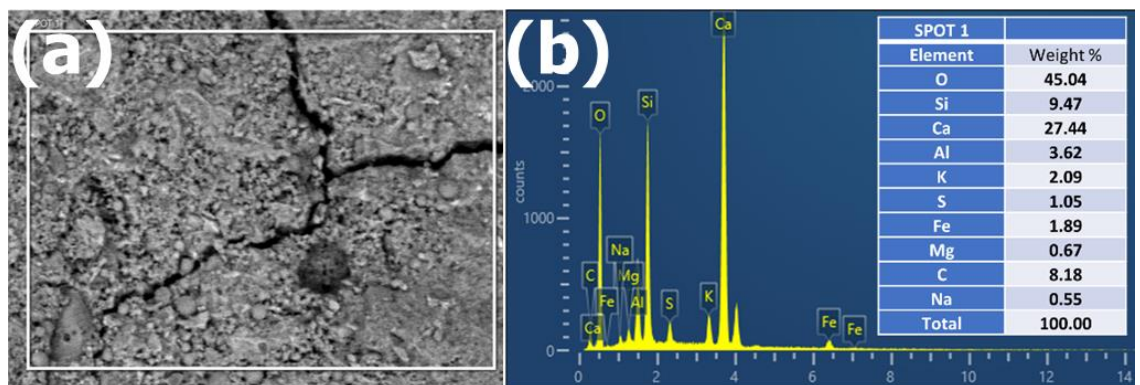


Figure 21: SEM-EDX of sample G3 (a) Image and (b) Weight (%)

The difference in the surfaces of the hybrid one-part alkali-activated mortar activated by different water-to-cement ratios was further investigated by the chemical element composition at a specific area using the EDX. The resulting SEM images at 28 days of curing with the corresponding EDX maps at 28 days of curing are shown in Figure 20a – Figure 21a. During the curing period, microstructures of all mortar samples become dense by reducing micro-pores, reflecting compressive strength development with time due to highly compacted and low porosity levels [48]. The formation and spatial distribution for both mortar samples consistently depict a well-blended elemental distribution for the formation of homogenous and dense microstructure [42]. The reaction process in AAMs requires a few steps starting with the dissolution of Ca, Si and Al from aluminosilicate precursors, a re-orientation process, re-interaction and condensation to develop the strength [80]. Additionally, the chemical compositions of Al/Si and/or Na/Si atomic ratios and K/Al molar ratio are beneficial to determining the AAMs' mechanical properties, which are connected with its product's dissolution rate [18][113]. It was explained in a past report on forming C-A-S-H gels that were regarded as aluminium substituted C-S-H phase in AAMs technology. Aluminium (Al) in C-A-S-H functioned in bridging tetrahedral sites. Still, the different extent was restricted by chemical limitations due to a defect of the tobermorite structure [76]. The overall constituent of geopolymerization products for mortar samples G2 and G3 have consisted of newly formed hybrid geopolymeric products N-A-S-H gels co-existing with C-A-S-H gels. New hydration products of C-(N)-A-S-H type gel was confirmed using EDX point analysis on dominant elemental phases in the reacted cement binder, mainly silicon, calcium, aluminium, and sodium.

The higher weight percentage of Ca/Si found in sample G3 (Figure 20b) than in sample G2 (Figure 21b) is a sign of a higher Ca/Si molar ratio beneficial for the early formation of C-S-H. Askarian et al.[38] reported that CaO to SiO<sub>2</sub> (Ca/Si) decreases with decreasing OPC content in geopolymer mixes. Mixing with a higher Ca/Si ratio is beneficial to form C-S-H gels, which can improve the early strength of mortar. The combination of OPC and FA/GGBFS creates different nature of C-S-H gels (stronger bond) compared to the typical C-S-H gels formed in OPC alone. Luukkonen et al.[72] reported that Ca/Si increases when sodium lignosulfonate – superplasticizer

introduced in the mortar with  $\text{Ca}^{2+}$  reaction from lignosulfonate could facilitate the dissolution of slag to increase the amount of calcium and likely to increase the compressive strength of mortar. It is worth noting that the roles of SP admixtures used as part of the mix design reacted well in assisting the dissolution process when a w/b ratio of 0.30 was added to ensure the efficiency of 30% OPC total weight reduction in the mixes and replaced with FA and slag yet still has a comparable Ca/Si ratio with sole OPC precursor.

#### **8.4 Conclusion**

The one-part AAMs experienced coarser pore fractions above 20nm, affecting their durability and mechanical strength compared to the two-part counterpart. A larger pore diameter will cause higher porosity and be prone to chemical attacks, especially when the location is exposed to adverse climate and temperature. This report established the effect of adequate water content through a w/b ratio to improve one-part alkali-activated mortar. Unlike the past report on hybrid one-part AAMs, the mortar samples in this study were activated with only 1.8% alkali activator and composed of 70% OPC with 25% FA and 5% GGBFS as main precursors sources. Three types of admixtures were added to stabilize the mortar's physical properties. As a result, the w/b ratio of 0.30 exhibit the best overall performance in the fresh and hardened mortar state. A lower w/b ratio also contributes to the low porosity level of hardened mortar by controlling its pore structure. It subsequently overcame the shortfall of the current one-part technology and achieved the aim of this study. The mix design formulation is now completed for the production of geopolymer binder as per class R4 – EN1504-3 standard for structural concrete repair materials applications.

Furthermore, this mix design formulation confirms that it successfully replaces 30% of OPC volume with industrial by-product precursors as the first step in diminishing reliance on the OPC and another effort to reduce clinker production, reuse waste products, and control  $\text{CO}_2$  emissions. This report also summarizes that the hardening mechanism and microstructures of hybrid one-part alkali-activated mortar changed significantly when the mortar was composed of different water-to-binder ratios, producing different mechanical strengths at early and later stages, affecting

the pore structure distribution. The ongoing geopolymerization process over time encourages continuous pore structure refinements, which is essential to control the total porosity level and guarantee mechanical strength growth beyond 28 days of curing age. A significantly lower porosity value below 20% was recorded for mortar samples G3, which is beneficial for controlling the drying shrinkage effect.

Nevertheless, the SEM images of the mortar specimen at 28 days of curing age for both mortar samples G2 and G3 show almost identical structures and similar final products. The only differences between different w/b ratios were the amount of reacted geopolymer gels (dense, homogenous, glass-like surface)/unreacted precursors (spherical structures) and micropores/microcracks elements. Unlike the conventional one-part AAMs, where the dissolution of precursors is not completed under low alkaline reactivity, leading to more unreacted particles, the mortar samples G2 and G3, on the other hand, have dense, compact, and homogenous reacted geopolymer gels.

Apart from the influence of water content discussed in this report, another finding showed that the usage of a low alkali activator reacted well with all precursors, in addition to the optimum content of solid admixtures for the geopolymerization process and offered reliable mechanical and microstructural properties for the hardened mortar. Although the hybrid one-part alkali-activated mortar has a significantly low porosity level and consistent mechanical strength, a future study must focus on the stability of its pore structures against severe environmental conditions and chemical attacks in a different climate to ensure its durability and efficacy for long-term application.

## 9 Discussion

### 9.1 Discussion of Manuscript 1

To produce a new concrete repair material based on one-part AAMs technology, each material's composition must be determined, formulated, and tested to establish a novel mortar mix design. The main element in a one-part system is precursors and alkali activator to produce cementitious binder. Therefore, it is vital to understand the type and composition of both sources before some adjustments can be made to ensure the reaction between them works properly. FA, slag and OPC were selected as aluminosilicate precursor sources, where potassium carbonate as a single alkali activator was employed for all mixes based on various dosage levels. The compressive strength of the repair mortar is the main aim of this experimental work as the first step to giving an overview of the characteristic of mortar and as an indication that the mortar samples have an adequately done. Therefore, three stages of mix proportions were designed to evaluate the compressive strength of all mortar samples based on 7, 14 and 28 days of age for all trial mix stages. It is essential to achieve a relevant strength at an early stage of the hardening process, where it provides a crucial indication of the strength development over time. Three admixtures were included in the mortar samples; SP, SRA and CaO and their effect on the mortar were thoroughly studied at stage 2. At 14 days of age, when the compressive strength trend is increasing, some adjustments on design ratios were made to determine their mechanical strength behaviour at 28 days of age. Mortar samples with better compressive strength at 7 days of age were selected for further testing at 14 and 28 days.

There are 30 mortar samples prepared and called Mix 1 – 30. At the first stage of the experiment, samples with reference Mix 1 – 9 were prepared. Mix 1 was selected as control sample no.1, where the main precursors were composed without OPC. The alkali activator concentration started at 6% of the total precursor's weight, which is considered a medium dosage as a first reference or benchmark to find the optimum activator volume. The volume of SP was consistently set at 1% as a reference from the past works of literature. The usage of SRA and CaO were set between 1 – 5% for the former and 0.5 – 1% for the latter. Generally, cementitious mortar is

composed of fine aggregate, unlike concrete with fine and coarse aggregate or paste samples without aggregates. Thus, the fine aggregate content was adjusted via an a/b ratio between 1 – 3, while the w/b ratio was adjusted between 0.30 to 0.50. Though the mechanical strength performance of all mortar samples was based on different trial mix designs or the try-and-error method, their composition was based on previous research, as elaborated in the literature review section. It is being reformulated to introduce new concrete repair materials with improved engineering properties.

Mix 10 was prepared without admixtures. For this regard, Mix 11 – 25 were tested to evaluate the strength performance with and without slag as a precursor and to analyze how the admixtures influenced the compressive strength of mortar if their dosage increased at a higher concentration. Other parameters remained consistent according to their first-stage volume. Finally, compressive strength results were analyzed based on stage two outcomes. Their final composition of precursors can be determined for mortar samples Mix 26 – 30, which is in the third stage of this trial mix study. The optimum dosage range of the activator also can be expected with some adjustment on SRA and CaO, where the volume of SP and a/b ratio were fixed to 1, before the final trial on the water content via w/b ratio carried out to activate the dry cementitious material for engineering application. Based on the compressive strength result, mix 5 and Mix 30 have significant strength levels at 28 days of age, where they were recorded at approximately 26 MPa and 28 MPa, respectively, complying with the minimum compressive strength requirement for class R3, EN1504-3 standard. Both mortar mix samples have a consistently increased strength development at 7, 14 and 28 days of age. As a result, these two samples were selected based on their mixed compositions. They were tested with other mechanical strength measurements to expand their potential, develop them as concrete repair materials, and aim for more comprehensive engineering applications.

Additional mechanical strength tests on flexural, modulus of elasticity and tensile strength were carried out on Mix 5 and Mix 30. These three types of mechanical strength are not required for concrete restoration application (all intended uses - EN1504) for applying mortar by hand.

Nevertheless, the outcome of this test will give a further indication of the performance level of the mortar, which can be applied as patching repair materials and perhaps can be utilized in the form of concrete comparable to the conventional OPC concrete in the market. For the flexural strength result, both mortar samples recorded a comparable strength of 8.10 MPa and 8.55 MPa at 28 days of age, showing that the mortar samples have an impressive bending resistance. Modules of elasticity (MOE) for Mix 5 and Mix 30 recorded 18.10 GPa and 19.60 GPa at 28 days of age and complied with class R3, EN1504-3 standard for specific intended uses category (exposed to extreme environment). Thus, the MOE result also proves this type of mortar can resist elastic deformation when force is applied. Splitting tensile test results for Mix 5 recorded about 1.80 MPa, and Mix 30 had 2.05 MPa at 28 days of age. Adhesive bond via pull-off bonding strength in Table 3, EN1504-3 standard emphasized the requirement bonding strength must be above 1.5 MPa for Class R3, thus result from the splitting tensile test give a clear signal on its ability to resist against tension and provide information on how good the mortar bonding performs when patch on a concrete substrate, to restore the concrete and prevent further delamination. Drying shrinkage measurement for mortar sample Mix 30 has recorded a lower shrinkage level at 260 microstrains than Mix 5, which recorded 350 microstrains. Nonetheless, both drying shrinkage measurements are within the allowable measurement below 400 microstrains as regulated under ASTM C157 specifications. A lower shrinkage level will ensure the durability of the mortar against an exposed environment for a longer concrete structure lifespan.

This study established a new design mix formulation for a one-part AAMs mortar based on its mechanical strength performance. The mortar can be employed as concrete repair materials and alternative cement binder to conventional Portland cement for concrete structure applications.

## **9.2 Discussion of Manuscript 2**

In manuscript 1, a new mix design was formulated for the one-part AAMs mortar and had a promising compressive strength at 28 days of age up to 28 MPa. Both mix compositions for mortar samples, referred to as Mix 5 and Mix 30 in manuscript 1 re-employed to analyze further their fresh properties and how their rheology behaviour influenced the mechanical strength of the

mortar from the perspective of compressive strength and pull-off bond strength. Seven mortar samples were prepared and called Mix 1 – Mix 7. However, the temperature and humidity when the mortar sample was prepared, cured and tested for compressive strength are different from the previous experiment in manuscript 1, where all the samples in this study were exposed to higher ambient lab temperature of 29 °C and low relative humidity (RH) of 65%. For the setting time of fresh mortar and pull-off bonding strength, the experiment was conducted under a controlled temperature of  $21 \pm 22$  °C and relative humidity of  $> 90\%$ .

Mix 2 was prepared without admixtures, referred to as control samples for fresh mortar, and has a longer initial and final setting time of 243 – 319 minutes. On top of that, Mix 1, which emulates the mix design of Mix 5 in manuscript 1, has the longest setting time, between 320 – 401 minutes. Both mortar samples recorded irrelevant initial setting times between 4-5 hours, making it impracticable for hand patching application at the actual site. Too long for the mortar to set will cause a loss in strength and durability with the potential to delaminate and early shrinkage crack. Nevertheless, both samples were activated with a higher w/b ratio of 0.50 which may have caused them to experience excessive water content. At a w/b ratio of 0.40, mortar samples Mix 3 – 5 has comparable setting time within the 170 – 300 minutes range.

On the other hand, the alkali activator dosage for these three samples was between 1.6 – 2.0 %, giving additional information to support findings on the optimum dosage level of the alkali activator as established in manuscript 1. Further reduction of the w/b ratio showed a significant effect on setting time Mix 6 and Mix 7, where both mortar samples recorded lower setting times between 158 – 279 minutes for the former and 147 – 274 minutes for the latter. Both mortar samples have an average below 2 hours of initial setting time which is more practical to apply at the site, whether for site mixing - in situ application or transporting from a batching plant. In addition, the setting time result indicates how admixtures and water content influence the rheology behaviour of one-part AAMs in fresh mortar. A better rheology performance is beneficial for workability and safeguards its mechanical strength. It is worth noting that the fast-setting problem in one-part AAMs technology has been improved with longer setting time, as

probed in this study. Temperature and humidity also play essential roles in lengthening the setting time, where a lower temperature with higher humidity will affect the kinetic reaction and limit the thermal effect on it.

Unlike the setting time experimental study, Mix 3 in this study emulates the design mix of mortar Mix 30 from manuscript 1, used as a control sample for hardened mortar. At higher temperatures and lower humidity levels, the mortar samples Mix 3 has dropped its compressive strength from about 28 MPa in the previous study (manuscript 1) to 26.75 MPa in this study. This phenomenon has shown that mortar sample Mix 3 has yet to achieve structural stability when applied in different environments. Mix 1 has a more stable structure since the compressive strength remains at 26 MPa, but a longer setting time becomes a setback to developing its mix design further. Mortar samples Mix 2,4, and 5 have a negative strength development trend where the compressive strength decreased over time.

On the other hand, the compressive strength result gives additional supporting information on the optimum dosage of SRA and CaO, as described in Manuscript 1. Interestingly, based on the findings above, water content becomes the final factor in deciding the ultimate mortar performance at the fresh and hardened stage. By reducing the w/b ratio to 0.35 for Mix 6 and 0.30 for Mix 7, compressive strength for both mortar samples achieved approximately 36 MPa at 28 days of age. Both strength levels have exceeded Class R3, EN1504-3 minimum compressive strength requirement but still fall behind in meeting with Class R4, EN1504-3 requirement.

In manuscript 1, tensile strength results for mortar sample Mix 30 have recorded significantly higher strength, about 2 MPa. It indicates that the mortar has a sufficient bond strength that can be used as patching materials on concrete. Pull-off bond strength was carried out in this study to evaluate the bonding strength capacity of one-part AAMs mortar according to the testing method specified in Table 3, EN1504-3 standard and compared to the tensile strength results in a previous experiment. Three mortar samples, Mix 3, 6 and 7, were selected based on their compressive strength achieved Class R3, EN1504-3 standard (> 25 MPa). Interestingly, the w/b ratio for each

sample was 0.40, 0.35 and 0.30, respectively. Mix 3 recorded 1.885 MPa, and Mix 6 had 1.757 MPa and Mix 7 recorded the best result of 2.565 MPa. In addition, mortar samples Mix 7 has demonstrated an A-substrate/cohesion type, indicating a stronger patch materials bonding strength than its concrete substrate. Both Mix 3 and Mix 6 have pull-off bond strength comply with Class R3 (>1.5 MPa), while Mix 7 has successfully exceeded Class R4, EN1504-3 minimum requirement (>2 MPa).

In this experimental study (manuscript 2), the one-part AAMs mortar samples have been tested in fresh and hardened states. The test on the setting time of mortar was carried out to determine the workability of the mortar when applied by hand to patch delaminated concrete surfaces. Faster setting time levels may not necessarily be practical to be employed in specific applications. It requires setting a time tolerance which is neither too fast nor too long. Mortar with a significant setting time level and acceptable compressive strength performance in this manuscript 2 indicates its potential to be developed further as concrete repair materials. The mix design of mortar was modified for this purpose, and further examination of its pull-off bonding strength revealed that this type of mortar could be utilized as concrete patching materials, especially for hand applications at least for Class R3, EN1504-3 for structural concrete repair applications.

### **9.3 Discussion of Manuscript 3**

The mixed design compositions of one-part AAMs mortar have been discussed thoroughly in manuscripts 1 and 2. The initial series of trial mix designs were carried out to understand a few parameters on; a) how different types of precursors and their dosage reacted with a low concentration level of alkali activator, b) the roles of admixtures, c) the effect of design ratios, and the relation between all these parameters between each other (a-b-c). The mix design composition obtained from Manuscript 1 was further analyzed in Manuscript 2 to ensure the final cementitious product has improved mechanical strength and workability. As a result, the pull-off bond strength of the mortar has complied with Class R4, EN1504-3 standard, while the compressive strength of the mortar has steadily exceeded the Class R3 strength requirement. Five main performance characteristics must be achieved for structural concrete repair applications, as referred to in Table 3, Class R3 and R4. While two characteristics were established accordingly

under mechanical performance in the previous study, the remaining three characteristics, on the other hand, are purposely to analyze durability performance. The one-part AAMs mortar in this study may be strong enough due to its mechanical performance. It was also valuable to operate, practical and easy to handle since it has recorded a significant workability level. However, its long-term resistance is still uncertain whether it can withstand the different environments that might affect its overall performance at specific periods. This study mainly focuses on the effort to control the shrinkage level of the mortar as a first step to determine and improve the durability level of the repair mortar for more extended applications. In addition, this study also confirmed the stability of the mortar with designated mix design composition, finalized its formulation and specified under which structural concrete repair materials class it will be classified following EN 1504-3 specifications.

In manuscript 2, it is well indicated that lower water content influences mortar performance. When w/b was reduced, the mortar's setting time was shortened, and compressive pull-off bonding strength improved. For this regard, three mortar samples, identified as Mix 1 – 3, have been prepared in this study with different levels of w/b: 0.40, 0.35 and 0.30, respectively. All experimental tests were conducted under a controlled temperature of  $20 \pm$  Celsius and relative humidity of  $RH > 90\%$  as per EN1504-3 requirements. At first, the rheology behaviour of mortar samples was tested to support the previous findings on the workability level of the mortar. Mix 3, which activated with w/b ratios 0.30, recorded the lowest initial and final setting time, about 2 hours. Mix 3 has a shorter spreading measurement of about 120mm compared to other mortar samples. This is the probe that a lower w/b ratio ensures higher workability of the fresh mortar. The workability test may not be specified in Table 3, EN1504-3, but this finding is necessary to understand the practicality of this repair mortar for real hand patching applications. Secondly, the compressive strength of these three mortar samples was tested from 7 days up to 56 days of age. All mortar samples have an increased mechanical strength trend over time. Mix 2 (w/b: 0.35) has recorded 48 MPa, and Mix 3 (w/b: 0.30) has the highest compressive strength of 54 MPa at 28 days of age. Both mortar samples satisfied the Class R4, EN1504-3 requirement. Interestingly, at 56 days, Mix 3 has the best compressive strength level of 63 MPa to prove that the

depolymerization reaction is still working at later stages, increasing durability, which is beneficial for long-term application.

To determine its porosity level, the pore structures of mortar with a low w/b ratio were evaluated using Mercury Intrusion Porosimetry (MIP) analysis. Higher porosity levels will cause the mortar to be exposed to chemical attack and water penetration. The mortar will not only be contracted during an early stage of the hardening process due to water loss, but it can also expand if intruded with excessive water levels when exposed to the environment. The expansion and contraction process may cause the mortar to experience shrinkage problems. Mix 3 has the lowest porosity level of 16.70%, which further justify on its higher pull-off bond strength overall performance. It recorded 2.35 MPa at 28 days of age, 2.21 MPa, and 2.09 MPa at 56 days under different curing methods: ambient lab temperature and wet conditions. The pull-off bond strength result explained how the mortar with a w/b ratio 0.30 can resist restrained drying shrinkage and expansion when exposed to different environments. Still, the bond strength results for Mix 3 have exceeded 2.0 MPa and complied with Class R4, EN1504-3. Furthermore, lower porosity and shrinkage levels indicate this mortar's physical structure to resist chloride and carbonation attacks. This study does not cover the other two remaining performance characteristics for durability.

As discussed above, the phenomenon of the experimental result was further investigated via microstructural analysis. Scanning electron Microscopy (SEM) was employed to view the image of the micromorphological features of the mortar. At the same time, Energy Dispersive X-Ray analysis (EDX) was used to identify elemental compositions of the mixes in the hardened mortar. The microstructural development of one-part AAMs mortar is crucial to understand how the water content influenced the reaction between aluminosilicate precursors, alkali activators and admixtures. The optimum w/b ratio will assist in the dissolution of raw materials, bond breaking and formation of gels. Sufficient water content improves the geopolymerization process, while excessive water will affect its chemical stability. As a result, a w/b ratio of 0.30 for one-part AAMs mortar in this study assisted in the creation of a more robust chain of N-A-S-H and C-A-

S-H gels subsequently contributed to the higher mechanical strength performance, better workability level, and improve the pore structure distribution.

Finally, this manuscript 3 established the report on the effect of the water-to-binder ratio on the pore structure of one-part AAMs mortar. Therefore, it has completed the continued research from manuscripts 1 and 2 on formulating a novel mix design of repair mortar. The main objectives of the overall study were successfully achieved, and the aim for Class R3, EN1504-3 has been fulfilled but with better achievement of Class R4, EN1504-3 standard.

## 10 Conclusion

The production of Portland cement has caused tons of CO<sub>2</sub> emissions into the air. Efforts have been taken to reduce the environmental impact due to the pollution. Industrial activities also contribute to environmental problems. Many industrial by-products were left abandoned and piling up the landfills. Waste materials such as Fly Ash from the coal-fired power station and Ground Granulated Blast Furnace Slag (GGBFS) produced from steel-making industry areas among types of industrial by-products that have been commercialized due to extraordinary properties that can be modified and produced as a cement binder, alternative compounds to Portland cement.

New concrete repair materials in this study were invented by applying engineering knowledge to develop advanced cementitious binder materials which are specifically designed for the improvement of engineering properties and performance in three main elements; mechanical, physical, and chemical behaviour of concrete to withstand pressures and stresses subsequently ensure the load-bearing design in the structural concrete system is functioning. The raw materials were then activated with a novel mix design formulation for structural concrete repair application in the form of mortar – for hand patching application to reinstate delaminated concrete surface, not only crucial to make sure concrete continues to resist and transfer the load between its structural element but also act as fire resistance and protect the steel reinforcement from corrosions. Interestingly, cementitious binders of one-part AAMs have a comparable performance with Portland cement for concrete application. It may not be necessary for its application in the form of concrete for superstructures or high-rise buildings. Still, perhaps it can be used to start with ancillary structures or infrastructures to cut dependency on Portland cement in the construction industry.

Many studies have been conducted on one-part AAMs performance, but its application mainly focuses on concrete. In addition, research is also extensively conducted to synthesize and calcinate raw materials to expand the selection of waste products. The application of one-part AAMs in the

form of mortar has been lacked behind since then. Nevertheless, one-part AAMs mortar has been studied in this report to understand its potential as a choice of concrete repair products in the market, offering comparable engineering performances and environmentally friendly products. Adding water lets the cementitious binder be applied immediately, is easy to patch, and is friendly to users. However, to ensure the sustainability of one-part AAMs as a repair material, its properties must be engineering modified so that its rheology and mechanical strength can achieve specific engineering standards. In comparison, AAMs mortar in the two-part system composed of metakaolin often has efflorescent problems. Also, in contrast, GGBFS-based mortar has failed to bind properly and delaminated when patched at both vertical and horizontal substrate surfaces.

Furthermore, the main objective of this study is to develop a cementitious binder with a new mix design formulation in the form of mortar for hand patching concrete repair application at ambient temperature conditions successfully complied. The mortar product has improved pore structure, lower shrinkage level and aim and satisfied class R4, EN1504-3 specifications for structural concrete repair materials. The formulation of mix design compositions was based on hybrid precursors content composed with FA, GGBFS and OPC, low concentration of carbonate type of alkali activator, three types of dry admixtures and adjusted design ratio of aggregate and water. The engineering performance of mortar was evaluated at fresh state, hardened state, and durability to find the optimum content of each raw material. Subsequently, the novel mix design formulation was completed. The main challenge for this study is the lack of literature review on one-part AAMs mortar for engineering application. Thus, three experiments were conducted, published in an academic journal, then presented in manuscript 1,2 and 3 of this report and concluded as follow:

Manuscript 1: The compositions of precursors, alkali activators, admixtures, aggregate and water were characterized based on compressive strength as a benchmark of one-part AAMs mortar performance. OPC and CaO compensated a low dosage of alkali activators as sources of alkali to activate the precursors via the geopolymerization process. An excessive amount of aggregate has caused the mortar to collapse early due to insufficient hydration gel products to wrap the aggregate

surface bonded with other particles. Too low water content has caused mortar to crack, brittle and fail because there is insufficient water to initiate the geopolymerization. The mix design composition was determined and subsequently tested for other mechanical performances and confirmed the mortar complied with class R3, EN1504-3 standard. The addition of admixtures assists in stabilizing the physical structure of the mortar both at the early and later stages of curing age.

Manuscript 2: Based on the mix composition formulation in Manuscript 1, the mix design of mortar reformulated by adjusting admixtures and water content to get a practical setting time for real hand patching repair application, increasing compressive strength and study its bonding strength via pull-off test for concrete patch mortar application. Adding admixtures and a low water-to-binder ratio have improved the workability of the mortar, improved the compressive strength over time and provided a better chemical bonding at the interface zone between repair material and substrate. The optimum admixture volume was determined, and the mix design composition's stability was further examined. The pull-off bond strength achieved class R4-EN1504-3 standard, yet the mechanical strength performance was still at class R3 level. The main shortfall of one-part AAMs in pull-off bonding performance (delamination) was overcome. In addition, superplasticizer (SP) admixtures work efficiently under low alkaline environments and improve fresh mortar workability at a low w/b ratio.

Manuscript 3: To improve the compressive strength of one-part AAMs mortar, the water-to-binder w/b ratio was adjusted, and its effect on pore structure and microstructure was analyzed in detail. The optimum w/b ratio ensures no excessive evaporation that affects the engineering properties of mortar, subsequently recording low porosity levels and denser microstructure. Adding shrinkage-reducing admixtures (SRA) and calcium oxide (CaO) powder has controlled both autogenous and drying mortar shrinkage at the early hardening and later stages, thus reducing the shrinkage level. As a result, the compressive strength and pull-off bond strength (drying shrinkage measurement) have exceeded the minimum requirement of Class R4, EN1504-3 and completed the novel mix design formulation of one-part AAMs mortar as structural concrete

repair materials. The 30% inclusion of aluminosilicate precursor as a cementitious binder successfully cut down the OPC volume, lesser clinker production, and reduced CO<sub>2</sub> emissions. A low dosage of potassium carbonate activator used instead of conventional sodium silicate and hydroxide activator has significantly cheaper cost, lowering CO<sub>2</sub> emissions and safer (lower corrosivity) besides less energy consumption in production. The microstructural study also confirms the inclusion of OPC, a more stable gels chain product of C-S-H, exists to support N-A-S-H and C-A-S-H cross-link, which were created in binding phases. Finally, the objective and aim of this study in Manuscript 3 were successfully fulfilled.

Future studies must focus on how to reduce and replace the OPC content. For this regard, the mix design may be reformulated with a higher dosage of alkali activator concentration and to include silica fume as additional aluminosilicate precursors to increase geopolymerization activities and quartz sand as a replacement for natural sand to improve the pore structure of cementitious repair materials. Investigation on freeze-thaw, chloride and carbonation mitigation, acid and sulphate attacks must be carried out to guarantee its durability for long-term applications. Geopolymer concrete or AAMs can also be tested with zero-OPC technology to produce binders for more concrete applications in the construction industry to reduce dependency on OPC. Therefore, a new mixed design formulation can be proposed to suit local weather to ensure a longer lifespan and less maintenance cost. The system can be practically applied for precast concrete production, which uses batching plants to mix and supply the concrete. Hence, the batch plant system does not need to be replaced with a new engineering system, saving more cost. Additional attention must be paid to designing water and aggregate ratios when a lack of calcium due to the absence of OPC may affect the hydration gel of AAM's cement binder.

## References

- [1] R. Robayo-Salazar, C. Jesús, R. Mejía de Gutiérrez, and F. Pacheco-Torgal, “Alkali-activated binary mortar based on natural volcanic pozzolan for repair applications,” *J. Build. Eng.*, vol. 25, no. April, p. 100785, 2019, doi: 10.1016/j.job.2019.100785.
- [2] J. Wang, T. Huang, G. Cheng, Z. Liu, S. Li, and D. Wang, “Effects of fly ash on the properties and microstructure of alkali-activated FA/BFS repairing mortar,” *Fuel*, vol. 256, no. July, p. 115919, 2019, doi: 10.1016/j.fuel.2019.115919.
- [3] I. Pol Segura, N. Ranjbar, A. Juul Damø, L. Skaarup Jensen, M. Canut, and P. Arendt Jensen, “A review: Alkali-activated cement and concrete production technologies available in the industry,” *Heliyon*, vol. 9, no. 5, 2023, doi: 10.1016/j.heliyon.2023.e15718.
- [4] I. Ramón-Álvarez, C. Marugán-Cruz, E. Enríquez, S. Sánchez-Delgado, and M. Torres-Carrasco, “Alkali-activated and hybrid materials: Alternative to Portland cement as a storage media for solar thermal energy,” *Bol. la Soc. Esp. Ceram. y Vidr.*, vol. 62, no. 2, pp. 160–173, 2023, doi: 10.1016/j.bsecv.2021.11.006.
- [5] O. G. Teixeira, R. H. Geraldo, F. G. da Silva, J. P. Gonçalves, and G. Camarini, “Mortar type influence on mechanical performance of repaired reinforced concrete beams,” *Constr. Build. Mater.*, vol. 217, pp. 372–383, 2019, doi: 10.1016/j.conbuildmat.2019.05.035.
- [6] M. Nodehi and F. Aguayo, “Ultra high performance and high strength geopolymer concrete,” *J. Build. Pathol. Rehabil.*, vol. 6, no. 1, pp. 1–29, 2021, doi: 10.1007/s41024-021-00130-5.
- [7] D. V. Val and M. G. Stewart, “Reliability assessment of ageing reinforced concrete structures - current situation and future challenges,” *Struct. Eng. Int. J. Int. Assoc. Bridg. Struct. Eng.*, vol. 19, no. 2, pp. 211–219, 2009, doi: 10.2749/101686609788220114.
- [8] T. de Larrard, E. Bastidas-Arteaga, F. Duprat, and F. Schoefs, “Effects of climate variations and global warming on the durability of RC structures subjected to

- carbonation,” *Civ. Eng. Environ. Syst.*, vol. 31, no. 2, pp. 153–164, 2014, doi: 10.1080/10286608.2014.913033.
- [9] A. S. E. Belaidi, B. Benabed, and H. Soualhi, “Physical and mechanical properties of concrete repair materials in dry and hot-dry environment,” *J. Adhes. Sci. Technol.*, vol. 29, no. 6, pp. 543–554, 2015, doi: 10.1080/01694243.2014.998001.
- [10] BASF, “European Standard EN 1504 A simplified, illustrated guide for all involved in concrete repair”.
- [11] M. Elzeadani, D. V. Bompa, and A. Y. Elghazouli, “One part alkali activated materials: A state-of-the-art review,” *J. Build. Eng.*, vol. 57, no. June, p. 104871, 2022, doi: 10.1016/j.jobbe.2022.104871.
- [12] Z. Abdollahnejad, S. Miraldo, F. Pacheco-Torgal, and J. B. Aguiar, “Cost-efficient one-part alkali-activated mortars with low global warming potential for floor heating systems applications,” *Eur. J. Environ. Civ. Eng.*, vol. 21, no. 4, pp. 412–429, 2017, doi: 10.1080/19648189.2015.1125392.
- [13] G. Xu and X. Shi, “Characteristics and applications of fly ash as a sustainable construction material: A state-of-the-art review,” *Resour. Conserv. Recycl.*, vol. 136, no. August 2017, pp. 95–109, 2018, doi: 10.1016/j.resconrec.2018.04.010.
- [14] I. Faridmehr, M. A. Sahraei, M. L. Nehdi, and K. A. Valerievich, “Optimization of Fly Ash—Slag One-Part Geopolymers with Improved Properties,” *Materials (Basel)*, vol. 16, no. 6, 2023, doi: 10.3390/ma16062348.
- [15] W. Teo, K. Shirai, J. H. Lim, and L. B. Jack, “Experimental Investigation on Ambient-Cured One-Part Alkali-Activated Binders Using Combined High-Calcium Fly Ash (HCFA) and Ground Granulated Blast Furnace Slag (GGBS),” 2022.
- [16] A. T. Almalkawi, S. Hamadna, and P. Soroushian, “One-part alkali activated cement based volcanic pumice,” *Constr. Build. Mater.*, vol. 152, pp. 367–374, 2017, doi: 10.1016/j.conbuildmat.2017.06.139.
- [17] Z. G. Ralli and S. J. Pantazopoulou, “State of the art on geopolymer concrete,” *Int. J. Struct. Integr.*, vol. 12, no. 4, pp. 511–533, 2020, doi: 10.1108/IJSI-05-2020-0050.
- [18] H. Choo, S. Lim, W. Lee, and C. Lee, “Compressive strength of one-part alkali activated

- fly ash using red mud as alkali supplier,” *Constr. Build. Mater.*, vol. 125, pp. 21–28, 2016, doi: 10.1016/j.conbuildmat.2016.08.015.
- [19] K. L. Aughenbaugh, P. Stutzman, and M. C. G. Juenger, “Identifying glass compositions in fly ash,” *Front. Mater.*, vol. 3, no. January, 2016, doi: 10.3389/fmats.2016.00001.
- [20] Y. C. Ding, T. W. Cheng, and Y. S. Dai, “Application of geopolymers for concrete repair,” *Struct. Concr.*, vol. 18, no. 4, pp. 561–570, 2017, doi: 10.1002/suco.201600161.
- [21] P. Chindaprasirt and T. Cao, *Setting, segregation and bleeding of alkali-activated cement, mortar and concrete binders*, no. 2012. Woodhead Publishing Limited, 2015. doi: 10.1533/9781782422884.2.113.
- [22] R. H. Geraldo, O. G. Teixeira, S. R. C. Matos, F. G. S. Silva, J. P. Gonçalves, and G. Camarini, “Study of alkali-activated mortar used as conventional repair in reinforced concrete,” *Constr. Build. Mater.*, vol. 165, pp. 914–919, 2018, doi: 10.1016/j.conbuildmat.2018.01.063.
- [23] S. Kramar, A. Šajna, and V. Ducman, “Assessment of alkali activated mortars based on different precursors with regard to their suitability for concrete repair,” *Constr. Build. Mater.*, vol. 124, pp. 937–944, 2016, doi: 10.1016/j.conbuildmat.2016.08.018.
- [24] T. Phoo-ngernkham *et al.*, “Low cost and sustainable repair material made from alkali-activated high-calcium fly ash with calcium carbide residue,” *Constr. Build. Mater.*, vol. 247, p. 118543, 2020, doi: 10.1016/j.conbuildmat.2020.118543.
- [25] T. Phoo-Ngernkham, S. Hanjitsuwan, L. Y. Li, N. Damrongwiriyanupap, and P. Chindaprasirt, “Adhesion characterisation of Portland cement concrete and alkali-activated binders,” *Adv. Cem. Res.*, vol. 31, no. 2, pp. 69–79, 2019, doi: 10.1680/jadcr.17.00122.
- [26] G. F. Huseien and K. W. Shah, “Performance evaluation of alkali-activated mortars containing industrial wastes as surface repair materials,” *J. Build. Eng.*, vol. 30, no. January, p. 101234, 2020, doi: 10.1016/j.jobbe.2020.101234.
- [27] E. Gomaa, A. Ghani, and M. A. ElGawady, “Repair of ordinary Portland cement concrete using ambient-cured alkali-activated concrete: Interfacial behavior,” *Cem. Concr. Res.*, vol. 129, no. December 2019, p. 105968, 2020, doi: 10.1016/j.cemconres.2019.105968.

- [28] S. Yousefi Oderji, B. Chen, M. R. Ahmad, and S. F. A. Shah, “Fresh and hardened properties of one-part fly ash-based geopolymer binders cured at room temperature: Effect of slag and alkali activators,” *J. Clean. Prod.*, vol. 225, pp. 1–10, 2019, doi: 10.1016/j.jclepro.2019.03.290.
- [29] A. Galvão Souza Azevedo and K. Strecker, “Kaolin, fly-ash and ceramic waste based alkali-activated materials production by the ‘one-part’ method,” *Constr. Build. Mater.*, vol. 269, no. xxxx, 2021, doi: 10.1016/j.conbuildmat.2020.121306.
- [30] M. Askarian, Z. Tao, B. Samali, G. Adam, and R. Shuaibu, “Mix composition and characterisation of one-part geopolymers with different activators,” *Constr. Build. Mater.*, vol. 225, pp. 526–537, 2019, doi: 10.1016/j.conbuildmat.2019.07.083.
- [31] Y. Alrefaei, Y. S. Wang, and J. G. Dai, “The effectiveness of different superplasticizers in ambient cured one-part alkali activated pastes,” *Cem. Concr. Compos.*, vol. 97, no. September 2018, pp. 166–174, 2019, doi: 10.1016/j.cemconcomp.2018.12.027.
- [32] S. Narimani Zamanabadi, S. A. Zareei, P. Shoaeei, and F. Ameri, “Ambient-cured alkali-activated slag paste incorporating micro-silica as repair material: Effects of alkali activator solution on physical and mechanical properties,” *Constr. Build. Mater.*, vol. 229, p. 116911, 2019, doi: 10.1016/j.conbuildmat.2019.116911.
- [33] V. A. Nunes, P. H. R. Borges, and C. Zanotti, “Mechanical compatibility and adhesion between alkali-activated repair mortars and Portland cement concrete substrate,” *Constr. Build. Mater.*, vol. 215, pp. 569–581, 2019, doi: 10.1016/j.conbuildmat.2019.04.189.
- [34] W. Chen, R. Peng, C. Straub, and B. Yuan, “Promoting the performance of one-part alkali-activated slag using fine lead-zinc mine tailings,” *Constr. Build. Mater.*, vol. 236, p. 117745, 2020, doi: 10.1016/j.conbuildmat.2019.117745.
- [35] Z. L. c Kangting Yin a, Yaqing Jiang a,\* , Hui He a, Jie Ren b, “Characterization of one-part alkali-activated slag with rice straw ash,” *Constr. Build. Mater.*, vol. 345, no. July 2022, p. 128403, 2022, doi: 10.1016/j.conbuildmat.2022.127328.
- [36] J. Ren *et al.*, “Experimental comparisons between one-part and normal (two-part) alkali-activated slag binders,” *Constr. Build. Mater.*, vol. 309, no. September, p. 125177, 2021, doi: 10.1016/j.conbuildmat.2021.125177.

- [37] B. Alsubari, P. Shafigh, M. Z. Jumaat, and U. J. Alengaram, "Palm Oil Fuel Ash as a Partial Cement Replacement for Producing Durable Self-consolidating High-Strength Concrete," *Arab. J. Sci. Eng.*, vol. 39, no. 12, pp. 8507–8516, 2014, doi: 10.1007/s13369-014-1381-3.
- [38] M. Askarian, Z. Tao, G. Adam, and B. Samali, "Mechanical properties of ambient cured one-part hybrid OPC-geopolymer concrete," *Constr. Build. Mater.*, vol. 186, pp. 330–337, 2018, doi: 10.1016/j.conbuildmat.2018.07.160.
- [39] L. Coppola, D. Coffetti, E. Crotti, G. Gazzaniga, and T. Pastore, "The durability of one-part alkali-activated slag-based mortars in different environments," *Sustain.*, vol. 12, no. 9, 2020, doi: 10.3390/SU12093561.
- [40] P. Nath and P. K. Sarker, "Use of OPC to improve setting and early strength properties of low calcium fly ash geopolymer concrete cured at room temperature," *Cem. Concr. Compos.*, vol. 55, pp. 205–214, 2015, doi: 10.1016/j.cemconcomp.2014.08.008.
- [41] T. Suwan and M. Fan, "Influence of OPC replacement and manufacturing procedures on the properties of self-cured geopolymer," *Constr. Build. Mater.*, vol. 73, pp. 551–561, 2014, doi: 10.1016/j.conbuildmat.2014.09.065.
- [42] M. H. Samarakoon, P. G. Ranjith, W. H. Duan, and V. R. S. De Silva, "Properties of one-part fly ash/slag-based binders activated by thermally-treated waste glass/NaOH blends: A comparative study," *Cem. Concr. Compos.*, vol. 112, no. December 2019, p. 103679, 2020, doi: 10.1016/j.cemconcomp.2020.103679.
- [43] Y. Alrefaei and J. G. Dai, "Effects of delayed addition of polycarboxylate ether on one-part alkali-activated fly ash/slag pastes: Adsorption, reaction kinetics, and rheology," *Constr. Build. Mater.*, vol. 323, no. December 2021, p. 126611, 2022, doi: 10.1016/j.conbuildmat.2022.126611.
- [44] E. Adesanya, K. Ohenoja, A. Di Maria, P. Kinnunen, and M. Illikainen, "Alternative alkali-activator from steel-making waste for one-part alkali-activated slag," *J. Clean. Prod.*, vol. 274, p. 123020, 2020, doi: 10.1016/j.jclepro.2020.123020.
- [45] J. C. Lao, L. Y. Xu, B. T. Huang, J. X. Zhu, M. Khan, and J. G. Dai, "Utilization of sodium carbonate activator in strain-hardening ultra-high-performance geopolymer concrete (SH-

- UHPGC),” *Front. Mater.*, vol. 10, no. February, pp. 1–12, 2023, doi: 10.3389/fmats.2023.1142237.
- [46] L. Xie and K. Liu, “Properties and Microstructure of Na<sub>2</sub> CO<sub>3</sub>-Activated Binders Modified with Ca(OH)<sub>2</sub> and Mg(OH)<sub>2</sub>,” *Materials (Basel)*, vol. 15, no. 5, 2022, doi: 10.3390/ma15051687.
- [47] L. Li, J. X. Lu, B. Zhang, and C. S. Poon, “Rheology behavior of one-part alkali activated slag/glass powder (AASG) pastes,” *Constr. Build. Mater.*, vol. 258, p. 120381, 2020, doi: 10.1016/j.conbuildmat.2020.120381.
- [48] H. A. Abdel-Gawwad, S. R. V. García, and H. S. Hassan, “Thermal activation of air cooled slag to create one-part alkali activated cement,” *Ceram. Int.*, vol. 44, no. 12, pp. 14935–14939, 2018, doi: 10.1016/j.ceramint.2018.05.089.
- [49] M. Nodehi, T. Ozbakkaloglu, A. Gholampour, T. Mohammed, and X. Shi, “The effect of curing regimes on physico-mechanical, microstructural and durability properties of alkali-activated materials: A review,” *Constr. Build. Mater.*, vol. 321, no. December 2021, p. 126335, 2022, doi: 10.1016/j.conbuildmat.2022.126335.
- [50] K. Yin *et al.*, “Effect of fine sand powder on the rheological properties of one-part alkali-activated slag semi-flexible pavement grouting materials,” *Constr. Build. Mater.*, vol. 14, no. December 2021, p. 125177, 2022, doi: 10.1016/j.jobe.2022.104263.
- [51] S. Haruna, B. S. Mohammed, M. M. A. Wahab, and M. S. Liew, “Effect of paste aggregate ratio and curing methods on the performance of one-part alkali-activated concrete,” *Constr. Build. Mater.*, vol. 261, p. 120024, 2020, doi: 10.1016/j.conbuildmat.2020.120024.
- [52] T. Luukkonen, Z. Abdollahnejad, J. Yliniemi, P. Kinnunen, and M. Illikainen, “One-part alkali-activated materials: A review,” *Cem. Concr. Res.*, vol. 103, no. October, pp. 21–34, 2018, doi: 10.1016/j.cemconres.2017.10.001.
- [53] N. Ye *et al.*, “Synthesis and strength optimization of one-part geopolymer based on red mud,” *Constr. Build. Mater.*, vol. 111, pp. 317–325, 2016, doi: 10.1016/j.conbuildmat.2016.02.099.
- [54] M. Gonçalves *et al.*, “Waste-based one-part alkali activated materials,” *Materials (Basel)*,

vol. 14, no. 11, pp. 1–17, 2021, doi: 10.3390/ma14112911.

- [55] M. Abdulkareem *et al.*, “Application of eco-friendly alternative activators in alkali-activated materials: A review,” *Constr. Build. Mater.*, vol. 286, no. 4, pp. 357–424, 2020, doi: 10.1016/j.jclepro.2020.125429.
- [56] S. Haruna, B. S. Mohammed, M. M. A. Wahab, M. U. Kankia, M. Amran, and A. M. Gora, “Long-term strength development of fly ash-based one-part alkali-activated binders,” *Materials (Basel)*, vol. 14, no. 15, pp. 1–14, 2021, doi: 10.3390/ma14154160.
- [57] Z. Abdollahnejad *et al.*, “Microstructural Analysis and Strength Development of One-Part Alkali-Activated Slag/Ceramic Binders Under Different Curing Regimes,” *Waste and Biomass Valorization*, vol. 11, no. 6, pp. 3081–3096, 2020, doi: 10.1007/s12649-019-00626-9.
- [58] M. H. Samarakoon, P. G. Ranjith, W. Hui Duan, A. Haque, and B. K. Chen, “Extensive use of waste glass in one-part alkali-activated materials: Towards sustainable construction practices,” *Waste Manag.*, vol. 130, pp. 1–11, 2021, doi: 10.1016/j.wasman.2021.04.060.
- [59] S. F. A. Shah, B. Chen, S. Y. Oderji, M. Aminul Haque, and M. R. Ahmad, “Comparative study on the effect of fiber type and content on the performance of one-part alkali-activated mortar,” *Constr. Build. Mater.*, vol. 243, p. 118221, 2020, doi: 10.1016/j.conbuildmat.2020.118221.
- [60] Z. Abdollahnejad, M. Mastali, M. Falah, K. M. Shaad, T. Luukkonen, and M. Illikainen, “Durability of the Reinforced One-Part Alkali-Activated Slag Mortars with Different Fibers,” *Waste and Biomass Valorization*, no. 0123456789, 2020, doi: 10.1007/s12649-020-00958-x.
- [61] Z. Abdollahnejad, M. Mastali, T. Luukkonen, P. Kinnunen, and M. Illikainen, “Fiber-reinforced one-part alkali-activated slag/ceramic binders,” *Ceram. Int.*, vol. 44, no. 8, pp. 8963–8976, 2018, doi: 10.1016/j.ceramint.2018.02.097.
- [62] T. Luukkonen, Z. Abdollahnejad, J. Yliniemi, P. Kinnunen, and M. Illikainen, “Comparison of alkali and silica sources in one-part alkali-activated blast furnace slag mortar,” *J. Clean. Prod.*, vol. 187, pp. 171–179, 2018, doi: 10.1016/j.jclepro.2018.03.202.
- [63] T. Yang *et al.*, “Effects of calcined dolomite addition on reaction kinetics of one-part

- sodium carbonate-activated slag cements,” *Constr. Build. Mater.*, vol. 211, pp. 329–336, 2019, doi: 10.1016/j.conbuildmat.2019.03.245.
- [64] M. Almakhadmeh and A. M. Soliman, “Effects of mixing water temperatures on properties of one-part alkali-activated slag paste,” *Constr. Build. Mater.*, vol. 266, p. 121030, 2021, doi: 10.1016/j.conbuildmat.2020.121030.
- [65] S. F. A. Shah, B. Chen, S. Y. Oderji, M. A. Haque, and M. R. Ahmad, “Improvement of early strength of fly ash-slag based one-part alkali activated mortar,” *Constr. Build. Mater.*, vol. 246, p. 118533, 2020, doi: 10.1016/j.conbuildmat.2020.118533.
- [66] C. Liu, X. Yao, and W. Zhang, “Controlling the setting times of one-part alkali-activated slag by using honeycomb ceramics as carrier of sodium silicate activator,” *Constr. Build. Mater.*, vol. 235, p. 117091, 2020, doi: 10.1016/j.conbuildmat.2019.117091.
- [67] G. Sadeghian, K. Behfarnia, and M. Teymouri, “Drying shrinkage of one-part alkali-activated slag concrete,” *J. Build. Eng.*, vol. 51, no. December 2021, p. 104263, 2022, doi: 10.1016/j.job.2022.104263.
- [68] H. A. Abdel-Gawwad, A. M. Rashad, and M. Heikal, “Sustainable utilization of pretreated concrete waste in the production of one-part alkali-activated cement,” *J. Clean. Prod.*, vol. 232, pp. 318–328, 2019, doi: 10.1016/j.jclepro.2019.05.356.
- [69] L. Coppola *et al.*, “The combined use of admixtures for shrinkage reduction in one-part alkali activated slag-based mortars and pastes,” *Constr. Build. Mater.*, vol. 248, p. 118682, 2020, doi: 10.1016/j.conbuildmat.2020.118682.
- [70] A. Alzaza, K. Ohenoja, and M. Illikainen, “One-part alkali-activated blast furnace slag for sustainable construction at subzero temperatures,” *Constr. Build. Mater.*, vol. 276, p. 122026, 2021, doi: 10.1016/j.conbuildmat.2020.122026.
- [71] T. Luukkonen, Z. Abdollahnejad, J. Yliniemi, P. Kinnunen, and M. Illikainen, “One-part alkali-activated materials: A review,” *Cem. Concr. Res.*, vol. 103, no. October 2017, pp. 21–34, 2018, doi: 10.1016/j.cemconres.2017.10.001.
- [72] T. Luukkonen, Z. Abdollahnejad, K. Ohenoja, P. Kinnunen, and M. Illikainen, “Suitability of commercial superplasticizers for one-part alkali-activated blast-furnace slag mortar,” *J. Sustain. Cem. Mater.*, vol. 8, no. 4, pp. 244–257, 2019, doi:

10.1080/21650373.2019.1625827.

- [73] N. You, Y. Liu, D. Gu, T. Ozbakkaloglu, J. Pan, and Y. Zhang, "Rheology, shrinkage and pore structure of alkali-activated slag-fly ash mortar incorporating copper slag as fine aggregate," *Constr. Build. Mater.*, vol. 242, p. 118029, 2020, doi: 10.1016/j.conbuildmat.2020.118029.
- [74] S. Y. Oderji, B. Chen, C. Shakya, M. R. Ahmad, and S. F. A. Shah, "Influence of superplasticizers and retarders on the workability and strength of one-part alkali-activated fly ash/slag binders cured at room temperature," *Constr. Build. Mater.*, vol. 229, p. 116891, 2019, doi: 10.1016/j.conbuildmat.2019.116891.
- [75] P. Perumal *et al.*, "High strength one-part alkali-activated slag blends designed by particle packing optimization," *Constr. Build. Mater.*, vol. 299, p. 124004, 2021, doi: 10.1016/j.conbuildmat.2021.124004.
- [76] W. Lv, Z. Sun, and Z. Su, "Study of seawater mixed one-part alkali activated GGBFS-fly ash," *Cem. Concr. Compos.*, vol. 106, no. June 2019, p. 103484, 2020, doi: 10.1016/j.cemconcomp.2019.103484.
- [77] A. Kadhim, M. Sadique, R. Al-Mufti, and K. Hashim, "Long-term performance of novel high-calcium one-part alkali-activated cement developed from thermally activated lime kiln dust," *J. Build. Eng.*, vol. 32, no. December 2019, p. 101766, 2020, doi: 10.1016/j.job.2020.101766.
- [78] T. Wei, H. Zhao, and C. Ma, "A comparison of water curing and standard curing on one-part alkali-activated fly ash sinking beads and slag: Properties, microstructure and mechanisms," *Constr. Build. Mater.*, no. xxxx, p. 121715, 2020, doi: 10.1016/j.conbuildmat.2020.121715.
- [79] Z. Abdollahnejad, M. Mastali, B. Woof, and M. Illikainen, "High strength fiber reinforced one-part alkali activated slag/fly ash binders with ceramic aggregates: Microscopic analysis, mechanical properties, drying shrinkage, and freeze-thaw resistance," *Constr. Build. Mater.*, vol. 241, p. 118129, 2020, doi: 10.1016/j.conbuildmat.2020.118129.
- [80] B. Yang and J. G. Jang, "Environmentally benign production of one-part alkali-activated slag with calcined oyster shell as an activator," *Constr. Build. Mater.*, vol. 257, p. 119552,

2020, doi: 10.1016/j.conbuildmat.2020.119552.

- [81] M. X. Peng *et al.*, “Alkali fusion of bentonite to synthesize one-part geopolymers cured at elevated temperature by comparison with two-part ones,” *Constr. Build. Mater.*, vol. 130, pp. 103–112, 2017, doi: 10.1016/j.conbuildmat.2016.11.010.
- [82] A. Adnan, M. Suhatri, and I. M. Taib, “The Mechanical Properties of High Strength Concrete for Box Girder Bridge Deck in Malaysia,” vol. 1, no. March 2010, pp. 35–44, 2012.
- [83] G. O. Carneiro, H. A. Santana, D. V. Ribeiro, M. S. Cilla, and C. M. R. Dias, “One-part alkali-activated binder produced from inertized asbestos cement waste,” *J. Clean. Prod.*, vol. 367, no. June, p. 132966, 2022, doi: 10.1016/j.jclepro.2022.132966.
- [84] S. A. Bernal and J. L. Provis, “Durability of alkali-activated materials: Progress and perspectives,” *J. Am. Ceram. Soc.*, vol. 97, no. 4, pp. 997–1008, 2014, doi: 10.1111/jace.12831.
- [85] Z. Shi, C. Shi, S. Wan, and Z. Zhang, “Effects of alkali dosage and silicate modulus on alkali-silica reaction in alkali-activated slag mortars,” *Cem. Concr. Res.*, vol. 111, no. June, pp. 104–115, 2018, doi: 10.1016/j.cemconres.2018.06.005.
- [86] P. K. M. Paulo and J. M. Monteiro, *Microstructures, Properties and Materials*, Third Edit. London: McGraw-Hill 2016. doi: 10.1036/0071462899\.
- [87] F. Pacheco-Torgal, Z. Abdollahnejad, A. F. Camões, M. Jamshidi, and Y. Ding, “Durability of alkali-activated binders: A clear advantage over Portland cement or an unproven issue?,” *Constr. Build. Mater.*, vol. 30, pp. 400–405, 2012, doi: 10.1016/j.conbuildmat.2011.12.017.
- [88] A. Kadhim, M. Sadique, R. Al-Mufti, and K. Hashim, “Developing one-part alkali-activated metakaolin/natural pozzolan binders using lime waste,” *Adv. Cem. Res.*, vol. 33, no. 8, pp. 342–356, 2021, doi: 10.1680/jadcr.19.00118.
- [89] X. Ke, S. A. Bernal, N. Ye, J. L. Provis, and J. Yang, “One-part geopolymers based on thermally treated red Mud/NaOH blends,” *J. Am. Ceram. Soc.*, vol. 98, no. 1, pp. 5–11, 2015, doi: 10.1111/jace.13231.
- [90] A. Alzaza, K. Ohenoja, and M. Illikainen, “Enhancing the mechanical and durability

- properties of subzero-cured one-part alkali-activated blast furnace slag mortar by using submicron metallurgical residue as an additive,” *Cem. Concr. Compos.*, vol. 122, no. February, p. 104128, 2021, doi: 10.1016/j.cemconcomp.2021.104128.
- [91] M. Liu, H. Wu, P. Yao, C. Wang, and Z. Ma, “Microstructure and macro properties of sustainable alkali-activated fly ash mortar with various construction waste fines as binder replacement up to 100%,” *Cem. Concr. Compos.*, vol. 134, no. June, p. 104733, 2022, doi: 10.1016/j.cemconcomp.2022.104733.
- [92] M. Liu, C. Wang, H. Wu, D. Yang, and Z. Ma, “Reusing recycled powder as eco-friendly binder for sustainable GGBS-based geopolymer considering the effects of recycled powder type and replacement rate,” *J. Clean. Prod.*, vol. 364, no. June, p. 132656, 2022, doi: 10.1016/j.jclepro.2022.132656.
- [93] I. L. Tchegnina Ngassam, P. Arito, and H. Beushausen, “A new approach for the mix design of (patch) repair mortars,” *African J. Sci. Technol. Innov. Dev.*, vol. 10, no. 3, pp. 259–265, 2018, doi: 10.1080/20421338.2018.1452845.
- [94] G. Fahim Huseien, J. Mirza, M. Ismail, S. K. Ghoshal, and A. Abdulameer Hussein, “Geopolymer mortars as sustainable repair material: A comprehensive review,” *Renew. Sustain. Energy Rev.*, vol. 80, no. May, pp. 54–74, 2017, doi: 10.1016/j.rser.2017.05.076.
- [95] M. N. Qureshi and S. Ghosh, “Effect of Si/Al ratio on engineering properties of alkali-activated GGBS pastes,” *Green Mater.*, vol. 2, no. 3, pp. 123–131, 2014, doi: 10.1680/gmat.14.00001.
- [96] S. Panda, P. Sarkar, and R. Davis, “Effect of Water-Cement Ratio on Mix Design and Mechanical Strength of Copper Slag Aggregate Concrete,” *IOP Conf. Ser. Mater. Sci. Eng.*, vol. 936, no. 1, 2020, doi: 10.1088/1757-899X/936/1/012019.
- [97] S. Thokchom, K. K. Mandal, and S. Ghosh, “Effect of Si/Al Ratio on Performance of Fly Ash Geopolymers at Elevated Temperature,” *Arab. J. Sci. Eng.*, vol. 37, no. 4, pp. 977–989, 2012, doi: 10.1007/s13369-012-0230-5.
- [98] C. K. Lau, M. R. Rowles, G. N. Parnham, T. Htut, and T. S. Ng, “Investigation of geopolymers containing fly ash and ground-granulated blast-furnace slag blended by amorphous ratios,” *Constr. Build. Mater.*, vol. 222, pp. 731–737, 2019, doi:

10.1016/j.conbuildmat.2019.06.198.

- [99] Y. Wang *et al.*, “Effects of Si/Al ratio on the efflorescence and properties of fly ash based geopolymer,” *J. Clean. Prod.*, vol. 244, p. 118852, 2020, doi: 10.1016/j.jclepro.2019.118852.
- [100] L. Coppola, D. Coffetti, and E. Crotti, “Pre-packed alkali activated cement-free mortars for repair of existing masonry buildings and concrete structures,” *Constr. Build. Mater.*, vol. 173, pp. 111–117, 2018, doi: 10.1016/j.conbuildmat.2018.04.034.
- [101] A. Z. Warid Wazien, M. M. Al Bakri Abdullah, R. Abd Razak, M. A. Z. Mohd Remy Rozainy, M. F. Mohd Tahir, and K. Hussin, “Potential of geopolymer mortar as concrete repairing materials,” *Mater. Sci. Forum*, vol. 857, pp. 382–387, 2016, doi: 10.4028/www.scientific.net/MSF.857.382.
- [102] G. F. Huseien *et al.*, “Performance of sustainable alkali activated mortars containing solid waste ceramic powder,” *Chem. Eng. Trans.*, vol. 63, no. 2010, pp. 673–678, 2018, doi: 10.3303/CET1863113.
- [103] L. Coppola, D. Coffetti, E. Crotti, A. Marini, C. Passoni, and T. Pastore, “Lightweight cement-free alkali-activated slag plaster for the structural retrofit and energy upgrading of poor quality masonry walls,” *Cem. Concr. Compos.*, vol. 104, no. May, 2019, doi: 10.1016/j.cemconcomp.2019.103341.
- [104] P. Sturm, G. J. G. Gluth, C. Jäger, H. J. H. Brouwers, and H. C. Kühne, “Sulfuric acid resistance of one-part alkali-activated mortars,” *Cem. Concr. Res.*, vol. 109, no. February, pp. 54–63, 2018, doi: 10.1016/j.cemconres.2018.04.009.
- [105] F. Pacheco-Torgal, R. E. Melchers, X. Shi, N. De Belie, K. Van Tittelboom, and A. Sa´ez, *Front-matter*. 2018. doi: 10.1016/b978-0-08-102181-1.00026-5.
- [106] Z. Luo, W. Li, K. Wang, A. Castel, and S. P. Shah, “Comparison on the properties of ITZs in fly ash-based geopolymer and Portland cement concretes with equivalent flowability,” *Cem. Concr. Res.*, vol. 143, no. February, p. 106392, 2021, doi: 10.1016/j.cemconres.2021.106392.
- [107] L. Jia, F. Zhao, K. Yao, and H. Du, “Bond performance of repair mortar made with magnesium phosphate cement and ferroaluminate cement,” *Constr. Build. Mater.*, vol.

279, p. 122398, 2021, doi: 10.1016/j.conbuildmat.2021.122398.

- [108] H. Y. Zhang, V. Kodur, B. Wu, L. Cao, and F. Wang, “Thermal behavior and mechanical properties of geopolymer mortar after exposure to elevated temperatures,” *Constr. Build. Mater.*, vol. 109, pp. 17–24, 2016, doi: 10.1016/j.conbuildmat.2016.01.043.
- [109] F. Pacheco-Torgal, Z. Abdollahnejad, S. Miraldo, S. Baklouti, and Y. Ding, “An overview on the potential of geopolymers for concrete infrastructure rehabilitation,” *Constr. Build. Mater.*, vol. 36, pp. 1053–1058, 2012, doi: 10.1016/j.conbuildmat.2012.07.003.
- [110] H. A. Khan, M. S. H. Khan, A. Castel, and J. Sunarho, “Deterioration of alkali-activated mortars exposed to natural aggressive sewer environment,” *Constr. Build. Mater.*, vol. 186, pp. 577–597, 2018, doi: 10.1016/j.conbuildmat.2018.07.137.
- [111] E. Hany, N. Fouad, M. Abdel-Wahab, and E. Sadek, “Compressive strength of mortars incorporating alkali-activated materials as partial or full replacement of cement,” *Constr. Build. Mater.*, vol. 261, p. 120518, 2020, doi: 10.1016/j.conbuildmat.2020.120518.
- [112] E. Yusslee and S. Beskhyroun, “The potential of one-part alkali-activated materials (AAMs) as a concrete patch mortar,” *Sci. Rep.*, vol. 12, no. 1, p. 15902, 2022, doi: 10.1038/s41598-022-19830-0.
- [113] A. Mobili, F. Tittarelli, and H. Rahier, “One-part alkali-activated pastes and mortars prepared with metakaolin and biomass ash,” *Appl. Sci.*, vol. 10, no. 16, 2020, doi: 10.3390/app10165610.
- [114] S. Candamano, P. De Luca, P. Frontera, and F. Crea, “Production of geopolymeric mortars containing forest biomass ash as partial replacement of metakaolin,” *Environ. - MDPI*, vol. 4, no. 4, pp. 1–13, 2017, doi: 10.3390/environments4040074.
- [115] A. Palomo, O. Maltseva, I. Garcia-Lodeiro, and A. Fernández-Jiménez, “Portland Versus Alkaline Cement: Continuity or Clean Break: ‘A Key Decision for Global Sustainability,’” *Front. Chem.*, vol. 9, no. October, pp. 1–28, 2021, doi: 10.3389/fchem.2021.705475.
- [116] E. Yusslee and S. Beskhyroun, “Performance Evaluation of Hybrid One-Part Alkali Activated Materials ( AAMs ) for Concrete Structural Repair,” *Buildings*, vol. 12, no. 11, 2022, doi: <https://doi.org/10.3390/buildings12112025>.
- [117] E. Pereira, E. Br, A. Resende, M. H. F. De Medeiros, and L. C. Meneghetti, “Chloride

accelerated test: influence of silica fume, water/binder ratio and concrete cover thickness  
Ensaio acelerado por cloretos: efeito da sílica ativa, relação água/aglomerante e espessura  
de cobrimento do concreto Chloride accelerated test: influence,” *IBRACON Struct. Mater.*  
*J.* • 2013 •, vol. 6, no. 4, p. 4, 2013.

## Glossary

a/b	activator-to-binder ratio
AAMs	Alkali-activated materials (AAMs)
AEA	air-entraining admixture
$Al_2O_3$	Aluminium oxide
ASTM	American Standard Testing Method
b	breadth
b/a	binder-to-aggregate
BFS	Blast furnace slag
BS	British Standards
Ca	Calcium
$Ca(OH)_2$	Calcium hydroxide
$CaCl_2$	Calcium chloride
CaO	Calcium Oxide
C-A-S-H	Calcium Alumino-Silicate Hydrate
CCRA	Climate Change Response Act
CCR	Calcium carbide residue
CD	calcined dolomite
CH	calcium hydroxide
cm	centimeter
$CO_2$	Carbon Dioxide
COS	Calcined Oyster Shell powder
C-S-H	Calcium Silicate Hydrate
CW	Coal Waste
d	depth
$D_1$	stress of longitudinal strain
$D_2$	compressive stress

DA	Dry Activator
DeS-dust	Desulphurization Dust
E <sub>2</sub>	longitudinal strain
EA	calcium oxide-based expansive agent
EA <sub>2</sub>	lateral strain
EDS	Energy Dispersive X-ray spectrometer
EN	European testing Standard
FA	Fly Ash
FA/GGBFS	Fly Ash/ Ground Granulated Blast Furnace Slag
FASB	ultra-fine fly ash sinking beads
Fe	Ferum
Fe <sub>2</sub> O <sub>3</sub>	ferric oxide
g/mL	Gram per miliLitre
GGBFS	Ground Granulated Blast Furnace Slag / slag
GGBFS/MK	Ground Granulated Blast Furnace Slag/ Metakaolin
GGBFS/OPC	Ground Granulated Blast Furnace Slag/ Ordinary Portland Cement
GP	glass powder
GPa	Giga Pascal
h	hour
HCC	honeycomb ceramic
IBZ	interfacial bonding zone
ITZ	interfacial transition zone
J/g	Joule/gram
K <sub>2</sub> CO <sub>3</sub>	Potassium Carbonate
K <sub>2</sub> O	Potassium oxide
K <sub>2</sub> SiO <sub>3</sub>	potassium silicate
kg/m <sup>3</sup>	density

KOH	potassium hydroxide
kN/s	kiloNewton per second
L	Length
LDA	Laser Diffraction Analysis
LiOH	Lithium hydroxide
LKD	Lime Kiln Dust
LOP	Limit Of Proportionality
LS	Sodium Lignosulfonate
MC	Methylcellulose
Mg	Magnesium
MgO	Magnesium oxide
MIP	Mercury Intrusion Porosimetry
MK	Metakaolin
mm	millimeter
min	minutes
m <sup>2</sup> /g	meter square per gram
MOE	Modulus of elasticity
MOR	Modulus of rupture
Mpa	Mega Pascal
MPa/s	Mega Pascal per second
MS	Micro Silica
MSt	Modified Starch
N	Newton
N/mm <sup>2</sup>	Newton per millimeter
N/mm <sup>2</sup> /s	Newton per millimeter per second
N/s	Newton per second
Na/Al	Sodium/aluminium
Na <sub>2</sub> CO <sub>3</sub>	Sodium carbonate

Na <sub>2</sub> O	Sodium oxide
Na <sub>2</sub> O/SiO <sub>2</sub>	Sodium oxide/silicon dioxide
Na <sub>2</sub> SiO <sub>3</sub>	Sodium Silicate or Anhydrous sodium metasilicate
Na <sub>2</sub> SiO <sub>3</sub> .5H <sub>2</sub> O or Na <sub>2</sub> SiO <sub>3</sub> .9H <sub>2</sub> O	Sodium metasilicate pentahydrate
Na <sub>2</sub> SO <sub>3</sub>	Sodium silicate anhydrous
NaOH	Sodium Hydroxide
NaOH/NS	Hydroxide/silicate solution
N-A-S-H or K-A-S-H	Sodium aluminosilicate hydrate
NHNS	Sodium silicate/sodium hydroxide
nm	nanometer
NP	Natural Pozzolan
OPC	Ordinary Portland Cement
P	Load
p/a	paste/aggregate
PCE	methacrylic acid monomer
PCEs	Polycarboxylate Ether
PVA	Polyvinyl Alcohol Fibre
RC	Reinforced concrete
RH	Relative Humidity
RM <sub>s</sub>	conventional repair materials
RSA	Rice Straw Ash
s/b	sand-to-binder
SCM	Supplementary Cementitious Materials
SEM	Scanning Electron Microscopy
SF	Silica Fume
SFA	Super-fine Fly Ash
SH	Sodium Hydroxide

Si/Al	silicon/aluminium
SiO <sub>2</sub>	silicon dioxide
SiO <sub>2</sub> /Al <sub>2</sub> O <sub>3</sub>	silicon dioxide/ Aluminium oxide
SP	Superplasticizer
SRA	Shrinkage-reducing Admixture
STP	Sodium Triphosphate
UHPGC	Ultra-High Performance Geopolymer Concrete
w/b	water-to-binder
WG	waste glass
XRD	X-Ray Diffraction analysis
μm	Miu meter
μm/m	Miu meter per meter

## Appendices

1. Manuscript 1: Performance Evaluation of Hybrid One-Part Alkali Activated Materials (AAMs) For Concrete Structural Repair.

MDPI – Buildings (Publication) 18 September 2022

[doi.org/10.3390/buildings12112025](https://doi.org/10.3390/buildings12112025)

2. Manuscript 2: The Potential of one-part Alkali-Activated Materials (AAMs) as a concrete patch mortar.

Springer Nature - Scientific Reports (Publication) 23 September 2022

[doi.org/10.1038/s41598-022-19830-0](https://doi.org/10.1038/s41598-022-19830-0)



3. Manuscript 3: The Effect of Water-To-Binder Ratio (w/b) on Pore Structure of One-Part Alkali Activated Mortar

Cell Press – Heliyon (Publication) 14 January 2023

[doi.org/10.1016/j.heliyon.2023.e](https://doi.org/10.1016/j.heliyon.2023.e)

## Article

# Performance Evaluation of Hybrid One-Part Alkali Activated Materials (AAMs) for Concrete Structural Repair

Eddy Yusslee \* and Sherif Beskhyroun 

School of Future Environments, Auckland University of Technology, Auckland 1010, New Zealand

\* Correspondence: eddy.yusslee@aut.ac.nz

**Abstract:** Alkali-activated materials (AAMs) have been widely used as an alternative to Portland cement. This production of AAMs emits lesser carbon dioxide by utilizing industrial waste products to make this cement binder technology greener and more sustainable. The conventional two-part system comprises solid aluminosilicate precursors with an alkali solution to activate the AAMs. However, higher alkalinity of the liquid activator is required to complete the geopolymerization process, making the cementitious materials costly and sticky, and thus not convenient to handle on the construction site, affecting the worker's safety. A one-part AAMs system was introduced to overcome the two-part system's shortcomings. The alkali solution is now replaced with a solid alkali activator which is easier and more practical to apply at construction sites. This study was carried out to evaluate the mechanical performance of one-part alkali AAMs in the form of mortar by conducting compressive and flexural strength, modulus of elasticity, and tensile strength tests at 28 days of curing age under laboratory experiments in the tropical climate of Malaysia. A drying shrinkage test was also performed to detect its durability. Three types of solid admixtures were added to complete the composition of the novel mix design formulation. According to the results obtained, the mechanical strength of one-part alkali-activated mortar achieved the minimum requirement for Class R3 structural concrete repair materials as per EN1504-3 specifications. This eco-friendly cement binder has excellent potential for further engineering development, particularly to become a new concrete repair product in the future.

**Keywords:** fly ash (FA); ground granulated blast furnace slag (GGBFS); ordinary Portland cement (OPC); potassium carbonate; C-A-S-H



**Citation:** Yusslee, E.; Beskhyroun, S. Performance Evaluation of Hybrid One-Part Alkali Activated Materials (AAMs) for Concrete Structural Repair. *Buildings* **2022**, *12*, 2025.

<https://doi.org/10.3390/buildings12112025>

Academic Editors: Zhihai He, Kunjie Fan, Dong Zhang and Nanting Yu

Received: 25 October 2022

Accepted: 17 November 2022

Published: 18 November 2022

**Publisher's Note:** MDPI stays neutral with regard to jurisdictional claims in published maps and institutional affiliations.



**Copyright:** © 2022 by the authors. Licensee MDPI, Basel, Switzerland. This article is an open access article distributed under the terms and conditions of the Creative Commons Attribution (CC BY) license (<https://creativecommons.org/licenses/by/4.0/>).

## 1. Introduction

Alkali-activated materials (AAMs) have been widely used and regarded as a green technology mainly composed of industrial waste materials to reduce carbon dioxide (CO<sub>2</sub>) emissions in the atmosphere. This technology was developed to reduce construction dependency on ordinary Portland cement (OPC). The OPC contributes to CO<sub>2</sub> emissions due to higher energy consumption and heat released from the calcination process [1]. In addition, many countries face deteriorated concrete structures as the building life spans approach their limit. This situation contributes to the higher demand for cementitious material to repair, refurbish, as well as reconstruct the buildings.

Furthermore, to keep the aesthetic value and heritage landmark for some buildings, many architects prefer those buildings to be refurbished to preserve them. As a result, sustainable building products are becoming popular among architects and engineers to ensure building elements can resist the load and keep maintenance costs minimum. Thus, the AAMs have become a substitute for conventional Portland cement, which has higher mechanical strength and more extended durability [2]. The conventional AAMs are prepared by two components, aluminosilicate precursor and alkali solution, to create an amorphous three-dimensional structure via the geopolymerization process. Common aluminosilicate

precursors used are alkaline by-products such as fly ash (FA), ground granulated blast furnace slag (GGBFS) and metakaolin (M) as alternative binders to replace OPC and produce a sustainable low-carbon cement material. Fly ash is an aluminosilicate product, mostly spherical particles but solid spheres and fines too, which react with  $\text{Ca}(\text{OH})_2$  to form gel products [3]. GGBFS is obtained when the iron is manufactured. It is generated in the blast furnace and then slaked. Lower silica and  $\text{Na}_2\text{O}$  modulus in GGBFS benefit higher hydration products due to the heat released [4]. Both FA and GGBFS are presented in powder form and have fine particle sizes beneficial for mechanical strength development. AAMs composed of FA or metakaolin will produce sodium aluminosilicate hydrate or N-A-S-H gels as the main reaction product, while AAMs composed of slag create calcium aluminosilicate hydrate or C-A-S-H gels, essential for cementitious binder materials [5]. In addition, FA and GGBFS have a higher content of amorphous phases favorable to accelerating the reaction scale for creating hardened products [6].

In addition, sodium hydroxide and sodium silicate are alkaline solutions frequently used to activate the precursors and form a hardened matrix comparable to OPC in a two-part AAMs system [7]. On the contrary, the two-part AAMs concept has setbacks in handling, mixing, and transportation issues besides heat curing requirements to achieve the required strength, making this product unsuitable for in situ construction [8]. Researchers introduce the innovative method of one-part alkali-activated materials as complementary to the traditional two-part concept. Aluminosilicate precursors are mixed with solid alkali activators to form a dry mixture, and water is added to initiate the geopolymerization process [9]. This ‘just add water’ method has improved AAMs properties in terms of mechanical strength, porosity, durability, and fast application, and it is easier to use. Kadhim et al. [10] explained the function of the alkali activator to provide an alkali medium and raise the pH for the reaction of mixtures by assisting the dissolution process of aluminosilicate precursors in AAMs technology. Four main alkali groups are commonly used to generate the hardened binder of this solid precursor: alkali hydroxide, alkali silicates, alkali carbonates, and alkali sulfates [11]. Anhydrous sodium metasilicate ( $\text{Na}_2\text{SiO}_3$ ) is reported as the most suitable activator for the geopolymerization process but possesses a higher  $\text{SiO}_2/\text{Na}_2\text{O}$  ratio that makes it challenging to handle as such a corrosive chemical. For that reason, the lower  $\text{SiO}_2/\text{Na}_2\text{O}$  ratio of solid sodium carbonate is being studied as an alkali activator due to its low alkalinity level to provide safe and easy activator handling, compared to the sodium silicate activator or alkali hydroxide, which costs more and entails high  $\text{CO}_2$  emission. On the contrary, besides its corrosivity, the total cost of sodium hydroxide is almost 5–6 times higher than the calcium oxide type of alkali activator. Hence, it is crucial to minimize the usage of alkali activators in AAMs and make this technology safe, practical, and cheap.

However, the investigation found that the one-part AAMs still have a low or inconsistent compressive strength, flexure strength, and shrinkage cracking [8,12]. Numerous studies have been conducted to improve the compressive strength of one-part AAMs, but most studies are limited to only the synthesis and characterization stage. As a result, the application of one-part AAMs technology in the form of mortar for concrete structural repair has still lagged. The class F fly ash (FA) is a low reactive precursor that was combined with calcium-rich slag to expedite the system’s reactivity, subsequently abolishing the heat curing prerequisite, but it causes rapid hardening, which is not applicable for actual site application. A 15% slag reported was the optimum dosage of one-part AAMs mixed with 85% FA that improved the mechanical strength of one-part AAMs. Unfortunately, it was also activated with an 8% activator dosage that is still considered corrosive and costly [13]. Another study on one-part alkali-activated mortar composed of 40% GGBFS/60% FA and 10% anhydrous sodium metasilicate ( $\text{Na}_2\text{SiO}_3$ ) showed higher compressive strength up to 80 MPa but only managed to record 7 MPa of flexural strength, less than 10% of its compressive strength [14], affecting its ability to resist bending for concrete repair application. The flexural strength (11  $\text{N}/\text{mm}^2$ ) and modulus of elasticity (27 GPa) for mortar composed of 100% GGBFS were the highest compared to a single precursor of FA and

metakaolin. Nevertheless, slag mortar could not bond vertically and horizontally, making it not applicable to concrete repair materials in the study conducted by [15]. The splitting tensile strength of up to 3.5–11 MPa for one-part alkali-activated mortar with the inclusion of fibre can be achieved, yet a higher alkali-activated dosage of between 8% and 10% is required to achieve that standard strength [8,16].

Including the OPC in AAMs mixtures can improve and accelerate the reaction rate for strength development [17]. Moreover, this type of mixed or blended cement is cheap. OPC is a type of hydraulic cement composed of hydraulic calcium silicates. This cementitious material creates calcium silicate hydrate or C-S-H gels as the main hydration products used as binding agents responsible for the strength. The combination of by-product precursor with the OPC can be activated by non-hygroscopic alkali, which is beneficial in preventing the inclination for efflorescence, high permeability, and more severe water absorption problems. A 60% OPC added in one-part AAMs concrete recorded 55.0 N/mm<sup>2</sup> compressive strength at 28 days of age provides essential information in designing one-part AAMs in the form of mortar for patching concrete repair techniques. This concrete consists of coarse aggregate and has also been activated with a significantly higher 12% potassium carbonate [18].

Furthermore, the inclusion of 15% waste concrete fines was reported to improve the mechanical strength of AAMs. Still, excessive waste construction (concrete) fines adversely impact the mechanical strength due to slow hydration degree and insufficient high calcium content, reducing C-A-S-H gels [19]. In addition, the recycled concrete powder also increases porosity in two-part AAMs due to low polymerization activity, creating a more porous microstructure [20].

The larger shrinkage level of AAMs was also the primary concern in both two-part and one-part systems. Hence, the presence of shrinkage-reducing admixtures (SRA) and calcium oxide (CaO) could control the expansion of hardened AAMs [21]. Moreover, combining SRA and CaO can stabilize the shrinkage effect [22]. A higher concentration of alkali activator may assist the degree of hydration, but higher heat release creates more expressive shrinkage after drying [23]. Adding CaO, which can provide extra alkalinity and calcium sources for forming C-S-H gels from the cement binder, can reduce reliance on the alkali activator and increase the mechanical strength. This is in agreement with the fact that strength development is reduced when calcium content decreases [24]. Still, excessive contents of both SRA and expansive additive of CaO may cause other side effects, such as fast setting and losses of water or moisture, and thus be ineffective in reducing drying shrinkage level [25]. To control the fast setting problems, a lignosulfonate-based superplasticizer (SP) was used to regulate the setting time of high calcium one-part AAMs and avoid setting too quickly, which is essential for transporting fresh materials from batching plant to the site [26]. The previous study on the potential admixtures for one-part alkali-activated materials (AAMs) also suggested that by adding SP to the mixtures, the water content can be optimized to improve the compressive strength of the mortar [27].

Therefore, this experiment's objective is to evaluate the mechanical strength performance of one-part alkali-activated mortar composed of different dosages of aluminosilicate precursors and activated with low dosages of solid alkali activators for concrete structural repair applications. The main precursor source used in this study was composed of the industrial by-product of fly ash (FA) and ground granulated blast furnace slag (GGBFS) combined with ordinary Portland cement (OPC), unlike typical one-part AAMs which are commonly composed of by-products powder only. Potassium carbonate (K<sub>2</sub>CO<sub>3</sub>) is a single solid alkali activator used to activate the precursors and as the source of alkali besides the existing sodium and potassium element (Na<sub>2</sub>O and K<sub>2</sub>O) in the OPC itself. In addition, three powder admixtures were added and tested to stabilize the hardened material's physical properties. Furthermore, a test for drying shrinkage level for durability was also carried out. To the author's knowledge, no previous studies were conducted to evaluate the potential of one-part alkali-activated mortar composed of hybrid precursors

and activated with a low alkaline solid alkali activator used for concrete structural repair application as an alternative to the conventional two-part AAMs system.

This study aims to comply with the compressive strength requirement with Class R3–EN1504 standard for structural concrete repair materials. According to the EN1504 standard, for non-structural concrete repair materials Class R2, compressive strength must be above 15 N/mm<sup>2</sup>. For structural concrete repair, Class R3  $\geq$  25 N/mm<sup>2</sup> and  $\geq$ 45 N/mm<sup>2</sup> for Class R4 [28]. The novel mix design formulation reported in this study is vital for the author’s continued research on utilizing one-part AAMS technology for green and sustainable building products. The experiment was conducted in Kuala Lumpur, Malaysia, a country with a tropical climate which is hot and humid throughout the year.

## 2. Materials and Methods

Class F fly ash (FA) and ground granulated blast furnace slag (GGBFS) were used as precursors under ASTM C618 and ASTM C989, respectively. Ordinary Portland cement (OPC) was added as the primary binder source and activated with alkali-activated powder-potassium carbonate (K<sub>2</sub>CO<sub>3</sub> Purity  $\geq$  90%). The chemical compositions and physical properties of all main precursors are shown in Table 1. Natural sand was used as fine aggregate with a specific gravity of 2.67 and an average particle size of 90.23  $\mu$ m (D50). In addition, a commercial ethylene glycol type shrinkage-reducing admixture (SRA) and calcium oxide (CaO) were added as an admixture in the form of solid powder. At the same time, the sodium lignosulfonate powder-based superplasticizer (SP) was also used in the experiment as a retarder for the mortar samples.

**Table 1.** Chemical compositions (%) and physical properties of Fly Ash (FA), Ground Granulated Blast Furnace Slag (GGBFS) and ordinary Portland cement (OPC) were obtained from the manufacturer.

Chemical Compositions	FA (%)	GGBFS (%)	OPC (%)
SiO <sub>2</sub>	55.94	35.91	23.97
Al <sub>2</sub> O <sub>3</sub>	22.60	16.56	5.27
Fe <sub>2</sub> O <sub>3</sub>	8.10	1.52	3.28
CaO	6.26	35.28	60.12
P <sub>2</sub> O <sub>5</sub>	0.36	0.36	-
MgO	1.21	6.01	1.36
K <sub>2</sub> O	1.66	-	0.51
TiO <sub>2</sub>	0.72	0.59	0.06
SO <sub>3</sub>	1.02	0.36	2.20
Na <sub>2</sub> O	0.62	1.76	0.23
Cl	0.03	-	-
LOI	1.48	-	2.00
Physical Properties			
Specific Gravity	2.20	2.90	3.15
Average Particle Size (D50)	14.08 $\mu$ m	19.99 $\mu$ m	16.32 $\mu$ m

### 2.1. Mix Proportions

The experimental study was conducted to understand the effect of aluminosilicate precursors with different volume ratios, with OPC as the main binder and activated with a low percentage of alkali-activated powder. Besides that, three powder-type admixtures were added to all mixtures to investigate the effect of these admixtures compared to the samples prepared without admixtures. There were three stages of the experiment. All the samples were marked as Mix 1 to Mix 30 and consisted of FA, GGBFS, and with/without OPC as main precursors with different volume percentages. Stage 1, Mix 1, was chosen

as a control sample no.1, where the mixture contained only FA and GGBFS without OPC. For the second stage, Mix 10 was prepared as control sample no.2, which contained no admixtures. At the third stage, Mix 26 was chosen as control sample no.3 based on the findings on mechanical strength results for Mix 16–25 at 7 days of age (within the second stage experiment). The admixtures proportion for every sample was added into the mortar samples between 1.0 to 15.0 wt% of weight (based on total aluminosilicate precursors weight). The water-to-binder ratio was set between 0.30 to 0.50, and the aggregate-to-binder ratio was between 1 and 3 to produce the mortar, tested in all 30 mortar mixture samples and cured under the lab ambient conditions. The mix design compositions of one-part alkali-activated mortars are further elucidated in Table 2.

**Table 2.** Mix composition and design of one-part Alkali Activated Materials (AAMs).

Samples	Binder		Alkali Activated		Admixtures			Design Ratio	
	FA (%)	GGBFS (%)	OPC (%)	K <sub>2</sub> CO <sub>3</sub> (%)	SRA (%)	CaO (%)	SP (%)	Aggregate-to-Binder	Water-to-Binder (W/B)
* Mix 1	85	15	0	6	5	1	1	3	0.30
Mix 2	25.5	4.5	70	6	1	0.5	1.5	3	0.30
Mix 3	60	10	30	6	5	1	1	3	0.35
Mix 4	59.5	10.5	30	6	5	1	1	1.5	0.46
Mix 5	25	5	70	6	2	1	1	1	0.49
Mix 6	45	5	50	5	2	1	1	1.5	0.45
Mix 7	59.5	10.5	30	6	5	1	1	1	0.35
Mix 8	81	9	10	6	4	1	1	1	0.35
Mix 9	60	10	30	6	5	1	1	1	0.35
** Mix 10	60	10	30	6	-	-	-	1	0.35
Mix 11	60	10	30	6	4	1	1	1	0.35
Mix 12	60	10	30	8	4	10	1	1	0.35
Mix 13	60	10	30	10	5	15	1	1	0.40
Mix 14	45	5	50	8	4	10	1	1	0.35
Mix 15	45	5	50	10	5	15	1	1	0.40
Mix 16	30	-	70	8	4	10	1	1	0.35
Mix 17	30	-	70	10	4	15	1.5	1	0.40
Mix 18	30	-	70	8	4	10	1.5	-	0.45
Mix 19	30	-	70	10	4	10	1	1	0.45
Mix 20	30	-	70	8	4	10	1	1	0.45
Mix 21	30	-	70	8	4	10	1	1	0.50
Mix 22	40	-	60	8	4	-	1	1	0.45
Mix 23	30	-	70	8	4	-	1	1	0.45
Mix 24	20	10	70	8	4	-	1	1	0.45
Mix 25	25	5	70	8	4	-	1	2	0.45
*** Mix 26	25	5	70	1.8	-	-	-	1	0.50
Mix 27	25	5	70	1.6	0.3	0.15	1	1	0.50

Table 2. Cont.

Samples	Binder		Alkali Activated		Admixtures			Design Ratio	
	FA (%)	GGBFS (%)	OPC (%)	K <sub>2</sub> CO <sub>3</sub> (%)	SRA (%)	CaO (%)	SP (%)	Aggregate-to-Binder	Water-to-Binder (W/B)
Mix 28	25	5	70	2	0.9	0.45	1	1	0.50
Mix 29	25	5	70	1.8	0.6	0.30	1	1	0.49
Mix 30	25	5	70	1.6	0.3	0.15	1	1	0.40

\* control sample no.1, \*\* control sample no.2, \*\*\* control sample no.3.

## 2.2. Sample Preparations

An electric mixer, EX-EM2000 EXTRAMAN 2000W, was used to prepare all mixes. The FA, GGBFS, PCC, K<sub>2</sub>CO<sub>3</sub>, SRA, CaO, sodium lignosulfonate (SP), and fine aggregates were blended in the mixture for 2 min according to their sample of mix compositions. After that, water was added slowly to the mixtures and continued blending for another 3 min to ensure the mortar paste was uniform. Then, all the fresh mortars were immediately cast into 50 mm × 50 mm × 50 mm cubes for the compressive strength test, 40 mm × 40 mm × 160 mm for the flexural strength test, 150 mm × 300 mm diameter cylinder for tensile strength test and modulus of elasticity test, and 75 mm × 75 mm × 280 mm for drying shrinkage measurement. All filled moulds were vibrated for 2 min using a shaking table. The mixtures were demolded after 24 h before being cured in an ambient lab temperature of 29 °C, with relative humidity (RH) of 65% until the testing on days 7, 14, and 28 of curing age. For the compressive strength test, samples were taken out for curing under standard laboratory climate (dry conditioning) for 7 days at 21+/-2 Celsius and 60+/-10% RH.

## 2.3. Experimental Procedures

To study mechanical strength, hardened mortar's compressive strength and flexure strength were evaluated at 7-d, 14-d, and 28-d curing age. Compression test machine AUTOMAX5 was used at a loading rate of 1000 N/s per the EN12190 test method and a three-point flexure test under a displacement-controlled condition where the load was applied at mid-span in compliance with BS EN 13892-2:2002. The mean value of three readings of each sample produced in triplicate for every test was recorded and taken as their final strength value. In addition, a test on the static modulus of elasticity mortars was conducted at 28-d of age with basic stress of 0.5 N/mm<sup>2</sup>, and the stress increased at a constant rate within the range of 0.6 N/mm<sup>2</sup>/s until the stress was equal to one-third of the compressive strength of the concrete is reached in compliance with BS 1881. Three cylindrical specimens of 150 mm × 300 mm size for the selected mortar sample formula were prepared, and the average and standard deviation were calculated and reported. Indirect tensile strength was employed using a tensile splitting method on cylindrical mortars for the selected mortar sample and assessed at 28-d of age following ASTM C496 at a loading rate of 1 MPa/s. For drying shrinkage measurement, a test was conducted on the prism samples according to BS 1920-8:2009, tested at 28 days of curing age.

## 3. Result and Discussion

### 3.1. Compressive Strength

The seven-day compressive strength for 30 samples ranged from 2 N/mm<sup>2</sup> to 23 N/mm<sup>2</sup>, as shown in Figures 1–3. Mix 30, composed of 25% FA, 5% GGBFS, and 70% OPC, recorded the highest compressive strength with 23.76 N/mm<sup>2</sup>, nearing the minimum strength requirement at 28 days of curing age for structural repair products class R3 of EN1504-3 standard. For the mortar samples, Mix 5, 26, 27, 28, and 29 all recorded compressive strength above 15 N/mm<sup>2</sup> and had the potential to comply with the minimum

strength requirement at 28 days of curing age for non-structural repair products class R2 of EN1504-3 standard.

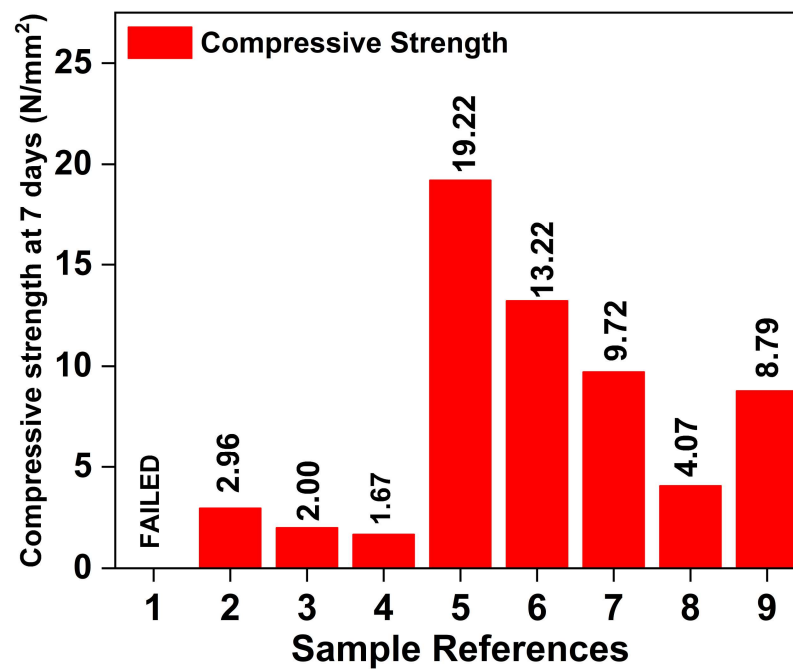


Figure 1. Compressive strength at 7 days of curing age—Stage 1.

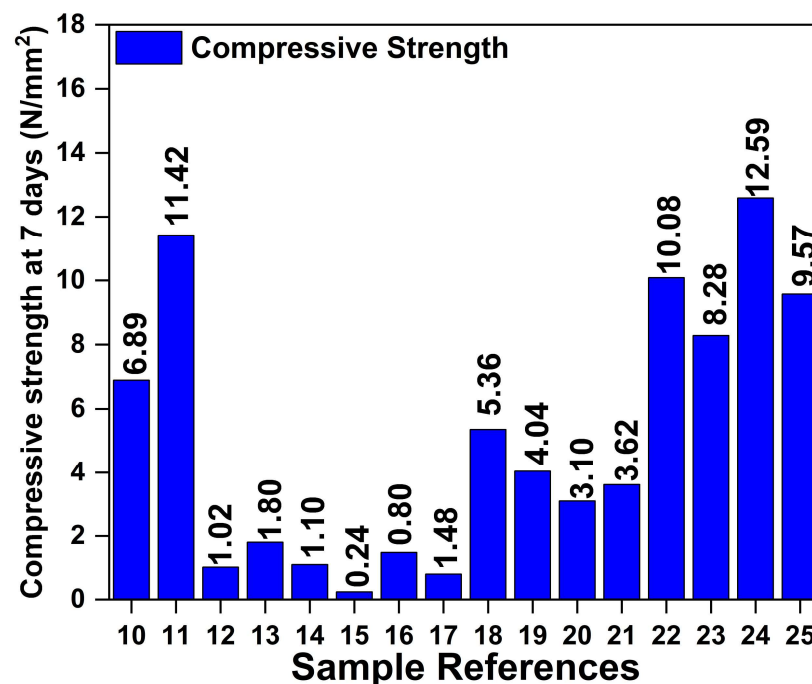


Figure 2. Compressive strength at 7 days of curing age—Stage 2.

Adding FA may slower the strength development of mortar at an early age and clarify the lowest compressive strength reported for samples. Mix 7–13 consisted of 60–80% FA. Without OPC, sample Mix 1 was prepared as a control sample consisting of 85% FA and 15% GGBFS and was activated by a 6% alkali activator, referred to as the first stage of this experiment for mortar samples 1–9 (Figure 1). It was reported that the total aggregate content did not affect the flexural strength development of one-part AAMs [29]. Thus, aggregate-to-binder ratios were set to 3 as a source of calcium and increased the mortar

volume for the first three mortar samples, Mix 1–3. However, as observed in these three samples, they were not hardened enough and immediately collapsed when the applied load was placed on the cube samples for testing.

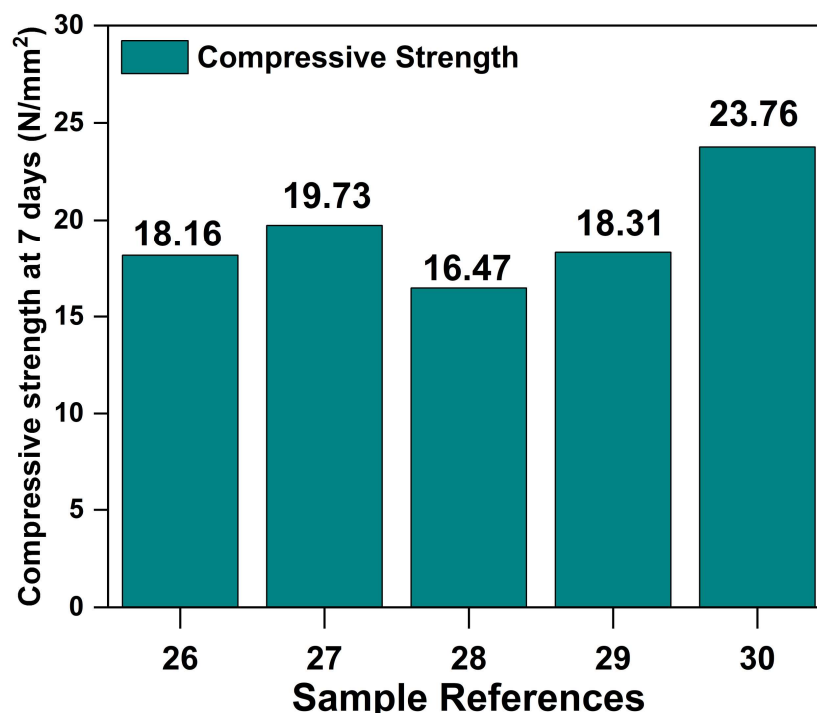


Figure 3. Compressive strength at 7 days of curing age—Stage 3.

Furthermore, these three samples were activated with a low water-to-binder (W/B) ratio of 0.3, contributing to lower compressive strength. As a result, the cube samples were brittle, sandy, cracked and failed due to insufficient water to initiate the geopolymeration process. The W/B ratio increased from 0.3 to 0.45 for Mix 3–9 and still only managed to get low compressive strength, except for Mix 5 (W/B ratio of 0.49), which was also designed with an aggregate-to-binder ratio of 1 and lower FA volume (than sample Mix 4) has recorded 13.22 N/mm<sup>2</sup> for seven days of curing age offered important indication on the optimum design of aggregate-to-binder ratio. A higher aggregate-to-binder ratio between 1.5 to 3.0 in this study led to low compressive strength at seven days of curing age because the insufficient hydration of main gel products of C-S-H could not wholly wrap the surface of the fine aggregate, creating more porous structures that make it physically not solid [30].

Mix 10 was designed as a control sample no.2 without admixtures to evaluate the compressive strength trend for mortar samples. Mixes 11–24 were prepared for the second stage (Figure 2) in this compressive strength test experiment. The mortar samples Mix 10 has a 6% alkali activator and W/B ratio of 0.35 and recorded compressive strength of 6.89 N/mm<sup>2</sup>. In addition, a 1–10% CaO was added to the mortar because the CaO could supply additional calcium, increase the exothermic level for the hydration process, and react with silica and alumina from FA to produce additional C-S-H and C-A-S-H. Furthermore, the higher silica content in FA increased the dissolution and polymerization process. A higher Si/Al ratio in FA promotes low porosity microstructures, ensuring high sample compactness and enhancing compressive strength [31]. Excessive CaO, however, could lead to strength loss due to the fast chemical reaction of the matrix, subsequently generating unbalanced gel binder structures that affect strength development [32].

Further investigation found that a higher volume of CaO between 10–15% of mix composition was one factor in the poor compressive strength recorded for Mix 12–21. As a result, the volume of FA was reduced to 45% and 40% in Mix 14, 15 and 22 but still showed poor compressive strength. At the same time, samples with 30% FA without

GGBFS continued a low compressive strength value trend below  $10 \text{ N/mm}^2$  as recorded for samples Mix 16–23, which gives a significant indication of the influence of GGBFS and its relation with FA to generate a stronger bond of prominent C-S-H gels.

A higher volume of GGBFS than FA in sample Mix 24 has shown slight improvement for 7-day compressive strength but is still within 50% of the targeted strength of class R3 standard. Nevertheless, it was reported that higher slag content is susceptible to autogenous shrinkage and cracking due to the rapid acceleration of the reactions [14]. Besides that, it was found that without CaO, the 4% SRA-only was inefficient in influencing the compressive strength performance of sample Mix 25. Therefore, based on the compressive strength result at seven days for Mix 10–15 (admixtures effect) and Mix 16–25 (GGBFS effect), Mix 26 was designed as a control sample no.3 for the mix composition consisting of 25% FA and 5% GGBFS with the presence of 70% OPC and 1.8% alkali activator to produce the mortar, subsequently referred as the third stage of the experiment (Figure 3). As a result, the compressive strength result for Mix 26 has an impressive early strength development up to  $18 \text{ N/mm}^2$  equivalent to 72% of the 28-day minimum compressive strength class R3 and successfully exceeded the 28-day minimum compressive strength for non-structural repair products class R2, both per EN1504-3 specification.

The concentration of alkali activators is crucial for early strength development [26]. A higher alkali activator dosage is required to complete the dissolution of raw materials. At lower alkali activator dosages, the dry mixtures were not fully reacted, causing the mortar to fail to harden at early curing ages. However, for this study, it was shown that a higher percentage negatively affected its mechanical strength, as explained in samples Mix 1–25, which, activated by 6–10% of alkali activators, were unable to react well with precursors and an excessive amount of SRA (1–5%) and CaO (0.5–15%). Therefore, the alkali activator was set between 1.6 and 2.0% for this third test stage. The SRA and CaO were adjusted to 0.3–0.9% of precursor volume for the SRA and 0.15–0.45% for CaO. The W/B ratio was maintained between 0.35–0.5. Moreover, a 1% superplasticizer (SP) and an aggregate-to-binder ratio of 1 were consistently applied to all samples. Therefore, the highest compressive strength value at seven days of age was obtained from sample Mix 30 at an optimum W/B ratio of 0.4, with a sufficient water supply for the geopolymerization process at an early age essential for heat equilibrium, especially with the inclusion of 70% OPC and chemical admixtures (SP, SRA, and CaO) that caused more heat to be released from the exothermic reaction.

Only six samples were selected out of 30 for compressive strength tests at 14 and 28 days of curing age, and the result is recorded in Figure 4. However, compressive strength for samples Mix 26, 27, 28, and 29 deteriorated on day 14 and dropped further toward day 28. It is worthwhile to understand that all mortar samples Mix 26, 27, 28, and 29 have higher water contents with W/B ratios of 0.50 and 0.49 (Mix 29). These findings agreed with [5] on the effect of higher water content reducing the rheology of fresh mortar, subsequently affecting the mechanical strength at the hardened stage. Excessive water content may be caused extra gaps to occur between aggregates, creating voids filled by air when moisture vaporizes. The hardened materials then experience insufficient compaction and become less solid, which affects their strength [33]. Additionally, insufficient alkali cation ( $\text{Na}^+$ ,  $\text{K}^+$ ) to keep the pH raised for the reaction mixtures affects the dissolution process at 28 days of curing age.

Moreover, Mix 26 as a control sample was composed without admixtures, affecting the stability of the C-A-S-H gels chains and making them prone to chemical attacks. Crack formation due to shrinkage has also lowered the mechanical strength development. The inclusion of a combination of CaO and SRA was reported to control the shrinkage efficiently [21,22]. Still, too much CaO and SRA content in Mix 28 and 29 did not react well with a low dosage of solid alkali activator in addition to higher water content level factors in this report. The reaction rate between precursors and admixtures decreased in low alkali medium, causing low mechanical strength and porous structures [34]. This phenomenon is due to the fact that low pH of carbonate delayed the initial reaction of one-part AAMs

and might not be able to fully break down the Al-O and Si-O bonds of the aluminosilicate precursors with the presence of excessive admixtures content. The highest compressive strength recorded at 28 days was 28.55 N/mm<sup>2</sup> for sample Mix 30, followed by Mix 5, which recorded 26.75 N/mm<sup>2</sup>. These two samples have strength increases over time consistently from seven days to 28 days of curing age, as shown in Figure 5, and exceed the minimum requirement for structural repair product Class R3 of EN1504-3 standard. The microparticle size of powder precursors FA, GGBFS, and OPC in this study exhibit higher specific areas, helpful in improving the reaction for better mechanical strength [6].

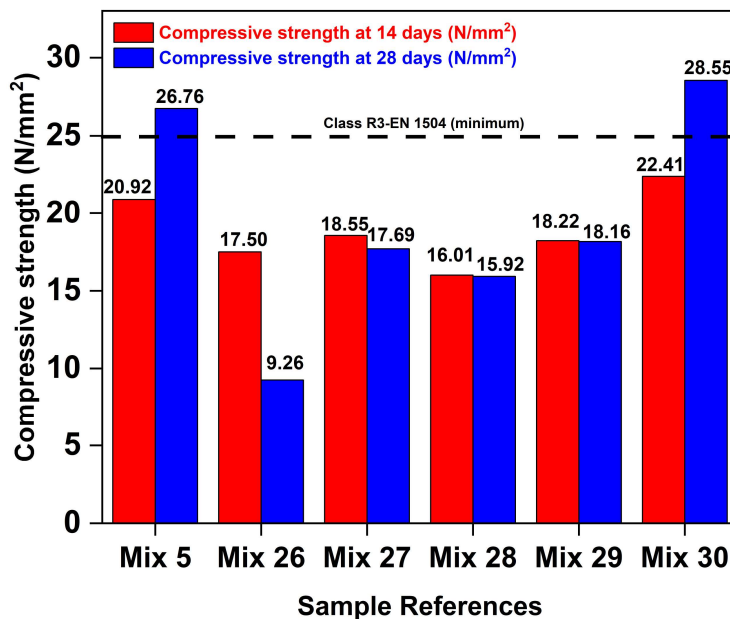


Figure 4. Compressive strength at 14 and 28 days of curing age.

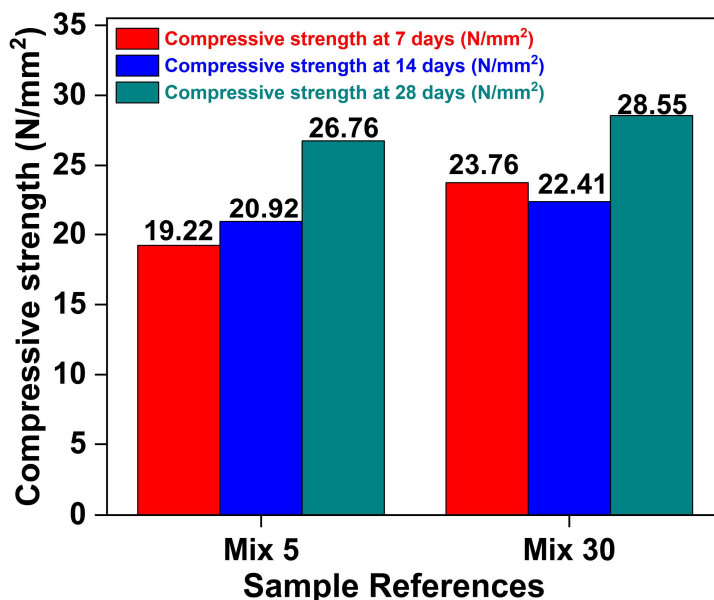
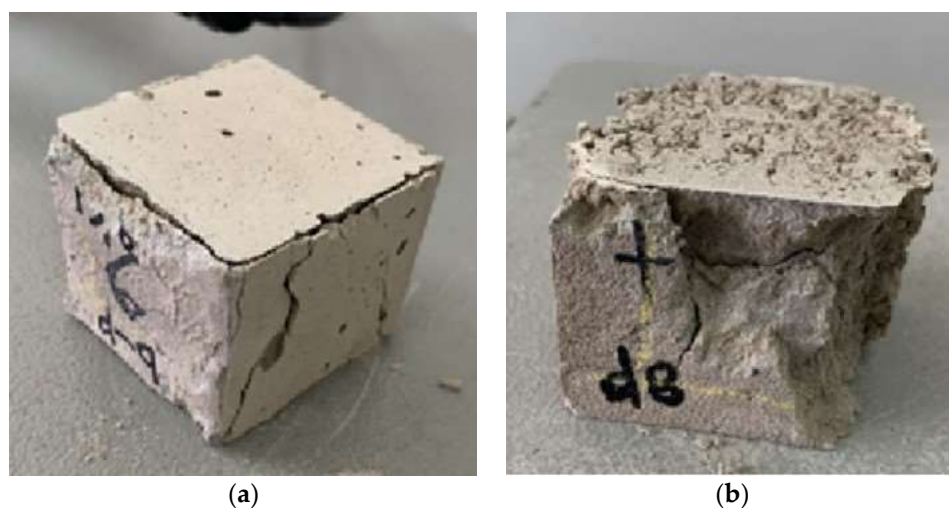


Figure 5. Compressive strength at 7, 14 and 28 days of curing age.

The cracked pattern of the cube samples for sample Mix 30 has little impact on faces in contact with the platens, cone, and shear with fewer macrocracks, generally reflecting its rigidity supporting on higher compressive strength value as shown in Figure 6a. In contrast, Mix 26 experienced an unsatisfactory type of cracked pattern failure, which indicates that it's brittle and not solid, as illustrated in Figure 6b. It was noted that a higher Si/Al ratio for

25% fly ash Class F used in this experiment is physically stable without significant structural disintegration, contributing to the excellent performance in compressive strength [35]. The Si/Al ratio for FA was above 2, within the recommended ratio for higher compressive strength suggested by [31,36,37]. In addition, the main precursors are composed of rich calcium content supplied from GGBFS and OPC sources. Calcium is beneficial for creating C-S-H gels. The combination of FA/GGBFS expands the C-S-H gels chain by creating new C-(A)-S-H co-existing with N-A-S-H gels for excellent mechanical properties [5]. Coppola et al. [38] reported that a one-part alkali-activated mortar activated with a 4% alkali activator recorded compressive strength of 26.4 N/mm<sup>2</sup> at 28 days of curing age, which is lower than the findings in this study which activated with a minimal dosage of alkali activator.



**Figure 6.** (a) Cracked pattern failure for mortar sample mix 30 under compressive strength test; (b) Cracked pattern failure for mortar sample mix 26 under compressive strength test.

### 3.2. Flexural Strength

The experiment in this report continues with the flexural test to determine the mechanical compatibility of the mortar and its bending resistance. The test will further explain its tensile strength ability indirectly. Sample Mix 5 and Mix 30 were selected to obtain their flexural strength because their compressive strength at 28 days achieved the minimum requirement as per EN 1504-3 class R3 standard, subsequently referred to as control samples used for the rest of the experiment in this report. At seven, 14 and 28 days, the flexural strength for Mix 30 was 7.4 N/mm<sup>2</sup>, 8.05 N/mm<sup>2</sup> and 8.55 N/mm<sup>2</sup>, and it was the highest flexural strength recorded between two control mortar samples, as shown in Figure 7, where the flexural strength development increased over time. Both mortar samples recorded above 8 N/mm<sup>2</sup>. The addition of 5% GGBFS improved the early mechanical strength of the mortar. At the same time, calcium from FA increased the pozzolanic reaction at the later stage. Besides, a more substantial bonding factor between the binder and the aggregate in the mortar is beneficial for bending resistance behaviour [29].

The flexural strength of Mix 30, however, was only around 30% of its compressive strength at 28 days of curing age. This result further explained that the unreinforced mortar cube samples used in this experiment are naturally brittle and very stiff. In addition, the growth of its mechanical strength over time dropped due to microcracks [39]. Nevertheless, the mortar used in the experiment was comparable to the conventional OPC concrete. The concrete standard's flexural strength or modulus of rupture is between 10% and 20% of its compressive strength, depending on the volume and size of the coarse aggregate used in the concrete. Moreover, the 8.55 N/mm<sup>2</sup> flexural strength of Mix 30 exhibited a higher strength value than other one-part alkali-activated materials, as published in past reports [14,21].

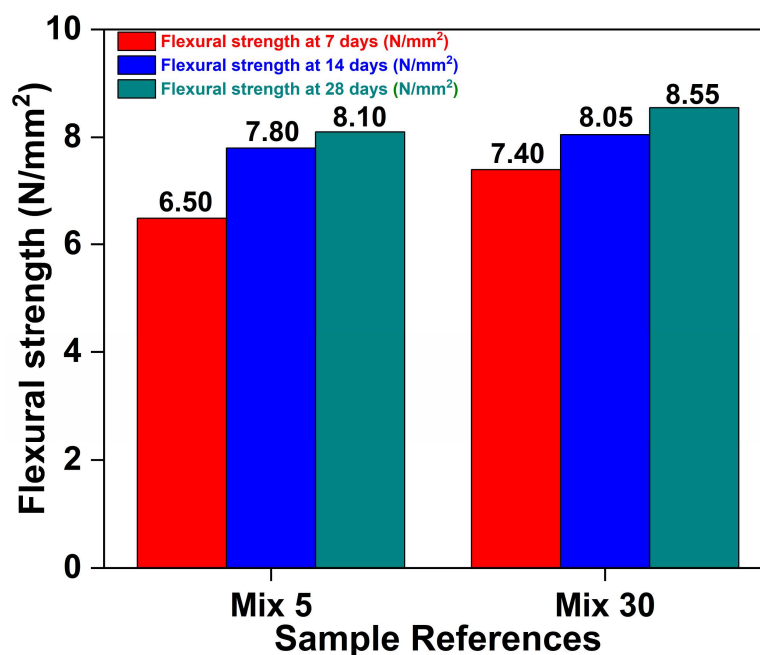


Figure 7. Flexural strength at 7, 14 and 28 days of curing age.

### 3.3. Modulus of Elasticity

Besides the mechanical strength, a higher modulus of elasticity of alkali-activated mortar is essential to offer durable repair materials by providing resistance against elastic deformation when force is applied. The lower aggregate-to-binder ratio reported increased the MOE of concrete activated by one-part AAMs according to [29]. The ratio of aggregate-to-binder in this experiment was 1, and the mortar samples for the MOE test were cured with water and ambient conditions.

As shown in Table 3, the modulus of elasticity of sample Mix 30 was recorded at 19.6 GPa, and Mix 5 has 18.10 GPa MOE, both complying with the minimum elastic modulus requirement for class R3-EN1504 standard, slightly higher than the modulus of elasticity for most of the two-part alkali-activated mortar, which has been recorded between 15–18 GPa [39,40]. Additionally, they did not require higher temperatures than the two-part AAMs [7]. However, similar to the flexural strength development, the presence of micro-cracks has affected the MOE of one part of alkali-activated mortar [41]. In addition, it is worth noting that repair materials and substrates may have different moduli of elasticity. For example, concrete substrates generally have an elastic modulus between 30 to 50 GPa. A lower modulus of elasticity of repair material than the substrates has more resilient elements that can take up more force and return to its initial structure [28], subsequently protecting mortar from cracking, thus providing better structural compatibility between the repair mortar and the existing concrete substrates [39].

Table 3. Modulus of Elasticity (MOE) at 28-day of age.

Sample References	Modulus of Elasticity (GPa)
Mix 5	18.10
Mix 30	19.60

### 3.4. Tensile Strength

The higher aggregate content would increase the splitting tensile strength, and the strength developed over time follows a similar trend with compressive and flexural strength. However, the tensile strength after 28 days was lower than the mixtures with lower aggregate content reported by [29]. The highest splitting tensile strength between these two samples is Mix 30, which recorded 2.05 MPa, equivalent to 10% of its compressive strength

at 28 days of curing age, as shown in Table 4, giving a good signal of its bond strength ability to achieve minimum adherence strength 2.0 MPa of class R4, EN1504-3 [42]. Nevertheless, Mix 30 with 2.05 MPa tensile strength was within the range of tensile strength for typical plain cementitious mortar, as reported by [43]. It turns out that the incorporation of slag as a replacement for fly ash for mortar Mix 30 enhanced splitting tensile strength, as reported by [44]. It is worth noting that mortar is good in compression but weak in tension, like typical concrete. The interface transition zone (ITZ) is the weakest link in the hardened mortar, as observed from its microstructure. When a compressive load is applied, the ITZ bridges the load from one aggregate to another in the mortar. On the contrary, the outer surface of aggregates will break from each other when tensile stresses are applied to leave the ITZ to absorb all forces and cause failure.

**Table 4.** Splitting tensile strength at 28 days of curing age.

Sample References	Splitting Tensile Strength (MPa)
Mix 5	1.80
Mix 30	2.05

### 3.5. Drying Shrinkage

Shrinkage is one of the significant problems for alkali-activated materials, mainly caused by alkali activator involvement in accelerating the reaction. Jixiang et al. [6] reported that a higher sodium silicate and slag content dosage in alkali-activated materials increased shrinkage. In this report, a lower dosage of alkali activator and slag for the one-part mortar Mix 30 has a length change measured of 260 microstrains at 28 days, while mortar sample Mix 5 documented 350 microstrains. Both recorded less than 400 microstrains under ASTM C157 specification for drying shrinkage measurement as shown in Table 5, which is much better than the shrinkage level of the two-part alkali-activated materials counterpart. This result also agreed with [45] on the beneficial effect of the shrinkage-reducing admixtures (SRA) in alkali-activated materials. The SRA admixture will limit the tensile stress stimulated by restrained shrinkage, thus avoiding the mortar from early cracks. Therefore, drying shrinkage measurement can indicate the mortar's ability to resist early crack formation and shrinkage-restraining stresses.

**Table 5.** Drying Shrinkage Measurement at 28 days of curing age.

Sample References	Drying Shrinkage Measurement (Microstrain)
Mix 5	350
Mix 30	260

On the other hand, the low water-to-binder ratio increased the mechanical strength of hardened mortar. Still, it could result in autogenous shrinkage and cracking, affecting the flexural strength over time. Sample Mix 30 mortar in this experiment has proved that even though it was composed of a lower water-to-binder ratio and a lower dosage of alkali activator yet recorded a lower level of drying shrinkage measurement within a maximum of 400 microstrains allowed. The result is also in agreement with [21,22], where the usage of shrinkage-reducing admixtures (SRA) and calcium oxide (CaO) as an expensive agent could reduce the shrinkage level of mortar. It is beneficial to determine CaO dosage in this experiment because the excessive level of calcium may precipitate as gypsum and expand, possibly damaging the mortar's physical structures. However, with an appropriate ratio, the gypsum may also block pores and minimize early corrosion attacks [46]. Furthermore, CaO is an expansive agent that induces a high exothermic reaction when it reacts with water to form a larger volume of hydrated lime particles, which helps the mortar to expand instead of shrinking and only stops expanding at the end of the curing process [22].

Other than that, the applied aggregate-to-binder of 1 for Mix 30 contributed to a better performance of tensile strength where it controlled the shrinkage level where the

fine aggregate served as reinforcement to compact and stabilize the materials [42]. It is worth noting that a higher percentage volume of all three admixtures created unbalanced gel structures and affected mechanical strength growth at the early and later stages of the hardening phase, as observed in all 30 mortar samples' compressive strength results in this study. Contrary to the conventional one-part alkali-activated mortar productions, the inclusion of admixtures and OPC reacted well with a low dosage of non-hygroscopic alkali activator, offering cheaper and safer construction products. This type of hybrid one-part AAMs has impressive mechanical strength and a low drying shrinkage level comparable to the conventional OPC mortar and the two-part AAMs mortar counterparts.

#### 4. Conclusions

This study investigated the mechanical strength performance of one-part alkali-activated mortar for concrete structural repair application. The mortar was composed with different mixed design compositions. As a result, mortar sample Mix 30 has the best mechanical strength performance out of 30 different mix design ratios, followed by mortar sample Mix 5. In Mix 30, the OPC binder content was replaced with 30% by-product precursors consisting of 25% class-F fly ash and 5% slag from the GGBFS source. Interestingly, dry mixed precursors were activated with only 1.8% powdered alkaline activator of Potassium carbonate ( $K_2CO_3$ ). As a result, mortar samples Mix 30 has a water-to-binder ratio of 0.40 compared to Mix 5 activated with a W/B of 0.49. The mechanical strength results for mortar sample Mix 30 complied with the minimum requirements for the compressive strength and modulus of elasticity (MOE) as per the Class R3-EN1504 standard for structural concrete repair materials and successfully achieved the aim of this study.

For one-part AAMs activated with low alkali activator dosage, a single aluminosilicate precursor will not be sufficient to produce the higher compressive strength of mortar. Combining two or three industrial by-product precursors with OPC demonstrates improved physical structures and mechanical strength. The combination of FA and GGBFS reacted well with the OPC under a low alkaline environment and exhibited acceptable mechanical strength performances. The flexural and splitting tensile strengths result for Mix 30 showed that the mortar has higher bending resistance and can resist the applied stress as a sign of solid bonding strength between mortar and concrete substrates, subsequently promoting its potential to be applied for concrete structural repair applications. Nevertheless, lower MOE of repair mortar than the concrete substrate is essential to ensure compatibility between two bonding materials to resist force while maintaining the bond at interface transition zone (ITZ).

The combination of three powder admixtures enhances the mechanical properties of the mortar compared to samples without admixtures. Using SRA and CaO reduced the internal stress, controlled the expansion of the mortar, and ensured reliable mechanical strength progress. Adding a superplasticizer (SP) lengthens the setting time and controls the hydration process rates.

Future studies will focus on the rheology behaviour of the fresh mortar using this new mix design formulation to ensure its consistency and flexibility adopted for in-situ application. In addition, improved workability of mortar will offer better mechanical strength, beneficial for the pull-off bond strength performance between the repair mortar and concrete substrate for concrete patching applications as part of concrete repair techniques.

**Author Contributions:** Conceptualization, E.Y.; Data curation, E.Y.; Formal analysis, E.Y.; Funding acquisition, E.Y.; Investigation, E.Y.; Methodology, E.Y.; Project administration, E.Y. and S.B.; Supervision, S.B.; Visualization, S.B.; Writing—original draft, E.Y. All authors have read and agreed to the published version of the manuscript.

**Funding:** This research received no external funding.

**Institutional Review Board Statement:** Not applicable.

**Informed Consent Statement:** Not applicable.

**Data Availability Statement:** Not applicable.

**Acknowledgments:** Special thanks to Makmal Kerja Raya Malaysia (MKRM), Engineering New Zealand, The Association of German Engineers (VDI) and the Public Service Department, Sabah (JPANS), Malaysia, for contributing to the outcome of this experiment.

**Conflicts of Interest:** The authors declare no conflict of interest.

## References

1. Ren, J.; Sun, H.; Li, Q.; Li, Z.; Ling, L.; Zhang, X.; Wang, Y.; Xing, F. Experimental comparisons between one-part and normal (two-part) alkali-activated slag binders. *Constr. Build. Mater.* **2021**, *309*, 125177. [[CrossRef](#)]
2. Peng, M.X.; Wang, Z.H.; Shen, S.H.; Xiao, Q.G.; Li, L.J.; Tang, Y.C.; Hu, L.L. Alkali fusion of bentonite to synthesize one-part geopolymeric cements cured at elevated temperature by comparison with two-part ones. *Constr. Build. Mater.* **2017**, *130*, 103–112. [[CrossRef](#)]
3. Xu, G.; Shi, X. Characteristics and applications of fly ash as a sustainable construction material: A state-of-the-art review. *Resour. Conserv. Recycl.* **2018**, *136*, 95–109. [[CrossRef](#)]
4. Ding, Y.-C.; Cheng, T.-W.; Dai, Y.-S. Application of geopolymer paste for concrete repair. *Struct. Concr.* **2017**, *18*, 561–570. [[CrossRef](#)]
5. Phoo-Ngernkham, T.; Hanjitsuwan, S.; Li, L.-Y.; Damrongwiriyanupap, N.; Chindaprasirt, P. Adhesion characterization of Portland cement concrete and alkali-activated binders. *Adv. Cem. Res.* **2019**, *31*, 69–79. [[CrossRef](#)]
6. Wang, J.; Huang, T.; Cheng, G.; Liu, Z.; Li, S.; Wang, D. Effects of fly ash on the properties and microstructure of alkali-activated FA/BFS repairing mortar. *Fuel* **2019**, *256*, 115919. [[CrossRef](#)]
7. Adesanya, E.; Ohenoja, K.; Di Maria, A.; Kinnunen, P.; Illikainen, M. Alternative alkali-activator from steel-making waste for one-part alkali-activated slag. *J. Clean. Prod.* **2020**, *274*, 123020. [[CrossRef](#)]
8. Shah, S.F.A.; Chen, B.; Oderji, S.Y.; Haque, M.A.; Ahmad, M.R. Comparative study on the effect of fiber type and content on the performance of one-part alkali-activated mortar. *Constr. Build. Mater.* **2020**, *243*, 11822. [[CrossRef](#)]
9. Luukkonen, T.; Abdollahnejad, Z.; Yliniemi, J.; Kinnunen, P.; Illikainen, M. Comparison of alkali and silica sources in one-part alkali-activated blast furnace slag mortar. *J. Clean. Prod.* **2018**, *187*, 171–179. [[CrossRef](#)]
10. Kadhim, A.; Sadique, M.; Al-Mufti, R.; Hashim, K. Developing one-part alkali-activated metakaolin/natural pozzolan binders using lime waste. *Adv. Cem. Res.* **2021**, *33*, 342–356. [[CrossRef](#)]
11. Li, L.; Lu, J.-X.; Zhang, B.; Poon, C.-S. Rheology behavior of one-part alkali activated slag/glass powder (AASG) pastes. *Constr. Build. Mater.* **2020**, *258*, 120381. [[CrossRef](#)]
12. Abdollahnejad, Z.; Mastali, M.; Falah, M.; Shaad, K.M.; Luukkonen, T.; Illikainen, M. Durability of the Reinforced One-Part Alkali-Activated Slag Mortars with Different Fibers. *Waste Biomass Valorization* **2020**, *12*, 487–501. [[CrossRef](#)]
13. Oderji, S.Y.; Chen, B.; Ahmad, M.R.; Shah, S.F.A. Fresh and hardened properties of one-part fly ash-based geopolymer binders cured at room temperature: Effect of slag and alkali activators. *J. Clean. Prod.* **2019**, *225*, 1–10. [[CrossRef](#)]
14. Shah, S.F.A.; Chen, B.; Oderji, S.Y.; Haque, M.A.; Ahmad, M.R. Improvement of early strength of fly ash-slag based one-part alkali activated mortar. *Constr. Build. Mater.* **2020**, *246*, 118533. [[CrossRef](#)]
15. Kramar, S.; Šajna, A.; Ducman, V. Assessment of alkali activated mortars based on different precursors with regard to their suitability for concrete repair. *Constr. Build. Mater.* **2016**, *124*, 937–944. [[CrossRef](#)]
16. Abdollahnejad, Z.; Mastali, M.; Luukkonen, T.; Kinnunen, P.; Illikainen, M. Fiber-reinforced one-part alkali-activated slag/ceramic binders. *Ceram. Int.* **2018**, *44*, 8963–8976. [[CrossRef](#)]
17. Alzaza, A.; Ohenoja, K.; Illikainen, M. Enhancing the mechanical and durability properties of subzero-cured one-part alkali-activated blast furnace slag mortar by using submicron metallurgical residue as an additive. *Cem. Concr. Compos.* **2021**, *122*, 104128. [[CrossRef](#)]
18. Alzaza, A.; Ohenoja, K.; Illikainen, M. Mechanical properties of ambient cured one-part hybrid OPC-geopolymer concrete. *Constr. Build. Mater.* **2018**, *186*, 330–337. [[CrossRef](#)]
19. Alzaza, A.; Ohenoja, K.; Illikainen, M. Microstructure and macro properties of sustainable alkali-activated fly ash mortar with various construction waste fines as binder replacement up to 100%. *Cem. Concr. Compos.* **2022**, *134*, 104733. [[CrossRef](#)]
20. Liu, M.; Wang, C.; Wu, H.; Yang, D.; Ma, Z. Reusing recycled powder as an eco-friendly binder for sustainable GGBS-based geopolymer considering the effects of recycled powder type and replacement rate. *J. Clean. Prod.* **2022**, *364*, 132656. [[CrossRef](#)]
21. Liu, M.; Wang, C.; Wu, H.; Yang, D.; Ma, Z. The combined use of admixtures for shrinkage reduction in one-part alkali activated slag-based mortars and pastes. *Constr. Build. Mater.* **2020**, *248*, 118682. [[CrossRef](#)]
22. Ngassam, I.L.T.; Arito, P.; Beushausen, H. A new approach for the mix design of (patch) repair mortars. *African J. Sci. Technol. Innov. Dev.* **2018**, *10*, 259–265. [[CrossRef](#)]
23. Ngassam, I.L.T.; Arito, P.; Beushausen, H. One-part alkali-activated binder produced from inertized asbestos cement waste. *J. Clean. Prod.* **2022**, *367*, 132966. [[CrossRef](#)]
24. Huseien, G.F.; Mirza, J.; Ismail, M.; Ghoshal, S.; Hussein, A.A. Geopolymer mortars as sustainable repair material: A comprehensive review. *Renew. Sustain. Energy Rev.* **2017**, *80*, 54–74. [[CrossRef](#)]

25. Yin, K.; Jiang, Y.; He, H.; Ren, J.; Li, Z. Characterization of one-part alkali-activated slag with rice straw ash. *Constr. Build. Mater.* **2022**, *345*, 128403. [[CrossRef](#)]
26. Liu, C.; Yao, X.; Zhang, W. Controlling the setting times of one-part alkali-activated slag by using honeycomb ceramics as carrier of sodium silicate activator. *Constr. Build. Mater.* **2020**, *235*, 117091. [[CrossRef](#)]
27. Luukkonen, T.; Abdollahnejad, Z.; Ohenoja, K.; Kinnunen, P.; Illikainen, M. Suitability of commercial superplasticizers for one-part alkali-activated blast-furnace slag mortar. *J. Sustain. Cem. Mater.* **2019**, *8*, 244–257. [[CrossRef](#)]
28. Teixeira, O.G.; Geraldo, R.H.; da Silva, F.G.; Gonçalves, J.P.; Camarini, G. Mortar type influence on mechanical performance of repaired reinforced concrete beams. *Constr. Build. Mater.* **2019**, *217*, 372–383. [[CrossRef](#)]
29. Haruna, S.; Mohammed, B.S.; Wahab, M.; Liew, M. Effect of paste aggregate ratio and curing methods on the performance of one-part alkali-activated concrete. *Constr. Build. Mater.* **2020**, *261*, 120024. [[CrossRef](#)]
30. Zhang, S.; He, Y.; Zhang, H.; Chen, J.; Liu, L. Effect of fine sand powder on the rheological properties of one-part alkali-activated slag semi-flexible pavement grouting materials. *Constr. Build. Mater.* **2022**, *333*, 127328. [[CrossRef](#)]
31. Qureshi, M.N.; Ghosh, S. Effect of Si/Al ratio on engineering properties of alkali-activated GGBS pastes. *Green Mater.* **2014**, *2*, 123–131. [[CrossRef](#)]
32. Phoo-Ngernkham, T.; Phiangphimai, C.; Intarabut, D.; Hanjitsuwan, S.; Damrongwiriyanupap, N.; Li, L.-Y.; Chindaprasirt, P. Low cost and sustainable repair material made from alkali-activated high-calcium fly ash with calcium carbide residue. *Constr. Build. Mater.* **2020**, *247*, 118543. [[CrossRef](#)]
33. Panda, S.; Sarkar, P.; Davis, R. Effect of Water-Cement Ratio on Mix Design and Mechanical Strength of Copper Slag Aggregate Concrete. *IOP Conf. Ser. Mater. Sci. Eng.* **2020**, *936*, 012019. [[CrossRef](#)]
34. Askarian, M.; Tao, Z.; Samali, B.; Adam, G.; Shuaibu, R. Mix composition and characterization of one-part geopolymers with different activators. *Constr. Build. Mater.* **2019**, *225*, 526–537. [[CrossRef](#)]
35. Thokchom, S.; Mandal, K.K.; Ghosh, S. Effect of Si/Al Ratio on Performance of Fly Ash Geopolymers at Elevated Temperature. *Arab. J. Sci. Eng.* **2012**, *37*, 977–989. [[CrossRef](#)]
36. Lau, C.K.; Rowles, M.R.; Parnham, G.N.; Htut, T.; Ng, T.S. Investigation of geopolymers containing fly ash and ground-granulated blast-furnace slag blended by amorphous ratios. *Constr. Build. Mater.* **2019**, *222*, 731–737. [[CrossRef](#)]
37. Wang, Y.; Liu, X.; Zhang, W.; Li, Z.; Zhang, Y.; Li, Y.; Ren, Y. Effects of Si/Al ratio on the efflorescence and properties of fly ash based geopolymer. *J. Clean. Prod.* **2020**, *244*, 118852. [[CrossRef](#)]
38. Coppola, L.; Coffetti, D.; Crotti, E. Pre-packed alkali activated cement-free mortars for the repair of existing masonry buildings and concrete structures. *Constr. Build. Mater.* **2018**, *173*, 111–117. [[CrossRef](#)]
39. Nunes, V.A.; Borges, P.H.; Zanotti, C. Mechanical compatibility and adhesion between alkali-activated repair mortars and Portland cement concrete substrate. *Constr. Build. Mater.* **2019**, *215*, 569–581. [[CrossRef](#)]
40. Huseien, G.F.; Shah, K.W. Performance evaluation of alkali-activated mortars containing industrial wastes as surface repair materials. *J. Build. Eng.* **2020**, *30*, 101234. [[CrossRef](#)]
41. Coppola, L.; Coffetti, D.; Crotti, E.; Gazzaniga, G.; Pastore, T. The durability of one-part alkali-activated slag-based mortars in different environments. *Sustainability* **2020**, *12*, 3561. [[CrossRef](#)]
42. Salazar, R.A.R.; Jesús, C.; de Gutiérrez, R.M.; Pacheco-Torgal, F. Alkali-activated binary mortar based on natural volcanic pozzolan for repair applications. *J. Build. Eng.* **2019**, *25*, 100785. [[CrossRef](#)]
43. Wazien, A.W.; Abdullah, M.M.A.B.; Razak, R.A.; Rozainy, M.M.R.; Tahir, M.F.M.; Hussin, K. Potential of geopolymer mortar as concrete repairing materials. *Mater. Sci. Forum* **2016**, *857*, 382–387. [[CrossRef](#)]
44. Huseien, G.; Ismail, M.; Tahir, M.; Mirza, J.; Hussein, A.; Khalid, N.; Sarbini, N. Performance of sustainable alkali-activated mortars containing solid waste ceramic powder. *Chem. Eng. Trans.* **2018**, *63*, 673–678. [[CrossRef](#)]
45. Coppola, L.; Coffetti, D.; Crotti, E.; Marini, A.; Passoni, C.; Pastore, T. Lightweight cement-free alkali-activated slag plaster for the structural retrofit and energy upgrading of poor quality masonry walls. *Cem. Concr. Compos.* **2019**, *104*, 103341. [[CrossRef](#)]
46. Sturm, P.; Gluth, G.; Jäger, C.; Brouwers, H.; Kühne, H.-C. Sulfuric acid resistance of one-part alkali-activated mortars. *Cem. Concr. Res.* **2018**, *109*, 54–63. [[CrossRef](#)]



OPEN

# The potential of one-part alkali-activated materials (AAMs) as a concrete patch mortar

Eddy Yusslee  & S. Beskhyroun 

One-part alkali-activated materials (AAMs) are developed to improve conventional two-part systems. One-part AAMs technology has been used in cement binders to produce concrete, mortar, and paste. Current research mainly focuses on synthesizing raw materials obtained from industrial and agricultural waste as the main aluminosilicate precursors of the cement binder for a concrete application. The one-part AAMs were reported to have higher early compressive strength at 7 days of age, contributed by its fast-setting time, mainly when the binder activates by a higher dosage of alkaline activator and containing OPC-rich. Due to bonding issues, single or combination, FA/GGBFS/MK precursors were reported as unsuitable for use as a concrete repair material. They were the reason for the lack of one-part AAMs application of mortar compared to concrete usage. This study was conducted to determine the potential of one-part AAMs used as concrete patch mortar by investigating its rheology and mechanical properties. The compressive strength of the mortar was tested under lab ambient temperature in the tropical climate country of Malaysia. The setting time of fresh mortar and bonding strength were set under controlled lab temperature. The one-part alkali-activated mortar was composed of hybrid aluminosilicate precursors between fly ash (FA), Ground Granulated Blast Furnace Slag (GGBFS) and ordinary Portland cement (OPC). A low alkaline activator of solid potassium carbonate was used for the geopolymerization process. Three types of solid admixtures were added to complete the composition of the new mix design. The experiment's outcome showed that the mortar composed with the combination of conventional Portland cement and industrial waste products has compressive and pull-off adherence strength that meets with Class R3—EN1504-3 standard for structural concrete repair materials requirement.

Many concrete buildings are approaching or exceeding their designed service life and require substantial maintenance to ensure the structure can function to the end of its service life. Typically, concrete infrastructures are designed for 50 to 100 years or more. However, most concrete buildings were built in the past 50 years, where sustainable construction materials are not widely used and established yet. For economic reasons, building owners tend to repair and upgrade these ageing buildings rather than demolish them, and also from the ecstatic or historical point of view, which makes them want to keep the existing building<sup>1</sup>.

Concrete degradation is most common due to corrosion, cracks, spalling, etc., and is repaired with different types of concrete repair techniques and strategies. Presently the maintenance program is focusing on developing eco-friendly materials such as geopolymer or other types of sustainable cement, which not only offers more environmentally friendly products but also improves its engineering properties like higher mechanical strength and better microstructure compared to the traditional ordinary Portland cement (OPC), which extensively used.

Ordinary Portland cement (OPC) has been used as a concrete binder due to its good mechanical properties and cheapness, making it a popular choice in construction<sup>2</sup>. However, many researchers have started looking for alternative binders to replace the OPC due to the environmental impact. Alkali-activated materials (AAMs) are a new binder introduced in the market. It is known for its recycle-friendly products by promoting and utilizing industrial waste as the primary aluminosilicate precursor source. Lately, the conventional two-part AAMs system has been deliberately replaced by one-part technology, also referred to as the 'just add water' concept, where the binder is composed of solid precursors, activated by a solid alkali activator before water is added to activate the mixture, unlike the two-part method that still required corrosive aqueous solutions of alkali activator, not convenient for handling purpose from mixing, transporting to the placing of the sticky concrete. The one-part AAMs used as concrete proved similar and had better mechanical performance than the OPC.

Auckland University of Technology (AUT), Auckland 1010, New Zealand. ✉ email: eddy.yusslee@aut.ac.nz

On the contrary, AAMs applications as concrete repair materials are still not popular compared to commercial polymer-modified cement mortar and epoxy resin. Therefore, the effort has been made to ensure the mechanical strength compatibility will be better or comparable to the conventional concrete repair materials available in the market. AAMs, as part of geopolymer cementitious technology reported has better flexural bond strength than the OPC due to the creation of chemical bonds, especially C-S-H gels for interfacial bonding at the interfacial transition zone (ITZ)<sup>2-5</sup>. A study on shear bond strength of two-part AAMs by<sup>2</sup> using a slant shear test suggested that the combination of fly ash and Portland cement improved the bonding strength of AAMs mortar and PCC substrates and recorded slightly above 25 MPa, comparable to the bonding strength that applied with the commercial repair materials. The developed bond strength in two-part AAMs mortar's trend is further supported by the findings from<sup>5</sup> on the combination of FA/GGBFS precursors exhibiting higher interfacial adhesion level as a result of conducting an interfacial flexural-tensile strength contributed to the better compressive strength of about 60 MPa and flexural strength of about 6 MPa at 28 days of age.

However, for structural concrete repair materials Class R3 and Class R4, the pull-off bonding strength test method is required and must exceed 1.5 MPa for Class R3 and 2.0 MPa for Class R4 as per EN1504-3 Standard<sup>6</sup>. Salazar et al.<sup>7</sup> reported that the two-part AAMs mortar composed of 70% natural volcanic pozzolan and 30% ground granulated blast furnace slag (GGBFS), activated with sodium hydroxide (NaOH) and sodium silicate ( $\text{Na}_2\text{SiO}_3$ ), only recorded 1.24 MPa despite highest compressive strength at 28 days of age about 65 MPa. Two-part alkali-activated mortar composed of a sole slag precursor collapsed when the patch was applied vertical and horizontally due to low pull-off bonding strength between repair materials and substrate. When the slag precursors were substituted and composed of Fly Ash (FA) only, the adhesion strength was recorded 2.3 MPa at the vertical surface and 1.8 MPa horizontally. The two-part AAMs mortar activated by metakaolin-only, however, recorded consistent pull-off bonding strength reading at 2.0 MPa, both tested at vertical and horizontal surfaces. It is worth mentioning that the alkali activator reported in this experiment was between 8 and 14% weightage from the precursor's total weight and demonstrated the influence of the alkali activator where bonding strength will increase when the amount of Si and Na is boosted<sup>6</sup>. Too much alkali content, however, will cost more and affect the mechanical strength with efflorescent, especially metakaolin-based cementitious<sup>8</sup>. Nunes et al.<sup>9</sup> explained that the precursors composed with GGBFS/ metakaolin under high alkalinity conditions tend to reduce adhesive strength due to the unreactive slag caused by high reactivity calcium precipitation that caused  $\text{Ca}(\text{OH})_2$  drops in the loss of C-S-H type of gels, risking the bond. The average pull-off bond strength recorded reported in this experiment showed that sole metakaolin precursor activated with a  $\text{SiO}_2/\text{Al}_2\text{O}_3$  molar ratio of 3.0 for alkali solution only achieved 1.78 MPa at 28 days of age and 1.74 MPa for precursors activated with 80% GGBFS & 20% metakaolin at a similar molar ratio of alkali solution. It is worth noting that both mortar samples recorded higher compressive strength of 50 MPa at 28 days of age.

In addition, the setting time of the one-part AAMs mortar is too fast if containing a higher percentage of OPC, as reported by<sup>10</sup>, where one-part geopolymer paste recorded 22 min for an initial setting time even though it has remarkable concrete mechanical strength at 7 days of age at around 27 MPa with the inclusion of 60% of OPC, nevertheless, accelerate setting time does not favour the production and handling process at the construction site. Therefore, to overcome the shortcomings of these alternative concrete repair materials, attention should be given more to the mix composition of one-part alkali-activated mortar, particularly on the selection of raw materials as aluminosilicates precursors, type of solid alkali activator, admixtures and the ratio of water and aggregates in the mixtures.

As for the solid alkali activator, the sodium metasilicate series has recorded the shortest setting time for a one-part alkali activator mortar. Increasing the alkali activator amount has a linear growth in compressive strength, for which the flexural strength will follow the same trend. Regular concrete's required initial setting time is more than 45–75 min depending on the strength class<sup>11</sup>. Liu et al.<sup>12</sup> used honeycomb ceramic (HCC) as a carrier for the alkaline activator to prolong the setting time of one-part alkali-activated slag paste to counter from short setting time of one-part AAMs. By taking into account, the lowest dosage of alkali activator used for one-part alkali-activated slag mortar in the experiment by Almakhadmeh et al.<sup>13</sup>, colder mixing water temperature at 0 °C recorded a longer initial setting time, followed by 10 and 20 °C, whereby 30 °C of mixing water temperature shortened the initial setting time up to 30%, or the average of 50–60 min dropped for every 10 °C of mixing water temperature difference compared to mortar samples activated with 0 °C of water which explained the influence of mixing water temperature in controlling the initial setting time of fresh one-part AAMs.

Askarian et al.<sup>10</sup> reported that one-part alkali-activated paste composed of fly ash and slag only did not set within the first 24 h. With the inclusion of ordinary Portland cement (OPC), the initial and final setting time for fresh paste was significantly decreased. The superplasticizer (SP) effect on one-part alkali-activated slag mortar was studied by Luukkonen et al.<sup>14</sup> and found that the lignosulfonate-based superplasticizer was the most suitable retarder admixture to lengthen the setting time of the AAMs slag mortar by increasing the SP and water amount. The delay in setting time was due to adsorption activities by the SP towards binder particles under an alkaline environment<sup>15</sup>. Coppola et al.<sup>16</sup> reported the influence of admixtures in one-part alkali-activated slag where the calcium oxide, CaO used as an expansive agent for the paste samples reduced both initial and final setting time and the combination of CaO and shrinkage reducing admixture (SRA) effectively decreased shrinkage level of the mortar samples.

Wang et al.<sup>5</sup> reported that three systems were applicable for the compatibility between repair material and its substrate: mechanical interlocking, Van de Waals forces, and chemical bonds. Teixeira et al.<sup>17</sup> explained the requirement for repair mortars according to EN 1504 standard used in Europe and highlighted the importance of AAMs properties in fresh and hardened states for sustainable repair and reinforcement elements.

Study on one-part AAMs has been conducted extensively at the synthesis stage to determine the new kind of by-products, chemical activator, and compositions. However, the usage of one-part AAMs as concrete repair materials have not been studied profoundly. Nevertheless, One-part AAMs can be used in concrete and are

Chemical compositions (%)				
Chemical compositions (%) OPC	CaO	SiO <sub>2</sub>	Fe <sub>2</sub> O <sub>3</sub>	MgO
	60–65%	17–25%	0.5–6.0%	0.1–4.0%
	Al <sub>2</sub> O <sub>3</sub>	Na <sub>2</sub> O + K <sub>2</sub> O	SO <sub>3</sub>	
	3–8%	0.2–1.0%	1.0–2.75%	

**Table 1.** Chemical compositions (%) of Ordinary portland cement (OPC) obtained from the cement manufacturer.

Samples	Binder			Alkali activated	Admixtures			Design ratio	
	FA (%)	GGBFS (%)	OPC (%)	K <sub>2</sub> CO <sub>3</sub> (%)	SRA (%)	CaO (%)	SP (%)	Binder to sand	Binder to water
Mix 1	25	5	70	6	2	1	1	1	0.49
Mix 2	25	5	70	1.8	–	–	–	1	0.50
Mix 3	25	5	70	1.6	0.3	0.15	1	1	0.40
Mix 4	25	5	70	2.0	0.9	0.45	1	1	0.40
Mix 5	25	5	70	1.8	0.6	0.30	1	1	0.40
Mix 6	25	5	70	1.6	0.3	0.15	1	1	0.35
Mix 7	25	5	70	1.6	0.3	0.15	1	1	0.30

**Table 2.** Mix design of one-part alkali-activated repair mortars.

helpful as mortar. In this experiment, a one-part alkali-activated mortar was carried out to establish its potential as a concrete repair material in terms of compressive strength and also the mortar's bonding strength which was evaluated by pull-off bonding strength method against OPC substrate to satisfy class R3 and Class R4–EN1504-3 specifications for structural concrete repair materials. In addition, the volume ratio for aluminosilicate precursors was kept constant (25% FA, 5% GGBFS and 7% OPC). The main objective of this paper is to determine the capability of the one-part alkali-activated mortar used as a patching mortar as an alternative concrete repair material product for structural repair purposes class R3 and R4 EN1504-3 specifications.

## Materials and method

Class f–Fly Ash (FA) and Ground Granulated Blast Furnace Slag (GGBFS) were used as precursors under ASTM C618 and ASTM C989, respectively. Table 1 shows the chemical composition of Ordinary Portland cement (OPC), which was added as the primary binder source and activated with alkali-activated powder-potassium carbonate (K<sub>2</sub>CO<sub>3</sub>, Purity ≥ 90%). Natural sand was used as fine aggregates with a specific gravity of 2.67 and an average particle size of 90.23 μm (D50). In addition, a commercial ethylene glycol type of shrinkage reducing admixtures (SRA) and calcium oxide (CaO) was added as admixture and expansion agent, respectively, in the form of solid powder. At the same time, the sodium lignosulfonate powder-based superplasticizer (SP) was also used as a water reducer in high-strength concrete.

**Mix Proportions.** The experimental study was conducted to understand the effect of aluminosilicate precursor and OPC as the main binder, activated with a different low dosage of alkali activator powder. Adjusted water content to improve the mortar workability, compressive strength, and bonding strength for patch mortar application and meet the Class R3, EN-1504 standard for structural concrete repair material.

All the samples were marked as Mix 1 to Mix 7 and consisted of FA, GGBFS and OPC as main precursors with different volume percentages. The admixtures proportion for every sample was added into the mortar samples between 1.0 to 15.0 wt% of weight based on total aluminosilicate precursors (binder) weight. The water to binder ratio ranged from 0.30 to 0.50, and the binder to sand ratio was constant at 1 to 1 to produce the mortar applied to all mixtures. The compositions of one-part alkali-activated mortars are further elucidated in Table 2.

**Sample preparations.** An electric mixer, EX-EM2000 EXTRAMAN 2000 W, was used to prepare all mixes. The FA, GGBFS, PCC, K<sub>2</sub>CO<sub>3</sub>, SRA, CaO, Sodium Lignosulfonate (SP) and fine aggregates were blended in the mixture for 2 min according to their sample of mix compositions. After that, water was added slowly to the mixtures and continued blending for another 3 min to ensure the mortar paste was uniform. Then, all the fresh mortars were immediately cast into a 50 mmx50 mmx50 mm cube for the compression strength test. All filled moulds were vibrated for 2 min using a shaking table. The mixtures were demoulded after 24 h before being cured at an ambient lab temperature of 29 °C, with Relative Humidity (RH) of 65% until the testing day on 7, 14 and 28 days of curing age.

For setting time test of fresh mortar, it follows the same procedure. Still, after 3 min of mixing with water, the samples are immediately cast into Vicat moulds (Fig. 1) before the penetrating process begins at a specific time interval. The preparation of fresh mortar for setting time and pull-off strength test was under a controlled

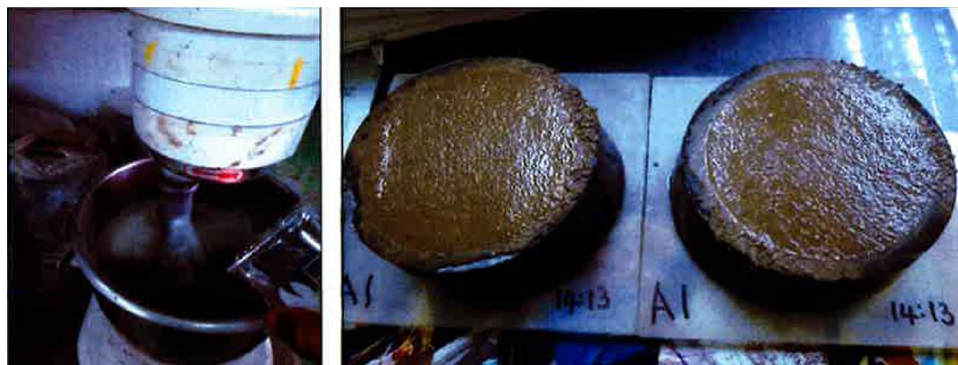


**Figure 1.** Vicat penetration test for setting one-part alkali-activated repair mortar.

Mix samples	Initial setting time (min)	Final setting time (min)
Mix 1	320	401
Mix 2 (control sample)	243	319
Mix 3	177	302
Mix 4	170	289
Mix 5	175	295
Mix 6	158	279
Mix 7	147	274

**Table 3.** Initial and final setting time of one-part alkali-activated repair fresh mortar.

temperature of 21 °C and Relative Humidity (RH) > 90%. The age of the concrete substrate is 56 days, and the age of the test specimen is 28 days after curing age.

**Experimental procedures.** The one-part AAMs mortar was mixed following the dry mixing method in previous studies. The compressive strength of hardened mortar was evaluated at 7-d, 14-d, and 28-d curing age to study mechanical strength and properties. The compression test machine AUTOMAX5 was used at a loading rate of 1000 N/s. The mean value of three readings of each sample produced in triplicate for every test was recorded and taken as their final strength value. Test on the setting time of mortar was conducted by penetrating the fresh mortar in Vicat moulds, set with 120 min for its first interval. The height of the Vicat mould is 40 ± 0.2 mm, and the initial setting time was recorded when the 34 ± 3 mm was obtained, and the final setting time was recorded at 0.5 mm penetration depth obtained as per MS EN 196-3: 2016 specification. A 50 mm dolly size was used for the pull-off strength test, and the core drill depth was 15 mm into the substrate material as per BS EN 1542:1999 requirement.

## Result and discussion

**Setting time of fresh mortar.** The initial setting time for the one-part alkali-activated mortar is essential for in situ application. The initial setting time is when fresh mortar starts losing its plasticity and the final setting time is when the mortar completely loses its plasticity. Too long of an initial setting time will cause mortar or concrete to lose strength. This parameter will control the handling process from mixing to the casting stage. The initial setting time for Mix 2 (control sample) was 243 min or 4 h compared with Mix 7, which recorded 147 min, a 39% reduction in initial setting time as shown in Table 3. The result also met the previous report's findings on the initial setting time range for one-part AAMs between 23 and 150 min<sup>11</sup>. Higher water to binder ratios for Mix 1 and Mix 2 affect the overall setting time of the fresh mortar, where the initial setting time was recorded at 320 min and 243 min, respectively. When the water content is reduced to a 0.40 water-binder ratio, both initial and final settings for Mix 3, Mix 4 and Mix 5 decrease in the range of 177 min to 170 min for the initial setting time and between 302 to 289 min or about 5 h for the final setting time. The fastest initial setting time was recorded for sample Mix 7 at 147 min, followed by sample Mix 6 at 158 min, where both samples contained low water-to-binder ratios of 0.30 and 0.35. As illustrated in Fig. 2, the overall pattern of initial setting time decreased against lower water (W/B) content levels.

It was reported that the common problem with one-part AAMs was they were set too fast and had a typical initial setting time in the range of 60 min, as reported by<sup>18</sup>. The longer setting time recorded in this experiment agrees with<sup>12</sup> that the presence of slag and solid potassium carbonate could reduce the workability of a one-part geopolymer. As shown in Fig. 3, three mortar samples Mix 3, Mix 4 and Mix 5, have similar water to binder ratios of 0.40. Still, the longer initial setting time for Mix 3 was mainly contributed by the low alkali activator dosage

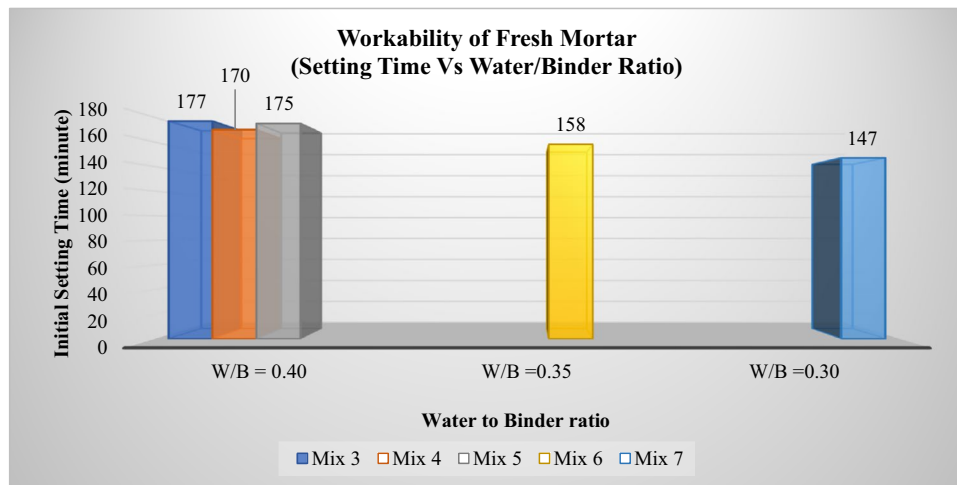


**Figure 2.** Initial time for a one-part alkali-activated repair mortar (Setting time Vs. Water/Binder ratio).

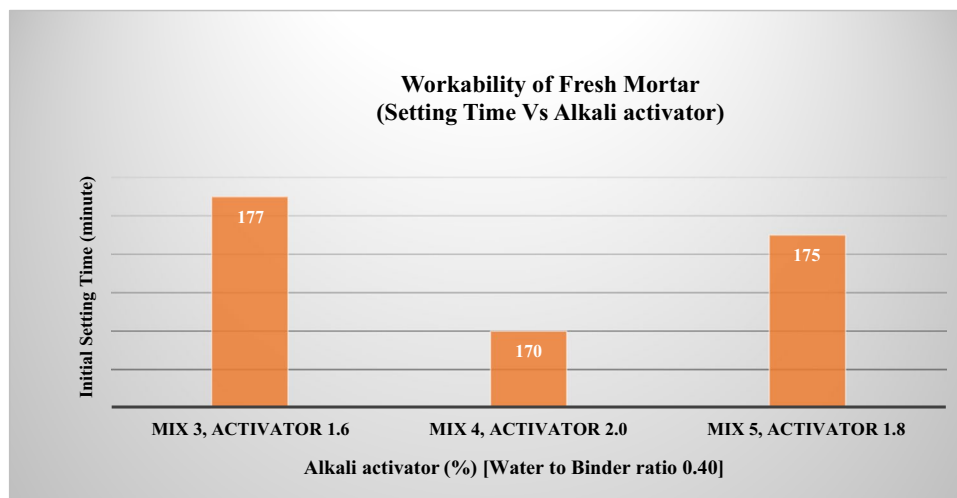


**Figure 3.** Initial setting time for a one-part alkali-activated repair mortar (Setting time Vs. Alkali activator).

of potassium carbonate, which only consists of 1.6% of total precursors weight because the higher the activator dosage, the shorter the setting time of one-part AAMs. Furthermore, all samples were prepared under a colder controlled temperature of 21 °C, which could be why lengthens the initial setting time due to the thermal effect factor as in the agreement with<sup>13</sup>. Furthermore, 70% OPC content used as primary aluminosilicate sources for the binder was also the possible reason for a longer initial setting time due to a large group of cement particles occurring when the former reacts with water for the hardening process subsequently increased yield stress and plastic viscosity of the mortar for a longer setting time<sup>19</sup>.

Potassium carbonate powder used in this experiment is a chemically non-hygroscopic alkaline type and reported to have a minimal impact than typical hygroscopic-based activators such as sodium hydroxide and sodium silicate that could harm the product in terms of efflorescence and water absorption level<sup>10</sup>. However, the slower dissolution of solid potassium carbonate activators, especially K ions in water, caused a slow hardening process at an early stage<sup>20</sup>. This experiment also confirmed the additional 1% (of binder weight) lignosulfonate-superplasticizer (SP) and higher water content could prolong the setting time of one-part alkali-activated mortar reported by<sup>14</sup>. Activated by a constant low dosage of alkali activator in resulting longer initial setting time of more than 100 min for both mortar samples respectively, the difference composition between the control samples Mix 2 and Mix 3 was that the addition of SRA and CaO provided more calcium to Mix 3 for a rapid reaction at an early stage on top of the existing 70% OPC for all mortar samples Mix 1 to Mix 7. Thus, SP was added to control the setting time of all samples with rich calcium examined in this experiment.

Comparing the initial setting time between Mix 2 (without admixtures) and Mix 1, 3–7, the strong influence of admixtures can shorten the setting time and improve the mechanical strength of one-part alkali-activated

Sample references	Compressive strength at 7 days (N/mm <sup>2</sup> )	Compressive strength at 14 days (N/mm <sup>2</sup> )	Compressive strength at 28 days (N/mm <sup>2</sup> )
Mix 1	19.22	20.92	26.35
Mix 2	18.16	17.50	9.26
Mix 3 (control sample)	23.76	22.41	26.75
Mix 4	19.16	19.03	14.41
Mix 5	18.0	18.83	13.88
Mix 6	21.90	29.24	36.27
Mix 7	21.45	31.14	36.80

**Table 4.** Compressive strength at 7, 14 and 28 days of curing age.

mortar. However, without admixtures, the control sample Mix 2 has recorded a longer initial setting time and low compressive strength at 28 days of curing age and does not comply with class R3 EN1504-3 standard.

It is worth noting that the non-hygroscopic alkaline with low alkali activator content of 1.6% was used in this experiment yet achieved not only mechanical strength comparable to the one-part AAMs activated by a conventional higher dosage of hygroscopic activator type but also a more extended initial setting for the mortar to become not too short or not too long and improved the setting time issues on one-part AAMs system.

**Compressive strength.** Table 4 above shows the compressive strength of one-part alkali-activated mortar composed of mixed ordinary Portland cement (OPC), by-products of fly ash and ground granulated blast furnace slag (GGBFS). All samples were activated by a low alkaline activator which is not corrosive, greener, yet cheaper. Mix 3 was referred to as a control sample based on the workability result activated by the lowest dosage of alkali activator at water to binder ratio of 0.40. At the same time, Mix 2 was composed without admixtures.

At the early stage, the highest compressive strength was recorded for Mix 3 with 23.76 N/mm<sup>2</sup>, followed by sample Mix 6 and sample Mix 7, 21.90 N/mm<sup>2</sup> and 21.45 N/mm<sup>2</sup>, respectively. It is understood that one-part AAMs have a rapid reaction at an early stage due to the dissolution process of solid alkali activator with the presence of rich-calcium oxide content in precursors. The least amount of slag in this experiment, however, has been compensated by adding calcium oxide (CaO) powder as an expansive agent<sup>16</sup> together with the higher volume of calcium-rich OPC to provide more calcium, subsequently offering additional nucleation sites for dissolved materials under rapid dissolution process at an early stage, contributed to the fast hardening<sup>10,21</sup>.

At 14 days of curing age, samples Mix 1, Mix 5, Mix 6, and Mix 7 recorded an increment in strength, contrary to samples Mix 2 (without admixtures), Mix 3 (control sample) and Mix 4, which recorded slightly decreased strength over time. Mix 7 recorded the highest compressive strength with 31.14 N/mm<sup>2</sup>, followed by Mix 6 with 29.24 N/mm<sup>2</sup> and Mix 5 with 22.42 N/mm<sup>2</sup>.

Further examination of the mortar's mechanical strength later confirmed the strong growth over samples Mix 1, Mix 3, Mix 6, and Mix 7. The highest compressive strength recorded was 36.80 N/mm<sup>2</sup> for Mix 7. The compressive strength slightly dropped for Mix 6 with 36.27 N/mm<sup>2</sup>, followed by Mix 3 and Mix 1, which recorded not much difference in the strength, 26.75 N/mm<sup>2</sup> for the former and 26.35 N/mm<sup>2</sup> for the latter. The compressive strength at 28 days of curing age for all four repair mortar samples also complied with a minimum requirement for class R3, EN1504-3 specification for concrete structural repair materials. On the other hand, Mix 2, Mix 4, and Mix 5 continue suffered strength inclination between 30 and 50% over time.

The early mechanical strength of one-part AAMs contributes to the fast reaction due to the rapid dissolution of solid alkali activator in the binder to generate heat and make them lose their plasticity earlier than the two-part AAMs system. Consistent compressive strength levels in the range of 18 N/mm<sup>2</sup> to 21 N/mm<sup>2</sup> recorded at an early stage proved the rapid geopolymerization process begins immediately after water is added. Samples Mix 3, Mix 4, and Mix 5 were composed with a low alkaline activator (below 2.0% dosage). In contrast, sample Mix 2 activated without admixtures caused low compressive strength compared with the samples containing added admixtures. Samples Mix 4 and Mix 5 mortar have a double and triple volume of SRA and CaO compared to the sample Mix 3 mortar, where SP dosage was kept constant at 1% for all samples. Samples Mix 1 – Mix 5 had compressive strength rise and dropped between – 5% to + 10% within 7 days to 14 days of age, in contrast with common hardened mortar, which is usually springing up to its strength and achieve 90% compressive strength at 14 days of curing age.

The reduction in activator concentration would decrease the mechanical strength of hardened one-part AAMs<sup>22</sup>; thus, the dosage of alkali activator increased to 1.8% and 2.0% for samples Mix 4 and Mix 5 and additional Ca was obtained from SRA and CaO powder. However, the trend showed that dissolution of alkali activator for both samples Mix 4 and Mix 5 reached its peak at 7 days, whereby the lack of alkali activator did not make sufficient to react with the excessive amount of calcium resulting in incomplete reaction and inadequate binding between precursor and aggregate, creating more pores and crack propagation prevent the compressive strength growth at a later stage. Also, declined compressive strength over time was found in the fact that one-part AAMs were not water-resistant compared to the two-part AAMs system and subsequently encountered a slow hydration rate<sup>8</sup>, associated with a higher water/binder ratio of 0.4 to 0.5, in addition to the low dosage of alkali activator used to compose these mortar samples.

Moreover, samples Mix 6 and Mix 7 recorded the highest compressive strength, about 36 N/mm<sup>2</sup>, which is higher than the 25 N/mm<sup>2</sup> set as minimum compressive strength at 28 days of age for class R3-EN1504-3

Samples references	Tensile bond strength (MPa)	Mode of failure
Mix 3 (control samples)	1.885	A and B interface/Adhesion
Mix 6	1.757	A and B interface/Adhesion
Mix 7	2.565	A-substrate/Cohesion

**Table 5.** Average pull-off bond strength results in protection and repair products of concrete structures at 28-d of curing age of one-part alkali-activated repair mortar.



**Figure 4.** Pull off mortar samples after 28 days of age (Mix 7).

specifications. Both mortar samples have similar mix compositions except for the water/binder ratio, 0.3 for Mix 7 and 0.35 for Mix 6.

Likewise, it is interesting to know that the low dosage of alkali activator has activated both mortar samples with 1.6% only than sample Mix 1 mortar activated by 6% yet achieved consistent and higher compressive strength. Insufficient Si and Al ions would dissolve due to a low alkalinity environment, and the resulting reduction in aluminosilicate precursors subsequently affects the rates of geopolymeric reaction<sup>23</sup>. On the other hand, Coppola et al.<sup>24</sup> reported that a higher dosage of alkali activator is required to lower the water demand. The lower alkaline activator incorporated with lower water to binder ratio contributed to the higher compressive strength. Li et al.<sup>19</sup> however, explaining the effect of the water to binder ratio plays a vital role in determining the rheological parameters of a one-part AAMs system. A lower w/b ratio will significantly increase yield stress and plastic viscosity for one-part AAMs and ordinary Portland cement (OPC). Luukkonen et al.<sup>25</sup> claimed that less water will increase the compressive strength of one-part AAMs, and adding a superplasticizer can further reduce and control the water. This experiment also confirmed that the presence of CaO and SRA restricted the growth of mechanical strength of one-part alkali-activated repair mortar as in the agreement with Coppola et al.<sup>16</sup>

**Pull-off bonding strength.** Based on the compressive strength result shown in Table 4, which was recorded above 25 MPa, only 3 samples were selected to be tested with compression. Pull-off bond strength for all samples complied with the required strength requirement Class R3–EN1504-3 standard for structural concrete repair materials. The highest pull-off bond strength was recorded for sample Mix 7 mortar with 2.565 MPa (Class R4–EN504-3 standard), Mix 3 with 1.885 MPa and Mix 6 with 1.757 MPa, as shown in Table 5 above. This experiment's pull-off test also confirmed the adhesion mode of failure at the interface between mortar and concrete substrate for Mix 3 and Mix 6, a cohesion mode of failure for Mix 7 (Fig. 4). Both types of failure are considered ideal types of failure classification for the pull-off test as per EN1542 standard, indicating the one-part AAMs repair mortar as a good bonding material. In addition, the higher pull-off bond strength recorded indicates that this type of mortar can provide higher adhesive force<sup>23</sup>. The variety of material compositions sought for mortar mix design in this experiment influences the bond strength of the one-part AAMs system<sup>26</sup>.

The reaction between alumina and silica from FA and calcium ions from ordinary Portland cement (OPC) could form C–(A)–S–H gel co-existed with N–A–S–H, enhancing the alkali-activated materials (AAMs) properties as reported by Phoo-ngernkham et al.<sup>2</sup>. The surface of OPC substrates is rich with calcium hydroxide (Ca(OH)<sub>2</sub>) will bond chemically by reacting with the alkaline one-part alkali-activated repair mortar for positive ions such as Ca<sup>++</sup> to balance the negative charge of the Al<sup>3+</sup> and Si<sup>4+</sup> from FA and GGBFS for geopolymeric reaction, in addition of the formation of calcium carbonate hydrate from the reaction between potassium carbonate powder and calcium hydroxide of OPC later improved the adherence between repair mortar and substrates<sup>7,27</sup>. Additional C–S–H and/or C–A–S–H gel was established with N–A–S–H gel enhancing the bonding concentration at the contact area<sup>28</sup>.

This experiment proved that one-part alkali-activated repair mortar, known as the third mortar category, can be used for concrete structural repair to replace conventional organic and inorganic binders in the construction sector<sup>29</sup>. Once again, the low dosage of alkaline activator used in this experiment successfully activated the one-part AAMs system and performed better than the two-part AAMs system counterpart.

## Conclusions

The experiments in this report were carried out to investigate the mechanical properties of compressive and the pull-off bonding strength of one-part alkali-activated mortar against OPC substrate used as concrete patching materials as stated in EN1504-3 guideline for structural concrete repair material specifications. Hybrid precursors of fly ash, ground granulated blast furnace slag and ordinary Portland cement (OPC) were used as the source of aluminosilicate binder. A low alkali activator of potassium carbonate in powder form was used to initiate the geopolymerization process and further adjusted with some admixtures, water, and aggregates for optimum mortar mix design. To maintain workability, a longer setting time is essential for transporting a large quantity of mortar to the construction site. The initial setting time for the mortar sample in this experiment achieved 147 min, in line with previous reports on the setting time of one-part AAMs. In addition, the highest compressive strength and bonding strength at 28 days of age were recorded for Mix 7 with 36.8 N/mm<sup>2</sup> and 2.565 MPa, respectively. Therefore, they complied with Class R4 – EN1504 for structural concrete repair materials.

Another conclusion that can be highlighted in this paper is as follow:

1. Two-part AAMs composed of a single precursor such as fly ash, slag or metakaolin only have higher early compressive strength and better mechanical properties but are not suitable for concrete repair material due to lower pull-off bonding strength. In addition, two-part AAMs mortar activating with sole precursors also does not comply with mechanical requirements for repair materials (pull-off strength class R3 and R4, EN1504 standard) and is often delaminated. However, all these industrial wastes can be utilized by incorporating Portland cement in one-part AAMs technology to promote better chemical bonding between repair mortar and concrete substrates at the interface zone in terms of pull-off bonding strength.
2. A short initial setting time for AAMs mortar is the main problem for supplying process at the construction site. Therefore, a longer initial setting time for the one-part alkali-activated repair mortar recorded in this experiment is beneficial for the in-situ application. The main aluminosilicate precursors of mortar sample Mix 7 were 25% FA, 5% GGBFS and 70% OPC. They exhibited 147 min for the initial setting time within the range of 23–150 min as reported for the initial setting time of one-part AAMs. Furthermore, it is worth noting that countries with hot and dry climates possess a higher rate of hydration. This result enlightened the sustainability of this type of repair mortar which has a flexible range of initial to final setting time when exposed to the higher surrounding temperature that may shorten the setting time of the fresh mortar up to a 30% reduction. Therefore, it is applicable to be applied in hot climate countries.
3. A lower dosage of solid admixtures is used to enhance the fresh and mechanical properties of one-part alkali-activated mortar that meet the requirement for class R3 and class R4, EN1504-3 specifications for structural concrete repair materials together with the optimum admixture dosage of 0.3% for SRA, 0.15% for CaO and 1% of SP from the total weight of precursors. In addition, lower water to binder ratio at 0.30 has increased the repair mortar's pull-off bonding strength following higher compressive strength recorded at 28 days of curing age.
4. The repair mortar assessed in this experiment is composed of fly ash and slag as part of the mix composition, whereby this type of by-product can be developed further to enhance its potential and exploited as cement binder used as concrete patching materials, subsequently overcoming the limitations on the pull-off bonding strength properties as the weakest part of the system as reported. Therefore, future studies should focus on the microstructure analysis of the one-part AAMs mortar to enhance their potential to be used as a concrete repair material.

## Data availability

The datasets used and/or analyzed during the current study are available from the corresponding author upon reasonable request.

Received: 2 June 2022; Accepted: 5 September 2022

Published online: 23 September 2022

## References

1. Pacheco-Torgal, F., Melchers, R. E., Shi, X., De Belie, N., Van Tittelboom, K & Sa'ez, A. (2018) Front-matter In: Eco-Efficient Repair and Rehabilitation of Concrete Infrastructures, Elsevier <https://doi.org/10.1016/b978-0-08-102181-1.00026-5>.
2. Phoo-Ngernkham, T., Hanjitsuwan, S., Li, L. Y., Damrongwiriyanyap, N. & Chindaprasirt, P. Adhesion characterization of Portland cement concrete and alkali-activated binders. *Adv. Cem. Res.* **31**(2), 69–79. <https://doi.org/10.1680/jadcr.17.00122> (2019).
3. Luo, Z., Li, W., Wang, K., Castel, A. & Shah, S. P. Comparison on the properties of ITZs in fly ash-based geopolymer and Portland cement concretes with equivalent flowability. *Cem. Concr. Res.* **143**(February), 106392. <https://doi.org/10.1016/j.cemconres.2021.106392> (2021).
4. Jia, L., Zhao, F., Yao, K. & Du, H. Bond performance of repair mortar made with magnesium phosphate cement and ferroaluminate cement. *Constr. Build. Mater.* **279**, 122398. <https://doi.org/10.1016/j.conbuildmat.2021.122398> (2021).
5. Wang, J. *et al.* Effects of fly ash on the properties and microstructure of alkali-activated FA/BFS repairing mortar. *Fuel* **256**(July), 115919. <https://doi.org/10.1016/j.fuel.2019.115919> (2019).

6. Kramar, S., Šajna, A. & Ducman, V. Assessment of alkali activated mortars based on different precursors with regard to their suitability for concrete repair. *Constr. Build. Mater.* **124**, 937–944. <https://doi.org/10.1016/j.conbuildmat.2016.08.018> (2016).
7. Robayo-Salazar, R., Jesús, C., Mejía de Gutiérrez, R. & Pacheco-Torgal, F. Alkali-activated binary mortar based on natural volcanic pozzolan for repair applications. *J. Build. Eng.* **25**(April), 100785. <https://doi.org/10.1016/j.jobbe.2019.100785> (2019).
8. Peng, M. X. *et al.* Alkali fusion of bentonite to synthesize one-part geopolymeric cements cured at elevated temperature by comparison with two-part ones. *Constr. Build. Mater.* **130**, 103–112. <https://doi.org/10.1016/j.conbuildmat.2016.11.010> (2017).
9. Nunes, V. A., Borges, P. H. R. & Zanotti, C. Mechanical compatibility and adhesion between alkali-activated repair mortars and Portland cement concrete substrate. *Constr. Build. Mater.* **215**, 569–581. <https://doi.org/10.1016/j.conbuildmat.2019.04.189> (2019).
10. Askarian, M., Tao, Z., Adam, G. & Samali, B. Mechanical properties of ambient cured one-part hybrid OPC-geopolymer concrete. *Constr. Build. Mater.* **186**, 330–337. <https://doi.org/10.1016/j.conbuildmat.2018.07.160> (2018).
11. Luukkonen, T., Abdollahnejad, Z., Yliniemi, J., Kinnunen, P. & Illikainen, M. Comparison of alkali and silica sources in one-part alkali-activated blast furnace slag mortar. *J. Clean. Prod.* **187**, 171–179. <https://doi.org/10.1016/j.jclepro.2018.03.202> (2018).
12. Liu, C., Yao, X. & Zhang, W. Controlling the setting times of one-part alkali-activated slag by using honeycomb ceramics as carrier of sodium silicate activator. *Constr. Build. Mater.* **235**, 117091. <https://doi.org/10.1016/j.conbuildmat.2019.117091> (2020).
13. Almkhadme, M. & Soliman, A. M. Effects of mixing water temperatures on properties of one-part alkali-activated slag paste. *Constr. Build. Mater.* **266**, 121030. <https://doi.org/10.1016/j.conbuildmat.2020.121030> (2021).
14. Luukkonen, T., Abdollahnejad, Z., Ohenoja, K., Kinnunen, P. & Illikainen, M. Suitability of commercial superplasticizers for one-part alkali-activated blast-furnace slag mortar. *J. Sustain. Cem. Mater.* **8**(4), 244–257. <https://doi.org/10.1080/21650373.2019.1625827> (2019).
15. Alrefaei, Y., Wang, Y. S. & Dai, J. G. The effectiveness of different superplasticizers in ambient cured one-part alkali activated pastes. *Cem. Concr. Compos.* **97**(September 2018), 166–174. <https://doi.org/10.1016/j.cemconcomp.2018.12.027> (2018).
16. Coppola, L. *et al.* The combined use of admixtures for shrinkage reduction in one-part alkali activated slag-based mortars and pastes. *Constr. Build. Mater.* **248**, 118682. <https://doi.org/10.1016/j.conbuildmat.2020.118682> (2020).
17. Teixeira, O. G., Geraldo, R. H., da Silva, F. G., Gonçalves, J. P. & Camarini, G. Mortar type influence on mechanical performance of repaired reinforced concrete beams. *Constr. Build. Mater.* **217**, 372–383. <https://doi.org/10.1016/j.conbuildmat.2019.05.035> (2019).
18. Adesanya, E., Ohenoja, K., Di Maria, A., Kinnunen, P. & Illikainen, M. Alternative alkali-activator from steel-making waste for one-part alkali-activated slag. *J. Clean. Prod.* **274**, 123020. <https://doi.org/10.1016/j.jclepro.2020.123020> (2020).
19. Li, L., Lu, J. X., Zhang, B. & Poon, C. S. Rheology behavior of one-part alkali activated slag/glass powder (AASG) pastes. *Constr. Build. Mater.* **258**, 120381. <https://doi.org/10.1016/j.conbuildmat.2020.120381> (2020).
20. Samarakoon, M. H., Ranjith, P. G., Duan, W. H. & De Silva, V. R. S. Properties of one-part fly ash/slag-based binders activated by thermally-treated waste glass/NaOH blends: A comparative study. *Cem. Concr. Compos.* **112**(December 2019), 103679. <https://doi.org/10.1016/j.cemconcomp.2020.103679> (2020).
21. Shah, S. F. A., Chen, B., Oderji, S. Y., Haque, M. A. & Ahmad, M. R. Improvement of early strength of fly ash-slag based one-part alkali activated mortar. *Constr. Build. Mater.* **246**, 118533. <https://doi.org/10.1016/j.conbuildmat.2020.118533> (2020).
22. Yousefi Oderji, S., Chen, B., Ahmad, M. R. & Shah, S. F. A. Fresh and hardened properties of one-part fly ash-based geopolymer binders cured at room temperature: Effect of slag and alkali activators. *J. Clean. Prod.* **225**, 1–10. <https://doi.org/10.1016/j.jclepro.2019.03.290> (2019).
23. Ding, Y. C., Cheng, T. W. & Dai, Y. S. Application of geopolymer paste for concrete repair. *Struct. Concr.* **18**(4), 561–570. <https://doi.org/10.1002/suco.201600161> (2017).
24. Coppola, L., Coffetti, D. & Crotti, E. Pre-packed alkali activated cement-free mortars for repair of existing masonry buildings and concrete structures. *Constr. Build. Mater.* **173**, 111–117. <https://doi.org/10.1016/j.conbuildmat.2018.04.034> (2018).
25. Luukkonen, T., Abdollahnejad, Z., Yliniemi, J., Kinnunen, P. & Illikainen, M. One-part alkali-activated materials: A review. *Cem. Concr. Res.* **103**(October 2017), 21–34. <https://doi.org/10.1016/j.cemconres.2017.10.001> (2018).
26. Fahim Huseien, G., Mirza, J., Ismail, M., Ghoshal, S. K. & Abdulameer Hussein, A. Geopolymer mortars as sustainable repair material: A comprehensive review. *Renew. Sustain. Energy Rev.* **80**(May), 54–74. <https://doi.org/10.1016/j.rser.2017.05.076> (2017).
27. Zhang, H. Y., Kodur, V., Wu, B., Cao, L. & Wang, F. Thermal behavior and mechanical properties of geopolymer mortar after exposure to elevated temperatures. *Constr. Build. Mater.* **109**, 17–24. <https://doi.org/10.1016/j.conbuildmat.2016.01.043> (2016).
28. Phoo-ngernkham, T. *et al.* Low cost and sustainable repair material made from alkali-activated high-calcium fly ash with calcium carbide residue. *Constr. Build. Mater.* **247**, 118543. <https://doi.org/10.1016/j.conbuildmat.2020.118543> (2020).
29. Pacheco-Torgal, F., Abdollahnejad, Z., Miraldo, S., Baklouti, S. & Ding, Y. An overview on the potential of geopolymers for concrete infrastructure rehabilitation. *Constr. Build. Mater.* **36**, 1053–1058. <https://doi.org/10.1016/j.conbuildmat.2012.07.003> (2012).

## Acknowledgements

Special thanks to Makmal Kerja Raya Malaysia (MKRM), Testech Sdn Bhd (Material Laboratory Test) and Sabah Public Service Department (JPANS), Malaysia, for contributing to the outcome of this experiment.

## Author contributions

All authors reviewed the manuscript.

## Competing interests

The authors declare no competing interests.

## Additional information

**Correspondence** and requests for materials should be addressed to E.Y.

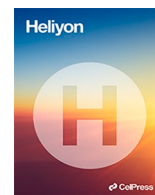
**Reprints and permissions information** is available at [www.nature.com/reprints](http://www.nature.com/reprints).

**Publisher's note** Springer Nature remains neutral with regard to jurisdictional claims in published maps and institutional affiliations.



**Open Access** This article is licensed under a Creative Commons Attribution 4.0 International License, which permits use, sharing, adaptation, distribution and reproduction in any medium or format, as long as you give appropriate credit to the original author(s) and the source, provide a link to the Creative Commons licence, and indicate if changes were made. The images or other third party material in this article are included in the article's Creative Commons licence, unless indicated otherwise in a credit line to the material. If material is not included in the article's Creative Commons licence and your intended use is not permitted by statutory regulation or exceeds the permitted use, you will need to obtain permission directly from the copyright holder. To view a copy of this licence, visit <http://creativecommons.org/licenses/by/4.0/>.

© The Author(s) 2022



## Research article

# The effect of water-to-binder ratio (W/B) on pore structure of one-part alkali activated mortar

Eddy Yusslee<sup>\*</sup>, S. Beskhyroun

Auckland University of Technology (AUT), Auckland, 1010, New Zealand



## ARTICLE INFO

## Keywords:

Microstructure  
Scanning electron microscope (SEM)  
Dispersive X-Ray analysis (XRD)  
Calcium oxide (CaO)  
Superplasticizer (SP)

## ABSTRACT

One-part alkali-activated materials (AAMs) are alternative cementitious materials to respond to the shortcoming of conventional two-part systems. Combining aluminosilicate precursor by-products with ordinary Portland cement (OPC) helps develop a robust performance. It can potentially be used as a patching product for concrete repair materials.

Mix design for the one-part AAMs in this report is formulated to ensure its application is according to the structural concrete repair materials Class R4, EN1504-3 specification. In addition, the lower alkalinity alkali activator employed is helpful for economic reasons and less harmful to handle. Furthermore, the addition of powdered admixture enhances the performance of hardened products for retarding effect, provides additional calcium for geopolymer reactions, and offers stable mechanical strength. Finally, an adequate water-to-binder (W/B) ratio has completed the mix design proportion and effectively activated the chemical reaction of the dry mixed ingredients in the geopolymerization process for binding purposes.

In this study, the water-to-binder ratio was set in the range of 0.30, 0.35 and 0.40 for all mortar samples at constant mix design formulation and activated by low alkalinity of solid potassium carbonate ( $K_2CO_3$ ). At 0.30 W/B ratio, the setting time is delayed to 120 min but shorter than other W/B ratios. Mechanical strength of the mortar increased over time up to 63 N/mm<sup>2</sup> at 56 days of curing age, recorded low porosity level of 16%, minimal pore structure area of 17.374 m<sup>2</sup>/g and documented above 2.0 MPa of pull-off bonding strength that encounters restrained drying shrinkage and expansion impact at 56 days of age under different curing conditions.

## 1. Introduction

Alkali-activated materials (AAMs) are synthesized from solid aluminosilicate precursors and alkali activator reactions. They become greener alternative cementitious materials to the traditional ordinary Portland cement (OPC) [1]. The AAMs technology does not require clinker for cement hydration products. In contrast, the excessive energy consumption required for clinker up to 5 GJ per ton is needed to burn limestone and silicious materials to manufacture clinker [2]. OPC emits tons of CO<sub>2</sub> that contributes up to 7% of greenhouse gas emissions resulting in global warming and climate crisis [3]. Therefore, industrial by-products in AAMs were introduced as a partial substitute for OPC cement for construction purposes. Conventional AAMs are produced with two products: solid aluminosilicate precursors and the aqueous solution of alkali activators. A higher alkalinity level is required to ensure the best performance of the cementitious products, although it means costly besides consists of highly corrosive chemicals that might risk the

<sup>\*</sup> Corresponding author.

E-mail address: [eddy.yusslee@aut.ac.nz](mailto:eddy.yusslee@aut.ac.nz) (E. Yusslee).

health and safety of the worker. Nevertheless, using a viscous aqueous activator makes it sticky and prevents it from an extensive in-situ application on the construction site. Therefore, the alkaline solution is replaced with a dry alkali activator in one-part AAMs technology for more practical applications.

However, without relevant formula, the one-part AAMs have some significant drawbacks on their long-term durability from the perspective of microstructural and nanostructural levels, which further affect the mechanical strength and durability, causing this type of geopolymer binder is still not famous for a commercial adaption at present [4]. Many reports have been established on the development of one-part AAMs. Fly ash consists of high silica content beneficial to improve the reaction rates in the geopolymerization process. However, it has low calcium, preventing it from strengthening the C-S-H gels for binding products. Adding calcium-rich slag filled the shortage by supplying additional calcium. Combining these two precursors creates an additional 3D network of N-A-S-H gels that co-exist with C-A-S-H gels from the main parent product of C-S-H [5,6]. The FA/GGBFS precursors exhibited higher mechanical strength in one-part AAMs in concrete. However, too high GGBFS content will cause rapid hardening, water loss and higher shrinkage. Thus, OPC, which has a significant amount of calcium, was added in one-part AAMs as part of the precursors. OPC has been widely used as concrete and cementitious mortar. Still, with the presence of by-product precursors, the dependency on the OPC can be reduced, indirectly cutting down its volume. Askarian et al. [7] explained on one-part AAMs activated with the combination of by-product precursors and OPC in concrete can achieve up to 55.0 MPa with 60% of OPC content at 28 days of curing age. However, its mechanical strength in the form of repair mortar is still not yet established. Luukkonen et al. [8] reviewed past studies on hybrid one-part AAMs performance and found that it has higher mechanical strength subject to a different percentage of OPC inclusion. The report comprises a few studies, including a 60% OPC mixed with 40% fly/bottom ash, which has recorded 32 MPa compressive strength at 28 days of curing age but has a higher W/B ratio of 0.5 and a tendency towards shrinkage. In addition, 20% OPC/40% GGBFS and 40% kaolin/bentonite mixtures recorded compressive strength with promising 32 MPa at 28 days of age but had inconsistent W/B ratio of 0.3/0.5 besides being triggered with slightly higher alkali activator (5% solid sodium carbonate). Solid sodium hydroxide was used to activate the mixed precursor composed of OPC/FA/kaolin has an efflorescence effect due to the lower reactivity that causes some sodium to be replaced by calcium. Nevertheless, this hybrid AAMs has recorded sufficient 27 MPa compressive strength (at 28 d). Moreover, in this review report, a patented geopolymeric cement containing 3–30% OPC has been tested at 28 days of age and recorded 35 MPa (30% OPC) of compressive strength. However, the pore structure of the hardened cement for all 43 patented dry mix cement compositions samples was not reported, making its durability uncertain.

In addition, minimal study on the effect of low alkaline activators is used to activate the one-part AAMs cementitious materials because higher alkalinity is more significant to complete the geopolymerization process to produce standard quality cement binder. Excessive alkalinity, on the other hand, causes significant drawbacks to the pore structures of the hardened products and is prone to chemical attacks in a harsh environment. Yang et al. [9] mentioned that the slag paste was activated with a 15% sodium carbonate alkali activator has demonstrated a bigger pore diameter and pore volume than a 10% sodium carbonate, suggesting an excessive alkali activator could be coarse in the pore structures. Another study reported by Azevedo et al. [10] proved that with a higher dosage of alkali activator, the average pore diameter decreased from 24.29 nm to 21.48 nm and documented higher compressive strength up to 41 MPa at 28 days, subsequently supporting the fact that the elevated concentration of alkali activator encourages the hardened product to be more dense and solid without decreasing any unreacted particles.

Still, it has also affected the porosity between 30 and 40% for one-part AAMs composed of calcined commercial kaolin and ceramic waste. Gel pores and capillary pores are two significant matters in the strength of cementitious products where gel pores are unlikely to affect much strength properties but are reported to be influential on creep and shrinkage [11]. However, not all finer pores are harmful. There are four ranges of pore sizes that influence the compressive strength of hardened AAMs, which are classified as harmless pores for sizes below 20 nm, less harmful pores for 20–50 nm, harmful pores if 50–200 nm and more harmful pores if exceed 200 nm [12]. It was reported that two-part AAMs composed with a single metakaolin precursor used as concrete repair materials recorded 2.0 MPa maximum bond strength, but 20% replacement with slag showed an increment in pull-off bonding strength as an indication of mixed aluminosilicate precursors exhibits greater strength than a single type of binder precursor source. Both compositions have documented about 14% porosity level [13].

A fully reacted microstructure pattern on the surface could be formed by increasing the alkali activator in a dry mixture, as reported by Ref. [10]. Yet, excessive alkali content in the mixture can migrate to the surface and react with CO<sub>2</sub> in the atmosphere, consequently causing carbonation. The use of hybrid one-part AAMs concrete studied by Ref. [7] explained that the inclusion of 30% OPC in the mixes has more compact microstructures and less unreacted fly ash particles compared to 0–20% of OPC content but has a more porous structure than 40% and 60% of OPC content. In that report, the compressive strength for one-part AAMs concrete with 60% OPC was about 55.0 MPa. In comparison, adding 40% OPC and 30% OPC in one-part AAMs concrete composed with a single precursor of metakaolin recorded compressive strength of about 52.0 MPa and 50.0 MPa at 28 days of age, which was activated by 3–5% of alkali activator. It is worth mentioning that one-part AAMs composed of single precursors of metakaolin promote a highly porous structure, heterogeneous with unreacted particles that affect its mechanical strength and durability as illustrated in SEM images [14]. In contrast, one-part AAMs composed of two aluminosilicate precursors of fly ash and slag have denser microstructure than fly ash only mixes to confirm that combination of aluminosilicate precursors contributes better mechanical strength, rich in Al but has a substantial low Ca/Si ratio which the hydrated OPC has the advantage to offer a higher Ca/Si ratio and compensate this shortage [15].

At the current stage, one-part AAMs technology mainly focuses on concrete product purposes as an alternative option to the conventional OPC based cementitious. One-part AAMs mortar is to be developed to reduce dependency on OPC mortar and be comparable to other mortar repair materials in the market. Combining more than one precursor was designed to be mixed with the OPC as an initial approach towards promoting green and sustainable construction materials by utilizing industrial by-products as the primary aluminosilicate precursors source and cutting down the volume of OPC as low as it can be. Furthermore, a lower dosage of the

solid alkaline activator is beneficial for a cheaper cost, lower health risks and is not harmful to the environment. First, the effect of a low alkaline activator used in one-part AAMs must be observed on its reaction with main precursors. For this reason, the water-to-binder effect will support the geopolymerization process before conducting a microstructural study to deliver more understanding of the mechanism of its physical property's behaviour. Yusslee et al. [16] reported that the one-part AAMs' mechanical strength has compressive strength and pull-of bond strength level that complied with Class R4-EN1504-3 standard, indicating the potential of this type of geopolymer binder to be used as concrete patch repair mortar. However, the constancy of pore structures of the hardened mortar has yet to be proved; thus, its durability stays doubtful.

It is crucial to understand how pores start created during the hardening process as the water content difference affected the hydration products and strength development. Many researchers activate dry mixtures for one-part AAMs application with different W/B of ratios [7,10,15]. Luukkonen et al. [8] reported that in one-part AAMs, four steps occur after water is added to cementitious materials, beginning with ion exchange, hydrolysis, network breakdown and release of Si and Al, which differentiate the one-part technology from the conventional two-part AAMs. It is worth mentioning that as the geopolymerization cycle continues, the cracks and pores formed at the early stage were filled with an increasing amount of gels and justify compressive strength development over time as the result of a reduction in the accumulated volume of the pores, mainly from C-A-S-H gels phase fill the pore structure to reduce the pore diameter [9,17]. The compressive strength of one-part AAMs containing fly ash, OPC and slag as the main component reacted with an alkali activator to produce gel formation of sodium aluminosilicate hydrate (N-A-S-H), calcium aluminosilicate hydrate (C-A-S-H) and stable 3D network of silico-aluminate structures that enhance polycondensation process that contributes to the higher compressive strength [18].

The addition of commercial solid additives will be added and formulated in the one-part AAMs dry mixtures to control and stabilize the hardened products of mortar. The inclusion of lignosulfonate (LS) type superplasticizer (SP) as high range water reducing admixtures improved the dissolution of slag and reduced water content for better mechanical properties [19,20]. At the same time, the addition of OPC and CaO powder provided more calcium. As a result, it increased the compressive strength on the effect of water content for high compressive strength of AAMs cementitious products [19]. Differences in SP effect on one-part AAMs depend much on the stability behaviour of admixtures in a different type of solid activator. Quicklime-type of Calcium Oxide (CaO) was used as an expansive agent in mortar. Adding the CaO with Shrinkage Reducing Admixture (SRA) has increased the mortar volume instead of shrinking it like conventional cementations materials. Hence, the initial impression on the selection and composition of solid admixtures for the mix design of this study was based on the above findings and the previous study by Ref. [16].

Undeniable, the one-part AAMs have become a popular option in the form of concrete. Current studies largely focus on the synthesis and characterization to determine the new type of precursor-green products. Researchers utilize various types of waste products from agriculture and construction on top of traditional industrial by-products, fly ash, slag and metakaolin [21,22,23,24]. However, the engineering application for the one-part AAMs in other cementitious-based materials has still lagged. On the contrary, mortar composed of two-part AAMs systems has been tested as concrete repair products and reported to have great potential to be commercial in the construction industry [25,26]. The one-part AAMs must be developed not only to focus on their compressive strength but must have robust physical structures, higher consistency and be chemically stable.

The motivation to carry out this study is to analyze further the fact that the higher water content could decrease the yield stress and plastic viscosity of fresh cementitious materials and affect their rheology behaviour and performance at the hardened stage [27]. Nevertheless, the water content in the water-to-binder (W/B) ratio can be adjusted to change yield stress and plastic viscosity. Still, in actual construction, the W/B are conventionally controlled to ensure homogeneity of the mortar or concrete, besides operated practical handling from mixing and transporting to pouring time. Moreover, unlike the conventional one-part AAMs, which traditionally utilize industrial waste or/with natural pozzolanic materials as main aluminosilicate precursors [28], hybrid one-part AAMs, on the other hand, combine the industrial by-products with the OPC used as the main source of the cementitious binder in this study [7,8].

Therefore, the objective of this study is to examine the effect of W/B content on the pore structures of fly ash/slag precursors mixed with the OPC for repair mortar application. This study aims to reduce the porosity level of one-part AAMs by controlling the pore structure size of the hardened mortar with appropriate water content and safeguarding its mechanical strength against shrinkage effect after 28 days of curing age for concrete patching mortar application. Consequently, the hybrid one-part alkali-activated mortar in this study was activated by different W/B ratios of 0.40, 0.35 and 0.30 to encounter previous findings, which stated that alkali-activated materials exhibit higher porosity levels and larger pore size than those reported in ordinary Portland cement (OPC), hence by controlling W/B ratio, it could produce less porous polymeric microstructure [29]. Thus, the optimum W/B ratio will complete the novel contribution of a new mix design formulation for Class R4 - EN1504-3 standard for structural concrete repair mortar application previously developed by the author [30]. Furthermore, the hybrid one-part alkali-activated in this study was activated with low alkalinity of solid alkali activator as part of the research in developing sustainable cementitious product technology by the author for engineering application.

This new type of repair mortar could efficaciously reduce clinker cement production and mitigate the carbon footprint linked to the construction industry. Furthermore, the reported result from this study will stipulate the prerequisite of understanding the interrelationship between compositions of solid materials ingredients with their physical properties when water reacts with a dry mixture of precursors, activators, aggregates, and admixtures (dissolution process of solid particles).

## 2. Materials and method

The experiment conducted in this report used three main aluminosilicate precursors: Fly Ash Class-F as per ASTM C618, Ground Granulated Blast Furnace Slag as per ASTM C989 and ordinary Portland cement (OPC). A powdered Potassium Carbonate (K<sub>2</sub>CO<sub>3</sub>),

purity  $\geq 90\%$ ) was used as the sole alkali activator. First, three solid admixtures were added to the mix design formulation: sodium lignosulfonate as a superplasticizer additive (SP), shrinkage-reducing admixture (SRA) – commercial ethylene glycol type, and calcium oxide power (CaO). Both SRA and CaO control the effect of drying shrinkage of the mortar. Next, natural sands were added to increase the mortar volume and source of additional calcium with a specific gravity of 2.67 and has an average particle size (D50) of 90.23 $\mu\text{m}$ . Finally, water is added to activate the mortar mix for testing in a fresh and hardened state. The chemical compositions of fly ash, slag and ordinary Portland cement are shown in Tables 1–3, respectively. In addition, the particle size for each material is measured with the Laser Diffraction Analysis (LDA) and elaborated in Table 4. This report's materials and mix design formulation were according to the author's previous study in developing novel mix design formulation for one-part alkali-activated mortar used as structural concrete repair materials [16,30].

#### a. Mix proportions

This study aims to reduce the porosity level of the one-part AAMs mortar by analyzing the pore structures of the structural repair mortar activated with one-part AAMs technology at three different water content levels of 0.40, 0.35 and 0.30 water-to-binder (W/B) ratio. Samples were marked with G1 composed with the highest W/B ratio of 0.40 (high water content), G2 has a W/B ratio of 0.35 (medium water content), and G3 has the lowest W/B ratio of 0.30 (low water content). Sample G1 was selected as the control sample in order to compare the pore structure behaviour if the W/B is decreased and its influence on determining the workability in the fresh state, mechanical strength and durability in the hardened state. Three admixtures were added in the mix design with a constant proportion of 0.30% of SRA, CaO (0.15%) and 1% SP from total aluminosilicate precursors weight. The sand content was fixed at 1 (binder/aggregate ratio) for all samples. The mix design formulation of the mortar is shown in Table 5. All samples were cured under controlled temperature per EN1504–3:2005 standard, part 3: structural and non-structural concrete repair materials.

#### b. Sample Preparation

Dry mixtures of FA, GGBFS, OPC, SP, SRA, CaO and fine aggregates were blended for 2 min using an electric mixer (EX-EM2000 EXTRAMAN, 2000W). Next, water was added to the mixtures and blended for 3 min until the mortar paste was uniform. Finally, the fresh mortar the filling into the 40 mm  $\times$  40mm  $\times$  160mm steel moulds for the compression strength test and vibrated for 2 min and dismantled form moulds after 24 h. All samples were cured under the lab-controlled temperature of 20  $\pm$  Celsius and relative humidity of RH > 90% before being tested at the 7th, 28th and 56th days of age. The experiment on the cementitious paste was done without aggregates using Vicat moulds for the penetration process to check its consistency. The setting time measurement and pull-off bonding strength test also used similar temperatures and RH. Additionally, the flow table test was carried out under lab temperature of 29–30 Celsius and RH between 55 and 60%. For this test, the fresh mortar was filled and compacted into truncated conical moulds at the flow table platen before jolting the samples.

#### c. Experimental and procedures

A compression strength test machine, AUTOMAX5, was used to determine the compressive strength of hardened mortar at the 7th, 28th and 56th days of age with an applied loading rate of 2.4  $\pm$  0.2 kN/s. Samples were produced in triplicate for each test, and the mean value of three readings was taken as the final strength value. Setting time cement paste was set for 120 min as the first interval time. The Vicat moulds used are 40  $\pm$  0.2 mm in height, and the first setting time is recorded when the penetration depth of 34  $\pm$  3 mm is obtained, while for final setting time, it is recorded when 0.5 mm penetration depth is achieved to comply with EN 196–3: 2016 standard. For the flow table test, after the truncated conical moulds are removed, the flow table is jolted 15 times and measured using a calibrated calliper. The average of two spread dimensions was recorded to get the flow value according to BS EN 13395-1-2002 standard. To examine the shear strength and tensile strength level, the pull-off test is carried out by means of determining restrained drying shrinkage or expansion impact after the hardening process stops at 28 and 56 days of curing age under three different curing conditions as per EN 12617–4 test method as part of the durability checking in EN1504-3 guidelines. Analyzing pore structural characterization, crushed samples from mechanical strength tests were used and measured with Mercury Intrusion Porosimetry (MIP) using a MicroActive Autopore V9600 machine. Scanning Electron Microscope (SEM) and Energy Dispersive X-Ray analysis (EDX) were employed to analyze micromorphological features and elemental compositions of the mixes in the form of hydrated particles. The SEM scanned the fractured mortar surfaces at 28 days of age while the EDX (BSE/20 KV) observed the elemental composition in the samples.

**Table 1**  
Chemical compositions (%) of Fly Ash obtained from XRF analysis.

Chemical Composition	Percentage (wt %)	Chemical Composition	Percentage (wt %)
SiO <sub>2</sub>	55.94	TiO <sub>2</sub>	0.72
Al <sub>2</sub> O <sub>3</sub>	22.60	Cr <sub>2</sub> O <sub>3</sub>	–
Fe <sub>2</sub> O <sub>3</sub>	8.10	MnO	–
CaO	6.26	SO <sub>3</sub>	1.02
P <sub>2</sub> O <sub>5</sub>	0.36	LOI	1.48
MgO	1.21	Cl	0.03
K <sub>2</sub> O	1.66	Na <sub>2</sub> O	0.62

**Table 2**

Chemical compositions (%) of Ground Granulated Blast Furnace Slag (GGBFS) obtained from XRF analysis.

Chemical Composition	Percentage (wt %)	Chemical Composition	Percentage (wt %)
SiO <sub>2</sub>	35.91	TiO <sub>2</sub>	0.59
Al <sub>2</sub> O <sub>3</sub>	16.56	Cr <sub>2</sub> O <sub>3</sub>	–
Fe <sub>2</sub> O <sub>3</sub>	1.52	MnO	–
CaO	35.28	SO <sub>3</sub>	0.36
P <sub>2</sub> O <sub>5</sub>	0.36	LOI	–
MgO	6.01	Cl	–
K <sub>2</sub> O	–	Na <sub>2</sub> O	1.76

**Table 3**

Chemical composition (%) of Ordinary Portland Cement (OPC).

Chemical Composition	Percentage (wt %)	Chemical Composition	Percentage (wt %)
SiO <sub>2</sub>	23.97	MgO	1.36
Al <sub>2</sub> O <sub>3</sub>	5.27	K <sub>2</sub> O	0.51
Fe <sub>2</sub> O <sub>3</sub>	3.28	TiO <sub>2</sub>	0.06
CaO	60.12	SO <sub>3</sub>	2.20
Na <sub>2</sub> O	0.23	LOI	2.00

**Table 4**

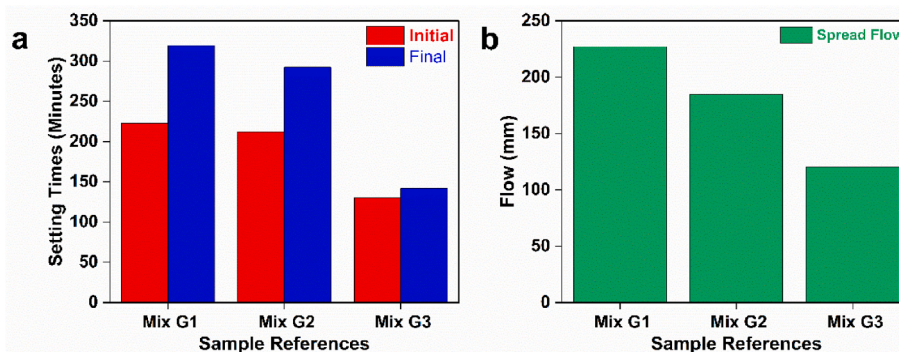
Laser Diffraction Analysis (LDA) measured the particle size distribution.

Samples	D10 (μm)	D50 (μm)	D90 (μm)
FA	2.682	14.08	54.92
GGBFS	2.819	19.99	57.25
OPC	2.690	16.32	47.96
K <sub>2</sub> CO <sub>3</sub>	299.1	448.4	645.6
SRA	2.334	12.81	35.20
CaO	1.728	4.949	20.61
SP	16.12	35.88	56.86
Sand	11.16	92.95	220.8

**Table 5**

Mix design ratio for one-part alkali-activated mortar.

Samples	Binder			Alkali activator	Solid admixtures			Design ratio	
	FA (%)	GGBFS (%)	OPC (%)	K <sub>2</sub> CO <sub>3</sub> (%)	SRA (%)	CaO (%)	SP (%)	Binder/Sand	Binder/Water
Mix G1	25	5	70	1.60	0.30	0.15	1	1	0.40
Mix G2	25	5	70	1.60	0.30	0.15	1	1	0.35
Mix G3	25	5	70	1.60	0.30	0.15	1	1	0.30

**Fig. 1.** Setting time and workability test result of one-part AAMs mortar (paste samples).

### 3. Result and discussion

#### 3.1. Setting time and workability test

The workability of the one-part AAMs mortar determines by observing how easily the fresh mortar deforms when stress is applied. Fig. 1a above shows that sample Mix G3, activated by the water-to-binder (W/B) ratio of 0.30, has the shortest initial and final setting time, followed by sample Mix G2 and control samples Mix G1. All cement paste samples recorded more than 2 h (>120 min) of initial setting time but what makes them different is low water content effectively expedited the final setting time to 142 min for cement paste sample G3 compared to mortar samples G1 and G2, which have recorded much longer time above 290 min (>4 h). An extended initial setting time in this result as a result of a low alkaline medium delayed the chemical reaction and geopolymerization process, contrary to the higher activator content, which has a more rapid reaction for a faster setting time. Furthermore, the inclusion of superplasticizer (SP) also has a retarder effect on the development of hardened mortar attributed to the adsorption properties of SP on the precursors material particles of FA, slag and OPC, as documented by [20].

Nevertheless, in this study, water content was the main factor differentiating between all paste samples. The lower W/B ratio can shorten the setting time due to heat generation from solid activators when reacted with water. Askarian et al. [7] found that the paste only contained FA and GGBFS and failed to harden in 24 h but recorded the shortest setting time by incorporating 60% OPC in the mixes. However, a short setting time could prevent proper casting at the construction site besides transporting issues from the batching plant. As for the flow table test, the higher water content in sample Mix G1 spread up to 227.24 mm makes it less viscous because of excess water compared to the samples with lesser water content, Mix G2 (184.95 mm) and G3 (120.40 mm) as shown in Fig. 1b. These findings represented a 47% reduction in mortar spreading capacity when the W/B ratio of 0.40 was reduced to 0.30. It is worth noting that the finer the particles are, the lower the spreading flow is [12]. Though all mortar samples were spread firmly, no segregation was found on the flow table. This trend also confirmed the roles of CaO as one of the admixtures used in mix design which favoured the formation of homogeneous materials, low viscosity and reduced segregation of fresh materials [28]. The workability of the mortar is beneficial when applied as a repair patching material to ensure the patched mortar remains firm, set, and bonded well on a substrate. Nevertheless, the W/B ratio has influenced cementitious mortar's yield stress and plastic viscosity. When cement particles come into contact with water, it begins to dissolve and are hydrated. Positive and negative charges will occur because of this reaction, encouraging electrostatic activities among cement particles and leading to the flocculation of the particles. Finally, cement particles absorb the amount of water, and as a sequence, the free amount of water will be diminished, leading to a higher content of solid volume fraction. As a result, yield stress and plastic viscosity level will subsequently rise, which improves the workability of the fresh one-part AAMs mortar [27]. In this study, the lower water content of the W/B ratio of 0.30 delayed the hardening process (low plastic viscosity) but was shorter than the W/B ratio of 0.35 and 0.40. Higher yield stress and lower plastic viscosity ensure the fresh mortar is more stable and flows consistently, but too viscous could be a disadvantage if applied as sprayable mortar as it is not easy to be pumped out from the pipe. On the contrary, lower W/B with higher slag content also reported a setback in autogenous shrinkage and cracking [18] due to its porosity and pore size reported larger than the OPC [29], which is further discussed in the later section in this report.

It can also be concluded that with the optimum water-to-binder ratio of 0.30, the reaction between precursors (composed with only 70% OPC content) with low alkaline activators as main synthesized products can lengthen the one-part AAMs setting time within an acceptable allowable range that beneficial for mixing, transporting, and pouring operation at the site.

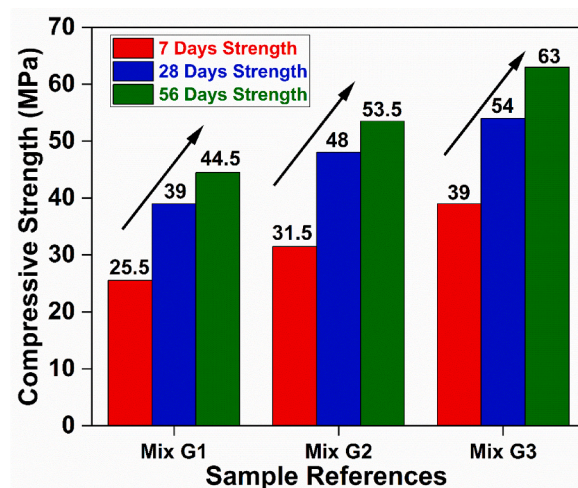


Fig. 2. Compressive strength result for mixed one-part AAMs repair mortar at 7, 28 and 56 days of curing age.

### 3.2. Compressive strength test

Compressive strength development for all mortars increases with time regardless of the water-to-binder (W/B) ratio, illustrated in Fig. 2. Mortar sample Mix G3 has recorded higher compressive strength for all curing periods beginning at 7 days of curing age and continues to develop later. Mortar sample Mix G3 has recorded the highest strength at 54.0 MPa, followed by mortar sample Mix G2 with 48.0 MPa and sample Mix G1 with 39.0 MPa at 28 days of age. Both mortar samples, Mix G2 and Mix G3 recorded above the minimum requirement for class R3 and subsequently met the class R4 - compressive strength standard as per EN1504-3 specification. At lower alkaline medium, mortar sample G3 managed to record the highest compressive strength at 63.0 MPa, followed by samples G2 and G1 at 53.5 MPa and 44.5 MPa, respectively, at 56 days of curing age.

The W/B ratio significantly influences cementitious materials for proper workability and strength. This result confirmed that the lower the W/B ratio, the higher the hardened mortar's compressive strength. Moreover, the lower binder-to-aggregate ratio used in this study was set to 1, beneficial to acting as reinforcement in the matrix and providing high dimensional stability to the mortar, improving mechanical performance and adherence level [31]. Apart from that, the compressive strength of one-part alkali AAMs product in this experiment keeps increasing after 28 days of age and confirms the geopolymerization process remains in force.

The use of a low W/B ratio of 0.30 successfully reduces the water content and has improved the compressive strength in line with the findings on the compressive strength development is correlated with the fine and large pore's diameter [20]. To understand it better, this report's latter part investigates the compressive strength result from the pore structure perspective. The inclusion of a

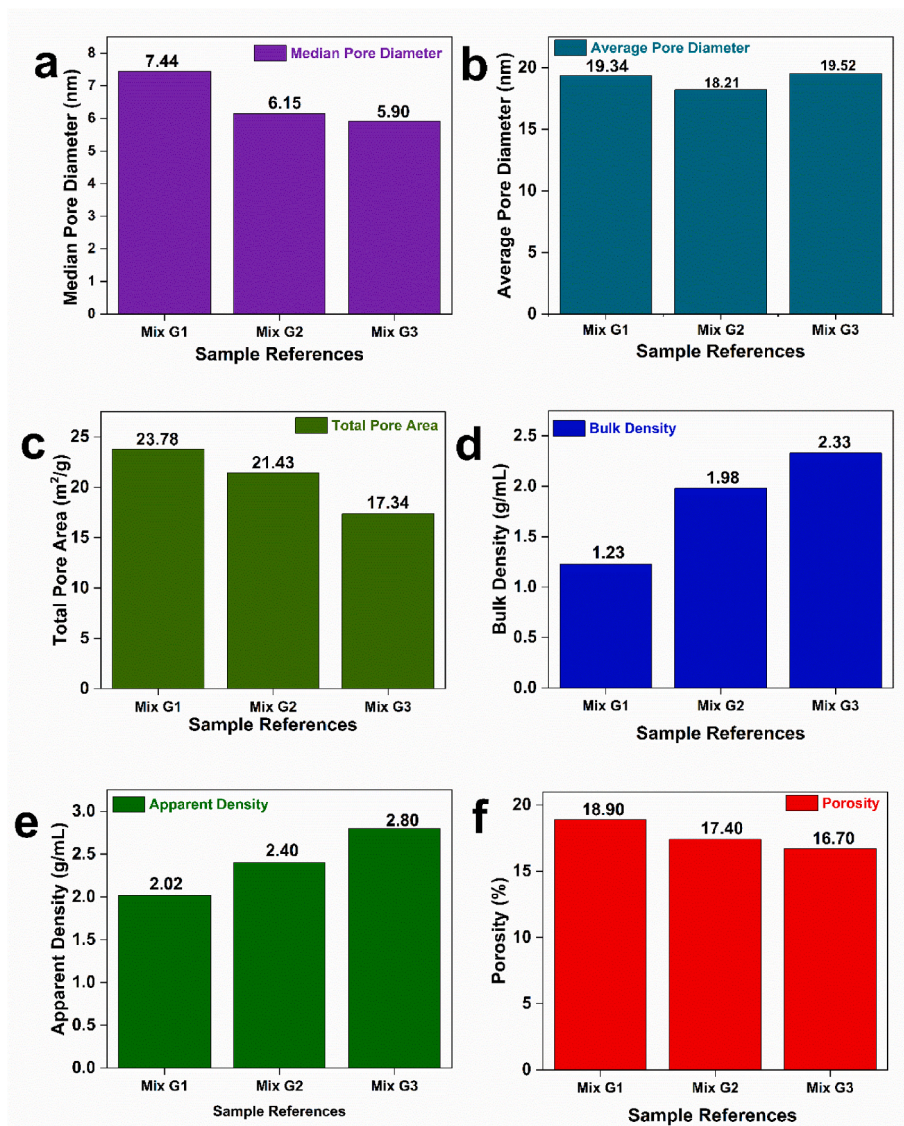


Fig. 3. Pore structure distribution of hybrid one-part alkali-activated mortars.

combination shrinkage-reducing admixture (SRA) and CaO – expansive agent contributed to the higher compressive strength for mitigating shrinkage by reducing the surface tension of pore water and micropores. When water is added, the SRA helps decrease internal stress during evaporation, while CaO counteracts the shrinkage's effect by reducing the capillary stress. The porosity level, however, can be controlled by diminishing the capillary stress of the water generated by SRA during the mortar mixing process, although the usage of ethylene-glycol-based admixture reported has a setback in affecting the elasto-mechanical properties [32]. The expansion of mortar is extended with the addition of CaO during the hydration process and only starts to shrink when the wet curing is stopped. The combination of CaO and SRA reported gave a better performance concerning the cracking resistance of the mortar due to the shrinkage effect, which is valuable for better mechanical properties of hybrid one-part AAMs [33].

### 3.3. Pore structure analysis

Pore structure distribution of mortar samples Mix G1, G2 and G3 were analyzed with Mercury Intrusion Porosimetry (MIP). The results are shown in Fig. 3a - f. The mortar specimens were collected from the crushed cube samples from the 28-d compressive strength test. The median pore diameter is mainly distributed between the range of 5.90 nm–7.44 nm (Fig. 3a). The average pore diameter for all mortar samples has no significant difference and is measured at 19.34 nm, 18.21 nm, and 19.52 nm for mortar samples G1 (W/B of 0.40), G2 (W/B of 0.35) and G3 (W/B of 0.30), respectively (Fig. 3b). It is worth noting that pores sizes in the range of 3.5–10 nm are commonly described as small gel pores type, while 10–100 nm are better known as large gel pores [1], 50 nm–10  $\mu\text{m}$  as capillary pores that cause detrimental to the strength of hardened samples and voids if the pore size is more than 10  $\mu\text{m}$  [17]. However, voids or air bubbles have less impact on the strength during the sample preparation process triggered by vibration or mould defects [34]. Gel pores size found in this experiment as a sign of the complete reaction process of the products that can fill capillary pores with the addition of slag may decrease polymerization degree and improve pore size distribution of the mixes and strength development as reported by Ref. [15].

The increase in porosity percentage will also reduce mechanical strength performance on the one-part AAMs [10]. The sample Mix G3 has an overall better pore structure distribution in terms of a low total pore area of 17.374  $\text{m}^2/\text{g}$  (Fig. 3c), higher density of 2.33  $\text{g}/\text{mL}$  (Fig. 3d), smaller median pore diameter (Fig. 3e) and as a result, Mortar G3 has a low percentage of porosity of 16.655% (Fig. 3f), compared to mortar sample Mix G2 and G1.

This contributed to the inclusion of the OPC able to decrease microstructure porosity with the formation of amorphous Ca–Al–Si gels [7] and was discussed further in this report's SEM images analysis section. In comparison to other one-part AAMs, Samarakoon et al. [11] reported that the porosity level for one-part fly ash/slag-based materials was 35.96% (activated by sodium silicate/sodium hydroxide solution), 39% porosity (activated by soda lime glass powder/sodium hydroxide) and 29% porosity activated by solid sodium silicate. On the other hand, for two-part AAMs, Kramar et al. [35] stated that a higher porosity level was recorded for metakaolin-based mortar (16.5%) followed by fly ash mortar (13.2%) and slag mortar (11.1%). As published in the report, it is interesting to note that only metakaolin-based mortar has complied with the class R4 standard and class R3 standard for fly ash-based AAMs, as per EN1504-3 specifications. However, a larger range of average pore diameter between 20 and 140 nm detected in two-part AAMs mortar samples in that report compared to the mortar samples in this study showed that the introduced hybrid one-part AAMs has not only improved the existing one-part AAMs performance but also comparable to the two-part AAMs system for concrete repair application.

Furthermore, the total pore area occupied under controlled lab temperature curing mortar at a W/B ratio of 0.35 is 23.778  $\text{m}^2/\text{g}$  but significantly reduced to 17.374  $\text{m}^2/\text{g}$  for mortar samples with a W/B ratio of 0.30. A 26% decrease in porosity is contributed to the enrichment of pore structures as an effect of the dense and compact hybrid one-part alkali-activated mortar where the group of

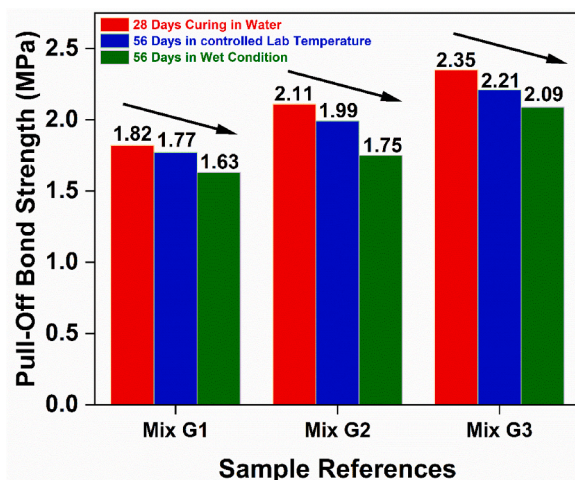


Fig. 4. Restrained drying shrinkage behaviour (pull-off bond strength result).

aluminosilicate C-A-S-H gels characterized the geopolymer matrix Si–O–Al network that reflects porous fundamental structure in geopolymerization process to refined the pores [17]. The ongoing alkali activation at a later stage encourages more pore structure refinements, contributing to the better compressive strength performance for samples Mix G2 and Mix G3 at 28 days in this report. On the other hand, one-part AAMs activated by the dry activator of NaOH micro-pearls powder have a coarser pore fraction of more than 20 nm at a W/B ratio of 0.1 and subsequently prone to chemical attacks and potentially lower resistance against severe curing conditions than two-part AAMs counterparts [11]. Contrary, findings from this report indicate that a lower dosage of potassium carbonate reacts well with the optimum water-to-binder ratio of 3.0 in the geopolymerization process, capable of refining the pore size of the mortar by filling the capillary pores, subsequently increasing the degree of microstructure densification and justified the higher compressive strength result in this report.

### 3.4. Restrained drying shrinkage and expansion

The hybrid one-part alkali-activated mortars continue to be tested to determine their shrinkage impact by conducting a pull-off bond strength test under three different curing conditions between 28 days and 56 days of age as per EN 12617–4 test method. The pull-off bond strength trend for all mortars declines over time for all mortar samples, as shown in Fig. 4 and confirms that each mortar sample was shrinking after the hydration process was completed or drying (loss) of capillary water/moisture for curing. When hardened mortar shrinks, tensile stress increases, leading to cracking and other internal deforming, thus affecting its homogeneity and compactness. Consequently, the shear and tensile bond strength of the hardened mortars at repair and the concrete substrate surface will be weakened and influence the adhesion interface. Mortar samples cured for 28 days were soaked in the water as control values showed the highest pull-off bonding strength for each mixed sample, followed by 56 days curing under lab temperature, and 56-day wet curing condition (wrapped with water bath) was the lowest pull-off bonding strength amongst all. It is interesting to understand that pull-off bond strength for mortar sample G3 activated with a W/B ratio of 0.30 has recorded above 2.0 MPa for all curing conditions and thus complied with the Class R4 ( $\geq 2.0$  MPa) while both mortar samples G1 and G2 even though recorded pull-off bond strength  $>1.5$  MPa, they were only satisfied the Class R3 standard. It is vital to note that the pull-off bond strength of control values for mortar samples G3 only dropped slightly to its lowest recorded strength ( $-2.55\%$ ) compared to its counterpart, G1 ( $-10.44\%$ ) and G2 ( $-17.06\%$ ) and explain on the little effect of internal stress because of low shrinkage level. It does not affect the shear and tensile strength of the hardened mortars, indicating higher adhesive force [16]. The result of this experiment was in good agreement with the fact that the lower alkali activator dosage will have lower shrinkage and thermal effects on the hardened samples [36]. It also confirmed water content's vital role in controlling porosity levels in limiting drying shrinkage in alkali-activated materials systems.

The correlation between the porosity level of one-part AAMs mortar and mechanical strength before and after hardened mortar shrink at 56 days of curing are shown in Fig. 5 above. At the constant mix design ratio for the mortar mixture, the influence of the water-to-binder (W/B) ratio is essential to activate the geopolymerization and control the microstructural properties of the mortar. Reduction in porosity and drying shrinkage depends on excessive hydration product content in alkali-activated binder technology. When the water is added, the chemical reaction known as hydration is initiated and produces the final hardened material products by forming the calcium silicate hydrate (C–S–H) gels to fill the open pores to form a solid microstructure. A lower W/B ratio ensures a low porosity level of mortar sample G3 (W/B of 0.30), with 16.7%, followed by mortar sample G2, with 17.4%, and mortar sample G1 recorded the highest porosity level at 18.9%. At a lower porosity level, Mix G3 recorded 54 MPa, the utmost recorded strength for 28-d age. Furthermore, at 56 days, the compressive strength continued to develop up to 63 MPa and recorded the highest pull-off bonding strength of 2.21 MPa. This understanding explained the intercorrelation between porosity level and mechanical strength to control the shrinkage level of the mortar.

A lower porosity level ensures that the hardened mortar has a compact microstructure and fewer pores to avoid intrusion of water,

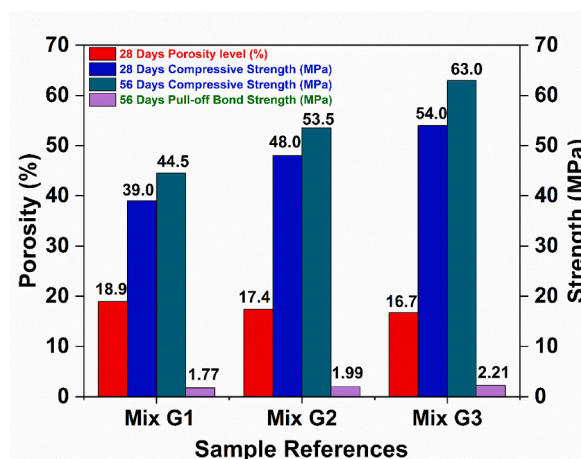


Fig. 5. Porosity level vs compressive strength of one-part AAMs mortar.

gas, or other potential chemical attacks helps to increase the mechanical strength on both compressive strength's development at 28 days of curing age uninterruptedly to a last 56 days of age as reported in this study. In addition, FA consists of rich silica content that improves the process of dissolution and polymerization, contributing to low porosity microstructures [37]. Moreover, the input of Si is more efficient with low water content [38]. As a result, the pull-off bond strength remains consistent above 2.0 MPa for of mortar sample with the lowest W/B ratio (mortar sample G3) encountering the shrink-hardened mortar at 56 days of age and shows the water content effect on monitoring drying shrinkage and expansion behaviour (by means of pull-off bond strength result) subsequently complies with structural repair products of class R4 – EN1504-3 standard. These findings also confirmed that hardened mortar with a low porosity level corresponds to the lowest drying shrinkage and better mechanical strength [39].

### 3.5. Scanning Electron Microscope (SEM)

The microstructure of one-part alkali-activated materials was studied using Scanning Electron Microscope (SEM). The hardened mortar was produced with different percentages of mix composition consisting of fly ash which contains 25% of total precursors weight, 5% slag and 70% ordinary Portland cement as main aluminosilicate precursors, which is donated to the densified microstructure of the mortar. Few spots were captured for the SEM images of mortar samples G2 and G3, and only images with overall textures, i.e., pores, cracks, and compacted surfaces, are shown in this report to understand the microstructures of the hydrated particles. Fig. 6 and Fig. 7 showed that both SEM images for samples G2 (Fig. 6a) and G3 (Fig. 7a) are well hydrated in general, compact and homogenous with new calcium sodium aluminosilicate hydrated gels on their surfaces. Interestingly, using a 1.8% dry activator type of potassium carbonate still contributes to lesser unreacted calcium as a sign of effective chemical reaction between precursors, admixtures, and low alkali activators with appropriate water content.

Nevertheless, the morphology of the two mortar samples is similar from the perspective of porosity and aggregate-mortar interface, including some unreacted particles pattern. Both images also depict the micropores and microcracks marks but exhibit a glass-like surface representing the geopolymeric gel. The microcracks frequently occur due to irregular shrinkage forces among gels and particles throughout the drying process, besides the loss of water in gels [1]. SEM images zoomed in to 20  $\mu\text{m}$ , focusing on spherically shaped areas, revealed that sample G2 has a less spherical structure than sample G3, which consists of more spherical spots, as shown in Figs. 6b and 7b. However, it can also observe in this image that the pores of sample G3 are more prominent, which supports the pore structure distribution result for the mortar sample with a low water content of W/B ratio of 0.30, has higher average pore diameters than the mortar sample G2.

### 3.6. Microstructural development

All raw materials used in this study, from aluminosilicate precursors, alkali activators and solid admixtures, have good reactivity, are chemically stable in reaction and are well dissolved when in contact with water. Optimum water-to-binder content ensures the hydrolysis of all these solid activators takes part to facilitate the network breakdown of solid precursors. Dissolved ions would undergo gelation and condensation, as reported by Lv et al. [40]. A higher Si/Al ratio obtained from fly ash is beneficial to encourage low porosity microstructure, improving sample compactness for better mechanical strength [37,41,42]. Adding GGBFS/OPC further supplies calcium and balances the short supply in FA, assisting in stronger chemical bonds for hydration products.

A higher volume of OPC is beneficial to wrap the water in the cement particles and reduce the amount of free water in the fresh mortar mixes, subsequently increasing adequate solid volume friction for better compactness and leading to higher mechanical strength [27]. Three exothermic reactions after the addition of water in one-part AAMs are the dissolution of raw materials (NaOH and hydration of CaO), bond breaking (attack of  $\text{OH}^-$  on Si–O and Al–O bonds) and release of Ca, Si and Al and formation of gels via polymerization as reported by Ref. [8]. Unreacted particles decrease in quantity with a longer curing time and a higher dosage of alkali activator in the system. However, lower alkali activator dosages were used in this experiment. Only 70% of OPC content was used in the mix, yet it contributed to a more compact and less porous structure and less unreacted fly ash particles, as agreed by Ref. [7]. Fly ash particles composed of microspheres, amorphous alumina and/or silica-rich materials can be dissolved in alkalinity [43]. The spherical particles will be embedded in the form of material and contribute to better mechanical strength over time. Spherical structures are spotted in this study's SEM image, commonly known as the unreacted fly ash component, in agreement with Azevedo et al. [10] on the fact that fly ash particles remain even after contact with alkaline materials in all curing periods, probably caused by low alkaline reactivity. In this report, mortar sample G3, which has more spherical shape particles, recorded growth compressive strength from 7 days (39.0 MPa) to 28 (54.0 MPa) and 56 days (63.0 MPa) of curing age and retained its pull-off bond strength at an

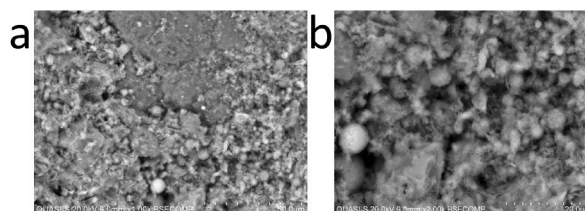


Fig. 6. SEM Image of sample G2 (a) Overview and (b) Spherical structure.

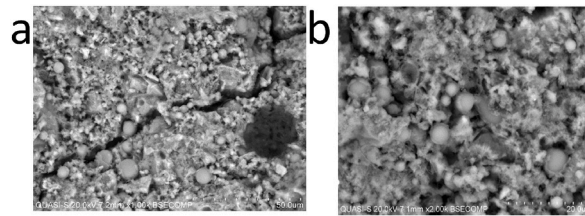


Fig. 7. SEM Image of sample G3 (a) Overview and (b) Spherical structure.

average of above 2.0 MPa at 56 days of age. It proves that the spherical/unreacted fly ash particles were still experiencing the geopolymerization process after 28 days of age. It was also helpful to understand that some unreacted particles are inherited from the parent material of hydration products, as suggested by Ref. [29].

A compact structure shows good adhesion and explains the increase in mechanical strength of the mortar. The compaction of microstructures improved with a more extended curing period, confirming the increment of strength over time for both mortar [39] samples as recorded in the compressive strength test at 7, 28 and 56 days of curing age in this report. Therefore, the unreacted particles in the SEM images may act as micro fillers in the mixes and improve their compactness. Both images have shown microcracks spots. Although a line of microcracks is more visible in the mortar sample, the G3 image may indicate the loss of water [44] or temperature cracks due to the heat generated from the reaction between the sodium oxide of the alkali activator and water [15] and uneven shrinkage forces between derivatized gel and the particles. All take place during the curing period [1]. The cracks' formation could degrade the mechanical performance of the mortar over time. Though, Almalkawi et al. [29] reported other factors on why microcracks could appear or get visible areas due to the drying process of the specimen for Scanning Electron Microscope (SEM). The clear microcracks image proves that the mortar sample G3 (19.52 nm) has a higher average pore diameter than G2 (18.21 nm), in line with the MIP test result for pore structure distribution. It was reported that an 8% solid activator (by weight %) used to activate FA/GGBFS one-part AAMs only achieved about 30 MPa at 28 days of curing age, where more unreacted particles were observed in SEM image [45]. In contrast, as the low alkaline level of the alkali activator (1.6%  $K_2CO_3$  by weight) used in this study observed, fewer unreacted particles were found on both SEM images for samples G2 and G3. Yet, they achieved significant compressive strength value, proving that this type of mortar samples initiated with a low amount of alkali activator have substantial potential to improve the current technology of one-part AAMs.

Alkali activated materials concept is much contributed by the dissolution of aluminosilicate precursors with the formation of geopolymeric gels of low atomic order favourable for hardened materials cementing properties [10]. The preparation of samples in this study was conducted under controlled temperatures and not exposed to high temperatures that could trigger dissolution. On the other hand, the geopolymerization begins with the calcium reacting with potassium carbonate to create C-S-H gels, consequently elevating the pH of the alkaline mix and reducing water content. Under an alkaline environment, the dissolution of aluminosilicate precursors was initiated, subsequently ameliorating polycondensation and polymerization reactions for the hardening process. The precipitated compounds and geopolymeric gels of N-A-S-H and C-A-S-H contributed strength and remained to develop higher over time as the geopolymerization continued.

On the contrary, at a higher temperature level of 65 Celsius, the dissolution of aluminosilicate precursors quickens to form geopolymeric compounds at an early age for higher early strength [18]. Still, it may also cause incomplete dissolution of aluminosilicate compounds given that geopolymeric slurries could cover the undissolved precursor, limiting further dissolution besides water evaporation and excessive shrinkage problem creating more cracks and pores and finally decreasing the strength of the mortar. Samarakoon et al. [11] reported that at the early age of curing, the hydration product for one-part AAMs is mainly composed of C-A-S-H type gels. However, the reaction products are moreover C-S-H dominant due to higher reactivity, and easier discharge of calcium ions can be found as early as 1 day of curing age. At the same time, the other portion of silicon and aluminium remains unreacted on the surface of the reacted phase. After 28 days, calcium content will be reduced. Still, silicon involvement in hydration products is increased because higher portions of fly ash could promote zeolite formation at the later curing stage when the composition of the binder is  $SiO_2$ -rich; the

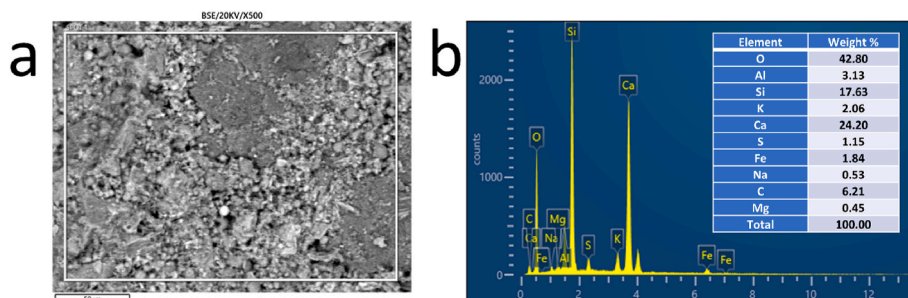


Fig. 8. SEM-EDX of sample G2 (a) Image and (b) Weight (%).

incorporation of Na is also favoured, later confirming the co-existence between C-A-S-H and N-A-S-H with a potential cross-linked structure of C-(N)-A-S-H type gels at subsequent curing. In this report an optimum W/B of 0.30 effectively initiate the chemical reaction and created C-(N)-A-S-H type gels which assist the hardened mortar with low porosity level not only able to resist leaching through its open pores but also offer more stable geopolymeric link gels against chemical attacks and maintaining its mechanical strength, beneficial for one-part AAMs long-term effectiveness.

### 3.7. Characterization of reaction products using – SEM-EDX

The difference in the surfaces of the hybrid one-part alkali-activated mortar activated by different water-to-cement ratios was further investigated by the chemical element composition at a specific area using the EDX. The resulting SEM images at 28 days of curing with the corresponding EDX maps at 28 days of curing are shown in Fig. 8a – Fig. 9a. During the curing period, microstructures of all mortar samples become dense by reducing micro-pores, reflecting compressive strength development with time due to highly compacted and low porosity levels [46]. The formation and spatial distribution for both mortar samples consistently depict a well-blended elemental distribution for the formation of homogenous and dense microstructure [11]. The reaction process in AAMs requires a few steps starting with the dissolution of Ca, Si and Al from aluminosilicate precursors, a re-orientation process, re-interaction and condensation to develop the strength [34]. Additionally, the chemical compositions of Al/Al and/or Na/Si atomic ratios and K/Al molar ratio are beneficial to determining the mechanical properties of the AAMs, which are in connection with its products dissolution rate [21,43]. It was explained in a past report on forming C-A-S-H gels that were regarded as aluminium substituted C–S–H phase in AAMs technology. Aluminium (Al) in C-A-S-H functioned in bridging tetrahedral sites. Still, the different extent was restricted by chemical limitations due to a defect of the tobermorite structure [40]. The overall constituent of geopolymerization products for mortar samples G2 and G3 have consisted of newly formed hybrid geopolymeric products N-A-S-H gels co-existing with C-A-S-H gels. New hydration products of C-(N)-A-S-H type gel were confirmed using EDX point analysis on dominant elemental phases in the reacted cement binder, mainly silicon, calcium, aluminium, and sodium.

The higher weight percentage of Ca/Si found in sample G3 (Fig. 9b) than in sample G2 (Fig. 8b) is a sign of a higher Ca/Si molar ratio beneficial for the early formation of C–S–H. Askarian et al. [7] reported that CaO to SiO<sub>2</sub> (Ca/Si) decreases with decreasing OPC content in geopolymer mixes. Mixing with a higher Ca/Si ratio is beneficial to form C–S–H gels, which can improve the early strength of mortar. The combination of OPC and FA/GGBFS creates different nature of C–S–H gels (stronger bond) compared to the typical C–S–H gels formed in OPC alone. Luukkonen et al. [47] reported that Ca/Si increases when sodium lignosulfonate – superplasticizer introduced in the mortar with Ca<sup>2+</sup> reaction from lignosulfonate could facilitate the dissolution of slag to increase the amount of calcium and likely to increase the compressive strength of mortar. It is worth noting that the roles of SP admixtures used as part of the mix design reacted well in assisting the dissolution process when a W/B ratio of 0.30 was added to ensure the efficiency of 30% OPC total weight reduction in the mixes and replaced with FA and slag yet still has a comparable Ca/Si ratio with sole OPC precursor.

## 4. Conclusion

The one-part AAMs experienced coarser pore fractions above 20 nm, affecting their durability and mechanical strength compared to the two-part counterpart. A larger pore diameter will cause higher porosity and be prone to chemical attacks, especially when the location is exposed to adverse climate and temperature. This report established the effect of adequate water content through a water-to-binder (W/B) ratio to improve one-part alkali-activated mortar. Unlike the past report on hybrid one-part AAMs, the mortar samples in this study were activated with only 1.8% alkali activator and composed of 70% OPC with 25% FA and 5% GGBFS as main precursors sources. Three types of admixtures were added to stabilize the mortar's physical properties. As a result, the W/B ratio of 0.30 exhibit the best overall performance in the fresh and hardened mortar state. A lower W/B ratio also contributes to the low porosity level of hardened mortar by controlling its pore structure. It subsequently overcame the shortfall of the current one-part technology and achieved the aim of this study. The mix design formulation is now completed for the production of geopolymer binder as per class R4 – EN1504-3 standard for structural concrete repair materials applications.

Furthermore, this mix design formulation confirms it successfully replaces 30% of OPC volume with industrial by-product precursors as the first step in diminishing reliance on the OPC and another effort to reduce clinker production, reusing waste products, and subsequently control the CO<sub>2</sub> emissions. This report also summarizes that the hardening mechanism and microstructures of hybrid one-part alkali-activated mortar changed significantly when the mortar was composed of different water-to-binder ratios, producing different mechanical strengths at early and later stages affecting the pore structure distribution. The ongoing geopolymerization process over time encourages continuous pore structure refinements, which is essential to control the total porosity level and guarantee mechanical strength growth beyond 28 days of curing age. A significantly lower porosity value below 20% was recorded for mortar samples G3, which is beneficial for controlling the drying shrinkage effect.

Nevertheless, the SEM images of the mortar specimen at 28 days of curing age for both mortar samples G2 and G3 show almost identical structures and similar final products. The only differences brought by different W/B ratios were in the amount of reacted geopolymer gels (dense, homogenous, glass-like surface)/unreacted precursors (spherical structures) and micropores/microcracks elements. Unlike the conventional one-part AAMs, where the dissolution of precursors is not completed under low alkaline reactivity, leading to more unreacted particles, the mortar samples G2 and G3, on the other hand, have dense, compact, and homogenous reacted geopolymer gels.

Apart from the influence of water content discussed in this report, another finding showed that the usage of a low alkali activator reacted well with all precursors, in addition to the optimum content of solid admixtures for the geopolymerization process and offered

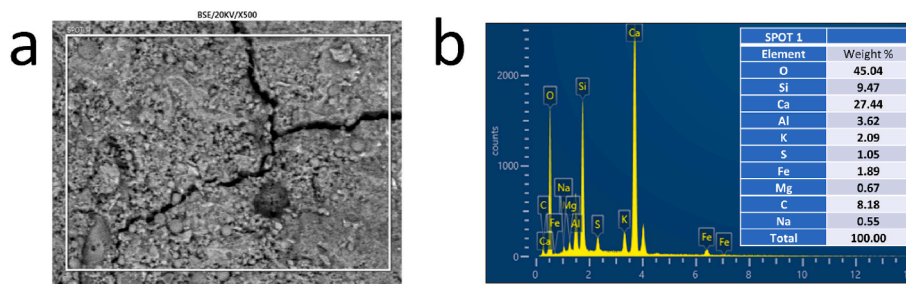


Fig. 9. SEM-EDX of sample G3 (a) Image and (b) Weight (%).

reliable mechanical and microstructural properties for the hardened mortar. Although the hybrid one-part alkali-activated mortar has a significantly low porosity level and consistent mechanical strength, a future study must focus on the stability of its pore structures against severe environmental conditions and chemical attacks in a different climate to ensure its durability and efficacy for long-term application.

#### Author contribution statement

Eddy Yusslee: Conceived and designed the experiments; Performed the experiments; Analyzed and interpreted the data; Contributed reagents, materials, analysis tools or data; Wrote the paper.

Sherif Beskhyroun: Contributed reagents, materials, analysis tools or data.

#### Funding statement

This research did not receive any specific grant from funding agencies in the public, commercial, or not-for-profit sectors.

#### Data availability statement

No data was used for the research described in the article.

#### Declaration of interest's statement

The authors have no conflicts of interest to declare.

#### Acknowledgements

Special thanks to Engineering New Zealand (ENZ), The Association of German Engineers (VDI) and the Sabah Public Service Department, Malaysia, which contributed to the outcome of this experiment.

#### References

- [1] C. Liu, X. Yao, W. Zhang, Controlling the setting times of one-part alkali-activated slag by using honeycomb ceramics as carrier of sodium silicate activator, *Construct. Build. Mater.* 235 (2020), 117091, <https://doi.org/10.1016/j.conbuildmat.2019.117091>.
- [2] H.A. Khan, M.S.H. Khan, A. Castel, J. Sunarho, Deterioration of alkali-activated mortars exposed to natural aggressive sewer environment, *Construct. Build. Mater.* 186 (2018) 577–597, <https://doi.org/10.1016/j.conbuildmat.2018.07.137>.
- [3] E. Hany, N. Fouad, M. Abdel-Wahab, E. Sadek, Compressive strength of mortars incorporating alkali-activated materials as partial or full replacement of cement, *Construct. Build. Mater.* 261 (2020), 120518, <https://doi.org/10.1016/j.conbuildmat.2020.120518>.
- [4] S.A. Bernal, J.L. Provis, Durability of alkali-activated materials: progress and perspectives, *J. Am. Ceram. Soc.* 97 (4) (2014) 997–1008, <https://doi.org/10.1111/jace.12831>.
- [5] T. Phoo-Ngernkham, S. Hanjitsuwan, L.Y. Li, N. Damrongwiriyanupap, P. Chindaprasirt, Adhesion characterization of Portland cement concrete and alkali-activated binders, *Adv. Cement Res.* 31 (2) (2019) 69–79, <https://doi.org/10.1680/jadcr.17.00122>.
- [6] P. Perumal, et al., High strength one-part alkali-activated slag blends designed by particle packing optimization, *Construct. Build. Mater.* 299 (2021), 124004, <https://doi.org/10.1016/j.conbuildmat.2021.124004>.
- [7] M. Askarian, Z. Tao, G. Adam, B. Samali, Mechanical properties of ambient cured one-part hybrid OPC-geopolymer concrete, *Construct. Build. Mater.* 186 (2018) 330–337, <https://doi.org/10.1016/j.conbuildmat.2018.07.160>.
- [8] T. Luukkonen, Z. Abdollahnejad, J. Yliniemi, P. Kinnunen, M. Illikainen, One-part alkali-activated materials: a review, *Cement Concr. Res.* 103 (October) (2018) 21–34, <https://doi.org/10.1016/j.cemconres.2017.10.001>.
- [9] T. Yang, et al., Effects of calcined dolomite addition on reaction kinetics of one-part sodium carbonate-activated slag cements, *Construct. Build. Mater.* 211 (2019) 329–336, <https://doi.org/10.1016/j.conbuildmat.2019.03.245>.
- [10] A. Galvão Souza Azevedo, K. Strecker, Kaolin, fly-ash and ceramic waste based alkali-activated materials production by the 'one-part' method, *Construct. Build. Mater.* 269 (2021), <https://doi.org/10.1016/j.conbuildmat.2020.121306>.
- [11] M.H. Samarakoon, P.G. Ranjith, W.H. Duan, V.R.S. De Silva, Properties of one-part fly ash/slag-based binders activated by thermally-treated waste glass/NaOH blends: a comparative study, *Cem. Concr. Compos.* 112 (2020), 103679, <https://doi.org/10.1016/j.cemconcomp.2020.103679>. December 2019.

- [12] W. Chen, R. Peng, C. Straub, B. Yuan, Promoting the performance of one-part alkali-activated slag using fine lead-zinc mine tailings, *Construct. Build. Mater.* 236 (2020), 117745, <https://doi.org/10.1016/j.conbuildmat.2019.117745>.
- [13] V.A. Nunes, P.H.R. Borges, C. Zanotti, Mechanical compatibility and adhesion between alkali-activated repair mortars and Portland cement concrete substrate, *Construct. Build. Mater.* 215 (2019) 569–581, <https://doi.org/10.1016/j.conbuildmat.2019.04.189>.
- [14] X. Ke, S.A. Bernal, N. Ye, J.L. Provis, J. Yang, One-part geopolymers based on thermally treated red Mud/NaOH blends, *J. Am. Ceram. Soc.* 98 (1) (2015) 5–11, <https://doi.org/10.1111/jace.13231>.
- [15] M. Askarian, Z. Tao, B. Samali, G. Adam, R. Shuaibu, Mix composition and characterization of one-part geopolymers with different activators, *Construct. Build. Mater.* 225 (2019) 526–537, <https://doi.org/10.1016/j.conbuildmat.2019.07.083>.
- [16] E. Yusslee, S. Beskhyroun, The potential of one-part alkali-activated materials (AAMs) as a concrete patch mortar, *Sci. Rep.* 12 (1) (2022), 15902, <https://doi.org/10.1038/s41598-022-19830-0>.
- [17] S. Haruna, B.S. Mohammed, M.M.A. Wahab, M.S. Liew, Effect of paste aggregate ratio and curing methods on the performance of one-part alkali-activated concrete, *Construct. Build. Mater.* 261 (2020), 120024, <https://doi.org/10.1016/j.conbuildmat.2020.120024>.
- [18] S.F.A. Shah, B. Chen, S.Y. Oderji, M.A. Haque, M.R. Ahmad, Improvement of early strength of fly ash-slag based one-part alkali activated mortar, *Construct. Build. Mater.* 246 (2020), 118533, <https://doi.org/10.1016/j.conbuildmat.2020.118533>.
- [19] T. Luukkonen, Z. Abdollahnejad, J. Yliniemi, P. Kinnunen, M. Illikainen, One-part alkali-activated materials: a review, *Cement Concr. Res.* 103 (2018) 21–34, <https://doi.org/10.1016/j.cemconres.2017.10.001>. October 2017.
- [20] Y. Alrefaei, Y.S. Wang, J.G. Dai, The effectiveness of different superplasticizers in ambient cured one-part alkali activated pastes, *Cem. Concr. Compos.* 97 (2019) 166–174, <https://doi.org/10.1016/j.cemconcomp.2018.12.027>. September 2018.
- [21] A. Mobili, F. Tittarelli, H. Rahier, One-part alkali-activated pastes and mortars prepared with metakaolin and biomass ash, *Appl. Sci.* 10 (16) (2020), <https://doi.org/10.3390/app10165610>.
- [22] M. Liu, H. Wu, P. Yao, C. Wang, Z. Ma, Microstructure and macro properties of sustainable alkali-activated fly ash mortar with various construction waste fines as binder replacement up to 100, *Cem. Concr. Compos.* 134 (2022), 104733, <https://doi.org/10.1016/j.cemconcomp.2022.104733>. June.
- [23] M. Liu, C. Wang, H. Wu, D. Yang, Z. Ma, Reusing recycled powder as eco-friendly binder for sustainable GGBS-based geopolymer considering the effects of recycled powder type and replacement rate, *J. Clean. Prod.* 364 (2022), 132656, <https://doi.org/10.1016/j.jclepro.2022.132656>. June.
- [24] S. Candamano, P. De Luca, P. Frontera, F. Crea, Production of geopolymeric mortars containing forest biomass ash as partial replacement of metakaolin, *Environ. - MDPI* 4 (4) (2017) 1–13, <https://doi.org/10.3390/environments4040074>.
- [25] R.H. Geraldo, O.G. Teixeira, S.R.C. Matos, F.G.S. Silva, J.P. Gonçalves, G. Camarini, Study of alkali-activated mortar used as conventional repair in reinforced concrete, *Construct. Build. Mater.* 165 (2018) 914–919, <https://doi.org/10.1016/j.conbuildmat.2018.01.063>.
- [26] O.G. Teixeira, R.H. Geraldo, F.G. da Silva, J.P. Gonçalves, G. Camarini, Mortar type influence on mechanical performance of repaired reinforced concrete beams, *Construct. Build. Mater.* 217 (2019) 372–383, <https://doi.org/10.1016/j.conbuildmat.2019.05.035>.
- [27] L. Li, J.X. Lu, B. Zhang, C.S. Poon, Rheology behavior of one-part alkali activated slag/glass powder (AASG) pastes, *Construct. Build. Mater.* 258 (2020), 120381, <https://doi.org/10.1016/j.conbuildmat.2020.120381>.
- [28] A. Palomo, O. Maltseva, I. García-Lodeiro, A. Fernández-Jiménez, Portland versus alkaline cement: continuity or clean break: 'A key decision for global sustainability, *Front. Chem.* 9 (2021) 1–28, <https://doi.org/10.3389/fchem.2021.705475>. October.
- [29] A.T. Almkaw, S. Hamadna, P. Soroushian, One-part alkali activated cement based volcanic pumice, *Construct. Build. Mater.* 152 (2017) 367–374, <https://doi.org/10.1016/j.conbuildmat.2017.06.139>.
- [30] E. Yusslee, S. Beskhyroun, Performance evaluation of hybrid one-Part Alkali activated materials (AAMs) for concrete structural repair, *Buildings* 12 (11) (2022), <https://doi.org/10.3390/buildings12112025>.
- [31] R. Robayo-Salazar, C. Jesús, R. Mejía de Gutiérrez, F. Pacheco-Torgal, Alkali-activated binary mortar based on natural volcanic pozzolan for repair applications, *J. Build. Eng.* 25 (2019), 100785, <https://doi.org/10.1016/j.jobbe.2019.100785>. April.
- [32] L. Coppola, et al., The combined use of admixtures for shrinkage reduction in one-part alkali activated slag-based mortars and pastes, *Construct. Build. Mater.* 248 (2020), 118682, <https://doi.org/10.1016/j.conbuildmat.2020.118682>.
- [33] I.L. Tchegnig Ngassam, P. Arto, H. Beushausen, A new approach for the mix design of (patch) repair mortars, *African J. Sci. Technol. Innov. Dev.* 10 (3) (2018) 259–265, <https://doi.org/10.1080/20421338.2018.1452845>.
- [34] B. Yang, J.G. Jang, Environmentally benign production of one-part alkali-activated slag with calcined oyster shell as an activator, *Construct. Build. Mater.* 257 (2020), 119552, <https://doi.org/10.1016/j.conbuildmat.2020.119552>.
- [35] S. Kramar, A. Sajna, V. Ducman, Assessment of alkali activated mortars based on different precursors with regard to their suitability for concrete repair, *Construct. Build. Mater.* 124 (2016) 937–944, <https://doi.org/10.1016/j.conbuildmat.2016.08.018>.
- [36] M. Almkhadme, A.M. Soliman, Effects of mixing water temperatures on properties of one-part alkali-activated slag paste, *Construct. Build. Mater.* 266 (2021), 121030, <https://doi.org/10.1016/j.conbuildmat.2020.121030>.
- [37] M.N. Qureshi, S. Ghosh, Effect of Si/Al ratio on engineering properties of alkali-activated GGBS pastes, *Green Mater.* 2 (3) (2014) 123–131, <https://doi.org/10.1680/gmat.14.00001>.
- [38] E. Pereira, E. Br, A. Resende, M.H.F. De Medeiros, L.C. Meneghetti, Chloride accelerated test: influence of silica fume, water/binder ratio and concrete cover thickness Ensaio acelerado por cloretos: efeito da sílica ativa, relação água/aglomerante e espessura de cobrimento do concreto Chloride accelerated test: influence, *IBRACON Struct. Mater. J.* • 2013 • 6 (4) (2013) 4.
- [39] H.A. Abdel-Gawwad, A.M. Rashad, M. Heikal, Sustainable utilization of pretreated concrete waste in the production of one-part alkali-activated cement, *J. Clean. Prod.* 232 (2019) 318–328, <https://doi.org/10.1016/j.jclepro.2019.05.356>.
- [40] W. Lv, Z. Sun, Z. Su, Study of seawater mixed one-part alkali activated GGBFS-fly ash, *Cem. Concr. Compos.* 106 (2020), 103484, <https://doi.org/10.1016/j.cemconcomp.2019.103484>. June 2019.
- [41] S. Thokchom, K.K. Mandal, S. Ghosh, Effect of Si/Al ratio on performance of fly ash geopolymers at elevated temperature, *Arabian J. Sci. Eng.* 37 (4) (2012) 977–989, <https://doi.org/10.1007/s13369-012-0230-5>.
- [42] Y. Wang, et al., Effects of Si/Al ratio on the efflorescence and properties of fly ash based geopolymer, *J. Clean. Prod.* 244 (2020), 118852, <https://doi.org/10.1016/j.jclepro.2019.118852>.
- [43] H. Choo, S. Lim, W. Lee, C. Lee, Compressive strength of one-part alkali activated fly ash using red mud as alkali supplier, *Construct. Build. Mater.* 125 (2016) 21–28, <https://doi.org/10.1016/j.conbuildmat.2016.08.015>.
- [44] T. Luukkonen, Z. Abdollahnejad, J. Yliniemi, P. Kinnunen, M. Illikainen, Comparison of alkali and silica sources in one-part alkali-activated blast furnace slag mortar, *J. Clean. Prod.* 187 (2018) 171–179, <https://doi.org/10.1016/j.jclepro.2018.03.202>.
- [45] S. Yousefi Oderji, B. Chen, M.R. Ahmad, S.F.A. Shah, Fresh and hardened properties of one-part fly ash-based geopolymer binders cured at room temperature: effect of slag and alkali activators, *J. Clean. Prod.* 225 (2019) 1–10, <https://doi.org/10.1016/j.jclepro.2019.03.290>.
- [46] H.A. Abdel-Gawwad, S.R.V. García, H.S. Hassan, Thermal activation of air cooled slag to create one-part alkali activated cement, *Ceram. Int.* 44 (12) (2018) 14935–14939, <https://doi.org/10.1016/j.ceramint.2018.05.089>.
- [47] T. Luukkonen, Z. Abdollahnejad, K. Ohenoja, P. Kinnunen, Suitability of commercial superplasticizers for one-part alkali-activated blast-furnace slag mortar, *J. Sustain. Cem. Mater.* 8 (4) (2019) 244–257, <https://doi.org/10.1080/21650373.2019.1625827>.